2013

Examining geochemical processes in acid sulphate soils using stable sulphur isotopes

Crystal A. Maher
Southern Cross University

Publication details

Maher, CA 2013, 'Examining geochemical processes in acid sulphate soils using stable sulphur isotopes', PhD thesis, Southern Cross University, Lismore, NSW.

Examining geochemical processes in acid sulfate soils using stable sulfur isotopes

Crystal A Maher

BAppSci (Hons)

A thesis submitted in fulfilment of the requirements of the degree of

Doctor of Philosophy

Southern Cross GeoScience

School of Environment, Science and Engineering

Southern Cross University Lismore NSW Australia

May 2013

Thesis Declaration

I certify that the work presented in this thesis is, to the best of my knowledge and belief, original, except as acknowledged in the text, and that the material has not been submitted, either in whole or in part, for a degree at this or any other university.

I acknowledge that I have read and understood the University's rules, requirements, procedures and policy relating to my higher degree research award and to my thesis. **I certify that I have complied** with the rules, requirements, procedures and policy of the University (as they may be from time to time).

Print Name: ……..

Signature: …….

Date: ……

Abstract

Acid sulfate soils occur in coastal and inland environments in Australia and elsewhere around the world. Disturbance of acid sulfate soil materials causes considerable environmental harm including acidification, release of toxic metals, fish kills and degradation of aquatic ecosystems. This thesis shows that stable sulfur isotope ratios ($\delta^{34}S$) are sensitive to environmental conditions and are a geochemical technique that promises to provide valuable information about the behaviour of acid sulfate soil materials.

The sulfide and sulfate fractions of acid sulfate soil materials from a range of environments were examined to establish a baseline for the use of sulfur isotopes in acid sulfate soils in eastern Australia. The $\delta^{34}S$ of these fractions were sensitive to their environment of formation according to whether the sulfate supply was open or restricted during bacterial sulfate reduction and sulfide formation. These results suggest sulfur isotopes could be used to identify the environment of formation, trace the source of sulfate in contemporary and relic sulfide accumulations and possibly quantify the amount of sulfate in waterways derived from the oxidation of acid sulfate soil materials during hydrological events.

When applied to an acid sulfate soil landscape undergoing tidal exchange remediation at East Trinity, $\delta^{34}S$ were shown to provide valuable information about the geochemical processes that were occurring during remediation. The $\delta^{34}S$ ratios of the more insoluble secondary sulfate fractions (e.g. jarosite) retained information on the conditions prior to remediation, whereas the water soluble and exchangeable sulfate $\delta^{34}S$ ratios reflected conditions post remediation and indicated the relative contributions from two potential sulfate sources – the oxidation of pyrite and the tidal water. Similarly, the contemporary sulfide accumulations reflected both sulfate sources and could be clearly distinguished isotopically using $\delta^{34}S$ ratios from the relic sulfides at depth that had formed solely under open tidal conditions.

$\delta^{34}S$ of dissolved sulfate was also examined in water from the waterways of a drained acidified acid sulfate soil landscape in the Tuckean Swamp. Oxidised acid sulfate soil materials produced sulfate that was clearly differentiated from other sulfate sources, such as seawater, using sulfur isotope techniques. There was a strong association between the $\delta^{34}S$ of dissolved sulfate and other parameters commonly used to identify the influence of acid sulfate soils on water quality, specifically pH and the chloride:sulfate ratio. It was determined that $\delta^{34}S$ ratios could be used to help identify acidic discharges in waterways from acid sulfate soils and has the potential to help quantify the contribution that drainage from acid sulfate soils makes to surrounding waterways.

Finally, $\delta^{34}S$ ratios were used to examine the cycling of sulfides and sulfates in a contemporary mangrove sediment representing currently-forming sulfidic materials in Ballina. The sulfide concentrations and $\delta^{34}S$ ratios showed considerable variation throughout the profiles and across a 12 hour long drainage period. Rather than being the product of geochemical processes these variations were attributed mainly to the inherent heterogeneity of mangrove sediments. The study indicated the occurrence of sulfide oxidation in subsurface layers likely contributed to lower $\delta^{34}S$ ratios in the soluble sulfate fraction relative to seawater and the surface layer, but not to a degree that would explain the similarity between the sulfide and sulfate $\delta^{34}S$ ratios typically found in subsurface sulfidic layers of acid sulfate soils.

Acknowledgements

Completing a PhD is without doubt an arduous process – as it should be. For me the process included a few side steps. I organised and helped develop the first acid sulfate soil management course that has since been rolled out across the country. I also opened and ran a successful café for 3 years. Ok, maybe that wasn't the best idea but I made it to the finish line eventually.

Throughout this process I have been fortunate to meet many great people and be part of some fantastic research initiatives. Many wonderful people have helped me with field work, lab work, research direction, proof reading, support and encouragement. There are a few people that deserve special mention because without them, it is unlikely I would have made it through.

The first is my partner Shane. He has been my rock throughout this entire journey and without his constant support and unfailing belief in me I might not have achieved my goal. He has helped me keep my perspective and focus (you need to finish so you can get a job!) and has been tolerant of my whims (hey I want to open a café!). Shane provides the balance in my life that ultimately makes it all worthwhile.

The second is my very good friend Diane Fyfe. Diane was part of the original CASSR group and she has always been available to assist in whatever manner possible. She has helped with field work, lab work, data analysis, proof reading and a host of other things. Most importantly she was always available to grab a cup of coffee and just vent my frustration and relieve the stress. Without our weekly meetings to keep me on track and challenge my progress the battle would have been much tougher and far less enjoyable.

The third person is Laurel Freedman, who I met when she came to work for Southern Cross GeoScience. To say she is efficient is an understatement – Laurel is the guru of all things administrative and has been a valuable buffer between me and the paperwork demons. Laurel has always encouraged me to finish and has helped me focus on the future rather than getting caught up in the problems of the past.

Last but not least is my awesome supervisor Professor Leigh Sullivan. I will forever admire his ability to identify the trends in the data and then to always see the big picture applications. Leigh has encouraged, supported and challenged me to do my best in his subtle, non-pushy way. I appreciate the time, effort and experience that he has contributed to my PhD throughout the entire process. Without his direction I would never have found the finish line, let alone crossed it.

I want to give a special thanks to my parents and to the other CASSR, SCGS and SESE staff and students (in no particular order) – Nadia, Vanessa, Mick, Trent, Mark, Nick, Ed, Mal, Annabelle, Scott, Debra – you have made this an incredible experience.

I would also like to acknowledge the Australian Government for the APA and CRC CARE for the top up scholarship. This work was partially funded by CRC CARE as part of the East Trinity project 6-6-01-06/07, with additional financial support from the School of Environment, Science and Engineering and Southern Cross GeoScience.

This thesis was edited by Nadia Toppler in accordance with Standards D (Language and Illustration and E (Completeness and Consistency) of the Australian Standard of Editing Practice. More information can be found at http://iped-editors.org/editing_theses

Table of Contents

List of Tables

List of Figures

Chapter 1

Introduction to acid sulfate soils and stable sulfur isotopes

Acid Sulfate Soils – A Definition

In common terms, acid sulfate soil is the name given to soils containing sulfide minerals (particularly pyrite) or the products of sulfide oxidation (Melville and White 2000; Sullivan *et al* 2001; Powell and Martens 2005). A slightly more technical definition provided by Dent and Pons (1993) describes soils or sediments that contain sufficient iron sulfides, which when oxidised, produce more sulfuric acid than can be neutralised by the inherent buffering capacity of the soil. Acid sulfate soils are grouped under Hydrosols in the Australian Soil Classification Scheme (Isbell 1996) and can be divided into potential acid sulfate soils and actual acid sulfate soils (Powell and Martens 2005.

Potential Acid Sulfate Soils

Potential acid sulfate soils (PASS) are sediments which, due to insulation from water logging, remain unoxidised (Ritsema *et al* 1992; Lines-Kelly 2000). They may be characterised by dark grey, unripe clay (i.e. soft buttery consistency with low bearing strength), often containing remnants of decomposed organic matter (Dent and Pons 1993; Morand 1993). Potential acid sulfate soils often have a pH near neutral although sometimes acid diffusion through the soil profile may lower the pH substantially (Rosicky *et al* 2000).

Signs of potential acid sulfate soils in the field may include a strong hydrogen sulfide (H_2S) smell, the presence of mud that contains organic matter, dominance of mangroves, reeds, rushes and other swamp tolerant vegetation in dark grey estuarine clay, indicating intermittent poor drainage (Lines-Kelly 2000). A more comprehensive identification of potential acid sulfate soils is also provided in the Australian Soil Classification Scheme (Isbell 1996):

- Sulfidic material (PASS): A subsoil, waterlogged, mineral or organic material that contains oxidisable sulfur compounds, usually iron disulfide (e.g. pyrite), that has a field pH of 4 or more but which will become extremely acid when drained. Sulfidic material is identified by a drop in pH by at least 0.5 units to 4

or less (1:1 by weight in water, or in a minimum of water to permit measurement) when a 10 mm thick layer is incubated at field capacity for 8 weeks. For a quick screening test that is not definitive, a 10 g sample treated with 50 mL of 30% H_2O_2 will show a fall in pH to 2.5 or less. Caution: H_2O_2 is a strong oxidant and sulfides and organic materials will froth violently in a test tube, which may become very hot.

Potential acid sulfate soils have the potential to produce sulfuric acid but will remain stable if anaerobic, waterlogged conditions are maintained (Smith *et al* 2003). If they are allowed to oxidise they may develop into actual acid sulfate soils (Ritsema and Groenenberg 1993; Melville and White 2000).

Actual Acid Sulfate Soils

Depending upon the acid neutralising capacity of the soil the oxidation of potential acid sulfate soils may or may not form actual acid sulfate soils (AASS) (Ritsema *et al* 1992). Signs of actual acid sulfate soils may include:

- the presence of yellow mottles of jarosite along soil cracks and decayed plant root channels
- iron staining on plants
- white surface salts (non-tidal)
- pH of 4 or less
- negligible plant growth when dry
- red iron staining in water or unusually clear water
- acid and salt tolerant plants such as water lilies, tea tree, swamp oak, tussocks and rushes (Lines-Kelly 2000).

Actual acid sulfate soils or ‘sulfuric soils’ are also described in the Australian Soil Classification Scheme (Isbell 1996):

- Sulfuric materials (AASS): Soil material that has a pH less than 4 (1:1 by weight in water, or in a minimum of water to permit measurement) when measured in dry season conditions as a result of the oxidation of sulfidic materials. Evidence that low pH is caused by oxidation of sulfides is one

of the following: yellow mottles and coatings of jarosite (hue 2.5Y or yellower and chroma of about 6 or more); presence of underlying sulfidic material.

The profile of an actual acid sulfate soil may contain three oxidation phases (pre-oxidation, active and post-oxidation, as defined by Fanning (1993)) in a depth sequence. The pre-oxidation phase is found at depth below the redox influence, the active stage at the redox boundary and the post oxidation stage at the surface, if it has been exposed for many years (Fanning 1993). Alternatively the pre, active and post oxidation stages may follow one another on a time scale. The generic term 'acid sulfate soil' describes an entire soil profile that contains both actual acid sulfate soils and potential acid sulfate soil layers (Melville and White 2000; Smith *et al* 2003) but is also used to describe soil profiles that contain only one of these types of soil materials (Fitzpatrick *et al* 2003).

The Transformation of Potential to Actual Acid Sulfate Soils

The transformation of potential acid sulfate soils to actual acid sulfate soils is effectively governed by the height of the water table (White *et al* 1996; Johnston *et al* 2003c) as this determines the ingress of oxygen in a soil profile (Kelly 1996). Acid sulfate soil environments are generally located in low lying areas where the water table is maintained at or near the surface by a variety of factors including tidal pressure, rainfall and freshwater stream inputs (Ferguson and Eyre 1996; Powell and Martens 2005). Under such conditions the potential acid sulfate soils are insulated from oxidation and remain stable (Figure 1.1).

When potential acid sulfate soil materials are exposed they oxidise and produce sulfuric acid. Such exposure may result from excavation, dredging or stockpiling of sediment (Evangelou 1998), however, the most common cause is the lowering of the water table for urban and agricultural development (Figure 1.2) (Dent and Pons 1995; Boman *et al* 2008, 2010; Burton *et al* 2011a). In eastern Australia, over the past one hundred years the introduction of engineered drainage systems and flood mitigation structures has substantially altered the natural hydrology of many coastal floodplains

(White *et al* 1996; Johnston *et al* 2003a, b; Smith *et al* 2003; Powell and Martens 2005). This alteration has a two-fold effect on the rate of acidification from potential acid sulfate soils; the drainage lowers the water table and exposes potential acid sulfate soil materials allowing oxidation, while the flood mitigation structures prevent regular inflow of tidal waters, which would otherwise neutralise the acid produced from oxidation and flush away other oxidation products (White *et al* 1996; Johnston *et al* 2003a, b; Johnston *et al* 2011a, 2012).

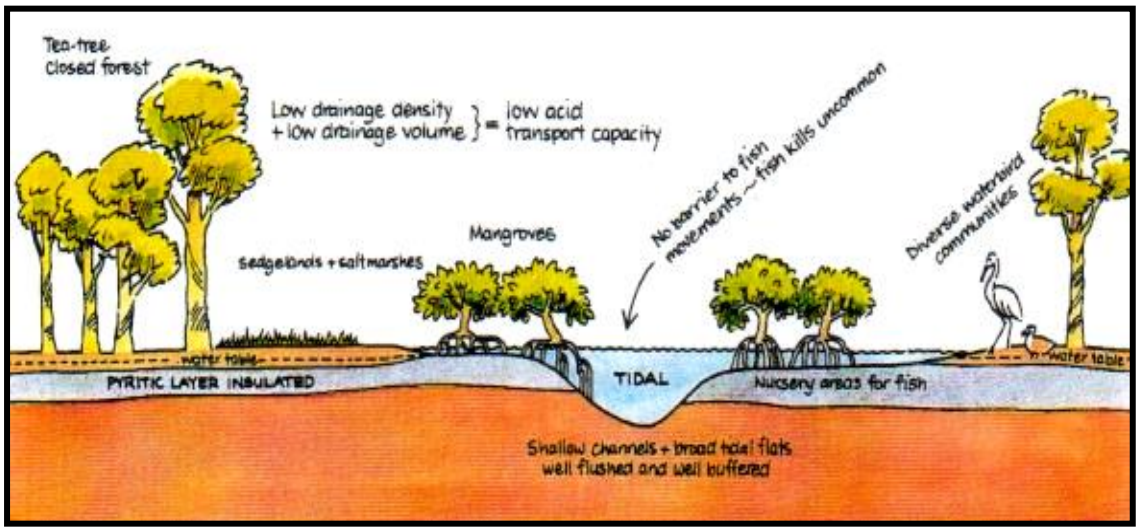

Figure 1.1. Diagram showing an undisturbed environment with sulfidic layers protected by water (Source: Sammut and Lines-Kelly 2000).

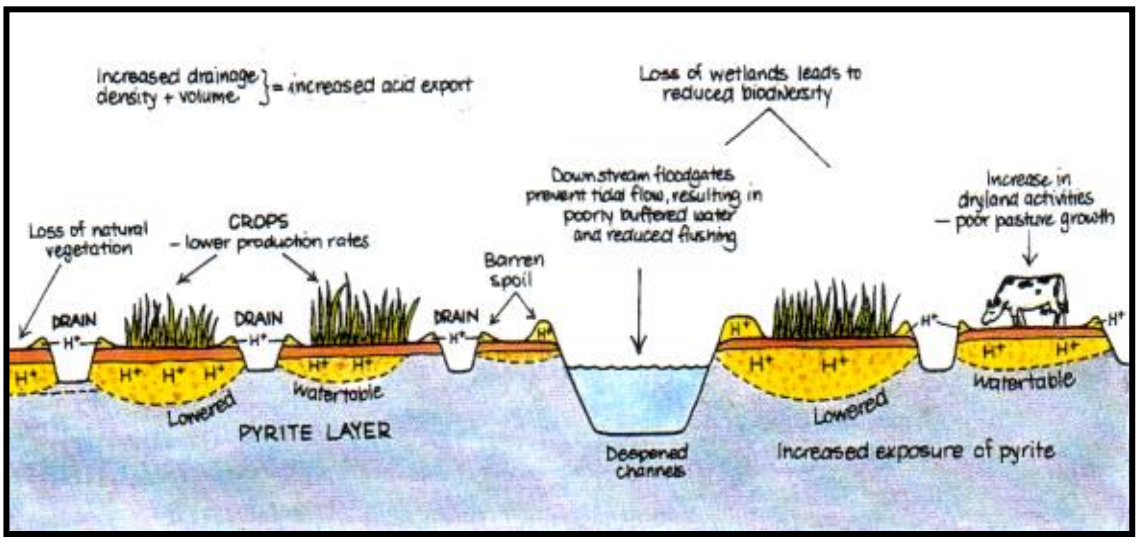

Figure 1.2. Draining acid sulfate soils leads to high frequency, high magnitude and persistent acidity (Source: Sammut and Lines-Kelly 2000).

The lowering of the water table also occurs naturally through evapotranspiration by vegetation, extreme drought or regional uplifting (Evangelou 1998; Astrom and Spiro 2000; Boman *et al* 2010). Most of the acid will be neutralised or buffered in the soil profile, although acid outflows do sometimes occur (White and Sammut 1995; Russell and Helmke 2002). In many areas however, human intervention has severely exacerbated the problem and caused acidification beyond what natural environmental processes can ameliorate (White and Sammut 1995; Williams *et al* 1996).

Distribution of Acid Sulfate Soils

Worldwide, acid sulfate soils are usually associated with tidal flushing zones (Macdonald *et al* 2002) and affect over 50 million hectares of land (Sullivan *et al* 2012). Acid sulfate soils affect significant portions of the Australian coastline (Sammut *et al* 1996a), particularly in New South Wales (Johnston *et al* 2003a; Burton *et al* 2006c; Claff *et al* 2011) (Figure 1.3), Queensland (Russell and Helmke 2002; Powell and Martens 2005; Johnston *et al* 2011a, b) and Western Australia (Kilmister and Cartwright 2011; Morgan *et al* 2012a, b). Acid sulfate soils have also been identified in many inland areas (Sullivan *et al* 2002; Fitzpatrick *et al* 2009; Isaacson *et al* 2009).

Coastal Acid Sulfate Soils

The majority of acid sulfate soils occur in coastal embayments and estuaries where wave action is limited and sedimentation occurs (Johnston *et al* 2003a). Acid sulfate soils that form in tropical and sub-tropical environments are expected to contain larger concentrations of pyrite. In addition, those environments with prolonged dry seasons have higher oxidation rates than those with more temperate climates (Yang 1997).

Inland Acid Sulfate Soils

In addition to coastal environments, acid sulfate soils have also been discovered at several inland locations in South Australia (Fitzpatrick *et al* 1993, 2009), New South

Wales (Isaacson *et al* 2009) and Victoria (Sullivan *et al* 2002). The occurrence of inland acid sulfate soils has been attributed to increasing salinisation, which is causing severe degradation over much of the Australian continent. In South Australia, inland acid sulfate soils are associated with dryland salinity, which is often caused by the replacement of native vegetation with annual pastures and crops. These crops cannot utilise enough of the rainfall resulting in increased recharge to groundwater and higher water tables. This brings salts in the soil closer to the surface thereby providing a source of sulfate for the formation of iron sulfides (Fitzpatrick *et al* 1993; Peck 1993).

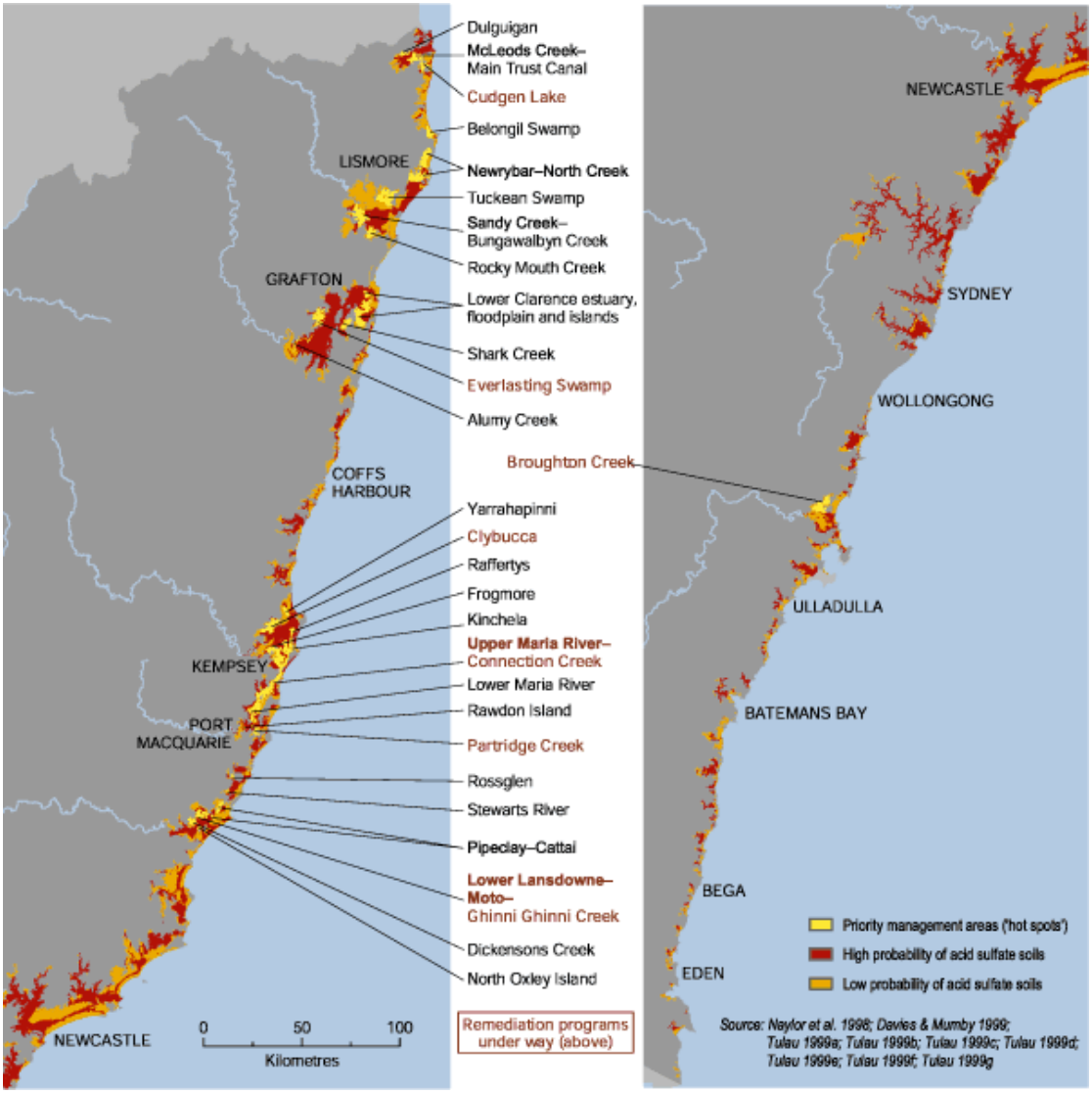

Figure 1.3. Acid sulfate soil hot spots along the NSW coast (Source: EPA 2000).

The inland acid sulfate soils investigated by Sullivan *et al* (2002) in New South Wales and Victoria are associated with irrigation activities. These activities have led to an increase in the sulfate concentrations of the freshwater river environments and water ways. Given sulfate availability is often a limiting factor in sulfate reduction and the formation of sulfides (Berner 1984), an increase in sulfate concentrations may enhance the accumulation of monosulfides and pyrite (Sullivan *et al* 2002).

Impacts of Acid Sulfate Soils

The oxidation of acid sulfate soils produces a plethora of environmental and economic problems. Amongst the most noticeable and publicised of these are fish kills, which may be caused by the formation and mobilisation of monosulfidic black ooze (MBO) which has the potential to rapidly reduce the dissolved oxygen content of the water (Fyfe 2001; Sullivan and Bush 2002; Bush *et al* 2004a, b). They may also result from the release of substantial quantities of acid and heavy metals into the aquatic environment (White *et al* 1993; Corfield 2000).

In additional to fish kills the oxidation of acid sulfate soils may also affect fish health. Repeated flows of acid increase the susceptibility of fish to fungal infections which may lead to diseases such as epizootic ulcerative syndrome, also known as red spot disease (Plate 1.1) (Callinan *et al* 1996). They may also cause reduced hatching, declines in growth rates, bone deformities and egg abnormalities (Leadbitter 1993; Sammut *et al* 1993). The oxidation of acid sulfate soils also affects fish populations indirectly by impacting on food resources, causing habitat degradation and releasing toxic levels of heavy metals, particularly aluminium into the waterways (Plate 1.2) (Sammut *et al* 1995; Russell and Helmke 2002; Powell and Martens 2005; Claff *et al* 2011).

Economic impacts associated with the oxidation of acid sulfate soils include soil toxicity due to the release of acid and heavy metals (Rassam *et al* 2001), low nutrient availability (White and Sammut 1995) and damage to engineering structures (Bloomfield and Coulter 1973; Blunden and Indraratna 2000). The severity and range

of impacts associated with acid sulfate soils suggest that research into their occurrence and remediation should be a management imperative.

Plate 1.1. The effect of 'Red Spot' disease on fish (Source: Sammut and Lines-Kelly 2000).

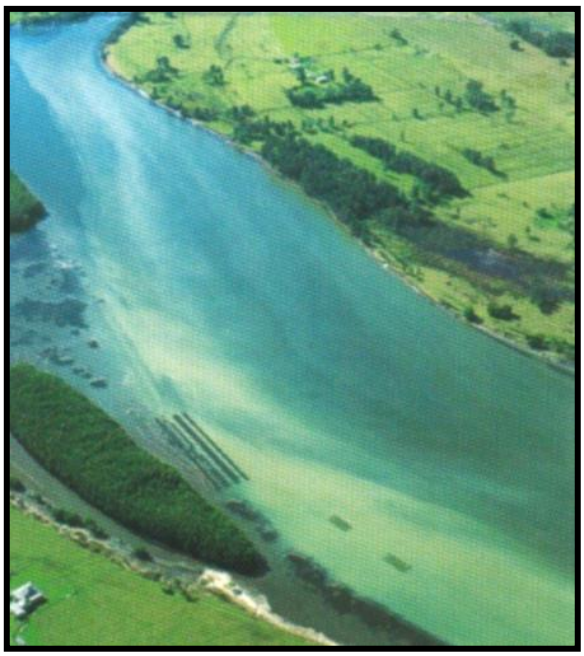

Plate 1.2. Blue-green acid water in the Richmond River indicates aluminium is present in the water (Source: Sammut and Lines Kelly 2000).

Iron Sulfide Minerals

Iron sulfide minerals occur as either monosulfides or disulfides, with the distinction made on the basis of their volatility in non-oxidising acids (Rickard and Morse 2005). Monosulfides or acid volatile sulfur (AVS) species, comprise pore-water sulfides and a suite of metastable iron sulfide minerals such as amorphous sulfides ($FeS_{0.89}$ – $FeS_{0.91}$), mackinawite (tetragonal $FeS_{0.94}$) (Schoonen and Barnes 1991; Wong *et al* 2013), and ferrimagnetic greigite ($FeS_{1.33}$) (Rickard *et al* 1995; Morse and Rickard 2004; Burton *et al* 2006c). Disulfide species include pyrite (cubic FeS_2) and marcasite (orthorhombic FeS_2) (Morse and Cornwell 1987). Pyrite is the most abundant iron sulfide mineral in soils and sediments as it is the most thermodynamically stable (Schoonen and Barnes 1991; Bush and Sullivan 2002; Burton *et al* 2006c; Burton *et al* 2011a, b).

Formation of Iron Sulfide Minerals

According to Melville *et al* (1993) and Goldhaber (2004) the formation of iron sulfides is dependent upon the following specific requirements:

- a continuous supply of sulfate
- generally anaerobic conditions alternating in time and space with limiting aeration
- chemically reducing microbes
- a large supply of metabolisable organic matter
- an adequate supply of iron
- tectonic stability
- the removal of carbonates formed during pyrite production

Formation of Iron Monosulfides

The formation of iron monosulfides begins as iron (III) oxides in the sediment and sulfates in water are bacterially reduced to produce iron (II) ions and dissolved sulfide (H_2S, S^{2-}, HS^-) (Berner 1964, 1970; Dent and Pons 1993; Sammut *et al* 1996b; Valdermarsen *et al* 2009). Such a reaction can only occur under intensely reducing

conditions and is greatly enhanced if significant quantities of organic matter are available to provide the bacteria with an energy source. In saturated sediment, the free oxygen is rapidly consumed and anaerobic bacteria turn to other compounds such as sulfates to act as electron acceptors (Raisewell 1982; Mulvey and Willett 1996). Equation 1.1 represents the reduction of sulfate by bacteria. According to Andrews *et al* (2000) organic matter is commonly represented by the generalised formula for carbohydrate, CH_2O.

$$2CH_2O_{(s)} + SO_4^{2-}{}_{(aq)} \rightarrow H_2S_{(g)} + 2HCO_{3(aq)} \quad \textbf{Equation 1.1}$$

Hydrogen Sulfide Pathway

According to the order of reduction sequence (Mulvey and Willett 1996), iron (III) oxides are reduced before sulfates. This means that soluble ferrous iron (Fe^{2+}) is likely to be present when sulfate is reduced to dissolved sulfide. When the structure of the soil prevents its release, the dissolved sulfide can react with the soluble Fe^{2+} ions to produce insoluble ferrous sulfides. The initial iron sulfide produced is amorphous iron monosulfide (Equation 1.2). This direct precipitation reaction has been termed the 'hydrogen sulfide pathway' by Rickard *et al* (1995).

$$Fe^{2+}{}_{(aq)} + H_2S_{(g)} \rightarrow FeS_{(mono)(s)} + 2H^{+}{}_{(aq)} \quad \textbf{Equation 1.2}$$

The Bisulfide Pathway

Another competing reaction mechanism for the formation of iron monosulfides is the 'bisulfide pathway', which involves the formation of the complex $FeSH^+$ and the solid $Fe(SH)_2$ (Rickard *et al* 1995) (Equation 1.3).

$$Fe^{2+}{}_{(aq)} + 2HS^{-}{}_{(aq)} \rightarrow Fe(SH)_{2(s)} \quad \textbf{Equation 1.3}$$

In the second stage of this reaction, $Fe(SH)_2$ is condensed to FeS with the release of dissolved sulfide back to solution (Equation 1.4).

$$Fe(SH)_{2(s)} \rightarrow FeS_{(mono)(s)} + H_2S_{(aq)} \quad \textbf{Equation 1.4}$$

The dominant mechanism in the formation of iron monosulfides will depend on the total dissolved sulfide concentration, iron concentration, pH and temperature (Rickard *et al* 1995; Burton *et al* 2006d; Boman *et al* 2008; Keene *et al* 2011).

Formation of Pyrite

Monosulfides are unstable minerals and will readily transform to more stable disulfide species (Hunger and Benning 2007; Rickard and Luther 2007). The process by which this occurs has been well researched and several reaction mechanisms have been proposed. The first of these has been dubbed the 'polysulfide pathway' and involves the reaction between iron monosulfides and polysulfides.

The Polysulfide Pathway

The polysulfide pathway was originally proposed by Rickard (1975) and later confirmed and refined by Luther (1991). According to this mechanism the dissolution of FeS (or an $FeSH^+$ complex) produces soluble Fe^{2+} and HS^-. The dissolved sulfide then attacks and reduces the polysulfide ions to produce FeS_2 according to the following reaction (Equation 1.5).

$$Fe^{2+}_{(aq)} + S_5S^{2-}_{(aq)} + HS^-_{(aq)} \rightarrow FeS_{2(s)} + S_4S^{2-}_{(aq)} + H^+_{(aq)} \qquad \textbf{Equation 1.5}$$

Research by Howarth and Teal (1979) suggested pyrite formed rapidly via the direct precipitation of iron and polysulfides. Luther (1991) however, demonstrated that when polysulfides react with Fe^{2+}, the first product produced is FeS, which on further reaction with polysulfides formed a dissolved complex, $[FeSH(S_x)]^-$. This complex then breaks down producing FeS_2 (Rickard *et al* 1995).

Hydrogen Sulfide Pathway

The second mechanism for pyrite formation is termed the 'hydrogen sulfide pathway'. This mechanism, initially demonstrated by Taylor *et al* (1979), involves the reaction of iron (II) monosulfides with H_2S (Equation 1.6).

$$FeS_{(mono)(s)} + H_2S_{(aq)} \rightarrow FeS_{2(aq)} + H_{2(aq)} \qquad \textbf{Equation 1.6}$$

This reaction may be of particular interest to the early evolution of life since the reaction produces a potent reductant, H_2, which is biochemically important. Hydrogen is an important microbial metabolite and its generation may have been significant in early ecosystems (Rickard and Luther 1997).

The Iron Monosulfide Oxidation Pathway

The last reaction mechanism considered to be responsible for pyrite formation has been dubbed the 'iron monosulfide oxidation pathway'. This progressive oxidation mechanism was confirmed by the careful experimental work of Schoonen and Barnes (1991). They found that pyrite or marcasite formed from the increasing sulfidation of the precursor iron monosulfide. In the first instance, amorphous iron monosulfide ($FeS_{0.89} - FeS_{0.91}$) aged to mackinawite ($FeS_{0.94}$). According to Rickard *et al* (1995) the rate of transformation is slow, possibly taking up to 2 years for the complete conversion.

The second stage involved the conversion of mackinawite to greigite ($FeS_{1.33}$). This may occur with the addition of elemental sulfur (Equation 1.7) however Schoonen and Barnes (1991) considered the conversion more likely to take place with aqueous sulfur species such as hydrogen sulfide (Equation 1.8), bisulfide, polysulfides, thiosulfate and polythionates acting as sulfur sources. This reaction only takes place under slightly oxidising conditions.

$$3FeS_{0.94(aq)} + S^0_{(aq)} \rightarrow FeS_{1.33(aq)} \qquad \textbf{Equation 1.7}$$

$$3FeS_{0.94(aq)} + HS^-_{(aq)} + 1/2O_{2(g)} + H^+_{(aq)} \rightarrow FeS_{1.33(s)} + H_2O_{(aq)} \qquad \textbf{Equation 1.8}$$

The final stage in this reaction is the conversion of greigite to pyrite. According to Schoonen and Barnes (1991) this conversion required a major crystallographic reorganisation of both iron and sulfur and the transformation to marcasite was more likely. Marcasite will then change to the stable pyrite through a solid state

transformation (Rickard *et al* 1995). The conversion of greigite to pyrite was also challenged by Burton *et al* (2011a) when it was found the reactants could be spatially decoupled in a soil profile following tidal inundation.

Oxidation of Acid Sulfate Soils

Iron sulfide minerals are generally considered inert while they remain in a chemically reduced state below the water table (Melville and White 2000). Once these minerals are exposed to air by a drop in the water table or otherwise, oxygen enters the soil profile and they begin to oxidise. As pyrite is the most abundant iron sulfide mineral in acid sulfate soil environments it is also the largest source of potential acidity (Burton *et al* 2008; Boman *et al* 2010; Claff *et al* 2011). As the following equation shows, the initial oxidation of one mole of pyrite to produce Fe^{2+} produces 2 moles of acid (Andrews *et al* 2000) (Equation 1.9).

$$2FeS_{2(s)} + 7O_{2(g)} + 2H_2O_{(l)} \rightarrow 2Fe^{2+}{}_{(aq)} + 4SO_4{}^{2-}{}_{(aq)} + 4H^{+}{}_{(aq)}$$ **Equation 1.9**

Fe^{2+} can be transported a considerable distance from the original pyrite source where it can further oxidise to ferric iron (Fe^{3+}) producing iron oxyhydroxide and hydroxide flocs that coat benthic communities and stream banks (Sammut *et al* 1996a; Isaacson *et al* 2009; Burton *et al* 2010). This reaction also produces 2 moles of acid for every mole of Fe^{2+} oxidised (Andrews *et al* 2000) (Equation 1.10).

$$4Fe^{2+}{}_{(aq)} + O_{2(g)} + 10\ H_2O_{(l)} \rightarrow 4Fe(OH)_{3(s)} + 8H^{+}{}_{(aq)}$$ **Equation 1.10**

At neutral or alkaline pH conditions oxygen is the dominate oxidant (Morse 1991) and the rate of pyrite oxidation is relatively slow (Mulvey and Willett 1996). Once the pH falls to less than 4, Fe^{3+} becomes the predominant pyrite oxidant and the rate of oxidation is accelerated by the action of iron-oxidising bacteria such as *Acidithiobacillus ferrooxidans*. These bacteria can accelerate the oxidation of Fe^{2+} by a factor of $>10^6$ (Singer and Stumm 1970). The bacterially catalysed oxidation of

pyrite through the indirect oxidation of Fe^{3+} is described in the Equation 1.11 (Dent 1986).

$$FeS_{2(s)} + 14Fe^{3+}_{(aq)} + 8H_2O_{(l)} \rightarrow 15Fe^{2+}_{(aq)} + 2SO_4^{2-}{}_{(aq)} + 16H^{+}_{(aq)} \quad \textbf{Equation 1.11}$$

Contemporary Pyrite Formation

The oxidation of acid sulfate soils should not be considered a one-way process. In many acid sulfate soil landscapes, a change in conditions may allow the products of oxidation to be reformed into sulfides (Johnston *et al* 2009b; Keene *et al* 2010, 2011; Burton *et al* 2011a). Where sulfides have reformed in the past 20 years they are considered contemporary in nature. As an example, Rosicky *et al* (2002a, b) found pyrite reforming on the surface of acid sulfate soil scalds. In addition, Bolton *et al* (2002a) while working on an effluent reuse project at Byron Bay, northern New South Wales, Australia, found surface reformation after long term treatment with effluent. There is also extensive research regarding the contemporary formation and accumulation of monosulfides in drainage channels (Sullivan and Bush 2002; Bush *et al* 2004a, b; Smith and Melville 2004; Burton *et al* 2006c; Morgan *et al* 2012c). Recently, considerable contemporary sulfide accumulations have occurred following remediation with tidal inundation on a degraded acid sulfate soil landscape in northern Queensland, Australia (Johnston *et al* 2009b; Keene *et al* 2010, 2011; Burton *et al* 2011a).

Contemporary sulfide formation is a concern for managers of acid sulfate soils, particularly where it occurs at the surface. The surface portion of a soil profile is highly dynamic, affected by seasonal variations in water table height and rapidly changing environmental conditions. Where a slight change in conditions allows sulfides to reform, a similar change may allow them to begin oxidising again. Contemporary sulfide formations have also been identified at the oxidation boundary of an acid sulfate soil profile. Bush (2000) found evidence of pyrite reformation using sulfur isotope ratios, a technique that has received little attention in acid sulfate soil research.

Isotopes

Isotopes are atoms of a given element that differ in the number of neutrons and therefore, have different masses. The symbol $^{12}_{6}C$ or simply ^{12}C (read 'carbon twelve') represents the carbon atom with six protons and six neutrons. The number of protons, which is called the atomic number, is shown by the subscript. Since all atoms of a given element have the same atomic number, the subscript is often omitted. The superscript is called the mass number; it is the total number of protons plus neutrons in the atom. For example, some carbon atoms contain six protons and eight neutrons and are represented as ^{14}C. The percentage of an isotope in a naturally occurring sample of an element is known as the percentage abundance of that isotope (Brown *et al* 2000).

Isotopes may be either stable or radioactive. Stable isotopes do not decay through radioactive processes over time, whereas radioactive isotopes have limited life times and undergo a decay to form a different element. As an example, carbon has two stable isotopes (^{12}C and ^{13}C) and six radioactive isotopes (^{9}C, ^{10}C, ^{11}C, ^{14}C, ^{15}C and ^{16}C) (Ehleringer and Cerling 2002).

Measuring and Reporting Stable Isotopes

Stable isotopes can be measured using a Gas Isotope Ratio Mass Spectrometer (Werner and Brand 2001; Rickard 2012). The mass spectrometer consists of a source to ionize the gas, a flight tube with a magnet to deflect the path of the ionised gas and a detector system at the end of the flight tube to measure the different isotopic species. In the first instance the element of interest must be converted to a gas for introduction into the mass spectrometer. As it is introduced the gas is ionised by removal of an electron as the gas is bombarded by a source. As the gas then travels down the flight tube (under vacuum), the paths of light and heavy isotopic species are deflected differently by a magnet. Detectors positioned at the end of the flight tube measure the abundance ratios of the heavy and light isotopic species (Ehleringer and Cerling 2002).

Stable isotope abundances are expressed as the ratio (R) of the two most abundant isotopes in the sample compared to the same ratio in an international standard. Results are typically presented in delta notation (δ) (Equation 1.12).

$$\delta = (R_{sample} / R_{standard} - 1) \times 1000 \qquad \textbf{Equation 1.12}$$

Since the differences in ratios between the sample and standard are relatively small, they are expressed as parts per thousand (‰) deviations from the standard (Andrews *et al* 2000; Johnston 2011; Rickard 2012).

Natural Variations in Stable Isotopes

Given that isotopes of the same element have an identical number of electrons they interact with other elements in much the same way. The difference in mass attributable to the neutrons however, may result in fractionation during chemical, physical or biological processes (Emery and Robinson 1993; Brownlow 1996). Fractionation of stable isotopes occurs because the strength of the chemical bonds varies slightly with the mass of the isotope (Brownlow 1996; Hatzinger *et al* 2012). In general, the light isotope forms weaker bonds than the heavier isotope, requiring less energy to break the molecule in a chemical reaction (Emery and Robinson 1993; McConville *et al* 2000). This gives rise to the three types of isotopic fractionation seen in natural systems:

1. equilibrium isotope effects – controlled by the differing thermodynamic properties of each isotope;
2. vital or biological isotope effects – observed in certain organisms which produce mineral skeletons which are out of isotopic equilibrium with the water from which they form;
3. kinetic isotope effects – arise because the lighter isotope reacts more rapidly than the heavier isotope (Emery and Robinson 1993; Habicht and Canfield 1997)

Sulfur Isotopes

Sulfur has four stable isotopes and numerous radioactive isotopes. Table 1.1 shows the stable isotopes of sulfur and their percentage abundances. The international standard for the detection of sulfur is the Vienna Canon Diablo Triolite (VCDT). The original Canon Diablo Triolite (CDT) was prepared from the FeS phase of a large iron meteorite found at Meteor Crater, Arizona (Werner and Brand 2001). It was revealed however, that CDT was not sufficiently homogenous to continue as the primary reference material and was consequently replaced with VCDT, whose generally accepted ratio of $^{34}S/^{32}S$ is 0.044151. Since the standard is defined as 0 ‰, samples enriched in ^{34}S (i.e. ratios of $^{34}S/^{32}S$ that are greater than 0.044151) will have positive delta values and samples depleted in ^{34}S (i.e. those with ratios of $^{34}S/^{32}S$ that are less than 0.044151) will have negative delta values (Bottrell *et al* 1994). More recently, a silver sulfide standard IAEA-S-1 with an assigned value of -0.3 ‰ has also been introduced (Hoefs 2009; Rickard 2012).

Table 1.1. Isotopes of sulfur and their percentage abundances (Andrews *et al* 2000; Berglund and Wieser 2011).

Isotope	Protons	Electrons	Neutrons	% Abundance
^{32}S	16	16	16	94.99
^{33}S	16	16	17	0.75
^{34}S	16	16	18	4.25
^{36}S	16	16	20	0.01

Fractionation of Sulfur Isotopes

The process of bacterial sulfate reduction is an example of kinetic fractionation and the major cause for the natural variation in the isotopic composition of sulfur (Bottcher *et al* 1998; Wijsman *et al* 2001; Farquhar *et al* 2008; Stam *et al* 2011). Sulfate reducing bacteria use the reduction of sulfate ion to hydrogen sulfide for their metabolism. Fractionation occurs because the rate at which $^{34}SO_4^{2-}$ goes to $H_2{}^{34}S$ is significantly slower than the rate at which $^{32}SO_4^{2-}$ goes to $H_2{}^{32}S$. Thus the result is light sulfide and heavy sulfate (Brownlow 1996; Wijsman *et al* 2001; Hatzinger *et al*

2012). The fractionation patterns in the sulfur cycle due to biological processes are shown in Figure 1.4.

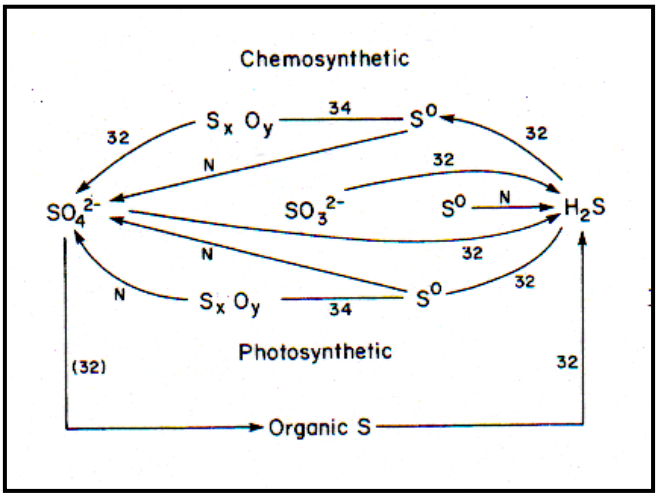

Figure 1.4. Fractionation patterns in the sulfur cycle due to biological processes. The isotope enrichment is indicated in the final and intermediate products. No fractionation is designated by N (Goldhaber and Kaplan 1974).

The reduction of sulfate through dissimilatory processes can be summarised in the following four steps (Figure 1.5), although the actual pathway may be more complicated and might vary between bacterial species (Goldhaber and Kaplan 1974; Widdel and Hansen 1992; Farquhar *et al* 2007).

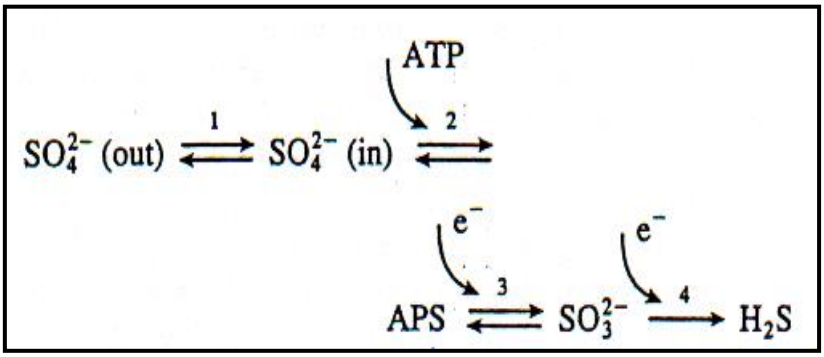

Figure 1.5. Steps in the reduction of sulfate to sulfide where fractionation may occur (Habicht and Canfield 1997).

There are several steps in this process where fractionation may occur. During step 1, the uptake of sulfate by bacteria, low or even positive fractionation values (3 ‰) may occur. The second step, the reaction of sulfate with ATP (adenosine triphosphate) to

form APS (adenosine-5'-phosphosulfate) proceeds without fractionation. Step 3, the reduction of APS to sulfite, and step 4, the reduction of sulfite to sulfide, may both produce a fractionation of 25 ‰ due to the splitting of S-O bonds. No fractionation is assumed during the backward reactions of steps 1, 2, and 3 (Habicht and Canfield 1997; Bradley *et al* 2011).

The overall isotope effect is the sum of the kinetic isotope effects from each step until the rate-limiting reaction is reached. The degree of isotope fractionation therefore, may depend on which step in the sulfate reduction pathway is rate-limiting (Rees 1973). Factors that affect fractionations include specific rates of sulfate reduction, sulfate concentration, substrates and depositional environment, temperature, pH, bacterial species and growth conditions (Habicht and Canfield 1997; McConville *et al* 2000).

The distribution and fractionation of sulfur isotopes makes them an ideal tool in many scientific investigations. Sulfur isotopes have been used to obtain information about Earths geological history (Scheiderich *et al* 2010; Johnston 2011; Berndmeyer *et al* 2012; Jones and Fike 2013), to understand microbial processes in sulfur cycling (Bradley *et al* 2011; Eckert *et al* 2011; Drake *et al* 2013) and to identify sulfate sources (Mayer *et al* 2010; Kilmister and Cartwright 2011) and assess groundwater contamination (Knoller *et al* 2005; Knoller and Schubert 2010; Wu *et al* 2011; Hartzinger *et al* 2012) in hydrological studies (Farquhar *et al* 2010; Johnston 2011; Rickard 2012).

Sulfur isotopes have also been used extensively in the study of sulfide ore deposits. Deposits that have similar $\delta^{34}S$ values throughout, probably formed from homogenous solutions, the source of which may also be identified. Sulfur brought to the crust from the mantle would probably be lighter than biogenic sulfur mobilised from a sedimentary rock while sulfur deposited at high temperatures should show less fractionation between minerals than that deposited at low temperatures (Drake *et al* 2013; Sahlstedt *et al* 2013). In general, deposits associated with igneous rocks display a narrow range of $\delta^{34}S$ values that are close to zero. Other deposits formed as a result of metamorphism, sedimentation, or groundwater activity usually show a wider range

of $\delta^{34}S$ values for a particular deposit (Sahlstedt *et al* 2013). For some deposits, the composition of the mineralising solutions was found to have changed with time, as indicated by regularly changing $\delta^{34}S$ values found in samples with known age relationships (Brownlow 1996).

Mazumdar *et al* (2012) examined diagenetic and paleoclimatic processes of Holocene sediments using sulfur isotopes in combination with reactive iron profiles. Their study showed diagenetic partitioning of sulfide into iron sulfide (pyrite) and organosulfur phases. Low $\delta^{34}S$ signatures in the pyrite phase corresponded with high pyrite concentrations indicating early diagenetic pyritization near the sediment water interface. Conversely, high $\delta^{34}S$ signatures combined with low pyrite concentrations was attributed to dominance of less or slowly reactive iron bearing minerals that resulted in late diagenetic pyritization (Mazumdar *et al* 2012).

Zhu *et al* (2013) also used sulfur isotopes to examine the formation and burial of pyrite and organic sulfur in mud sediments. Their study found low concentrations of acid volatile sulfur and pyrite which was attributed to sulfate reduction rates being limited by the availability of labile organic matter. A study by Stam *et al* (2011) also found sulfate reduction rates may be linked to organic matter availability and can also be affected by temperature and depth. Microbial sulfate reduction has also been studied by Bradley *et al* (2011) and Eckert *et al* (2011) in greater detail.

A study by Knoller *et al* (2005) examined the source of sulfate in drinking water using sulfur isotopes. Their study identified three anthropogenic sources of sulfate including atmospheric sulfate, inorganic fertilizers and the dissolution of gypsum. These sources overlapped in their isotope signature and could not be individually distinguished. Sulfate from the oxidation of sedimentary sulfides however could be readily recognised by its negative isotope signature (Knoller *et al* 2005).

A similar approach was employed by Mayer *et al* (2010) to identify sulfate in stream water in a catchment in Vermont, USA. Using sulfur isotopes in combination with hydrological and chemical approaches, their study indicated that the source of sulfate was related to changing hydrological conditions. During a wet period the sulfate

isotope values decreased by 13‰, indicating the presence of sulfates derived from the oxidation of secondary sulfides (Mayer *et al* 2010).

Studies by Knoller and Schubert (2010) and Hatzinger *et al* (2012) employed sulfur isotopes to examine sulfur cycling and biodegradation in contaminated groundwaters. Sulfur cycling was also examined by Wu *et al* (2011) in a wetland constructed to treat contaminated groundwater. In other hydrological studies Kamyshny *et al* (2011) examined sulfur cycling and the role of bacterial sulfate reduction in the water column of a stratified sea water lake. In addition to examining a range of dissolved sulfur species, their study employed all four of the stable sulfur isotopes (i.e. ^{32}S, ^{33}S, ^{34}S, and ^{36}S) (Kamyshny *et al* 2011).

Quadruple sulfur isotope studies were also utilised by Scheiderich *et al* (2010) and Johnston (2011) to examine biogeochemical processes and Earths surface evolution. Other recent techniques such as secondary ion mass spectrometry (SIMS) are being used to supplement conventional bulk-grain analysis and provide *in situ* sulfur isotope values on individual sulfide grains (Drake *et al* 2013; Sahlstedt *et al* 2013).

Sulfur Isotopes in Acid Sulfate Soils

Despite the regular adoption of isotopic studies in many related fields, they have received little attention in acid sulfate soil research. In 1992, Dowuona *et al* used sulfur and oxygen isotope data to determine the origin of soluble sulfate salts in Canada and the USA. Their study found a strong relationship between the $\delta^{34}S$ of the sulfide and sulfate fractions at each of the sites examined and concluded that pyrite oxidation was the dominant mechanism for the source of sulfate salts.

Dowuona *et al* (1992) also found the hydrolysis of jarosite was another contributing source of soluble sulfate. Similarities between the $\delta^{34}S$ of pyrite and jarosite indicated pyrite oxidised to jarosite in situ without major fractionation. From this they concluded that by knowing the $\delta^{34}S$ of jarosite, the isotopic composition of the pyrite from which it formed could be inferred.

Astrom and Spiro (2000) examined the isotope signature of dissolved sulfate in 40 first and second order streams during a high flow event in mid-western Finland. Their study gave two populations of $\delta^{34}S_{(sulfate)}$ values with medians of -6.2 and +3.2 ‰. The first of these populations they attributed to the oxidation and mobilisation of ^{32}S enriched sulfides in the acid sulfate soils.

The second more positive population, Astrom and Spiro (2000) associated with secondary sulfide formation processes. The oxidation of isotopically negative sulfides produces sulfates that are also isotopically negative. When conditions are favourable, bacteria will preferentially reduce $^{32}SO_4^{2-}$ which is reprecipitated as sulfides. The removal of light sulfate by this process results in an abundance of isotopically heavy sulfate in the soil profile.

A similar conclusion was reached by Bush (2000) by examining the greater enrichment of ^{32}S in the sulfide fraction. By combining SEM analysis with sulfur isotope studies Bush (2000) confirmed secondary sulfide formation at the oxidation boundary of an acid sulfate soil in northern NSW. That study however, did not show a change in the $\delta^{34}S$ of the sulfate fraction.

Backlund *et al* (2005) developed an analytical procedure for the determination of sulfur species in acid sulfate soils. They tested the procedure by examining the sulfur isotope signature of various sulfur fractions at a site in western Finland. $\delta^{34}S$ of the sulfide fractions were positive and ranged from +5.1 to +5.6 ‰. Organic sulfur was slightly lower with an average of +4.1 ‰. Backlund *et al* (2005) determined that the organic sulfur originated from assimilatory sulfate reduction which results in the $\delta^{34}S$ being similar to $\delta^{34}S$ of the sulfate in the growth medium. In combination with the $\delta^{34}S$ of the sulfide fraction, the researchers were able to establish that the acid sulfate soils were deposited in a freshwater environment.

In a study examining contemporary pedogenesis Johnston *et al* (2009b) used sulfur isotopes to identify the depth to which tidal inundation was impacting on an acid sulfate soil profile and consuming acidity. Their study found that prior to tidal inundation the $\delta^{34}S$ of the soluble sulfate fraction was similar to the $\delta^{34}S$ of the sulfide

fraction indicating the primary source of sulfate was the oxidation of pyrite. Following tidal inundation there was a shift in the $\delta^{34}S$ of the sulfate fraction which reflected the input of isotopically heavier marine sulfate. This trend was only evidenced in the sulfuric horizons which indicated the tidal water was not reaching the underlying sulfidic materials.

A recent study by Kilminster and Cartwright (2011) used sulfur isotopes in dissolved sulfate as a screening tool for assessing the impact of acid sulfate soils in Western Australia. An indicator was developed based on $\delta^{34}S$ and chloride and sulfate concentrations that categorised samples into groups with similar isotopic influences (iso-groups). Signals of disturbed acid sulfate soils were identified in <5% of the sites examined but statistical analysis showed water quality had deteriorated at those sites. Their study suggested the $\delta^{34}S$ values could be used to provide an early warning indicator for water affected by disturbed acid sulfate soils.

Many factors can contribute to changes in the sulfur isotope signature. In particular sulfate concentration, sulfate reduction rates, substrates and depositional environment, and pH (Habicht and Canfield 1997; McConville *et al* 2000; Mazumdar *et al* 2007; Stam *et al* 2011) are likely to be an influence in acid sulfate soils. The purpose of this research is to expand the current knowledge base for the application of sulfur isotopes in acid sulfate soils.

Aim

The overall aim of this thesis is to examine the use of stable sulfur isotopes to understand the geochemical processes occurring in a range of acid sulfate soil environments.

Objectives

The specific objectives of this thesis are:

To establish a baseline for the use of stable sulfur isotopes in acid sulfate soils by examining the isotope signature of samples from different acid sulfate soil environments (Chapter 2).

To examine the use of sulfur isotope ratios in understanding the geochemical processes operating in acid sulfate soils subject to remediation by lime assisted tidal exchange (Chapter 3).

To examine the use of stable sulfur isotopes in water to identify sites where acid sulfate soils may be oxidising and discharging acidity into waterways (Chapter 4).

To examine the use of sulfur isotope signatures to help understand the cycling between the sulfide and sulfate fractions of acid sulfate soil materials as they are being deposited (Chapter 5).

Chapter 2

Stable sulfur isotopes in acid sulfate soils: Baseline studies for south-eastern Australia

Introduction

Acid sulfate soil is the term used to describe soils or sediments that contain sulfide minerals (particularly pyrite) or the products of sulfide oxidation (Melville and White 2000; Sullivan *et al* 2001). Acid sulfate soils affect significant portions of the Australian coastline (Sammut *et al* 1996a), particularly in New South Wales (Johnston *et al* 2003a; Burton *et al* 2006c; Claff *et al* 2011), Queensland (Russell and Helmke 2002; Powell and Martens 2005; Johnston *et al* 2011a, b) and Western Australia (Kilmister and Cartwright 2011; Morgan *et al* 2012a, b). The majority of acid sulfate soils occur in coastal embayments and estuaries where wave action is limited and sedimentation occurs (Yang 1997). Although the formation of pyrite continues today in estuarine environments, the majority of acid sulfate soils formed during the last sea level rise between 6000 and 10000 years ago (Powell and Martens 2005). As the sea level rose it created a new coastline which was colonised by mangroves. This provided a source of organic matter that led to sulfate reduction and sulfide mineral formation and accumulation (Naylor *et al* 1998; Bouillon *et al* 2008; Fan *et al* 2012). Former mangrove forests extended in around 20 to 30 km from the current coastline, however a drop in sea level followed by terrestrial sedimentation has meant many of the sulfide accumulations have since been buried (Ferguson and Eyre 1996).

Acid sulfate soils formed during the last sea level rise are typically dark grey, gel-like clays. They often contain remnants of decomposed organic matter and have a near-neutral pH (Smith *et al* 2004; Powell and Martens 2005). Such soils are termed coastal clayey acid sulfate soils in this chapter. Samples of these soils were collected from Kempsey, McLeods Creek, Shark Creek and the Tuckean Swamp.

Following the drop in sea level many coastal backswamp areas became influenced by freshwater runoff which created shallow water environments where peat sediments could accumulate (Bush *et al* 2002a). Peat soils are dominated by slowly decomposing plant material (Anderson *et al* 2013) and are another common soil type in acid sulfate soil landscapes (Allery 2002). Peat acid sulfate soils differ from clayey

acid sulfate soils in that they are generally acidic (pH <5.5), have a large buffering capacity and high permeability. Coastal peats may contain either fresh or brackish water depending on the amount of freshwater runoff and the degree of isolation from tidal water (Dellwig *et al* 2002). Coastal peat acid sulfate soils studied in this chapter were collected from Byron Bay, Boggy Creek and Bora Codrington.

Another common environment for the formation of iron sulfides is in drainage channels associated with acid sulfate soil landscapes (Fyfe 2001; Sullivan *et al* 2002; Burton *et al* 2009). In these drainage channels sediments referred to as monosulfidic black oozes (MBO) accumulate in large quantities (Sullivan and Bush 2001; Bush *et al* 2004a, b). These sediments contain very high concentrations of iron monosulfides which are highly reactive and can oxidise rapidly (Smith 2004). They are also extremely gel-like with up to 90% water content and can cause a significant drop in dissolved oxygen in the water column when disturbed (Sullivan and Bush 2000, 2001; Fyfe 2001; Sullivan *et al* 2002).

Iron monosulfides are considered a necessary precursor for the formation of pyrite (Berner 1984; Burton *et al* 2006c). However in many drainage channels associated with acid sulfate soils, the abundance of reduced iron in relation to sulfate means monosulfides form in preference to pyrite (Rickard *et al* 1995; Mulvey and Willett 1996; Burton *et al* 2006a, b; Keene *et al* 2010, 2011; Johnston *et al* 2011b). MBO accumulates in drainage channels during periods of low flow, however they are readily mobilised during flood events and have been linked to significant fish kills in northern New South Wales (Sullivan and Bush 2002; Smith 2004). Coastal MBO samples were collected from drains at Boggy Creek and the Tuckean Swamp.

Iron sulfide minerals in the form of monsulfides and pyrite have been found in many inland areas of New South Wales, South Australia and Victoria (Fitzpatrick *et al* 1993; Isaacson *et al* 2009). Inland acid sulfate soils are associated with the increasing salinisation that is causing severe degradation across Australia. In South Australia, inland acid sulfate soils are associated with dryland salinity, often caused by the replacement of native vegetation with annual pastures and crops. These crops cannot utilise enough of the rainfall resulting in increased recharge to groundwater and

higher water tables. This brings salts in the soil closer to the surface thereby providing a source of sulfate for the formation of iron sulfides (Fitzpatrick *et al* 1993; Peck 1993).

In New South Wales and Victoria, inland acid sulfate soils are linked to irrigation activities. Irrigation has led to an increase in sulfate concentrations in the freshwater rivers and water ways. This provides a source of sulfate and leads to the formation of iron sulfides (Sullivan *et al* 2002). One of the principle differences between coastal and inland acid sulfate soil environments is the ratio of monosulfide to pyrite formation. In a study by Maher (2005), monosulfide:pyrite ratios ranged from 0.001 to 0.354 for coastal acid sulfate soil with the highest value recorded at the surface of a remediated acid sulfate soil scald. Gagnon *et al* (1995) considered a monosulfide:pyrite ratios of between 0.3 and 1.6 to be relatively high. Five of the inland sites recorded values within this range but at Leonards Lane the ratio was over double the upper value. In inland environments the very low sulfate concentrations associated with predominately fresh water means sulfate supply limits the formation of pyrite and allows the accumulation of monosulfides relative to disulfides such as pyrite (Boman *et al* 2008; Isaacson *et al* 2009; Morgan *et al* 2012c). Inland MBO samples were collected from New South Wales in the Murrumbidgee Irrigation Area (Calabria Road, Leonards Lane), in central New South Wales on the Talbragar River near Dubbo (Boomley), in the Hunter Valley of New South Wales (Widden) and in northern central Victoria in the Loddon River Basin (Piccaninny Creek and Barr Creek).

The environment that existed when acid sulfate soils formed is often imprinted on their geochemical properties. For example, the production of organic acids often gives peat acid sulfate soils a naturally lower pH than clay sediments (Dent 1986). In addition, the sulfate and iron concentration can determine the species and relative abundance of the iron sulfide minerals that form (Rickard *et al* 1995; Mulvey and Willett 1996; Tulau 2000; Burton *et al* 2006a, b; Keene *et al* 2010, 2011; Johnston *et al* 2011b). This affects the stability of the sulfides given that monosulfides are far more reactive than disulfide species (Sullivan *et al* 2002; Burton *et al* 2006b; Burton *et al* 2011a, b).

The formation and oxidation of acid sulfate soils can be further understood using stable sulfur isotopes. Sulfur isotopes have been used as tracers of sources, mixing processes and transformations of sulfur compounds (Stam *et al* 2011), to determine the formation environment of sulfide ores, differentiate between mantle sulfur and sedimentary sulfur and separate high and low temperature sulfur deposits (Brownlow 1996; Canfield 2004). The natural variation and fractionation of stable sulfur isotopes has made them an ideal tool in many geochemical studies (Bottcher *et al* 1998; Bottcher and Lepland 2000; Wijsman *et al* 2001; Mazumdar *et al* 2007; Mayer *et al* 2010).

Fractionation of stable isotopes occurs because the strength of the chemical bonds varies slightly with the mass of the isotope. In general, the light isotope forms weaker bonds than the heavier isotope, requiring less energy to break the molecule in a chemical reaction. The principle reaction in the formation of acid sulfate soils is the reduction of sulfate to produce H_2S (Dent and Pons 1993; Sammut *et al* 1996b; Burton *et al* 2011a, b). This bacterially mediated process results in kinetic fractionation because the rate at which $^{34}SO_4^{2-}$ goes to $H_2{}^{34}S$ is significantly slower than the rate at which $^{32}SO_4^{2-}$ goes to $H_2{}^{32}S$. Thus the result of such fractionation is lighter sulfide and heavier sulfate (Brownlow 1996).

Some of the factors that affect the degree of fractionation include sulfate concentration, sulfate reduction rates, substrates and depositional environment, temperature, pH, bacteria species and growth conditions (Habicht and Canfield 1997; McConville *et al* 2000; Farquhar *et al* 2007; Stam *et al* 2011). Many of these factors are likely to vary under the different acid sulfate soil formation environments that have been identified. This suggests stable sulfur isotopes may provide valuable insights into the geochemistry of acid sulfate soils and acid sulfate soil landscapes.

Aim

The aim of this chapter is to establish a baseline to examine stable sulfur isotopes in acid sulfate soils in south-eastern Australia. This study will also relate any observed

changes in the sulfur isotope signatures to different processes occurring in acid sulfate soil environments. These include coastal clay and peat dominated sediments, coastal monosulfidic black oozes and inland acid sulfate soils. In this study the term baseline is used to refer to the first or preliminary investigation into the use of sulfur isotopes in a range of acid sulfate soil environments.

Methodology

Sample collection and preparation

Sediments analysed for this study were collected from a variety of locations representing both coastal and inland acid sulfate soil environments. The sites were selected to allow a comparison between contemporary and ancient sediments as well as different environments during formation. The coastal sites included 7 acid sulfate soil sites (4 clay dominated and 3 peat dominated) and 2 monosulfidic black ooze samples from drainage channels (Figure 2.1a). Inland samples consisted of monosulfidic black ooze from 6 sites (Figure 2.1b).

Figure 2.1a. Google Earth image showing coastal acid sulfate soil sampling sites. Coastal MBO samples were also collected from Boggy Creek and the Tuckean Swamp.

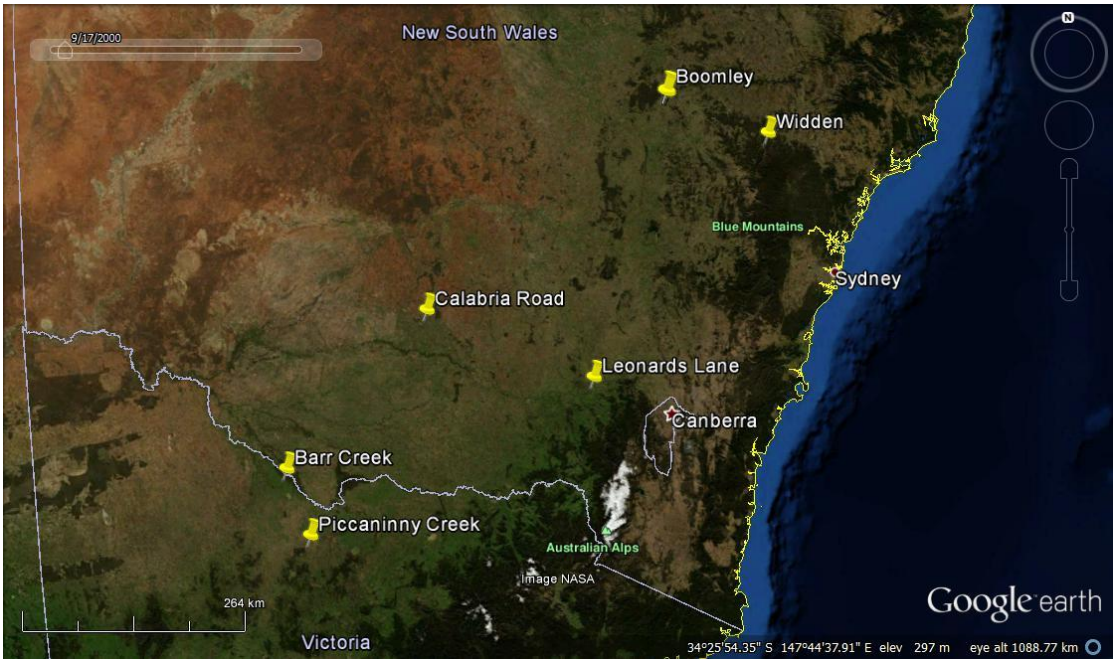

Figure 2.1b. Google Earth image showing inland acid sulfate soil sampling sites.

Coastal sediment samples were collected using a Russian D-Section corer. At each site 2–3 replicate cores were taken and cut into depth increments. Replicate increments were combined in thick plastic bags to form a homogenous composite. Bags were sealed and stored on ice for transport to the laboratory and then frozen.

Coastal MBO samples were collected with a sleeve corer to maintain the stratigraphy of the profiles. As with the sediment samples, replicate cores were taken and stored on ice for transport to the laboratory. At the laboratory the cores were placed in the freezer for approximately 3 hours to 'firm up' slightly without freezing through. They were then cut into depth increments and replicate sub-samples combined to form a composite of each depth. The composites were then returned to the freezer.

Surface accumulations of MBO were collected from the inland sites and placed in sealed plastic containers, purged with nitrogen, then stored on ice for transport to the laboratory. At the laboratory, the outer oxidised portion was removed and the remainder frozen. All analyses were conducted at Southern Cross University unless otherwise stated.

Background soil characteristics

Moisture content

Prior to freezing, a small amount of each sample was weighed for gravimetric moisture content determination (θg). These samples were placed in a fan-forced oven and dried at 105 °C for seven days, then reweighed (Rayment and Lloyd 2011). The moisture content of the soils dried to 65 °C for total carbon analysis was determined in the same manner. Where applicable results are calculated on an oven dried mass.

pH & electrical conductivity

pH was measured in a 1:5 soil:water suspension. For each depth increment, 6.00 g of frozen soil was placed in a centrifuge tube with 30 mL of Milli-Q water. The mixture was shaken for 1 hour then allowed to settle for 15 minutes. pH readings were taken using a calibrated Ionode IJ44 pH electrode. EC readings were also taken from the suspension using a calibrated TPS Conductivity Sensor.

Total carbon

For total carbon analyses, previously frozen soil was dried for 48 hours at 65 °C. The soil was then finely ground with a mortar and pestle. Total carbon analyses were conducted by LECO^{TM} CNS 2000 induction furnace analyser. The detection limit is 0.01%.

Water soluble sulfate

Water soluble sulfate was extracted in a 1:10 soil:water suspension. In accordance with recommendations by Maher *et al* (2004) analyses were conducted on frozen soil. The samples were shaken for 1 hour and centrifuged for 5 minutes at 3000 rpm. The supernatant was extracted and filtered through a 0.45 µm filter and analysed by Inductively Coupled Plasma Optical Emission Spectrometry (ICP-OES). Duplicate analysis gave a precision of ±8% with a detection limit of 0.05 mg/L.

Acid volatile sulfur

Acid volatile sulfur (AVS) was determined using the procedure adopted by the Acid Sulfate Soil Laboratory Methods Guidelines (Ahern *et al* 2004). Approximately 10 g of frozen soil or 5 g of frozen ooze was weighed into a 200 mL conical flask. A vial containing 15 mL of 20% zinc acetate trapping solution was gently placed in the flask. To the flask, 2 mL of ascorbic acid was added and the stopper loosely fitted. The flask was then purged with nitrogen gas for approximately 30 seconds. With the stopper firmly in place, a syringe was used to insert 15 mL of either 6 M HCl for soil samples or 9 M HCl for ooze samples. The flasks were then left for 24 hours to react.

After 24 hours, the stopper was opened and the vial containing the trapping solution carefully removed. The contents of the vial were placed in a 100 mL Erlenmeyer flask. Approximately 1 mL of starch indicator and 15 mL of 6 M HCl was added. The solution was then titrated with iodine on a magnetic stirrer to a permanent blue end point. The molarity of the iodine solution was checked daily and a blank of the zinc acetate was titrated at the beginning of each sampling session. The amount of iodine used to titrate the blank and the samples was used to calculate the AVS content using the following formula:

$$\textbf{AVS (\%S)} = \frac{\textbf{(A – B) x C x 1600}}{\textbf{Mass of soil (mg)}} \qquad \textbf{Equation 2.1}$$

Where:

A = the volume of iodine (mL) used to titrate the soil sample

B = the volume of iodine (mL) used to titrate the blank

C = the molarity of the iodine solution as determined by titration of this solution with standardised 0.025 M sodium thiosulfate solution

$$C = \frac{0.025 \text{ x titration volume of standard thiosulfate solution (mL)}}{\text{Volume of iodine solution titrated (mL)}}$$

Duplicate analysis gave a precision of ±8% with a detection limit of 0.001 %S

Chromium reducible sulfur

In accordance with recommendations by Maher *et al* (2004), chromium reducible sulfur (CRS) analyses were performed on frozen soil using the method of Sullivan *et al* (2000). At the commencement of each sampling session a blank of chromium metal was completed as well as a daily check of the molarity of the iodine solution.

According to this method frozen soil was weighed into a reaction vessel. 2.059 g of chromium metal powder and 10 mL of ethanol (95% concentration) were added. The flask was swirled to wet the sample then placed on the heating mantle and connected to the condenser. A Pasteur pipette was attached to the outlet tube at the top of the condenser and inserted into a 100 mL Erlenmeyer flask containing 40 mL of zinc acetate trapping solution. The nitrogen gas flow rate was adjusted to obtain a bubble rate in the zinc acetate of approximately 3 bubbles per second, then the system was allowed to purge for approximately 3 minutes before 60 mL of 5.65 M HCl was added. The system was purged for an additional 2 minutes then the solution was brought to the boil and allowed to digest for 20 minutes.

At the completion of the digest the Erlenmeyer flask was removed and any zinc sulfide on the Pasteur pipette washed into the flask with Milli-Q water. To the flask, 1 mL of starch indicator solution and 20 mL of 5.65 M HCl were added and gently stirred on a magnetic stirrer. The trapping solution was titrated with iodine to a permanent blue endpoint. The concentration of CRS was then calculated as follows:

$$\textbf{CRS (\%S)} = \frac{\textbf{(A – B) x C x 1600}}{\textbf{Mass of soil (mg)}} \qquad \textbf{Equation 2.2}$$

Where:

A = the volume of iodine (mL) used to titrate the soil sample

B = the volume of iodine (mL) used to titrate the blank

C = the molarity of the iodine solution as determined by titration of this solution with standardised 0.025 M sodium thiosulfate solution

$$C = \frac{0.025 \text{ x titration volume of standard thiosulfate solution (mL)}}{\text{Volume of iodine solution titrated (mL)}}$$

Duplicate analysis gave a precision of ±9% with a detection limit of 0.001 %S.

Isotope analysis

Sulfur isotope analyses were conducted on the AVS, CRS and soluble sulfate fractions of selected samples. To extract the sulfide fractions, additional AVS and CRS runs were performed. The trapping solutions were vacuum filtered through a 0.45 µm cellulose acetate filter, rinsed repeatedly with Milli-Q water then allowed to air dry.

The soluble sulfate fraction was extracted for isotope analysis by shaking a 1:5 soil:water suspension for 1 hour. Care was taken throughout the extraction procedure to limit the oxygen exposure. The Milli-Q water used in the suspension was deoxygenated by purging with nitrogen for 30 minutes prior to use and the centrifuge tubes were completely filled with water then capped to prevent oxygen being incorporated into the solution. The suspension was centrifuged then filtered through a 0.45 µm syringe filter into a solution of 1 M barium chloride, precipitating the sulfate as barium sulfate. The precipitate was rinsed several times with Milli-Q water then oven dried.

Extracted sulfides and sulfates were submitted to the Environmental Isotope Laboratory, Sydney, Australia. Barium sulfate (mixed with vanadium pentoxide) and zinc sulfide precipitates were combusted in a tin cup using a Roboprep Elemental Analyser (EA) attached to a Finnigan 252 Mass Spectrometer (MS). Samples were analysed relative to an internal gas standard and calibrated using international standards IAEA-S1 ($\delta^{34}S$ = -0.3 VCDT) and NBS-127 ($\delta^{34}S$ = +20.3 ‰ VCDT). Replicate analysis gave an error of ±0.3 ‰.

Isotope ratios are reported relative to the Vienna Canyon Diablo Triolite (VCDT). Fractionation was calculated as the difference in isotope ratio between the sulfate and sulfide values. For example, if the $\delta^{34}S$ of the sulfate was +20 ‰ and the sulfide was -10 ‰, the fractionation would be 30 ‰. In this chapter fractionation was calculated as the difference between the sulfate and sulfide from both the soluble sulfate and from a generally accepted seawater sulfate value. The sulfur isotope composition of seawater is constant throughout the world's ocean but has varied between +10 ‰ to +30 ‰

through geological time (Claypool *et al* 1980). According to Bottcher *et al* (2004), $\delta^{34}S$ for modern seawater sulfate is +20.6 ‰ and this value has been adopted.

Results and Discussion

The sites selected in this study have been grouped into 4 categories (coastal clay acid sulfate soils, coastal peat acid sulfate soils, coastal monosulfidic black ooze and inland acid sulfate soils). Kempsey, McLeods Creek, Shark Creek and Tuckean Swamp represent coastal clayey acid sulfate soils (Category 1). Byron Bay, Boggy Creek and Bora Codrington are classified as coastal peat dominated acid sulfate soils (Category 2). The distinction between clay and peat acid sulfate soils is based on the total carbon concentration. Soils with layers containing greater than 30% total carbon are classified as peat acid sulfate soils. Soils with less than 30% total carbon as considered clay acid sulfate soils. Category 3 is comprised of coastal monosulfidic black ooze samples collected from drainage channels in the Tuckean Swamp and Boggy Creek. Category 4 represents the inland acid sulfate soil samples. Each of these categories provided widely differing environmental conditions during the formation of sulfides.

Coastal clay acid sulfate soils

Kempsey (30°55’19.38”S, 152°58’4.91”E), McLeods Creek (28°18’0.00”S, 153°18’0.00”E), Shark Creek (29°31’57.36”S, 153°12’40.60”E), Tuckean Swamp (28°58’1.20”S, 153°22’9.12”E) samples represent coastal clay dominated acid sulfate soils. Although each of these sites display a spike in total carbon concentrations at the surface, these accumulations are the result of contemporary vegetation rather than an indicator of the environment in which the acid sulfate soils were laid down. The remainder of the profile is clay dominated, hence their classification.

Kempsey

The Kempsey site is located on an 880 acre cattle farm. At the time of sampling, the site was overlain by approximately 30 cm of water and a thick vegetation layer had

established. According to the property owner the site had previously contributed to one of the worst acid sulfate scalds in the country (R Yerbury pers comm. 2003). The soi characteristics for this site are presented in Figure 2.2. As these graphs indicate there is a considerable accumulation of sulfides at the surface of the profile accompanied by an increase in pH. Given the site was previously scalded, these sulfides are considered to be contemporary accumulations formed since water flooded the site (Rosicky *et al* 2002a, b, 2004). The established vegetation is contributing to the increased total carbon levels recorded at the surface. During repeated cycles of wetting and drying the vegetation establishes and dies off contributing to the carbon levels in the soil. Once anaerobic conditions are established this organic matter is used as a food source for sulfate reducing bacteria and iron sulfides are formed (Habicht and Canfield 1997; Stam *et al* 2011).

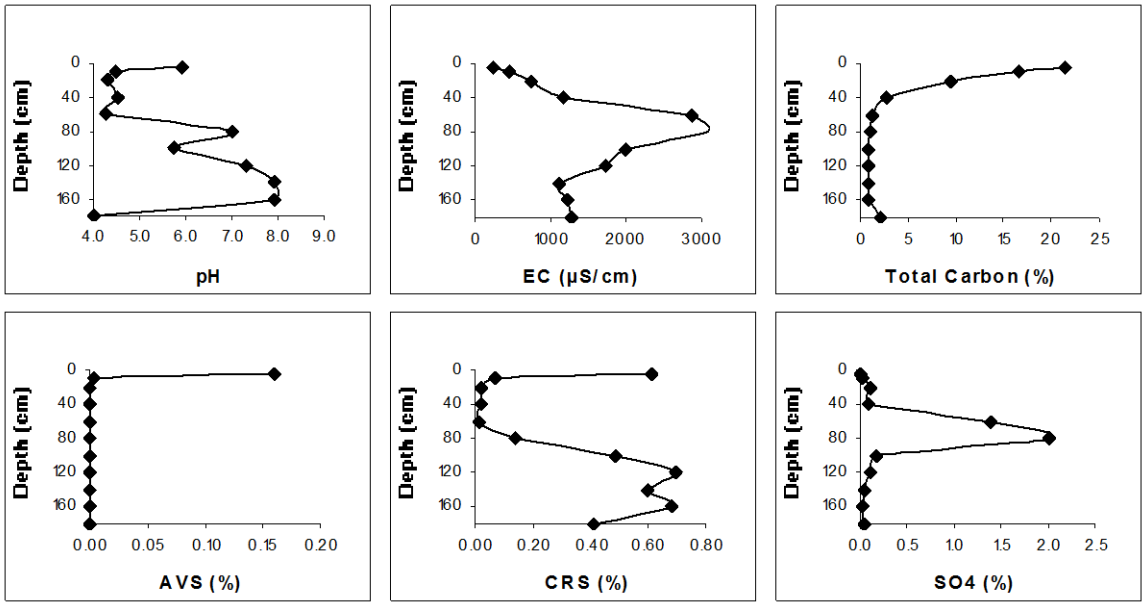

Figure 2.2. Selected soil properties for the Kempsey site including pH, electrical conductivity (EC), total carbon, acid volatile sulfur (AVS), chromium reducible sulfur (CRS) and water soluble sulfate (SO_4).

The stable sulfur isotope results for the Kempsey site are displayed in Table 2.1. Isotope ratios for the sulfide fractions at this site are negative and show a maximum fractionation from seawater sulfate of 49.17 ‰. These values are consistent with fractionation due to bacterial sulfate reduction (Bottcher and Lepland 2000; Stam *et al* 2011). According to Goldhaber and Kaplan (1974) the extent of fractionation due to bacteria preferentially metabolising isotopically lighter sulfate is highly variable.

Values between 0 and -50 ‰ have been measured, although sulfide is commonly 25 ‰ to 50 ‰ lighter than the precursor sulfate (Emery and Robinson 1993; Bruchert 1998; Wijsman *et al* 2001).

Table 2.1. $\delta^{34}S$ of the AVS, CRS and soluble SO_4 fractions at Kempsey. Fractionation is calculated between $\delta^{34}S$ CRS and both seawater SO_4 (SWS = 20.6 ‰) and soluble SO_4 (SS = $\delta^{34}S$ SO_4).

Depth (cm)	$\delta^{34}S$ AVS (‰)	$\delta^{34}S$ CRS (‰)	$\delta^{34}S$ SO_4 (‰)	Fract. from SWS (‰)	Fract. from SS (‰)
Overlying water	-	-	-18.0		
0–5	-19.0	-20.1	-2.7	40.7	17.4
60–80	-	-28.6	-17.3	49.2	11.3
160–180	-	-18.3	-16.4	38.9	1.9

The isotopic signature of the sulfates in the 60–80 cm and 160–180 cm zones are similar to the sulfide signatures. Assuming minimal fractionation during oxidation (Taylor *et al* 1984; Balci *et al* 2007), these isotopic signatures indicate the sulfates in these zones are derived from the oxidation of sulfides and are not sourced from either brackish tidal water or rainwater containing seawater aerosols (Bridgman 1989; Kilminster and Cartwright 2011). A similar situation was recorded by Bush (2000) for the Tuckean Nature Reserve and McLeods Creek. At all three sites it is interesting to note that the enrichment of soluble sulfate in ^{32}S continued below the oxidation boundary. This is perhaps due to oxidation processes that operated as the sediments were laid down or due to diffusion through the profile (Rosicky *et al* 2000).

Recent work corroborates the potential of sulfur isotopes in tracing the source of sulfate (Mayer *et al* 2010; Unland *et al* 2012). Dold and Spangenberg (2005), using isotopes of sulfur and oxygen, also concluded water soluble sulfate resulted from the oxidation of pyrite in mine tailings. In addition, their study was able to differentiate the isotopic signature of sulfate derived from pyrite oxidation from the isotopic signature of primary sulfate dissolution. In acid sulfate soil environments, this type of finding may be used to determine the contribution pyrite oxidation makes to the sulfate concentration of surface and ground water as well as in waterways. It may also be used to track the source of sulfate to the site of oxidation.

In the 60–80 cm zone there is a greater enrichment in ^{32}S in CRS compared to either the surface layer or the 160–180 cm layer. Given this layer is where the oxidation front occurs in this profile, the greater enrichment in ^{32}S is likely due to sulfur cycling processes. Several authors have reported small fractionations occurring during the oxidative part of the sulfur cycle (Jorgensen 1990; Canfield and Thamdrup 1994; Habicht and Canfield 1997; Bruchert 1998). Canfield and Thamdrup (1994) and Habicht and Canfield (1997) found that disproportionation of elemental sulfur during repeated oxidation cycles enabled sulfides to become more enriched in ^{32}S than would be possible with sulfate reducing bacteria alone. Jorgensen (1990) drew a similar conclusion for the disproportionation of thiosulfate. The fractionation of elemental sulfur and thiosulfate, while producing an enrichment of ^{32}S of between 7.0 ‰ and 8.9 ‰ in the sulfides, also produces an enrichment of ^{34}S of between 12.6 ‰ and 16.7 ‰ in the sulfates (Canfield and Thamdrup 1994). Given that the $\delta^{34}S$ of the sulfate at the Kempsey site is not enriched in ^{34}S, these fractionation processes are unlikely to dominate.

At this site, the greater fractionation at the oxidation front may have resulted from the oxidation of ^{32}S enriched sulfides to produce ^{32}S enriched sulfates. As these isotopically lighter sulfates are reduced the light isotope is again preferentially incorporated causing further ^{32}S enrichment in the resulting sulfides. A similar decrease in $\delta^{34}S$ values was recorded by Bush (2000) at the oxidation boundary of the McLeods Creek acid sulfate soil profile.

The sulfate in the overlying water at this site was isotopically similar to the sulfates at depth. This value of -18.0‰ is well outside the range of present freshwater sulfate (+5 to +15‰) determined by Holser and Kaplan (1966) (Figure 2.3). This is undoubtedly due to the sulfates in these waters being derived from the oxidation of the underlying sulfidic materials. This result clearly shows that $\delta^{34}S$ of fresh water cannot be assumed to be 10 ‰ ± 5 ‰ without verification, especially in coastal acid sulfate soil landscapes.

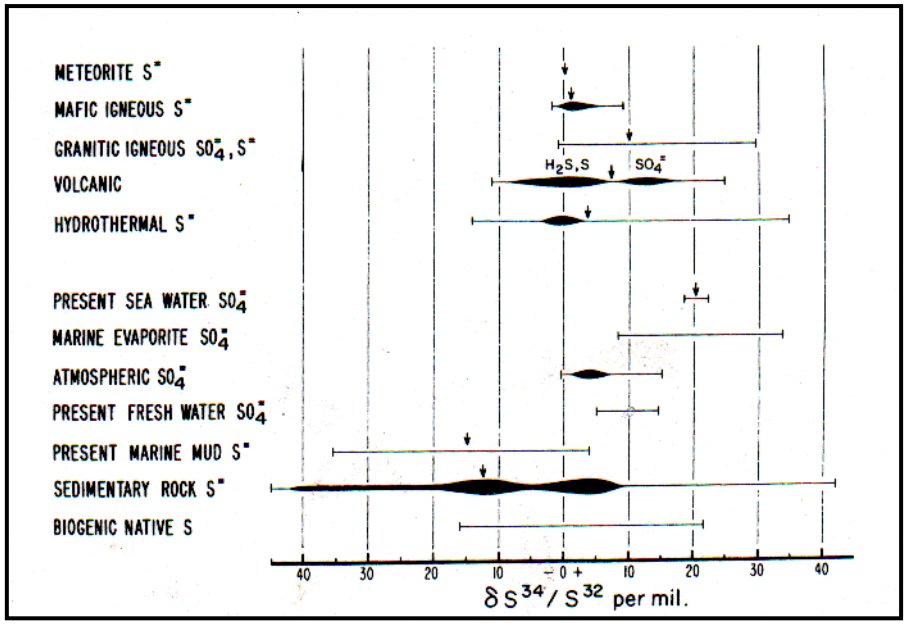

Figure 2.3. Summary of $\delta^{34}S$ ranges for sulfur from various terrestrial materials (Holser and Kaplan 1966).

The $\delta^{34}S$ of the sulfate in the surface soil layer at Kempsey (-2.2‰) is less negative than either the layer below (-17.3‰) or the overlying water (-18.0‰) and quite different to the $\delta^{34}S$ of the sulfide fractions (-20.1‰). Given this is a zone of active sulfide formation the comparatively less negative value is likely due to ^{32}S incorporation into the sulfide fraction. When isotopically light sulfate is removed from the pool the remaining sulfate becomes increasingly heavier (Brownlow 1996; Wijsman *et al* 2001; Farquhar *et al* 2008).

The similarities between the $\delta^{34}S$ for the AVS and CRS at this site suggest they were formed at approximately the same time under similar conditions (Wijsman *et al* 2001; Fan *et al* 2012). It should be noted however, that the sulfides were not extracted with a sequential extraction procedure and that the CRS fraction includes the AVS fraction.

The strong consistently negative $\delta^{34}S$ CRS values recorded at the Kempsey site are an example of a system that is open with respect to sulfate supply. Soils in this area form part of the Seven Oaks Soil Landscape and comprise Holocene estuarine sediments (Enginuity Design 2003). At this site seashells were abundant in the estuarine clay at depth. Since the early 1900s 'improvements' to the area restricted the inflow of seawater and the site became predominantly freshwater influenced (Enginuity Design

2003). This meant the major source of sulfate replenishment was cut off and the area became less open. A fresh supply of sulfate may still be transported to the site from seawater aerosol and rainfall. The primary source of sulfate however, is the oxidation of sulfides. Sulfate transported to the site by overland flow from within the catchment may have a varied isotopic composition reflecting both sources. This may further explain the slightly negative $\delta^{34}S\ SO_4$ value in the surface layer.

McLeods Creek

McLeods Creek is a right bank tributary which joins the Tweed River approximately 4.5 km downstream of Tumbulgum, near Tweed Heads in northern New South Wales. The creek forms part of the McLeods Creek – Main Trust Canal Acid Sulfate Soil Hot Spot for which a remediation plan has been developed and implemented (Cibilic 2003a). The main land use is sugar cane production which required the land to be extensively drained (Smith *et al* 2003; Green *et al* 2006). Historically, the area has been subjected to significant acid discharges from the high density drainage network (Easton 1989).

According to Figure 2.4, McLeods Creek contains actual acid sulfate soil layers between 60 cm and 110 cm where pyrite is actively oxidising. This is overlying potential acid sulfate soils layers which are not oxidising. Similar results were recorded by van Oploo (2000) for the same site.

The stable sulfur isotope signatures for McLeods Creek are displayed in Table 2.2. Throughout the profile $\delta^{34}S$ for the CRS fraction are negative and show a maximum fractionation from seawater sulfate of 43.20 ‰. These values are similar to the Kempsey profile and indicate the sulfides formed from the reduction of an abundant seawater sulfate source (Bottcher and Lepland 2000; Fan *et al* 2012).

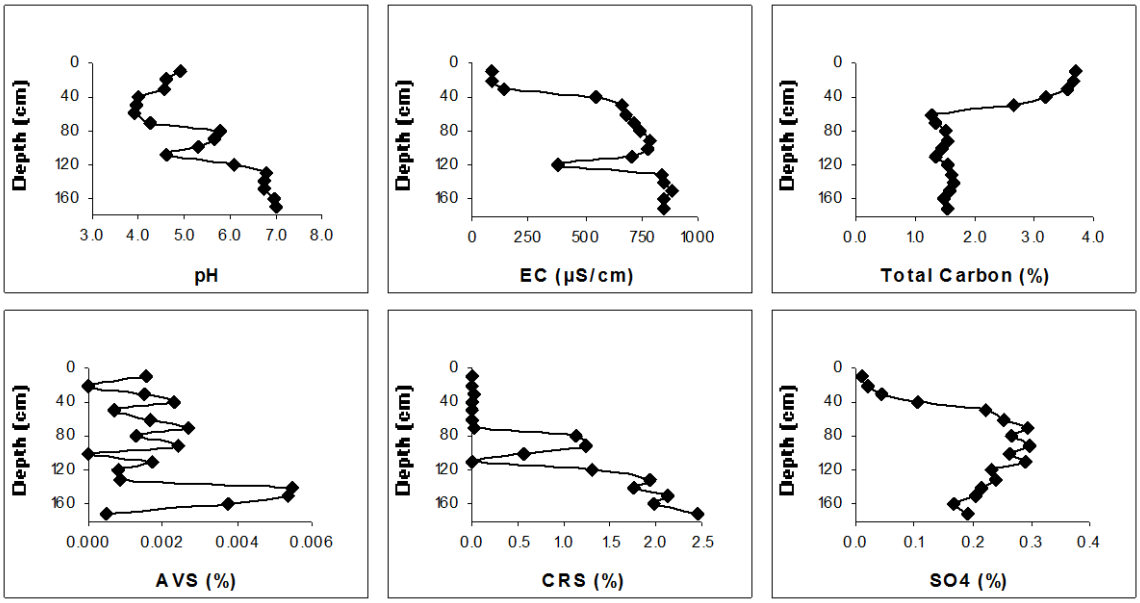

Figure 2.4. Selected soil properties for the McLeods Creek site including pH, electrical conductivity (EC), total carbon, acid volatile sulfur (AVS), chromium reducible sulfur (CRS) and water soluble sulfate (SO_4).

There is a significant increase in the enrichment of ^{32}S in the 110–120 cm layer compared with the 90–100 cm layer. This layer corresponds with the upper zone of the oxidation boundary between actual and potential acid sulfate soils. In this zone the redox conditions may cycle between oxidising and reducing which means isotopically light sulfate may be utilised in the reformation of sulfides (Bruchert 1998; Wijsman *et al* 2001). A similar pattern was recorded by Bush (2000) at this site and was attributed to a secondary accumulation of pyrite.

Table 2.2. $\delta^{34}S$ of the CRS and soluble SO_4 fractions at McLeods Creek. Fractionation is calculated between $\delta^{34}S$ CRS and both seawater SO_4 (SWS = 20.6 ‰) and soluble SO_4 (SS = $\delta^{34}S$ SO_4).

Depth (cm)	$\delta^{34}S$ CRS (‰)	$\delta^{34}S$ SO_4 (‰)	Fract. from SWS (‰)	Fract. from SS (‰)
20–30	-9.0	-5.4	29.6	3.5
60–70	-	-7.1	-	-
70–80	-13.6	-6.7	34.2	6.9
80–90	-10.5	-8.6	31.1	1.9
90–100	-10.9	-7.4	31.5	3.5
110–120	-22.6	-	43.2	-
160–170	-16.5	-6.3	37.1	10.2

The $\delta^{34}S$ of the sulfate fraction showed considerably less variation than the CRS fraction. However the values were all negative, which suggests the principle sulfate source in these sediments is the oxidation of pyrite. Again, as was seen in the Kempsey samples, the negative sulfate values continue below the oxidation boundary, suggesting either oxidation as they sediments were deposited or diffusion of the overlying oxidation products into the lower layers.

Shark Creek

Shark Creek is located approximately 35 km north east of Grafton in New South Wales on the lower Clarence River estuary (Johnston *et al* 2003a). Many of the background soil characteristics for Shark Creek (Figure 2.5) are quite similar to both Kempsey and McLeods Creek. There are slightly elevated (0.1 %S) CRS concentrations at 80–90 cm depth and a sharp increase in CRS after 120 cm depth.

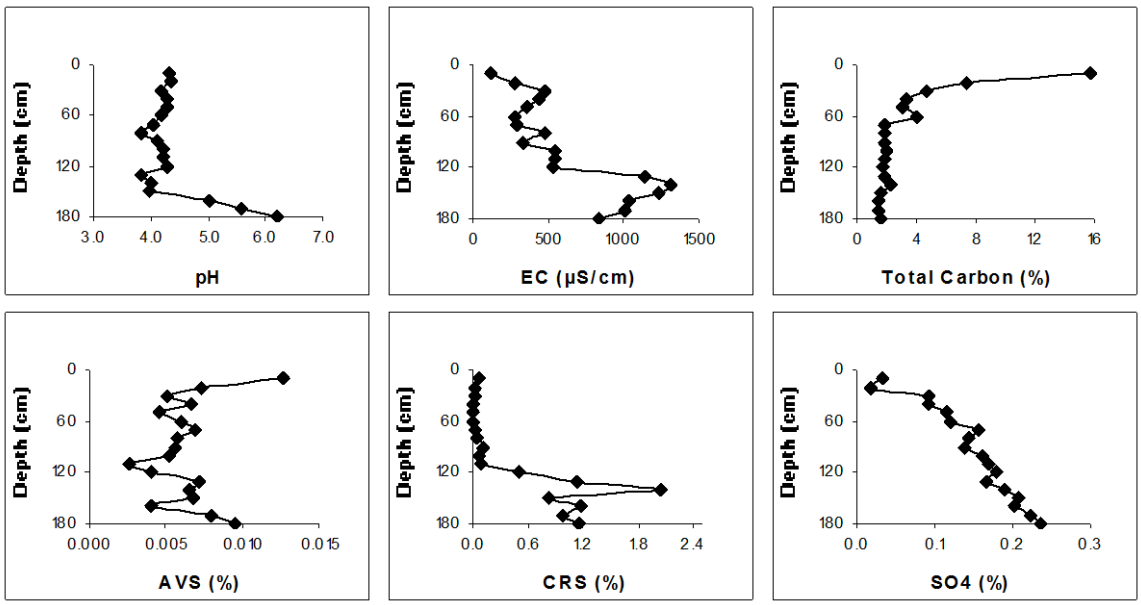

Figure 2.5. Selected soil properties for the Shark Creek site including pH, electrical conductivity (EC), total carbon, acid volatile sulfur (AVS), chromium reducible sulfur (CRS) and water soluble sulfate (SO_4).

The stable sulfur isotope signatures at Shark Creek (Table 2.3) are also similar to Kempsey and McLeods Creek. $\delta^{34}S$ CRS are all negative, indicating sulfide formation from an abundant sea water sulfate source (McConville *et al* 2000; Wijsman *et al* 2001; Stam *et al* 2011). In addition, $\delta^{34}S$ SO_4 is also negative and similar to the CRS

fraction suggesting the sulfate was derived from the oxidation of isotopically light sulfides (Mayer *et al* 2010; Kilminster and Cartwright 2011; Unland *et al* 2012).

Table 2.3. $\delta^{34}S$ of the CRS and soluble SO_4 fractions at Shark Creek. Fractionation is calculated between $\delta^{34}S$ CRS and both seawater SO_4 (SWS = 20.6 ‰) and soluble SO_4 (SS = $\delta^{34}S$ SO_4).

Depth (cm)	$\delta^{34}S$ CRS (‰)	$\delta^{34}S$ SO_4 (‰)	Fract. from SWS (‰)	Fract. from SS (‰)
0–10	-12.4	-2.8	33.0	9.6
10–20	-22.2	-5.1	42.8	17.1
90–100	-17.3	-8.7	37.9	8.6
100–110	-12.9	-8.4	33.5	4.5
110–120	-14.6	-8.6	35.2	6.0
170–180	-13.1	-6.0	33.7	7.1

The principle difference between the isotope signatures at Shark Creek and the two previous sites is that the lowest CRS value does not correspond with the oxidation front. At this site the lowest $\delta^{34}S$ CRS occurs in the 10–20 cm layer, however the soil characteristics indicate that the oxidation front is occurring much deeper in the profile. According to Figure 2.5, there is a very slight increase in AVS concentration in the upper soil layers. These reformed sulfides may be contributing to the high $\delta^{34}S$ of the CRS which represents both monosulfide and disulfide fractions. There is also a slight bump in the CRS concentration in the 80–90 cm layer. This layer is more isotopically negative then the layer below which could also be attributed to contemporary sulfide reformation (Bush 2000).

Tuckean Swamp

The Tuckean Swamp is located on the lower Richmond River floodplain in northern New South Wales. It comprises an area of approximately 5000 ha with a catchment of approximately 22 000 ha (Sammut *et al* 1996a). Tuckean Swamp is dissected by an extensive artificial drainage system, which has modified the natural drainage pattern (Sammut *et al* 1995). Hagley (1996) suggested this drainage has resulted in approximately 3000 ha becoming strongly acidic with another 1000 ha having the potential to become acidic.

Drainage of the Tuckean Swamp has caused significant oxidation of the underlying acid sulfate soils (Burton *et al* 2006a; Wong *et al* 2010; Claff *et al* 2011). This site recorded the lowest pH values and the highest pyrite concentrations for this study (Figure 2.6). These results suggest that although the site is already degraded, if not managed correctly there is still enormous potential for environmental damage.

There are several features to consider in the isotope signatures recorded for the Tuckean Swamp (Table 2.4). Between 80 and 120 cm $\delta^{34}S$ (CRS) are not as enriched in ^{32}S as the three previous sites. These less negative values are most likely a function of the depositional environment when the sulfides were formed. The fractionation values still fall within the range expected for bacterial sulfate reduction, however the source of sulfate may not have been as abundant as the other sites (Farquhar *et al* 2008; Stam *et al* 2011). At this site there may have been some influence from fresh water or it may have only received intermittent tidal water. According to Zaback and Pratt (1992) lower fractionation can result if the sulfate supply is limited or sulfate reduction rates are increased.

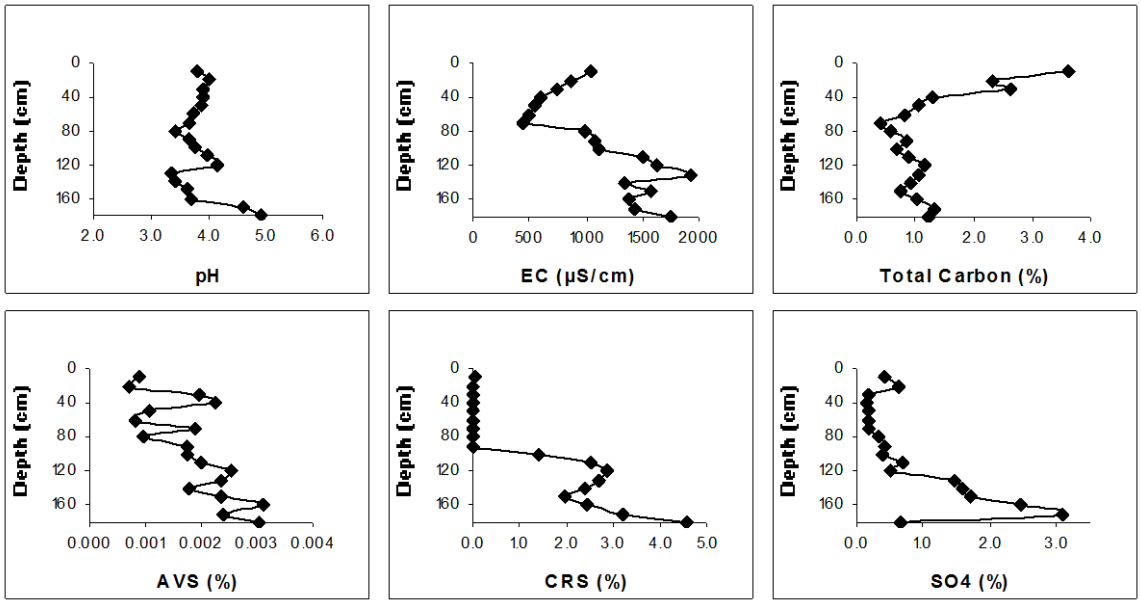

Figure 2.6. Selected soil properties for the Tuckean Swamp site including pH, electrical conductivity (EC), total carbon, acid volatile sulfur (AVS), chromium reducible sulfur (CRS) and water soluble sulfate (SO_4).

$\delta^{34}S$ in the sulfate fraction is consistent throughout the Tuckean Swamp profile. Between 80 and 120 cm the $\delta^{34}S$ SO_4 is similar to the $\delta^{34}S$ of the CRS fraction indicating they have likely resulted from the oxidation of pyrite. In the surface layer and the 170–180 cm depth layer the $\delta^{34}S$ of the CRS fraction varies significantly.

Table 2.4. $\delta^{34}S$ of the CRS and soluble SO_4 fractions at Tuckean Swamp. Fractionation is calculated between $\delta^{34}S$ CRS and both seawater SO_4 (SWS = 20.6 ‰) and soluble SO_4 (SS = $\delta^{34}S$ SO_4).

Depth (cm)	$\delta^{34}S$ CRS (‰)	$\delta^{34}S$ SO_4 (‰)	Fract. from SWS (‰)	Fract. from SS (‰)
0–10	-20.5	-4.4	41.1	16.1
80–90	-2.1	-2.2	22.7	-0.1
90–100	-2.5	-2.5	23.1	0.0
100–110	-4.8	-2.4	25.4	2.4
110–120	-4.1	-2.5	24.7	1.6
170–180	12.4	-2.8	8.2	-15.2

At the surface of the Tuckean Swamp $\delta^{34}S$ CRS is considerably more enriched in ^{32}S than the underlying layers. This result is probably due to sulfide reformation processes. Although the sulfide concentration in this layer is only 0.03% it is still higher than the layers below. The greater fractionation during reformation is indicative of isotopically light sulfate being used during sulfate reduction (Bruchert 1998). A similar value (-20.09 ‰) was recorded at the surface of the Kempsey profile where sulfide reformation was much higher.

In the deepest layer examined at this site the $\delta^{34}S$ (CRS) was positive. A study by Bush (2000) also showed a sharp change in the pyrite isotope signature for Tuckean Swamp from -15 ‰ at 1.5 m depth to +25 ‰ at 1.8 m depth. At 2.3 m depth Bush (2000) recorded +50 ‰ for $\delta^{34}S$ (CRS). According to that study hydrothermal pyrite often has a $\delta^{34}S$ value of >40 ‰ (McKibben and Eldridge 1989) but diagenic pyrite enriched to these levels has not previously been reported. A more detailed study of these zones in the Tuckean Swamp is warranted.

Coastal peat dominated acid sulfate soils

Byron Bay (28°37'8.48"S, 153°24'21.60"E), Boggy Creek (29°8'22.84"S, 153°21'43.22"E) and Bora Codrington (29°2'16.50"S, 153°13'31.40"E) represent acid sulfate soils that exhibit a peat layer where total carbon levels exceed 30%.

Byron Bay

The Byron Bay site is located on a 24 hectare site adjacent to the West Byron Sewage Treatment Plant in northern New South Wales. The site is underlain by a 1.5 m peat layer, embedded midway with a pyrite layer (Bolton *et al* 2002a). The Byron Shire Council has adopted an environmental management strategy that combines effluent reuse with acid sulfate soil management and Melaleuca wetland regeneration for the site (Bolton 2001; Bolton *et al* 2002b). Since commencement of the project in November 2001, nearly 500 000 Melaleuca seedlings have been planted on the site.

Seedlings are irrigated with tertiary treated effluent, which is used to manage acid sulfate soils in two ways. Firstly, the alkaline effluent (pH ~ 8.0) buffers existing acid products, increasing the pH of the groundwater. Secondly, it maintains water levels above the pyrite layer, preventing oxidation and the subsequent production of acid products (Bolton *et al* 2002a). Samples were collected from the area designated as Site 7, which receives regular irrigation with effluent.

As part of a previous study significant pyrite concentrations of >1% were recorded on the surface of the site after long term treatment with tertiary treated effluent (Bolton *et al* 2002a). During the current study, concentrations at the surface were only 0.163%, which is considerably less than the value recorded previously for the same site (Figure 2.7). This suggests that at the time of sampling, the site was relatively dry and that the surface sulfides that formed after treatment with effluent were oxidising.

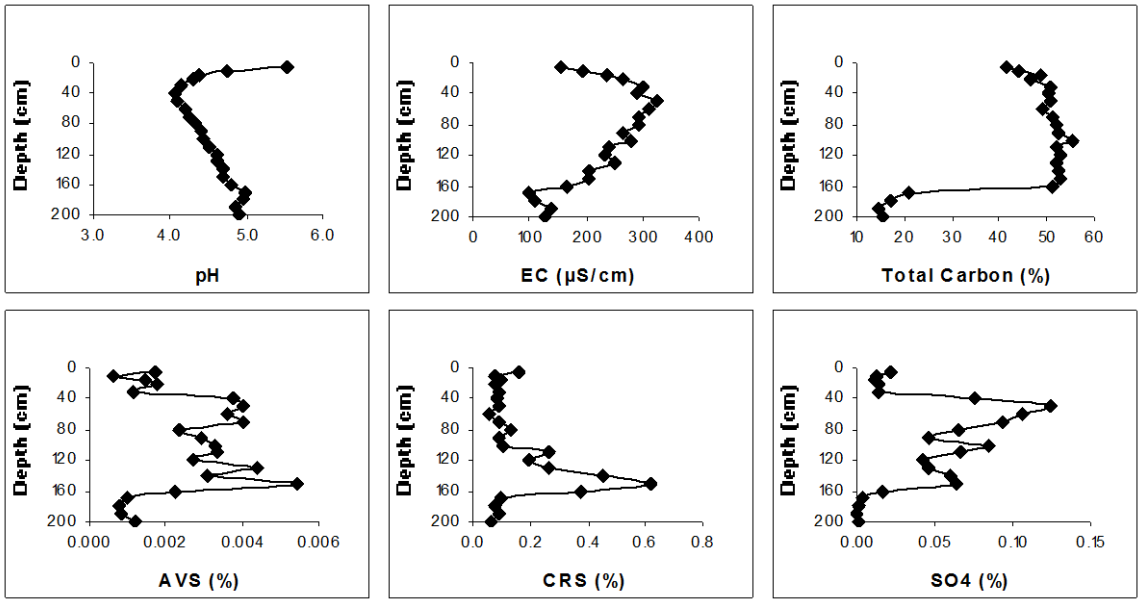

Figure 2.7. Selected soil properties for the Byron Bay site including pH, electrical conductivity (EC), total carbon, acid volatile sulfur (AVS), chromium reducible sulfur (CRS) and water soluble sulfate (SO_4).

The relatively high pH in the surface layer is probably due to the application of the alkaline effluent (Bolton *et al* 2001), however it may also provide further evidence of reformation processes, given pyrite formation is an acid consuming process (Rosicky *et al* 2004). The very low pH values throughout the remainder of the profile may result from acidic oxidation products diffusing down the profile (Rosicky *et al* 2000) and the naturally acidic conditions often associated with peat soils (Bush *et al* 2004). AVS concentrations at the Byron Bay site are consistently low. This was true even during periods when sulfides were reforming on the surface and the CRS was high, such as during the previous study (Bolton *et al* 2002a). Such low concentrations indicate the conditions are more conducive to pyrite formation than to AVS accumulation (Gagnon *et al* 1995; Burton *et al* 2011a, b; Johnston *et al* 2011b, 2012).

Unfortunately, there was insufficient sample to extract enough sulfate and sulfide for isotope analysis for all zones of interest. It was hoped the isotope data would show whether the tertiary treated effluent was providing a sulfate source and enabling the reformation of sulfides on the surface. The negative values of the layers that were examined represent a fractionation from seawater sulfate of 22.34 ‰ in the 100–110

cm layer and 27.96 ‰ in the 170–190 cm layer (Table 2.5). As with the Kempsey site, these fractionation values fall within the range expected for bacterial sulfate reduction (Emery and Robinson 1993).

Table 2.5. $\delta^{34}S$ of the CRS fraction at Byron Bay. Fractionation is calculated between $\delta^{34}S$ CRS and seawater SO_4 (SWS = 20.6 ‰).

Depth (cm)	$\delta^{34}S$ CRS (‰)	$\delta^{34}S$ SO_4 (‰)	Fract. from SWS (‰)
0–5	-	-	
100–110	-1.5	-	22.1
140–150	-7.2	-	27.8

The degree of fractionation from seawater sulfate was not as strong at Byron Bay when compared to the depth samples at Kempsey. The high degree of organic matter at Byron Bay may have a positive influence on the rate of bacterial sulfate reduction, which according to Habicht and Canfield (1997), often results in lower fractionations being recorded. The $\delta^{34}S$ values for the Byron Bay CRS fraction indicate an environment that is less open than Kempsey with respect to sulfate supply (Bloch and Krouse 1992).

Boggy Creek

The Boggy Creek site is located adjacent to Bungawalbyn Creek approximately 10 km south of Coraki in northern New South Wales. The primary use for the property is tea-tree production, however sheep and cattle are also present. The Boggy Creek drainage system is part of the Sandy Creek – Bungawalbyn Creek Acid Sulfate Soil Hot Spot, indicating it is a priority area for acid sulfate soil management. The current management program for the site involves active floodgate management and the use of dropboards (Cibilic 2003a).

According to the soil characteristics for Boggy Creek (Figure 2.8), appreciable CRS concentrations were not encountered until approximately 70 cm depth, which is where the oxidation front is occurring. Like the Byron Bay site, this site was dominated by

peat sediments from 10 cm to 150 cm, which may explain the consistently low pH levels throughout the profile.

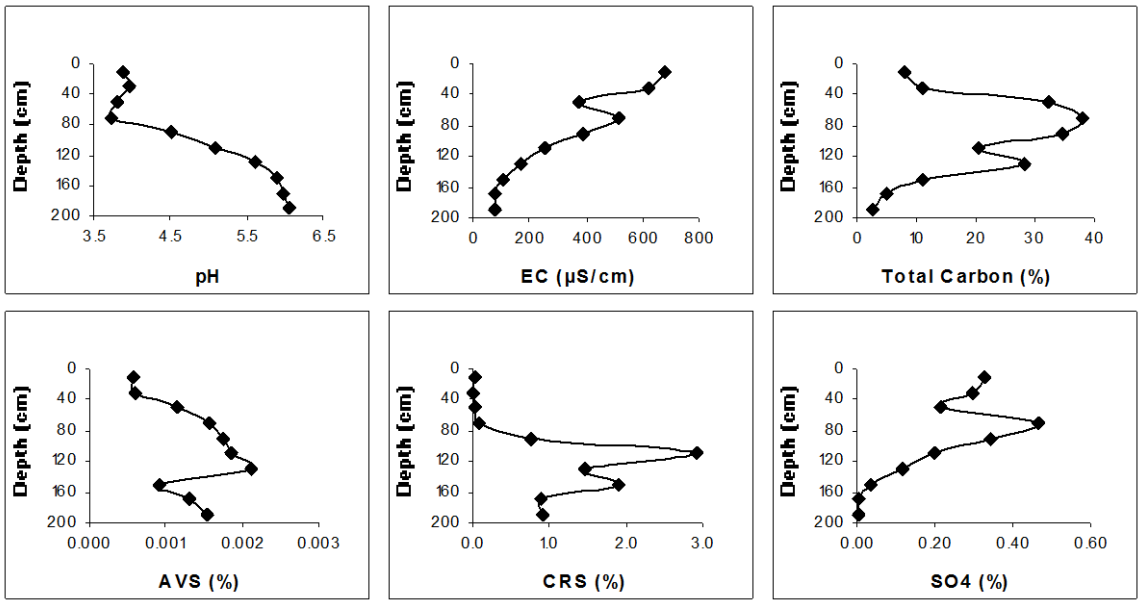

Figure 2.8. Selected soil properties for the Boggy Creek site including pH, electrical conductivity (EC), total carbon, acid volatile sulfur (AVS), chromium reducible sulfur (CRS) and water soluble sulfate (SO_4).

Isotope ratios for the CRS and soluble sulfate fractions are displayed in Table 2.6. Fractionation of the CRS has been calculated from both a known seawater sulfate value and from the corresponding soluble sulfate value. In contrast to the Byron Bay site, the $\delta^{34}S$ of the sulfide fraction at Boggy Creek were positive. Maximum fractionation from seawater sulfate was 10.79 ‰ which, although low, still falls within the range for bacterial sulfate reduction (Goldhaber and Kaplan 1974; Bottcher *et al* 1997).

The fractionation between the CRS and soluble sulfate however, was only 3.09 ‰. These values highlight the differences that may occur between fractionation values calculated from a known seawater sulfate value and from soluble sulfate values. In many acid sulfate soil landscapes, the degree of seawater influence may be limited, non-existent or unknown. As such, the use of the soluble sulfate values in fractionation calculations is likely to be more indicative of the precursor sulfate source.

Table 2.6. $\delta^{34}S$ of the CRS and soluble SO_4 fractions at Boggy Creek. Fractionation is calculated between $\delta^{34}S$ CRS and both seawater SO_4 (SWS = 20.6 ‰) and soluble SO_4 (SS = $\delta^{34}S$ SO_4).

Depth (cm)	$\delta^{34}S$ CRS (‰)	$\delta^{34}S$ SO_4 (‰)	Fract. from SWS (‰)	Fract. from SS (‰)
0–10	-	13.0		
90–110	9.8	12.9	10.8	3.1
170–190	10.5	-	10.1	

At Boggy Creek the $\delta^{34}S$ of the sulfate fraction indicates a closer association with freshwater sulfate, which according to Holser and Kaplan (1966) (Figure 2.3), typically range between +5 ‰ to +15 ‰. The influence of freshwater at this site is further supported by the abundance of peat which is usually associated with freshwater or brackish environments (Dellwig *et al* 2002; Bush *et al* 2004). The reduced concentration of sulfate in fresh or brackish water may lead to the positive $\delta^{34}S$ values recorded in the sulfide fraction at this site, however the extremely high rates of sulfate reduction often associated with high levels of organic matter may also be a factor (Farquhar *et al* 2008; Stam *et al* 2011; Morgan *et al* 2012c).

The Boggy Creek sulfate was enriched in ^{34}S by an average of 12.95 ‰. This value corresponds with $\delta^{34}S$ values recorded by Mandernack *et al* (2000) for soluble sulfates in wetland peats. In contrast to Boggy Creek however, Mandernack *et al* (2000) recorded $\delta^{34}S$ values for sulfide species of between -8.7 ‰ and -19.6 ‰.

Bora Codrington

The Bora Codrington site is located 12 km west of Woodburn in New South Wales; approximately 18 km north west of Boggy Creek. Both sites are detailed in the Sandy Creek – Bungawalbyn Creek Acid Sulfate Soil Remediation Concept Plan (Cibilic 2003b). The main land use in this area is cattle grazing (Allery 2003). The peat zone at this site is much thinner than either Boggy Creek or Byron Bay. The peat sediments were extremely moist which may contribute to pyrite reformation in these layers. Soluble sulfate concentrations are also considerably higher than the other peat sites examined, particularly between 130 and 160 cm depth (Figure 2.9).

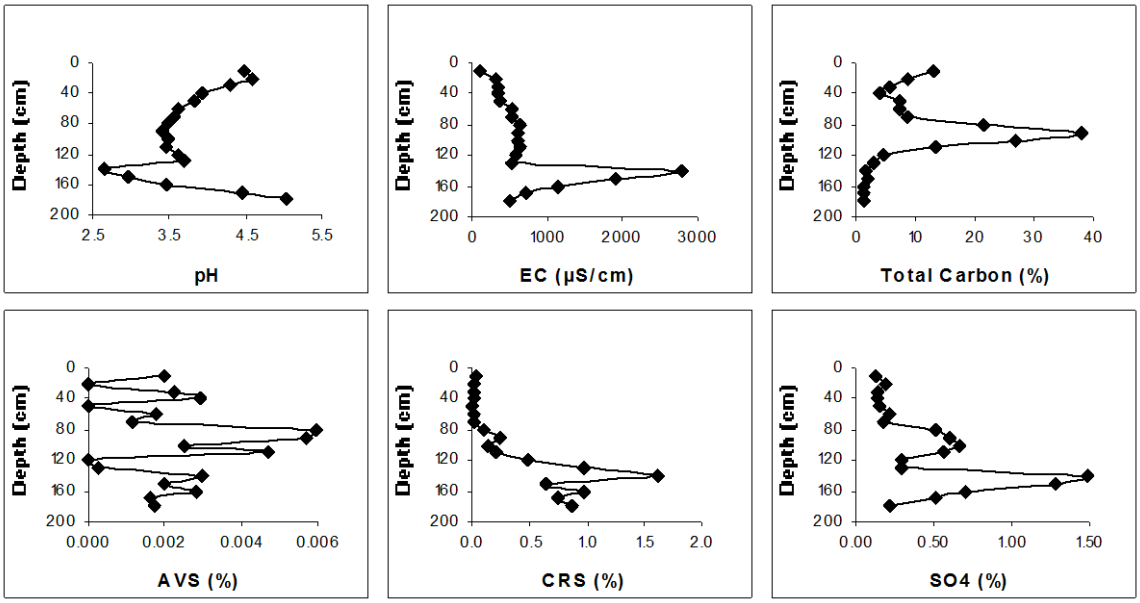

Figure 2.9. Selected soil properties for the Bora Codrington site including pH, electrical conductivity (EC), total carbon, acid volatile sulfur (AVS), chromium reducible sulfur (CRS) and water soluble sulfate (SO_4).

The isotope signatures for Bora Codrington show a range of both positive and negative values (Table 2.7). At the deepest layer the $\delta^{34}S$ for the CRS was quite negative and indicative of sulfide formation from the reduction of sea water sulfate (Wijsman *et al* 2001; Stam *et al* 2011). These sediments were likely deposited during the last sea level rise before the area was cut off from tidal influence (Mazumdar *et al* 2012).

Table 2.7 $\delta^{34}S$ of the CRS and soluble SO_4 fractions at Bora Codrington. Fractionation is calculated between $\delta^{34}S$ CRS and both seawater SO_4 (SWS = 20.6 ‰) and soluble SO_4 (SS = $\delta^{34}S$ SO_4).

Depth (cm)	$\delta^{34}S$ CRS (‰)	$\delta^{34}S$ SO_4 (‰)	Fract. from SWS (‰)	Fract. from SS (‰)
0–10	5.6	11.3	15.0	5.7
80–90	-7.4	12.5	28.0	19.9
90–100	-6.4	12.7	27.0	19.1
110–120	9.9	11.4	10.5	1.5
120–130	10.8	10.6	9.8	-0.2
170–180	-17.4	7.3	38.0	24.7

Between 110 and 130 cm depth $\delta^{34}S$ in the CRS fraction is very similar to the values recorded at Boggy Creek and are more likely associated with fresh water sulfate

where closed systems and limited sulfur supply exists (Fan *et al* 2012). It is likely sediments in this zone were deposited after the sulfate supply became restricted. According to Bloch and Krouse (1992) and Habicht and Canfield (1997) minimal fractionation between sulfate and sulfide occurs when the sulfate supply is limited or when the sulfate reduction rate exceeds supply. This could have been the case following a drop in the sea level which limited the tidal influence and meant sulfate was primarily derived from fresh water. Under these conditions bacteria will initially uptake the light sulfate but as the supply diminishes they will continue to utilise the heavy sulfate as well. If the entire supply of sulfate is reduced, the sulfides will have the same isotope signature as the precursor sulfate (Gautier 1985).

Between 80 and 100 cm $\delta^{34}S$ CRS is again negative. These layers correspond with the highest levels of total carbon which would facilitate increased sulfate reduction rates (Kristensen and Alongi 2006; Farquhar *et al* 2008). Given there is an abundant supply of sulfate in these layers, the negative $\delta^{34}S$ values are indicative of contemporary sulfide reformation (Bruchert 1998). Reformed sulfides would be formed from two sulfate sources; the freshwater sulfate and sulfate derived from the oxidation of pyrite. While the original pyrite formed in these layers may have carried a positive isotope signature, repeated cycles of oxidation and reduction have resulted in contemporary pyrite being isotopically negative.

In the surface layer, $\delta^{34}S$ in the sulfide fraction is positive. This signature may indicate relic pyrite that has not oxidised, however it is more likely to indicate more recently reformed pyrite. If the pyrite is reformed, the positive signature may be a function of limited sulfate supply (as described in the soil characteristics) or increased sulfate reduction rates due to the abundant supply of organic matter (Kristensen and Alongi 2006; Farquhar *et al* 2008).

Coastal monosulfidic black ooze samples

Coastal MBO samples were collected from drainage channels at Boggy Creek (29°8’22.84”S, 153°21’43.22”E) and Tuckean Swamp (28°58’1.20”S, 153°22’9.12”E). Samples were collected with a sleeve corer to maintain profile stratigraphy.

Boggy Creek MBO

Boggy Creek MBO samples were collected from within a drainage channel on the same property as the Boggy Creek soil samples. The samples were black and gelatinous and appeared to be monosulfidic black ooze. It was a surprise therefore, when the AVS concentrations were very low, particularly in the upper layers of the profile (Figure 2.10). Soluble sulfate concentrations were obviously sufficient to allow the transfer of AVS to pyrite as evidenced by the extremely high concentrations of CRS throughout the profile (almost 200 times the actionable limit; Ahern *et al* 2000).

As with the Boggy Creek soil profile, the Boggy Creek MBO $\delta^{34}S$ values were all positive (Table 2.8). At this site however, there was considerable variation in results throughout the profile. At the surface and between 50 and 55 cm depth, the isotope values for sulfate fall within the range of freshwater sulfate. In the 20–25 cm layer, sulfate is more depleted in ^{34}S and falls just outside the lower freshwater sulfate range (Holser and Kaplan 1966) with a $\delta^{34}S$ value of 4.76 ‰.

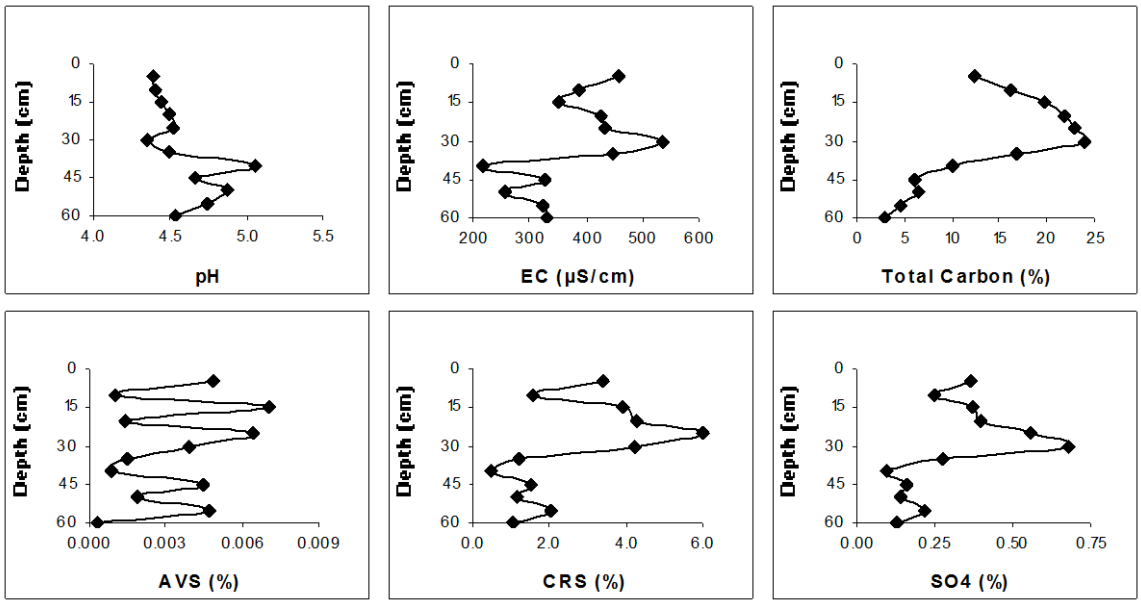

Figure 2.10. Selected soil properties for the Boggy Creek MBO including pH, electrical conductivity (EC), total carbon, acid volatile sulfur (AVS), chromium reducible sulfur (CRS) and water soluble sulfate (SO_4).

The slightly less positive value recorded for the $\delta^{34}S$ (CRS) fraction in the 20–25 cm layer corresponds with the highest CRS concentration (6%). While sulfide concentration does not have a direct effect on fractionation, a greater degree of cycling between oxidative and reductive phases may cause a stronger depletion in ^{34}S (Canfield and Thamdrup 1994; Bruchert 1998; Mazumdar *et al* 2012).

Table 2.8. $\delta^{34}S$ of the CRS and soluble SO_4 fractions for the Boggy Creek MBO. Fractionation is calculated between $\delta^{34}S$ CRS and seawater SO_4 (SWS = 20.6 ‰) and soluble SO_4 (SS = $\delta^{34}S$ SO_4).

Depth (cm)	$\delta^{34}S$ CRS (‰)	$\delta^{34}S$ SO_4 (‰)	Fract. from SWS (‰)	Fract. from SS (‰)
0–5	8.8	14.4	11.8	5.6
20–25	2.8	4.8	17.8	2.0
50–55	12.3	10.0	8.3	-2.3

In the 50–55 cm layer the $\delta^{34}S$ CRS was slightly higher than the soluble sulfate. There are limited occurrences in the literature where this phenomenon is reported, but it is suggested sulfide formed from organic sulfur may be a few per mille (‰) heavier than the organic sulfur source (Emery and Robinson 1993; Fan *et al* 2012). This is an area that would benefit greatly from a more detailed investigation.

Tuckean Swamp MBO

The primary regulatory structure for the Tuckean Swamp is the Bagotville Barrage, an eight-cell floodgate installed in 1971 to reduce periodic inundation by tidal influence (Hagley 1996). The barrage was constructed along a large drain commonly referred to as Hendersons Drain. Monosulfidic black ooze was sampled from this drain approximately 500 m upstream from the Barrage near a permanent weather station.

There has been considerable research regarding the occurrence and mobility of MBO along Hendersons Drain in the Tuckean Swamp (Fyfe 2001; Sullivan *et al* 2002). Unlike the Boggy Creek drain, at this site AVS was detected throughout the entire profile with considerable accumulations occurring in the upper layers (Figure 2.11). Generally the Tuckean Swamp MBO profile contains greater concentrations of iron and lower soluble sulfate compared to the Boggy Creek MBO. Such conditions are

conducive to the formation of AVS rather than pyrite (Gagnon *et al* 1995; Burton *et al* 2011a, b; Johnston *et al* 2011b, 2012).

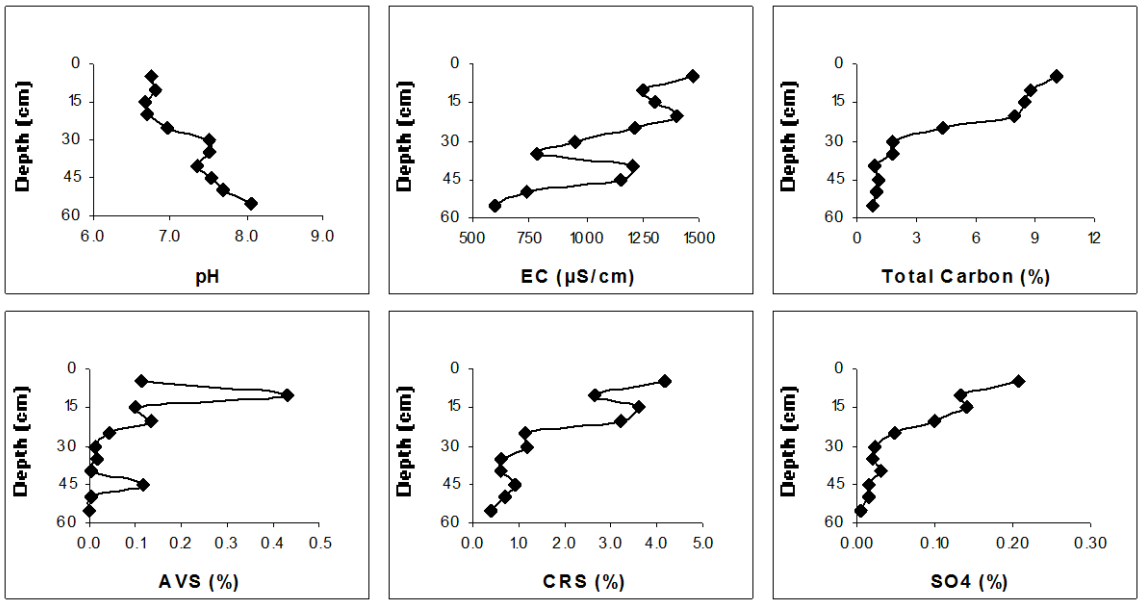

Figure 2.11. Selected soil properties for the Tuckean Swamp MBO including pH, electrical conductivity (EC), total carbon, acid volatile sulfur (AVS), chromium reducible sulfur (CRS) and water soluble sulfate (SO_4).

The isotopic ratios of the AVS, CRS and soluble sulfate fractions for the Tuckean Swamp are displayed in Table 2.9. At this site the isotopic composition of the AVS and CRS fractions showed both positive and negative values down the profile. In the 5–10 cm and 15–20 cm layers the AVS and CRS fractions were isotopically similar, however in the 40–45 cm layer the two fractions show considerable variation. The $\delta^{34}S$ of the soluble sulfate in this deep layer also showed a greater enrichment in ^{34}S than seawater sulfate and causes a higher fractionation from the CRS.

Table 2.9. $\delta^{34}S$ of the AVS, CRS and soluble SO_4 fractions for the Tuckean Swamp MBO. Fractionation is calculated between $\delta^{34}S$ CRS and both seawater SO_4 (SWS = 20.6 ‰) and soluble SO_4 (SS = $\delta^{34}S$ SO_4).

Depth (cm)	$\delta^{34}S$ AVS (‰)	$\delta^{34}S$ CRS (‰)	$\delta^{34}S$ SO_4 (‰)	Fract. from SWS (‰)	Fract. from SS (‰)
5–10	-2.0	-5.0	-	25.6	
15–20	4.0	2.3	-	18.3	
40–45	16.8	-6.3	24.6	26.9	30.9

The isotopic ratios of the sulfide fractions at this site ranged from -6.26 ‰ to +16.8 ‰. This variation is possibly a function of the accretionary nature of drain sediments. In 2001, Hendersons Drain in the Tuckean Swamp was flooded and a considerable portion of the MBO were mobilised downstream by the floodwater (Fyfe 2001). When the water levels receded the floodgates where closed and MBO began to re-accumulate in the drains. At this time the primary water input into the system was freshwater runoff from the catchment. In 2003, prior to these samples being collected, the floodgates were opened and seawater flowed into the drainage channel. This sequence of events may have affected the depositional environment under which the Tuckean Swamp MBO formed and may have contributed to the isotope variations.

Although the exact depth of MBO that was removed during the flood cannot be determined, it may have been eroded down to where the marine clay dominates the profile at approximately 20–25 cm depth. During the time between the flood in 2001 and the opening of the floodgates in 2003, the MBO that formed would have utilised sulfate from a freshwater sulfate source, that is, runoff from the catchment, and the resulting sulfides would have a lower degree of fractionation (as evidenced by the Boggy Creek MBO). However in 2003, with the opening of the floodgates, the system would have changed from freshwater dominated to seawater dominated and the MBO that formed after this time would reflect this sulfate source and have recorded greater levels of fractionation. It is reasonable to expect that over time the $\delta^{34}S$ values of the sulfide fraction at this site will become increasingly negative as sulfate is regularly replenished by the inflowing seawater and lighter isotopes are preferentially incorporated into sulfides.

Such a large variation between the AVS and CRS fraction in the 40–45 cm layer suggests the fractions formed under different conditions (Bruchet 1998; Fan *et al* 2012; Mazumdar *et al* 2012). During periods when sulfate supply is limited, lower fractionations will occur (Habicht and Canfield 1997). Such periods would also favour the formation of AVS in preference to CRS (Johnston *et al* 2009b; Keene *et al* 2010, 2011; Burton *et al* 2011a, b). However, when conditions change and sulfate becomes readily available, CRS will form with greater fractionation. Pyrite formed under these conditions may contain sulfur that is representative of both the lesser

fractionation stage and the greater fractionation stage (Butler *et al* 2004). This two stage process may explain why the $\delta^{34}S$ of the CRS in the 40–45 cm layer at this site is not as depleted in ^{34}S as the CRS at the Kempsey site.

Inland acid sulfate soils

Inland acid sulfate soil samples were collected from Calabria Road (34°16'34.35"S, 146°4'51.42"E), Leonards Lane (35°1'51.67"S, 148°7'8.42"E), Boomley (32°5'35.18"S, 149°7'10.85"E), Widden (32°31'40.18"S, 150°21'52.73"E), Piccaninny Creek (36°29'51.88"S, 144°28'41.83"E) and Barr Creek (35°48'30.19"S, 144°13'31.55"E). In many respects the inland sites represent contrasting environments to the coastal acid sulfate soils examined. In particular, the inland sites had monosulfide:pyrite ratios considerably higher than many coastal sites (Maher 2005). Gagnon *et al* (1995) considered a monosulfide:pyrite ratio of between 0.3 to 1.6 to be relatively high. Five of the inland sites recorded ratios within this range but at Leonards Lane the ratio was over double the upper range. Other soil characteristics for the inland sites are displayed in Figure 2.12.

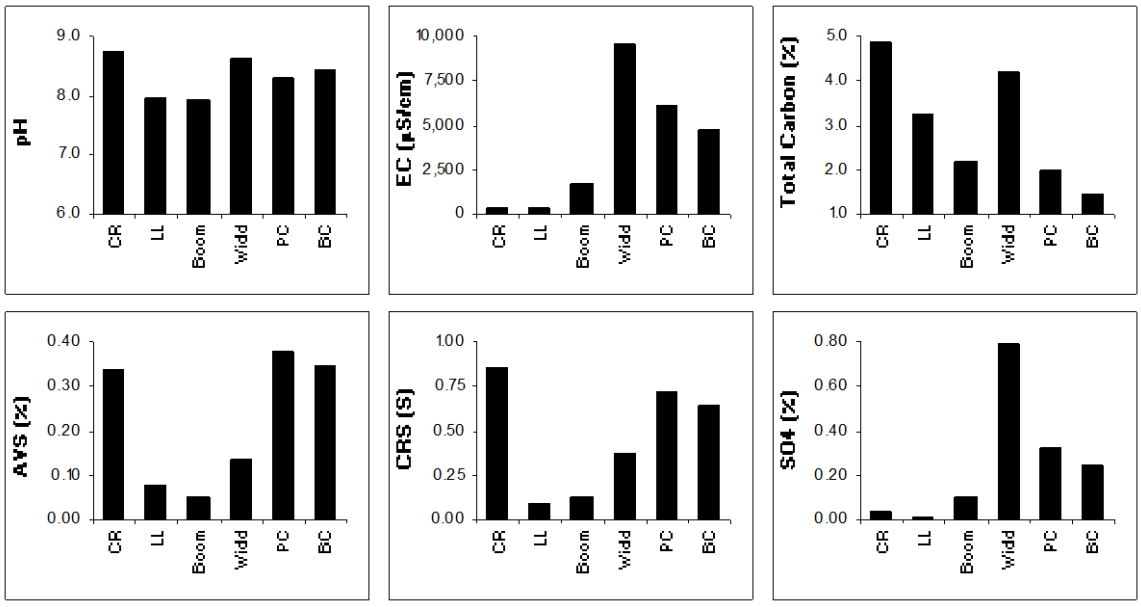

Figure 2.12. Selected soil properties for the Inland sites including pH, electrical conductivity (EC), total carbon, acid volatile sulfur (AVS), chromium reducible sulfur (CRS) and water soluble sulfate (SO_4). Sites include (from left to right) Calabria Road, Leonards Lane, Boomley, Widden, Piccaninny Creek and Barr Creek.

The isotopic ratios of the inland sites varied markedly from those recorded at the coastal sites (Table 2.10). With the exception of Boomley and Leonards Lane (insufficient sample quantity for analysis), sulfate in the inland samples were strongly positive with $\delta^{34}S$ values greater than seawater sulfate. At these sites, sulfate may be derived from weathering of gypsum and other minerals or from anthropogenic sources such as the application of fertilisers (Moncaster *et al* 2000; Kilminster and Cartwright 2011). Identifying the source of sulfate at these sites may prove instrumental in the development of a management strategy to prevent further accumulations of sulfides in these environments.

The $\delta^{34}S$ of the sulfides in the inland samples also showed variations between sites. Three of the sites, Leonards Lane, Boomley and Barr Creek had positive $\delta^{34}S$ values and may be displaying semi-closed system conditions either due to burial of the sediment or very rapid sulfate reduction rates. The other three sites, Calabria Road, Widden and Piccaninny Creek had negative $\delta^{34}S$ signatures, suggesting a more open supply of sulfate. The sulfides at the inland sites were not as enriched in ^{34}S as the Kempsey sulfides however, fractionation from the precursor sulfate is still considerably high.

Table 2.10. $\delta^{34}S$ of the AVS, CRS and soluble SO_4 fractions for the Inland sites. Fractionation is calculated between $\delta^{34}S$ CRS and both seawater SO_4 (SWS = 20.6 ‰) and soluble SO_4 (SS = $\delta^{34}S$ SO_4).

Site	$\delta^{34}S$ AVS (‰)	$\delta^{34}S$ CRS (‰)	$\delta^{34}S$ SO_4 (‰)	Fract. from SWS (‰)	Fract. from SS (‰)
Calabria	-8.6	-9.2	26.7	29.8	35.9
Leonards	5.1	2.3	-	18.3	
Boomley	8.8	8.4	11.1	12.2	2.7
Widden	-12.4	-13.5	24.0	34.1	37.5
Piccaninny	-9.5	-7.5	29.1	28.1	36.6
Barr Ck	4.4	3.0	26.0	17.6	23.0

General Discussion

Across each of the different environments there was considerable variation in the stable sulfur isotope signatures (Figure 2.13). In the clay dominated acid sulfate soil

sites $\delta^{34}S$ in the sulfide fractions ranged from -28.6 ‰ to -2.1 ‰. All the values recorded were negative with the exception of the value recorded in the deepest layer at the Tuckean Swamp. $\delta^{34}S$ of the sulfates were also negative and ranged from -17.3 ‰ to -2.2 ‰.

The signatures at the peat dominated sites displayed both positive and negative values. Nearly all the $\delta^{34}S$ CRS values ranged from -7.3 ‰ to +10.8 ‰. The only exception to this was the 170–180 cm clay sediment layer at Bora Codrington. Sulfate signatures from the peat sites were all positive and gave a $\delta^{34}S$ range of +7.3 ‰ to +13.0 ‰.

Samples collected from the inland sites gave a $\delta^{34}S$ CRS range of -13.5 ‰ to +8.4 ‰ and a $\delta^{34}S$ SO_4 range of +11.1 ‰ to +29.1 ‰. $\delta^{34}S$ CRS for both monosulfidic black ooze (MBO) samples fell within the range given for the peat sediments. The sulfate range for the Boggy Creek MBO was +4.8 ‰ to +14.4 ‰ extending the range of the peat sulfate slightly. Only one sulfate sample was analysed for the Tuckean Swamp MBO and it fell within the range given for inland sulfates.

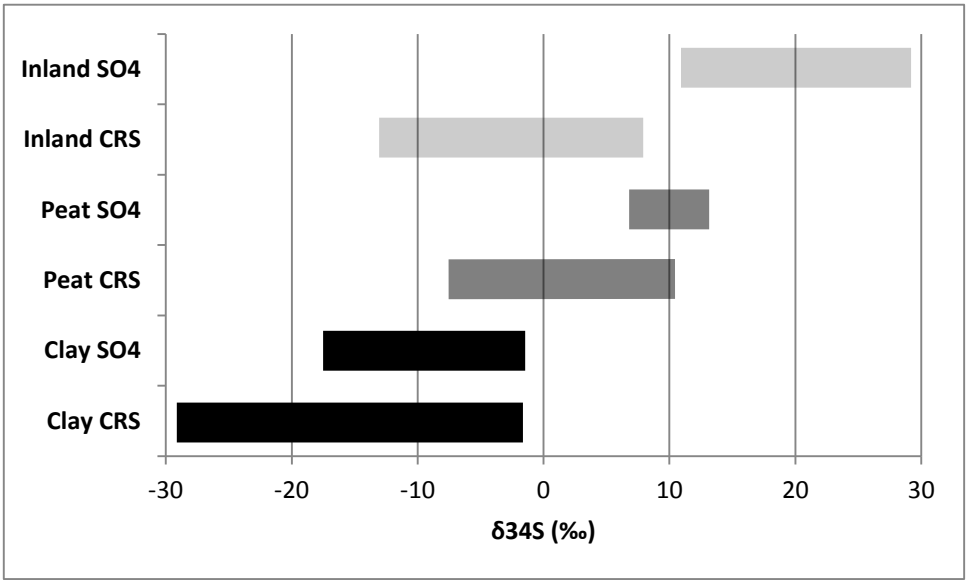

Figure 2.13. Range of $\delta^{34}S$ values recorded in the sulfide (CRS) and sulfate fractions from the clay and peat dominated coastal acid sulfate soil and inland acid sulfate soil sites in eastern Australia.

The variations in the sulfide fractions can be attributed to the formation environment and the effect it has on sulfate supply and sulfate reduction rates (Bottcher and Lepland 2000; Stam *et al* 2011; Mazumdar *et al* 2012). Strongly negative $\delta^{34}S$ CRS values are representative of environments in which sulfate is supplied more rapidly than it can be reduced (Bloch and Krouse 1992; Emery and Robinson 1993). Where the sulfate supply is continuously replenished, such as during tidal cycles, sulfate reducing bacteria preferentially incorporate the lighter isotope and $\delta^{34}S$ values become increasingly negative (Goldhaber and Kaplan 1974). Such environments are referred to as being 'open' with respect to sulfate replenishment (Figure 2.14). In an open system preferential removal of ^{32}S as sulfides does not significantly alter the isotopic composition of the remaining sulfate (McConville *et al* 2000). These open system conditions can be linked to the deposition and formation of clay dominated acid sulfate soils.

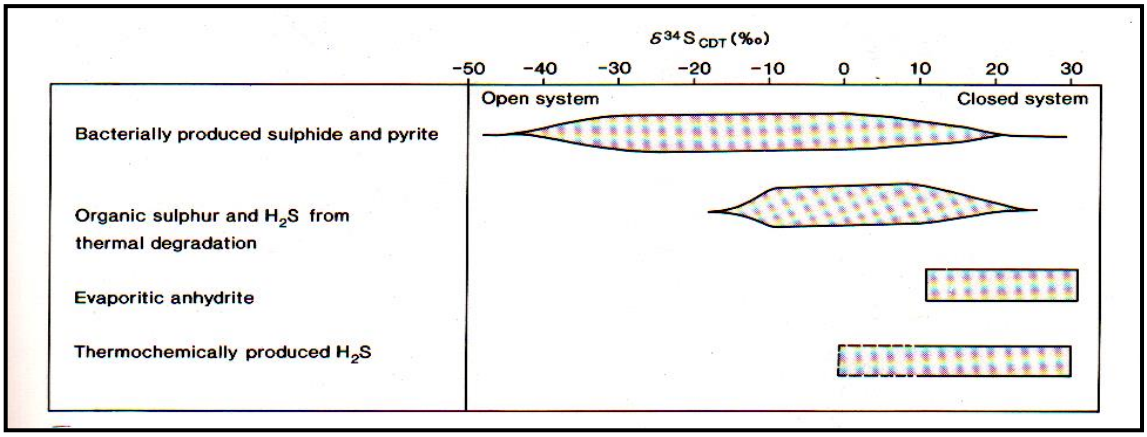

Figure 2.14. Range of isotopic compositions of sulfur compounds in sedimentary basins (Emery and Robinson 1993).

Where the sulfate supply is finite or when sulfate reduction exceeds supply, closed system conditions are said to exist (Zaback and Pratt 1992; Mandernack *et al* 2000). Under such conditions $\delta^{34}S$ values become more positive and may show larger variations between samples (Bloch and Krouse 1992; Brownlow 1996).

Closed system conditions may occur on any scale (McConville *et al* 2000). For example, enrichment in ^{34}S may occur if the sediment pore-fluid cannot exchange

freely with the overlying water column or if the reservoir is restricted (Bloch and Krouse 1992). It may also occur if the sediments are buried and the rate of sulfate reduction is faster than the rate of supply (McConville *et al* 2000). If the system remains closed the precipitating sulfides will become progressively enriched in ^{34}S. This may also be referred to as the 'reservoir' effect and may be described mathematically by the Rayleigh distillation equations (Goldhaber and Kaplan 1974; Emery and Robinson 1993; McConville *et al* 2000). If complete reduction of the sulfate occurs, the resulting sulfide will have the identical isotopic composition as the sulfate from which it was derived (Gautier 1985).

Closed system conditions would have dominated during the formation of the peat acid sulfate soils. When the sea level dropped, back swamp areas became fresh water dominated and restricted the supply of sulfate from sea water. Supply was further limited as sediments were buried. In addition, the accumulation of organic rich sediments may have significantly increased the sulfate reduction rate.

At most of the sites examined there was an increased enrichment in ^{32}S where contemporary sulfides were forming. At some sites this coincided with the oxidation boundary and at some sites it occurred in the upper soil layers. This increased enrichment was linked to the reduction of sulfate that was derived from the oxidation of existing sulfides. At many sites the oxidation of sulfides provided the dominant source of sulfate.

At the clay dominated acid sulfate soil sites the $\delta^{34}S$ CRS was generally more negative than the other environments examined. When these sulfides oxidise it produces sulfates that are also more negative than the other sites. As a result, when bacteria undertake sulfate reduction processes, they have a ready supply of isotopically negative sulfate which they utilise to produce sulfides. Repeated cycling of this process produces sulfides that are more enriched in ^{32}S.

The same process occurs at the peat sites however the initial sulfides that form in these environments are more likely to carry a positive $\delta^{34}S$ signature. Oxidation of these sediments therefore, gives a positive $\delta^{34}S$ sulfate signature as well. Although

bacteria will preferentially uptake the lightest sulfate the fractionation that results in the reformed sulfides may not be as great. Repeated cycles of oxidation and reformation however, should eventually produce negative $\delta^{34}S$ signatures.

The variations in the isotope signature of the sulfides could be further used to discern the provenance of sulfate in surface and ground water following oxidation. Sulfur isotopes have been used to identify and trace sulfate sources from the oxidation of sulfidic materials (Mayer *et al* 2010; Kilminster and Cartwright 2011; Unland *et al* 2012) and this technique could be further developed to quantify the sulfate contributed from various environments into the surrounding waterways.

The isotope signatures for the inland sites suggest another very different environment for the formation of acid sulfate soils. The $\delta^{34}S$ signatures for sulfides were fairly similar to those recorded at the peat sites, however the sulfate $\delta^{34}S$ signatures were considerably higher. The range of $\delta^{34}S$ sulfide values recorded could not be definitively linked to the sulfate source since it was not identified in this study. At these sites sulfate is probably derived from the weathering of parent rocks or from anthropogenic sources but further study is needed to confirm this.

Conclusion

This study has indicated large and consistent differences in the stable sulfur isotopes of different classes of acid sulfate soil materials in south-eastern Australia. These observed changes in the sulfur isotope signatures were related to the different geochemical processes occurring in the varying environments of formation.

Clay dominated acid sulfate soils deposited during the last sea level rise gave strongly negative $\delta^{34}S$ signatures in both the sulfide and sulfate fractions. Peat dominated acid sulfate soils which form in more fresh water environments showed both positive and negative values in the sulfide fraction and only positive values in the sulfate fraction. The isotope signatures recorded in these different environments are linked to whether the environments were open or closed with respect to sulfate supply. The sulfate

supply in sea water was abundant and therefore negative isotope signatures were recorded in the clay sediments. The sulfate supply in the fresh water was more limited which resulted in positive sulfur isotope signatures recorded in the peat sediments. The MBO samples were similar to the peat sediments and also closely aligned with their respective soil samples. The inland samples also gave both positive and negative $\delta^{34}S$ signatures in the sulfide fraction however the $\delta^{34}S$ signature in the sulfate fraction was strongly positive indicating a very different source from the other sites.

This study has clearly indicated stable sulfur isotopes can be used to provide valuable information on the nature of acid sulfate soil materials in south-eastern Australia, as well as on the likely geochemical environment of their formation. It also provides a basis from which to discern the provenance of sulfates in both surface and ground waters.

Acknowledgements

This study was made possible with financial assistance from CRC CARE as part of project 6-6-01-06/07 East Trinity and the School of Environment, Science and Engineering. At the various sites different people assisted with the collection of samples including Diane Fyfe, Vanessa Wong, Leigh Sullivan, Ed Burton, Simon Allery, Salirian Claff, Nadia Toppler, Scott Henderson, Nick Ward and Mark Rosicky.

Chapter 3

Understanding the geochemical processes in acid sulfate soils undergoing remediation, using stable sulfur isotopes

Introduction

The CRC CARE National Acid Sulfate Soil Demonstration Site is located on the eastern side of Trinity Inlet, near Cairns in far north Queensland (145°48' E, 16°56' S; Figure 3.1). The site, simply referred to as East Trinity, comprises 940 ha of deeply stratified Holocene sediments overlying Pleistocene basement strata down to 80 m (Smith *et al* 2004). The far north Queensland climate is characterised by very humid, wet summers and mild relatively dry winters. The mean annual rainfall for Cairns is 2223 mm and monthly temperatures range from a minimum of 16 °C in July and August to a maximum of 32 °C in December and January (Bureau of Meteorology 2012).

In the early 1970s the East Trinity property was developed for sugarcane production. This involved the construction of a bund wall to prevent tidal entry and the installation of pumps to assist with drainage of the intertidal wetland (Smith *et al* 2004). Floodgates installed in the bund wall at the creek outlets allowed excess wet season water to escape more rapidly and reduced the period of inundation. The drainage program reduced water levels to approximately -0.6 to -0.8 m relative to mean sea level (Johnston *et al* 2009a).

At the time of the development little was known of the impacts of acid sulfate soils and it was not until the early 1990s that acid sulfate soils were identified on the site, by which time considerable degradation had already occurred. The development of the site had a two-fold impact on the environment. Firstly, the drainage of the land lowered the natural water table and allowed oxygen to enter the soil. This initiated the oxidation of the acid sulfate soil materials, producing a variety of iron compounds and sulfuric acid. Secondly, the exclusion of tidal water from the site severely limited the areas ability to neutralise any acid that was produced and exacerbated the environmental degradation (Smith *et al* 2004).

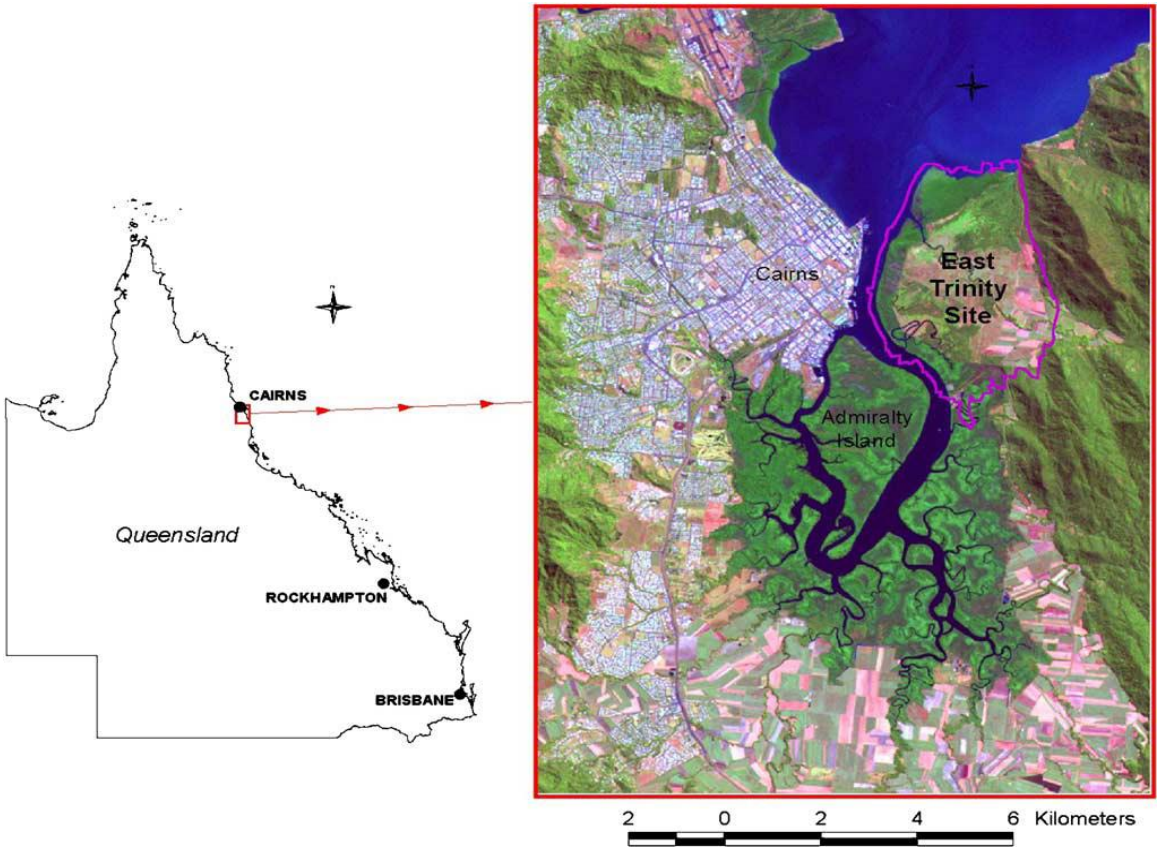

Figure 15 Location of the East Trinity site (Powell and Martens 2005).

The oxidation of acid sulfate soils at East Trinity produced an array of both on-site and off-site environmental problems. In particular, the disturbance of pyritic material produced sulfuric acid, which lowered the pH of the soil. This acid was then flushed into the surrounding creeks where the low pH water caused the mobilisation of iron, aluminium and other heavy metals. Often these extreme concentrations of acid and metals were discharged off-site into Trinity Inlet resulting in severely diminished populations of aquatic biota and significant fish kills (Russell and Helmke 2002; Smith *et al* 2004).

The problem at East Trinity is indeed critical. Hicks *et al* (1999) estimated the property had produced 72 000 t of sulfuric acid since it was disturbed and would continue to produce acid at a rate of 34 t/ha/yr. Soil investigations have shown approximately 65% of the floodplain area contains at least some acid sulfate soils and approximately 110 ha are severely acidified (Fitzpatrick *et al* 1999). Water discharged

into Trinity Inlet has been recorded containing up to 6000 times the Australian and New Zealand Environmental and Conservation Council (ANZECC) guidelines for aluminium and a pH average of 3.4 (Fitzpatrick *et al* 1999; Hicks *et al* 1999).

Prior to drainage the site was an ecologically diverse area, comprising an estuarine floodplain with five distinct mangrove communities and supratidal flats supporting samphire communities (Smith *et al* 2004; Powell and Martens 2005). As shown in Plate 3.1 much of these communities have been replaced by regrowth *Melaleuca* woodlands. Other acid-tolerant plant species and weeds have invaded the site. Ironically, the degradation of the site caused by the oxidation of acid sulfate soils ultimately meant it was unsuitable for the purpose for which it was originally drained – sugarcane production.

Following the failed agricultural attempt, ownership of the property passed through several developers, none of which were able to gain the necessary planning approvals to further develop the site. The area was neglected and continued to degrade. In May 2000 the Queensland State Government purchased the East Trinity property and a remediation plan was developed.

The remediation of acid sulfate soil landscapes has two principle directives. Firstly, to neutralise any existing acidity generated from the oxidation of pyritic material to prevent further degradation of the surrounding environment. Secondly, remediation should prevent further oxidation of the pyrite. This is usually achieved by reestablishing a higher water table to limit oxygen intrusion into the soil profile. At East Trinity these objectives where achieved with a remediation plan that involved lime assisted tidal exchange.

Plate 3.1 Historic photo from 1980s showing acidified and iron stained land and waterways on the inside of the bund wall and the death of mangroves on the outside as a result of acid sulfate soil oxidation (Powell and Martens 2005).

Prior to the adoption of the lime assisted tidal exchange strategy other strategies were considered and ultimately dismissed as being impractical or uneconomical. The adopted strategy had several advantages over other treatments:

- The East Trinity site was originally an intertidal wetland with dominant mangrove and samphire communities. The reintroduction of tidal exchange allows the site to revert to a pre-drainage state.
- The buffering capacity of seawater with the added assistance of hydrated lime neutralises existing sulfuric acid and precipitates iron, aluminium and toxic metals.
- Daily tidal exchange raises the level of the permanent water table and halts the process of oxidation of the pyritic layers, thereby preventing further generation of acid from these areas.

- Daily flooding hydraulically forces acidic cations deeper into the soil profile, limiting their export from the soil via slow diffusion into surface waters.
- The use of hydrated lime helps maintain bicarbonate and calcium levels in seawater, which is fundamental to the health of aquatic biota (especially shelled organisms) (Smith *et al* 2004).

The extent of tidal exchange was managed through the manipulation of flap gates and automatic tidal regulators to ensure neighbouring farms were not affected by saline water. After careful consideration it was decided +0.5 m AHD would be the upper limit of daily tidal exchange.

There have been numerous studies examining the geochemical changes that have occurred at East Trinity since the introduction of the lime assisted tidal exchange remediation strategy. Some of these studies have examined the hydrology and water chemistry of the site (Johnston *et al* 2009a, 2011a), contemporary pedogenesis (Johnston *et al* 2009b) and the abundance and reactivity of aluminium, iron and trace metals (Grogan *et al* 2003; Johnston *et al* 2010; Keene *et al* 2010; Burton *et al* 2011a, b).

In addition to providing a solution to a severe environmental problem, the strategy to allow tidal inundation to the site provided the opportunity to study the behavior of acid sulfate soils during a climate change induced sea level rise.

The use of stable sulfur isotopes is a geochemical technique that has been given minimal attention at East Trinity. In a study examining contemporary pedogenesis Johnston *et al* (2009b) used sulfur isotopes to identify the depth to which tidal inundation was on impacting the soil profile and consuming acidity. Their results indicated tidal inundation was only affecting the sulfuric horizons and not the underlying sulfidic material. This chapter will expand on the use of this technique and provide further insights into the geochemical changes occurring at East Trinity.

Aim

The aim of this chapter is to examine the use of stable sulfur isotopes to assist in the understanding of the geochemical processes operating in acid sulfate soils subject to remediation by lime assisted tidal exchange. The findings of this study could also be used to infer geochemical changes as a result of sea level rise in acid sulfate soil landscapes.

Methodology

Sampling sites

A total of 5 sites were examined across the East Trinity property. Sites 1, 2 and 3 represent a toposequence across the site. Site 1 has a surface elevation of ~0.5 m AHD and has been unaffected by tidal inundation. Site 2 is at a slightly lower elevation (~0.1 m AHD) and receives some tidal flushing (Johnston *et al* 2011a). Site 3 is again topographically lower (~ –0.1 m AHD) and remains inundated by seawater for most of the time (Johnston *et al* 2009b). This site has been receiving tidal inundation since 2002, and for the purpose of this study, is considered to be long term remediated.

Sites 4 and 5 have not received any tidal flushing. Site 4 has not been remediated at all and Site 5 has been inundated by predominately fresh water. These sites will be compared to determine the influence the remediation strategy is having both temporally and spatially on the geochemistry of the site.

Sample collection and preservation

Soil samples were collected using a Russian D-section corer to a depth of 1.5 m. At each site multiple cores were taken, then sectioned into 10 cm depth increments. Replicate depth increments were combined and homogenised to provide sufficient soil sample for analysis. Soil samples were placed in thick plastic bags to reduce oxidation, then frozen.

Chemical analysis

In the laboratory the following chemical analyses were performed on each depth increment for each site. The moisture content of all samples was determined by drying a sub sample of the frozen soil at 105 °C for 7 days (Rayment and Lloyds 2011). The moisture content of the soils dried to 65 °C for total carbon, sulfur and nitrogen analysis was also determined. Where applicable, results are calculated on an oven dried mass. All analyses were conducted at Southern Cross University.

pH, electrical conductivity

Frozen soil samples were placed in a centrifuge tube with Milli-Q water in a 1:5 soil:water ratio (Rayment and Lloyds 2011). The tubes were shaken in an end-over-end tumbler for 1 hour, then allowed to settle for 15 minutes. pH was recorded using an Ionode IJ44 pH electrode and electrical conductivity recorded with a TPS Conductivity sensor.

Total carbon, nitrogen and sulfur

Soil samples were dried at 65 °C then finely ground in a mortar and pestle for analysis of total carbon, nitrogen and sulfur using a LECO-CNS 2000 induction furnace analyzer (detection limit 0.01 % C, N, S). The carbon:nitrogen ratio was also calculated.

Water soluble chloride and sulfur analysis

Chloride and sulfur was analysed by ICP-OES following extraction in a 1:5 soil:water suspension. Frozen soil samples were placed in centrifuge tubes with deoxygenated Milli-Q water and shaken for 1 hour. Samples were centrifuged for 5 minutes at 3000 rpm and 10 mL of the supernatant extracted and filtered through a 0.45 µm filter for analysis by ICP-OES according to APHA Method 3120 (APHA 2005). Sulfur results were converted to sulfate according to the method provided in the Acid Sulfate Soils Laboratory Methods Guidelines (Ahern *et al* 2004). The chloride:sulfate ratio was calculated. The remaining supernatant was retained for isotope analysis. Duplicate

analysis gave a precision of ±9% for chloride and ±7% for sulfur with a detection limit of 0.05 mg/L).

Exchangeable and acid soluble sulfur analysis

In acid sulfate soils one of the principle products of oxidation is sulfate, which can exist in a variety of forms. According to the Acid Sulfate Soils Laboratory Methods Guidelines (Ahern *et al* 2004), sulfate can be determined in exchangeable and acid soluble forms. For this study, exchangeable and acid soluble sulfate was extracted using a sequential extraction procedure.

Exchangeable sulfate was measured using a 1 M KCl extract in a 1:40 soil:solution ratio (McElnea and Ahern 2004). In accordance with recommendations from Maher *et al* (2004) the analysis was conducted on frozen soil samples. Centrifuge tubes were shaken for 4 hours then allowed to stand for 12 hours before being centrifuged for 5 minutes at 3000 rpm. The supernatant was filtered with a 0.45 µm filter and analysed for sulfur by ICP-OES. The remaining soil was rinsed with Milli-Q water and retained for acid soluble sulfate analysis.

The acid soluble sulfate extraction is principally targeting the relatively insoluble iron and aluminium hydroxy sulfate compounds such as jarosite and natrojarosite. For this procedure 4 M HCl was added to the centrifuge tube in a 1:40 soil:solution ratio (McElnea and Ahern 2004). The solution was shaken for 16 hours then centrifuged at 3000 rpm for 5 minutes and filtered through a 0.45 µm filter. The supernatant was analysed by ICP-OES. Duplicate analysis gave a precision of ±6.5% and ±8% for KCl and HCl SO_4 respectively with a detection limit of 0.05 mg/L.

Sequential Iron Analysis

A sequential extraction procedure was employed to differentiate readily available and less available forms of iron. Readily available iron (termed reactive iron) was extracted using 1 M HCl from frozen soil (Wallman *et al* 1993). The suspensions were shaken for 16 hours then centrifuged. Extracts were analysed for ferrous and total iron using the 1,10 phenanthroline method (APHA 3500) (APHA 2005). Both

ferrous and total iron trapping solutions contained a phenanthroline ammonium acetate buffer solution. Total iron traps also contained hydroxyl ammonium chloride as a reducing agent. Samples were analysed by HACH spectrophotometer. Ferric iron is represented by total iron minus ferrous iron. Reactive iron species are reported as FeR^{2+} for reactive ferrous iron and FeR^{3+} for reactive ferric iron.

Residual soil samples were rinsed with 1 M $MgCl_2$ before the less available forms of iron was extracted using a citrate dithionite extraction procedure of Kostka and Luther (1994). Accordingly, 40 mL of a solution containing 0.2 M sodium citrate, 0.35 M acetic acid and sodium dithionite was added to the centrifuge tubes. The tubes were shaken for 16 hours then centrifuged. Aliquots were pipetted into phenanthroline ammonium acetate traps and analysed by HACH spectrophotometer. Results are reported as FeCDE. Duplicate analysis gave a precision of ±7% with a detection limit of 0.05 mg/L Fe.

Reduced inorganic sulfur analysis

In acid sulfate soils, reduced inorganic sulfur species typically include iron monosulfides – operationally defined as acid volatile sulfides (AVS), elemental sulfur (ES) and iron disulfides defined as chromium reducible sulfur (CRS). A procedure to sequentially extract AVS, ES and CRS was employed.

Acid volatile sulfide analysis was conducted on frozen soil (Maher *et al* 2004) following the diffusion method of Hseih *et al* (2002) and a modified apparatus described by Burton *et al* (2007). Accordingly, frozen soil was weighed into 50 mL centrifuge tubes under a nitrogen atmosphere to minimise oxidation. A 10 mL aliquot of 6 M HCl was added with 1 mL of 0.1 M ascorbic acid and the samples shaken for 18 hours. Evolved hydrogen sulfide gas was trapped in 10 mL vials containing 5 mL of zinc acetate and sodium hydroxide trapping solution. Following shaking the trapping solutions were removed and quantified by iodometric titration. Residual soil samples were centrifuged for elemental sulfur analysis and the supernatant discarded.

Samples were rinsed with Milli-Q water before 10 mL of toluene was added (Burton *et al* 2011a, b). Centrifuge tubes were shaken for 18 hours and allowed to settle. A

subsample of the toluene fraction was extracted for analysis of elemental sulfur by high performance liquid chromatography (HPLC) with a Dionex UltiMate 3000 system. The supernatant was discarded and the residual soil was rinsed for chromium reducible sulfur analysis.

Chromium reducible sulfur analysis was conducted according to the method of Sullivan *et al* (2000). Soil samples were reacted with chromium metal powder and 6 M HCl to evolve hydrogen sulfide gas which was trapped in a zinc acetate trapping solution. The trapping solutions were quantified by iodometric titration to give the residual pyrite fraction. Duplicate analysis gave a precision of ±10% with a detection limit of 0.001 %S.

Sulfur isotope analysis

Stable sulfur isotope analysis was conducted on selected layers from each site. Both sulfide and sulfate fractions were examined. The sulfide fraction was extracted using the chromium reducible sulfur procedure detailed previously. When used as a stand-alone technique this process will extract all reduced inorganic sulfur species including acid volatile sulfur, elemental sulfur and pyrite sulfur (Sullivan *et al* 2000). To extract samples for isotope analysis additional chromium reducible sulfur runs were performed on the selected soil samples. For these runs the trappings solutions were not titrated and the zinc sulfide (ZnS) precipitate was rinsed three times with Milli-Q water. The samples were centrifuged, the remaining water decanted and the precipitate dried in the oven overnight.

A range of sulfate fractions were examined including water soluble, exchangeable and acid soluble sulfate. Water soluble sulfate was examined on the supernatant remaining after the chloride and sulfate analysis. The solution was extracted and syringe filtered into a new centrifuge tube. Approximately 10 mL of 1 M barium chloride ($BaCl_2$) solution was added to precipitate barium sulfate ($BaSO_4$). The precipitate was then rinsed, centrifuged and oven dried.

Exchangeable and acid soluble sulfate for isotope analysis was extracted using nearly the same sequential procedure detailed previously. The only difference was a 1:10

soil:solution ratio. Following extraction, the suspension was centrifuged and transferred to a new centrifuge tube. $BaSO_4$ was precipitated with a 1 M $BaCl_2$ solution, which was then rinsed, centrifuged and oven dried.

ZnS and $BaSO_4$ precipitates were analysed for $\delta^{34}S$ by Continuous Flow Isotope Ratio Mass Spectrometry (CF-IRMS) using a Thermo Flash EA 1112 coupled to a Thermo Delta V Plus IRMS. NIST reference material 8555 was used for calibration. Results are presented as $\delta^{34}S_{(CRS)}$ for the sulfide fraction, $\delta^{34}S_{(WS\ SO4)}$ for the water soluble sulfate fraction, $\delta^{34}S_{(KCl\ SO4)}$ and $\delta^{34}S_{(HCl\ SO4)}$ for the exchangeable and acid soluble sulfate fractions, respectively. Duplicate analysis gave a precision of ± 0.3‰.

Results

Sites 1, 2 and 3 represent a sequence of the remediation strategy across the site. Site 1 has not received any tidal inundation and remains in a drained and severely acidified state. Site 3 was previously drained and acidified but has been completely inundated with tidal water since the program commenced in 2002. Site 2 is a transition environment between sites 1 and 3 and receives intermittent tidal exchange.

Figures 3.2–3.4 show some of the geochemical changes across the site from an unremediated post-drainage state to long term remediated. Site 1 is typical of an acid sulfate soil profile that has been oxidising for some time. The pH at the surface was ~4.0 and the chloride:sulfate ratios (Figure 3.5) are below 1 throughout the majority of the profile. The spike in sulfate concentration at approximately 80 cm depth indicates this is where the oxidation front is occurring. It is also at this depth that appreciable pyrite concentrations are encountered. The peak in HCl extractable SO_4 seen between 20 and 60 cm depth, suggest previous oxidation of pyrite and accumulation of relatively insoluble iron hydroxy sulfate compounds such as jarosite, as observed by Johnston *et al* (2009b, 2010) and Keene *et al* (2010, 2011).

Site 2 is showing some influence from the remediation strategy. pH has increased to almost 6.0 and remains relatively steady down the profile to approximately 120 cm

depth. There has also been an increase in EC at the surface and the chloride:sulfate ratio has risen to 2. Although still quite low, this ratio indicates the chloride concentration is now higher than the sulfate concentration. Below 90 cm the chloride:sulfate ratio falls below 1 and this layer appears to be unaffected by the tidal waters used in the remediation strategy at present (Johnston *et al* 2009b). Figure 3.4 indicates some reformation of sulfides in the upper 50 cm of the profile at this site – a process noted in other studies (Johnston *et al* 2009b, Burton *et al* 2011a, b).

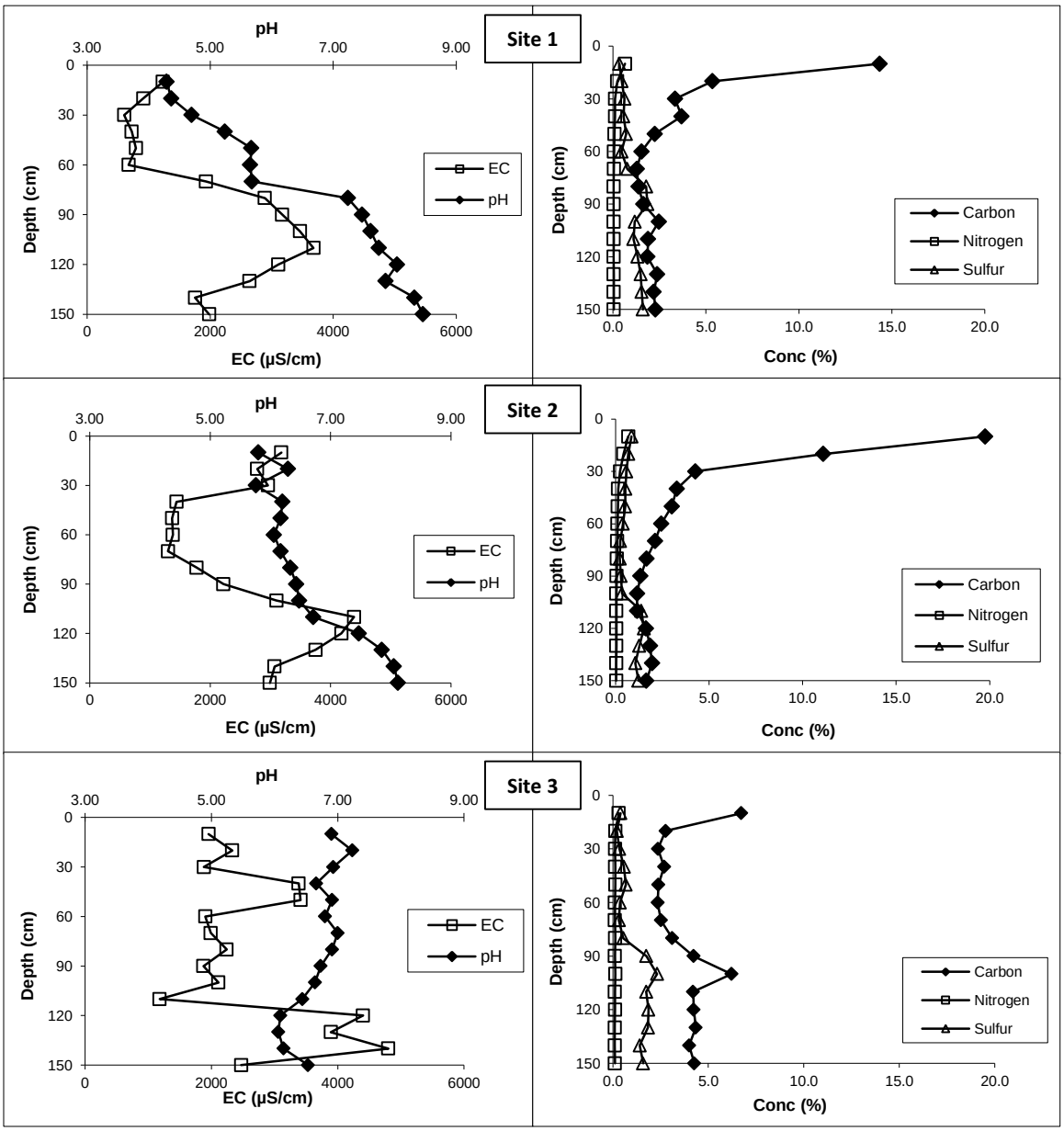

Figure 3.2. pH and electrical conductivity (EC) (left) and total carbon, nitrogen and sulfur (right) for Sites 1, 2 and 3.

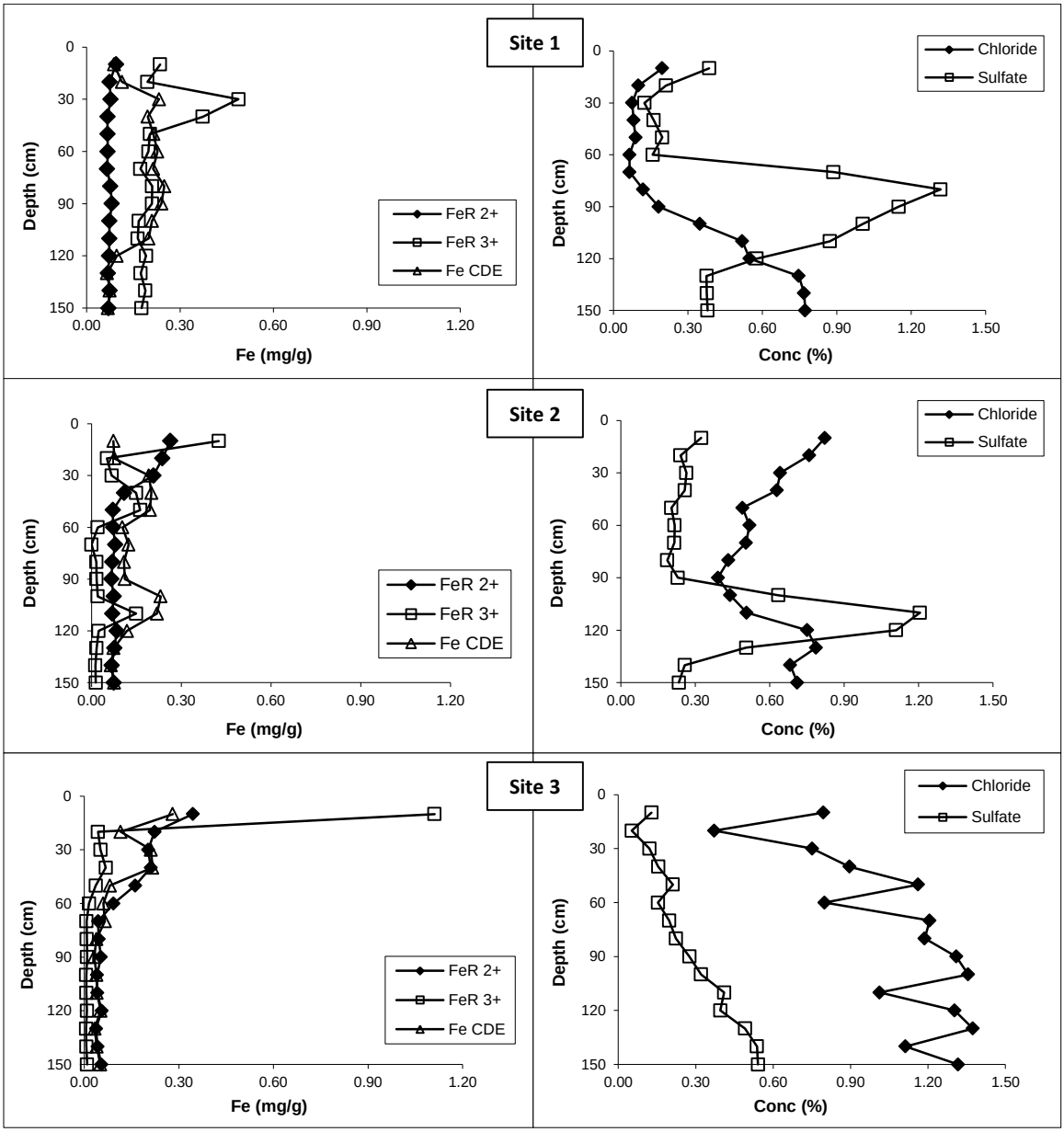

Figure 3.3. Reactive ferrous (FeR 2+), ferric (FeR 3+) and insoluble Fe (FeCDE) (left) and chloride and sulfate concentrations (right) for Sites 1, 2 and 3.

Site 3 has even higher concentrations of reformed sulfides in the upper 50–60 cm. In particular there is a greater abundance in AVS and ES forms as also seen by Burton *et al* (2011a, b) and Johnston *et al* (2011b, 2012). pH has risen to circum-neutral and the chloride:sulfate ratio is approaching that of seawater. There is considerably less total carbon at the surface of this site compared to the previous two sites (Figure 3.2). This may be due to organic matter consumption during the sulfate reduction process following inundation (Bottcher and Lepland 2000; Morgan *et al* 2012a, b).

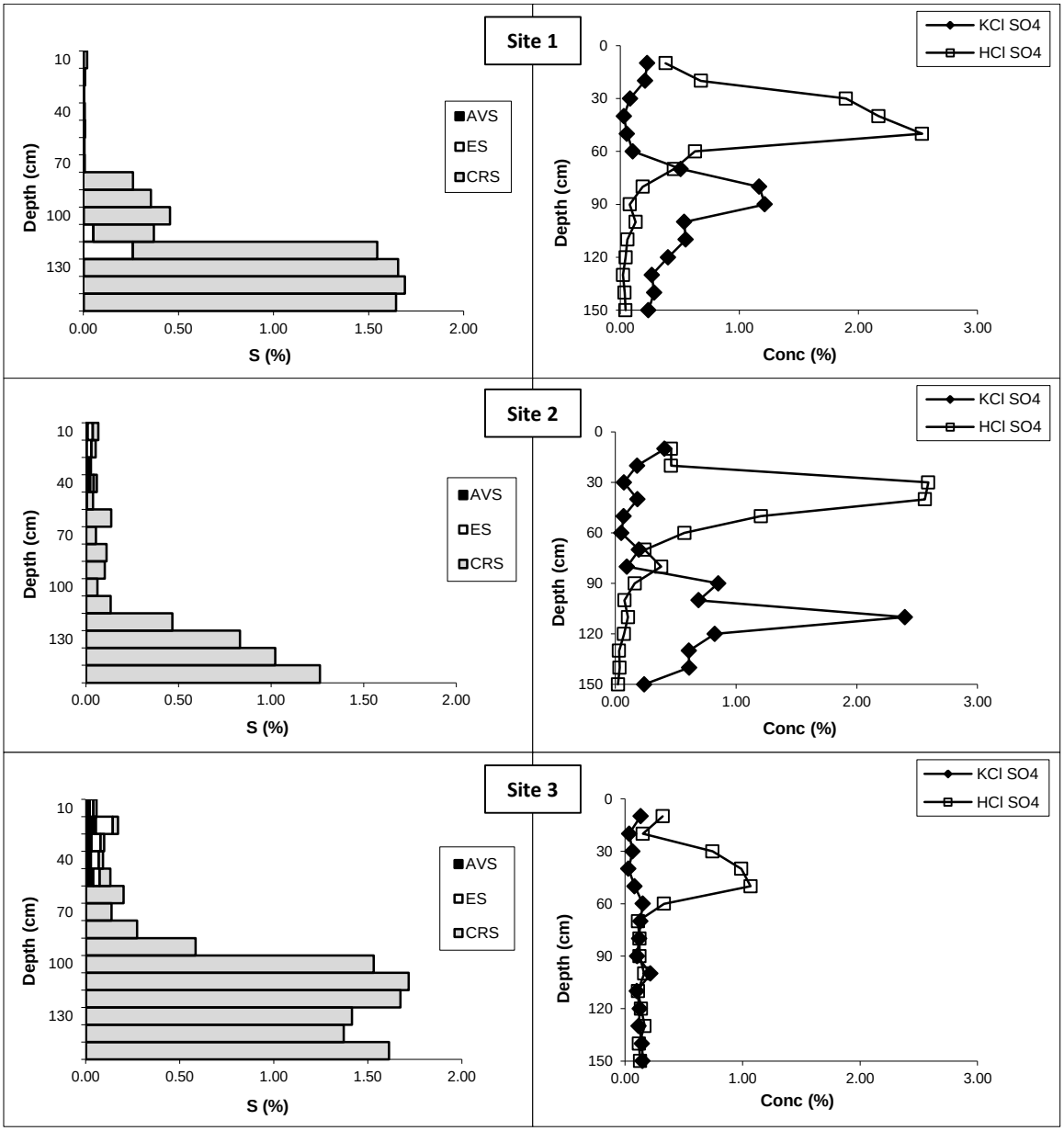

Figure 3.4. Acid volatile sulfur (AVS), elemental sulfur (ES) and chromium reducible sulfur (CRS) (left) and KCl and HCl extractable SO_4 (right) for Sites 1, 2 and 3.

The spikes in KCl extractable SO_4 observed at Sites 1 and 2 are not evident at Site 3. It is likely that exchangeable sulfate at this site has been converted by sulfate reduction processes into sulfides (Burton *et al* 2011a, b; Stam *et al* 2011). The peak in HCl extractable SO_4 is also smaller and there is a significant spike in FeR^{3+} at the surface. According to Johnston *et al* (2010) the long term inundation with sea water allows the establishment of reducing conditions which favour the dissolution of

jarosite and the mobilisation of Fe^{3+} that accumulates as surficial iron-rich layers at this site.

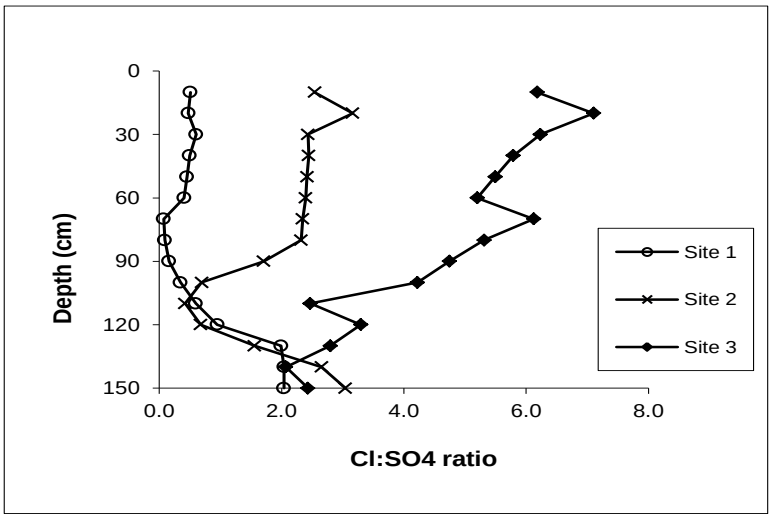

Figure 3.5 Chloride:sulfate ($Cl:SO_4$) ratios for Sites 1, 2 and 3.

The results indicate there has also been considerable geochemical change in the stable sulfur isotope signatures across Sites 1–3 (Figure 3.6). At Site 1, $\delta^{34}S_{(CRS)}$ ranges from -28.4 ‰ to -33.6 ‰ and shows a maximum fractionation from seawater sulfate of 54.2 ‰. This maximum value occurs at 80 cm depth at the oxidation front. $\delta^{34}S_{(WS\ SO4)}$ values are also strongly negative throughout the profile suggesting the dominant source of sulfate is from the oxidation of isotopically negative pyrite. The lowest $\delta^{34}S_{(WS\ SO4)}$ also corresponds with the most negative $\delta^{34}S_{(CRS)}$ suggestive of cycling between sulfide and sulfate fractions (Maher 2005).

A few of the $\delta^{34}S_{(KCl\ SO4)}$ at Site 1 are less depleted in ^{34}S than other layers. This is the only occurrence in this study where the exchangeable sulfate fraction has a markedly different isotope signature to the corresponding water soluble sulfate fraction.

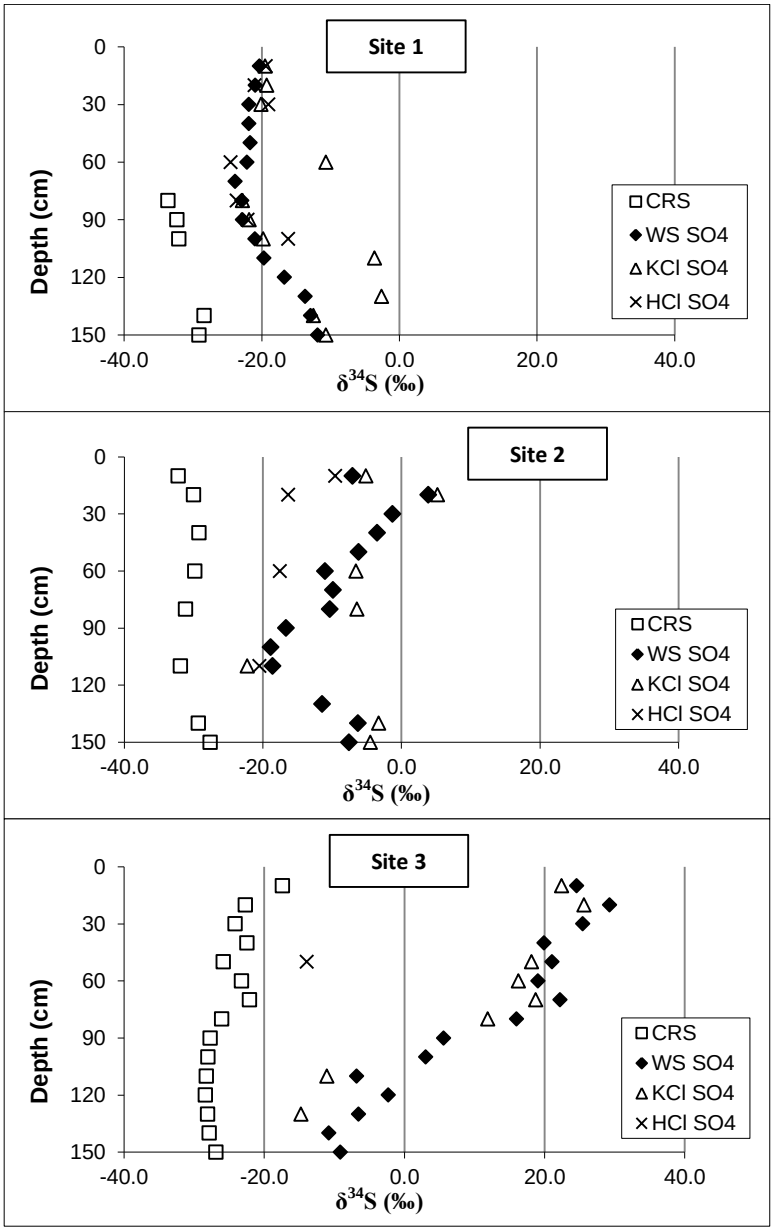

Figure 3.6. $\delta^{34}S$ of the sulfide and sulfate fractions for Sites 1, 2 and 3. Sulfides are represented by the chromium reducible sulfur fraction (CRS). The sulfate fraction includes water soluble sulfate (WS SO_4), exchangeable sulfate (KCl SO_4) and acid soluble sulfate (HCl SO_4).

At Site 2, the introduction of tidal water is starting to have some effect on the sulfur isotope signatures particularly in the sulfate fractions. The $\delta^{34}S_{(CRS)}$ are fairly similar to Site 1 with a range of -27.6 ‰ to -32.2 ‰, however the water soluble sulfate fraction shows a marked increase in $\delta^{34}S$ up to +3.8 ‰ near the surface. In the 20 cm and 60 cm layers the $\delta^{34}S_{(HCl\ SO4)}$ lies between the sulfide and water soluble sulfate fractions.

At Site 3 the geochemical shift in the sulfur isotope signature is even more pronounced. In the upper 100 cm of the profile the $\delta^{34}S_{(WS\ SO4)}$ is positive with a maximum value of +25.6 ‰. This is higher than the $\delta^{34}S$ of seawater sulfate (+20.6 ‰ – Bottcher *et al* 2004) and may be a function of light sulfate removal through sulfate reduction (Wijsman *et al* 2001; Farquhar *et al* 2008). There has also been a shift in $\delta^{34}S_{(CRS)}$. In the upper 70 cm the $\delta^{34}S_{(CRS)}$ averages -22.5‰ (SD=2.6, n=7), whereas in the lower half of the profile the $\delta^{34}S_{(CRS)}$ averages -27.6 ‰ (SD=0.8, n=8). At this site only 1 sample was extracted for acid soluble sulfate, however it is also much lower than the $\delta^{34}S_{(WS\ SO4)}$ and higher than the $\delta^{34}S_{(CRS)}$.

Non-tidal affected sites

Sites 4 and 5 have not been affected by the tidal exchange remediation strategy. Site 4 remains in a completely untouched state and is used to demonstrate the severity of acid sulfate soils at East Trinity (Plate 3.2). Site 5 has undergone some remediation through the use of fresh/brackish water rather than tidal water.

Plate 3.2. Iron oxide accumulations on the surface at Site 4 (width approximately 50 cm).

Site 4 was extremely degraded with some areas completely scalded (Plate 3.3). At the time of sampling there was fresh water pooling on the site and extensive accumulations of iron oxide minerals on the surface (Plate 3.2).

Plate 3.3. Site 4 showing iron staining and scalded areas.

The lack of tidal exchange at Sites 4 and 5 is quite evident from the soil properties (Figures 3.7–3.9). EC was quite low at both sites and remained low throughout the profile at Site 4. The pH at Site 4 was slightly higher than expected given the obvious degradation but this may be due to sulfide reformation processes occurring near the surface (Figure 3.9). The low total carbon concentrations recorded at Site 4 may also be due to sulfate reduction processes and sulfide formation or may be a function of the surface scalding. According to Rosicky *et al* (2002a, b, 2004) scalds occur where top soil conditions are too hostile to support plant growth.

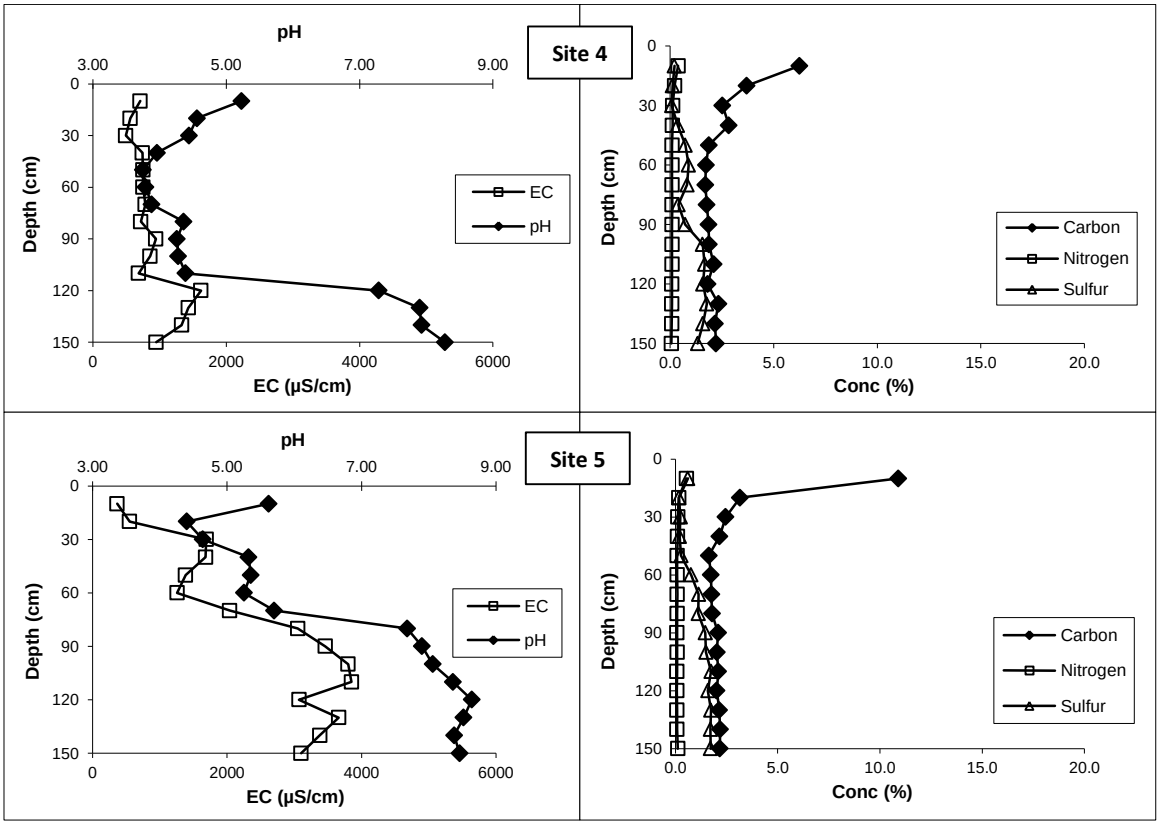

Figure 3.7. pH and electrical conductivity (EC) (left) and total carbon, nitrogen and sulfur (right) for Sites 4 and 5.

Both Sites 4 and 5 displayed peaks in iron concentrations at or near the surface with a dominance of FeR^{3+}. The extreme FeCDE concentrations combined with elevated HCl SO_4 at Site 4 are indications of abundant jarosite formation and suggest the site has experienced considerable oxidation at depth. This is also supported by the low chloride:sulfate ratios (Figure 3.10). Site 4 has oxidised to almost 90 cm below the surface but considerable pyrite concentrations still remain at depth.

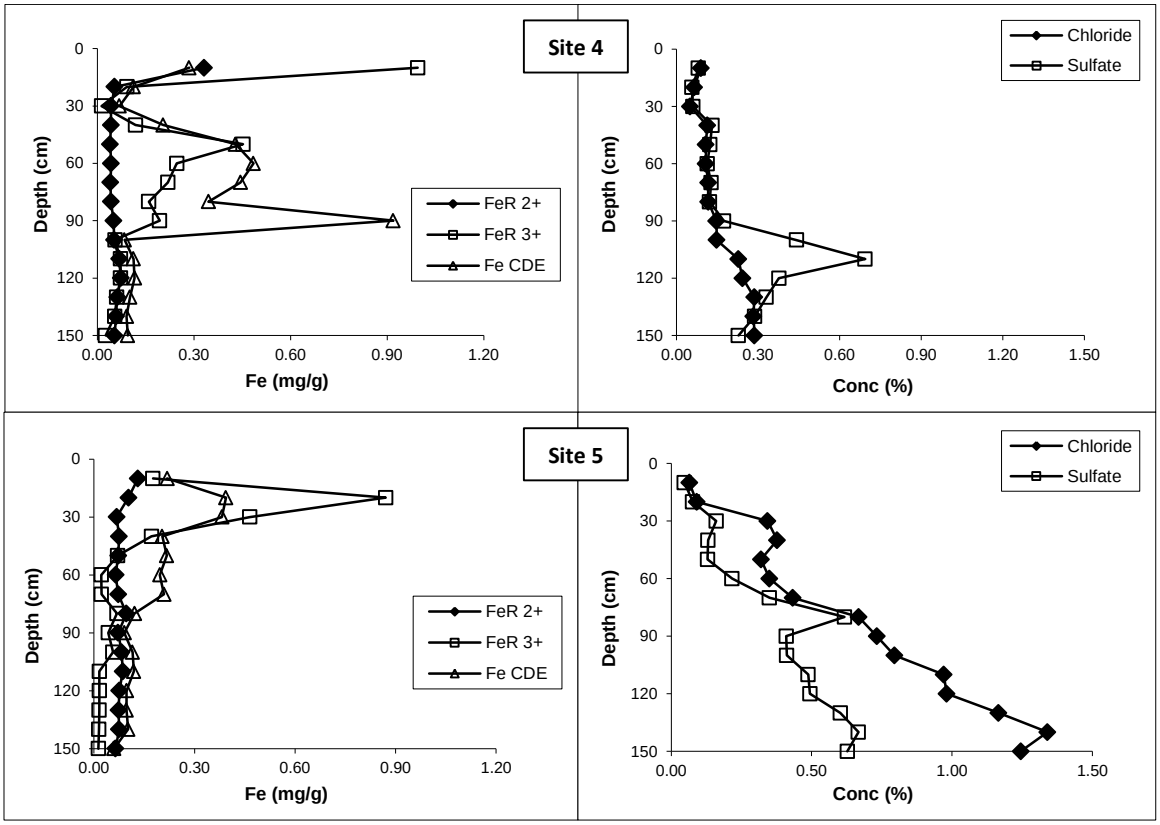

Figure 3.8. Reactive ferrous (FeR 2+), ferric (FeR 3+) and insoluble Fe (FeCDE) (left) and chloride and sulfate concentrations (right) for Sites 4 and 5.

The sulfur isotope signatures for Sites 4 and 5 are displayed in Figure 3.11. At Site 4, $\delta^{34}S_{(WS\ SO4)}$ is strongly negative below 40 cm. Interestingly, the $\delta^{34}S_{(WS\ SO4)}$ above 40 cm was less depleted in ^{34}S. This may be due to reformation of sulfides near the surface. As with other sites the lowest $\delta^{34}S_{(WS\ SO4)}$ coincided with the zone most probably experiencing pyrite oxidation. $\delta^{34}S_{(CRS)}$ and $\delta^{34}S_{(WS\ SO4)}$ are similar at Site 4 suggesting oxidation of pyrite is the dominant source of sulfate.

Site 5 stable isotope signatures show more variation down the profile than Site 4. At the surface $\delta^{34}S_{(WS\ SO4)}$ values were slightly positive then became more negative down the profile. Below 80 cm depth $\delta^{34}S_{(WS\ SO4)}$ increased slightly. At each measured point down the profile $\delta^{34}S_{(CRS)}$ is more depleted in ^{34}S than the corresponding $\delta^{34}S_{(WS\ SO4)}$, suggesting oxidation of pyrite may not be the only source of sulfate at this site. Prior to freshwater ponding, this site received tidal water, as evidenced by the high EC and chloride concentrations below 30 cm depth.

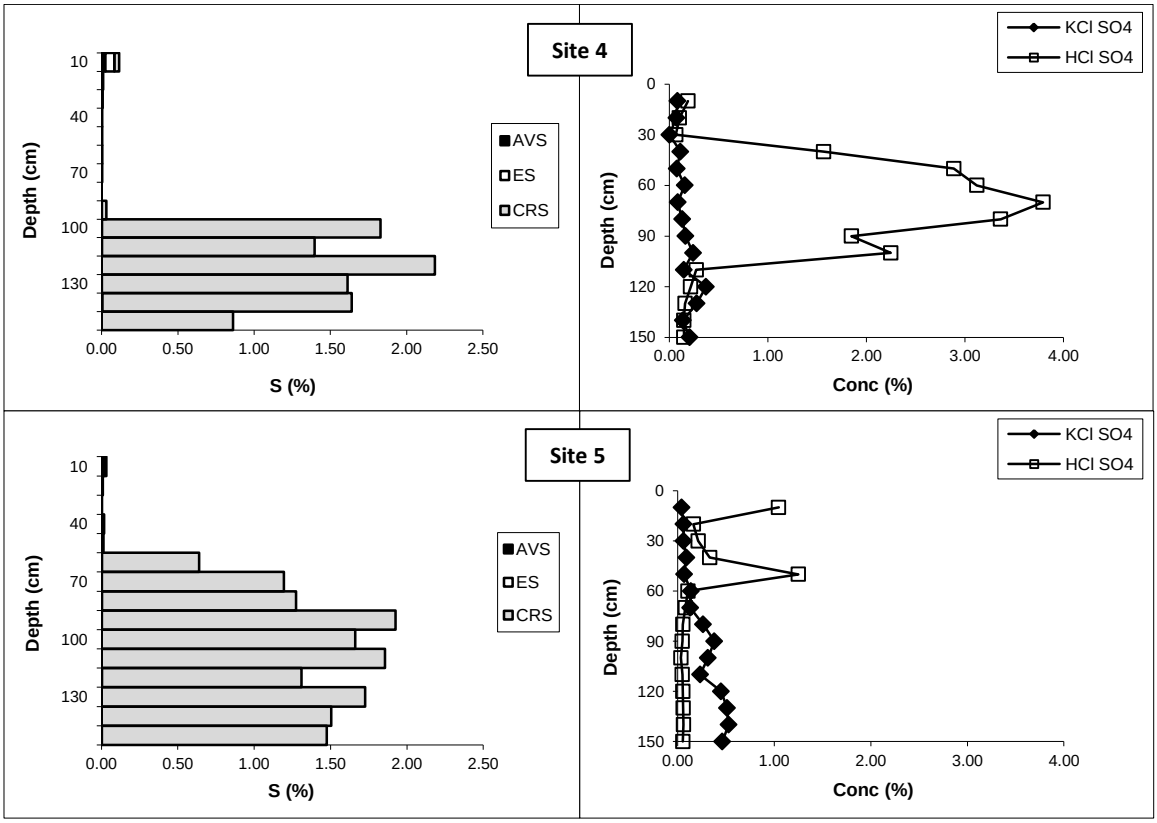

Figure 3.9. Acid volatile sulfur (AVS), elemental sulfur (ES) and chromium reducible sulfur (CRS) (left) and KCl and HCl extractable SO_4 (right) for Sites 4 and 5.

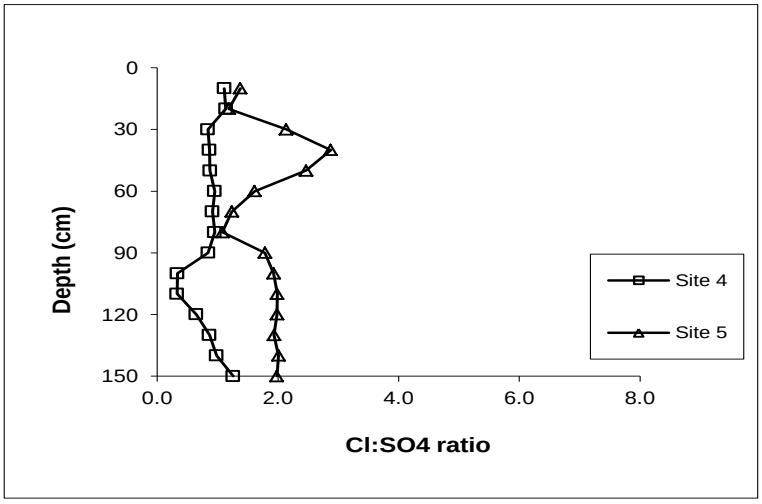

Figure 3.10. Chloride:sulfate ($Cl:SO_4$) ratios for Sites 4 and 5.

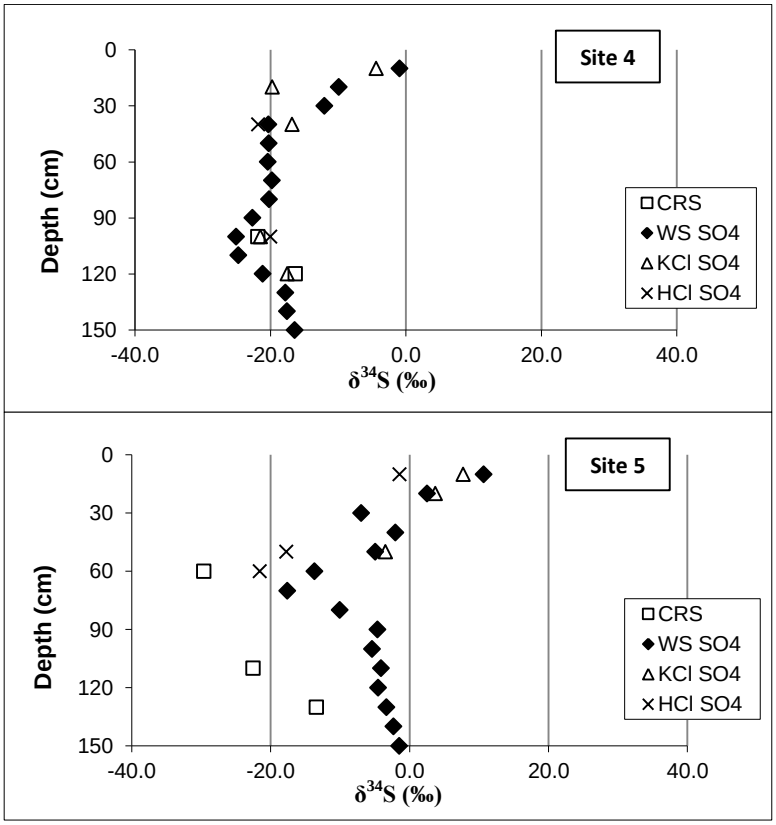

Figure 3.11. $\delta^{34}S$ of the sulfide and sulfate fractions for Sites 4 and 5. Sulfides are represented by the chromium reducible sulfur fraction (CRS). The sulfate fraction includes water soluble sulfate (WS SO_4), exchangeable sulfate (KCl SO_4) and acid soluble sulfate (HCl SO_4).

Discussion

The effect of tidal inundation on soil geochemistry

The lime assisted tidal exchange remediation strategy is having considerable effect on the geochemistry of the East Trinity property. The difference in surface elevation between Sites 1–3 means that a toposequence, as provided here, can be used as a proxy temporal sequence of tidal inundation. This suggests pH has increased at Sites 1, 2 and 3 (Figure 3.2) with salt water intrusion, particularly in the upper soil layers, indicating the tidal water is providing sufficient buffering capacity to neutralise existing acidity and raise the pH to nearly neutral (Johnston *et al* 2009a; 2011a). There has also been a significant change in the chloride:sulfate ratio at these sites with

an increase in values from <1 at Site 1 to >6 at Site 3 (Figure 3.5). Below approximately 120 cm depth the chloride:sulfate ratios are very similar suggesting tidal influence may be limited to this depth (Johnston *et al* 2009b).

There have also been marked changes in the abundance of the different iron species between Sites 1–3 (Figure 3.3). Following long term tidal inundation there is a decrease in FeCDE below 50 cm and an increase in FeR^{2+} above 50 cm. Studies by Keene *et al* (2010, 2011) and Burton *et al* (2011a, b) showed an abundance of FeR^{2+} in the surface and subsurface layers, whereas this study shows a peak of FeR^{3+} at the surface of Site 3. According to Johnston *et al* (2011b) this peak is likely to be an accumulation of poorly crystalline goethite and lepidocrocite.

The accumulations of sulfides in the upper layers of Sites 2 and 3 (Figure 3.4) are contemporary formations (Johnston *et al* 2009b; Keene *et al* 2010, 2011; Burton *et al* 2011a). Both of these sites underwent considerable oxidation due to drainage, hence sulfide formation could only have occurred following a geochemical shift in the redox conditions from oxidising to reducing (Smith *et al* 2004, Johnston *et al* 2011a). The relative abundance of AVS and ES fractions suggests the current conditions favour the accumulation of these forms. Similar results were returned by Burton *et al* (2011a, b) and Keene *et al* (2011) with the AVS mineral identified as greigite. At depth pyrite is the dominant sulfide mineral.

Changes in sulfur isotope signature following inundation

The use of stable sulfur isotopes is a technique that can be used to examine geochemical processes and identify or trace different sulfur sources (Hendry *et al* 1989; Dold and Spangenberg 2005; Unland *et al* 2012). In coastal acid sulfate soil landscapes, iron sulfide minerals, particularly pyrite are formed by the reduction of sulfate (most commonly from seawater) in the presence of reduced iron. The process of sulfate reduction is bacterially mediated and often brings about a shift in the isotopic signature of the resultant sulfide (Bottcher *et al* 1998; Bruchert and Pratt 1999; Stam *et al* 2011). According to Bottcher *et al* (2004), $\delta^{34}S$ for seawater sulfate is +20.6 ‰, whereas the resulting sulfide may have a $\delta^{34}S$ of -10 to -30 ‰.

In this study $\delta^{34}S$ of the sulfide fraction is measured as chromium reducible sulfur and includes the acid volatile, elemental sulfur and pyrite fractions combined. At Sites 1, 2 and 3 (Figure 3.6), the $\delta^{34}S_{(CRS)}$ values are all negative indicating sulfides formed from bacterial reduction of sulfate (McConville *et al* 2000;Wijsman *et al* 2001; Stam *et al* 2011). At Site 1 the maximum fractionation from seawater sulfate (54.2 ‰) was recorded in the zone where oxidisation is still occurring. Enrichment of ^{32}S at the oxidation boundary of acid sulfate soils was also reported at most of the sites examined in Chapter 2 and likely resulted from sulfur cycling processes (Jorgensen 1990; Canfield and Thamdrup 1994; Bush 2000).

At Site 3, $\delta^{34}S_{(CRS)}$ in the upper half of the profile (-22.5 ‰) is different from the $\delta^{34}S_{(CRS)}$ in the lower half of the profile (-27.6 ‰). This distinction is indicative of the difference between contemporary and older sulfide accumulations. It has already been established that sulfide concentrations near the surface must have occurred since the tidal exchange strategy was introduced as prior to this the site was undergoing oxidation (Johnston *et al* 2009b; Keene *et al* 2010, 2011; Burton *et al* 2011a). Below 70 cm $\delta^{34}S_{(CRS)}$ indicates the pyrite is part of the original Holocene sediments (Smith *et al* 2004; Powell and Martens 2005; Johnston *et al* 2010).

Reformed sulfides in the upper 40 cm of Site 2 gave an average $\delta^{34}S_{(CRS)}$ of -30.5 ‰ which is slightly more negative than the upper layers at Site 3. At this site, which lies topographically between Sites 1 and 3, the tidal exchange is intermittent and redox conditions regularly oscillate between reducing and oxidising (Johnston *et al* 2009b; Burton *et al* 2011a, b). Such conditions provide two sources of sulfate which can be reduced by bacteria (Poulton *et al* 1998; Johnston *et al* 2009b). When the site experiences tidal inundation the dominate sulfate source is seawater and the $\delta^{34}S_{(CRS)}$ would be similar to that recorded at Site 3. When the site is not inundated, oxidising conditions again prevail producing a source of isotopically light sulfate. Once reducing conditions are again established bacteria uptake this light sulfate first, thereby producing sulfides more enriched in ^{32}S. In this instance the change in redox conditions causes cycling similar to that seen at the oxidation boundary.

The $\delta^{34}S_{(HCl\ SO4)}$ was greater at all sites than the corresponding $\delta^{34}S_{(CRS)}$ (Figure 3.6). Acid soluble sulfate is taken as a measure of jarosite, which in acid sulfate soils is a product of pyrite oxidation (McElnea and Ahern 2004). Dowuona *et al* (1992) found similar sulfur isotope signatures in the jarosite and pyrite fractions indicating pyrite oxidised to jarosite without major fractionation. However in this study, the fact the $\delta^{34}S_{(HCl\ SO4)}$ was always slightly less negative than $\delta^{34}S_{(CRS)}$ suggests there may be some fractionation occurring during oxidation. According to Canfield and Thamdrup (1994) the fractionation of elemental sulfur through disproportionation can cause enrichment in ^{34}S of between 12.6 ‰ and 16.7 ‰ in the sulfate. Disproportionation is a specific type of redox reaction in which a species is simultaneously reduced and oxidized to form two different products. Fractionation between $\delta^{34}S_{(CRS)}$ and $\delta^{34}S_{(HCl\ SO4)}$ ranged from 10.0 ‰ at Site 1 to 22.7 ‰ at the surface of Site 2.

At Site 1, the $\delta^{34}S_{(HCl\ SO4)}$ is similar to $\delta^{34}S_{(KCl\ SO4)}$ and $\delta^{34}S_{(WS\ SO4)}$, however at Sites 2 and 3 the water soluble and exchangeable sulfate is more enriched in ^{32}S than the HCl extractable sulfate. Jarosite sulfate is more stable than the exchangeable or water soluble sulfate forms examined. The jarosite sulfate signatures in this study are more likely to reflect conditions that pre-date the introduction of tidal water, whereas the exchangeable and water soluble sulfate signatures reflect the remediation strategy and the degree of exposure to tidal water.

The greatest isotopic changes were seen in the $\delta^{34}S_{(WS\ SO4)}$ between Sites 1, 2 and 3 (Figure 3.6). At Site 1, $\delta^{34}S_{(WS\ SO4)}$ are negative indicating the dominant sulfate source is the oxidation of isotopically negative sulfides (Mayer *et al* 2005; Kilminster and Cartwright 2011; Unland *et al* 2012). This is further supported by the chloride:sulfate ratios which are <1 throughout the majority of the profile. The chloride:sulfate ratio is useful for identifying when additional sulfate is present (Mulvey 1993), whereas the isotope signature provides evidence of the source of the sulfate (Mayer *et al* 2005; Kilminster and Cartwright 2011; Unland *et al* 2012). When used in combination the two techniques improve the accuracy with which the hydrogeochemistry of acid sulfate soil landscapes can be identified and managed.

At Site 1 the lowest $\delta^{34}S_{(WS\ SO4)}$ correspond with the most recently oxidized layers. At the oxidation boundary the redox conditions change and sulfate reduction again begins to take place. In these zones the dominant source of sulfate is isotopically light, which bacteria can reduce to produce sulfides with an even greater fractionation (relative to sea water) than the original sulfides (Poulton *et al* 1998; Johnston *et al* 2009b).

At Site 2 $\delta^{34}S_{(WS\ SO4)}$ values show a distinct increase from the values recorded at Site 1, particularly above 110 cm depth. This indicates a shift to a different source of sulfate – in this case sulfate derived from the tidal exchange strategy. At this site, the sulfate signature is showing a combination of pyrite derived sulfate and seawater sulfate. Below 110 cm the $\delta^{34}S_{(WS\ SO4)}$ at Site 2 is similar to Site 1 suggesting this depth represents the limit of tidal water effect at Site 2 to date (Johnston *et al* 2009b).

The $\delta^{34}S_{(WS\ SO4)}$ at Site 3 shows even greater influence from seawater. Above 100 cm $\delta^{34}S_{(WS\ SO4)}$ values are positive and range from 3.1 ‰ to 29.3 ‰. The $\delta^{34}S_{(WS\ SO4)}$ signatures confirm the much lower influence of pyrite derived sulfate than was observed at the other sites. In the upper 30 cm of this profile $\delta^{34}S_{(WS\ SO4)}$ are higher than seawater sulfate (+20.6 ‰ – Bottcher *et al* 2004). In Chapter 2, high $\delta^{34}S_{(WS\ SO4)}$ values were recorded at depth in the Tuckean Swamp monosulfide and at most of the Inland sites. In each of these cases, high $\delta^{34}S_{(WS\ SO4)}$ values occur where contemporary sulfides are forming, indicating the removal of light sulfate through the process of sulfate reduction, with an abundance of heavy sulfate remaining (Brownlow 1996; Wijsman *et al* 2001; Farquhar *et al* 2008).

Non tidal sites

Sites 4 and 5 have not been affected by the tidal exchange remediation strategy. Site 4 in particular was extremely degraded with much of the area scalded and coated with surficial iron oxide accumulations (Figure 3.8). Below 40 cm depth the isotope signatures at Site 4 are similar to those recorded at Site 1, another unremediated site (Figure 3.11). $\delta^{34}S_{(CRS)}$ and $\delta^{34}S_{(WS\ SO4)}$ are both strongly negative and closely aligned, indicating pyrite oxidation is the dominant source of sulfate. Above 40 cm $\delta^{34}S_{(WS\ SO4)}$

is less enriched in ^{34}S suggesting another source of sulfate, most likely contained in the freshwater seen ponding on the surface (Plate 3.2). According to Holser and Kaplan (1966) freshwater sulfate has a range of +5 ‰ to +15 ‰. The slightly higher $\delta^{34}S_{(WS\ SO4)}$ may also be due to sulfate reduction given there are sulfidic accumulations on the surface. It may also be the result of sulfate from sea spray, rainfall, or both, given the location of the site adjacent to the ocean and estuary (Bridgman 1989; Kilminster and Cartwright 2011). According to Bridgman (1989), rainfall in much of Australia is likely to have a $\delta^{34}S_{(SO4)}$ value close to that of seawater.

At Site 4, the freshwater at the surface is only temporary following rainfall. Site 5 however, has been bunded so the freshwater remains ponded for extended periods of time. Below approximately 80 cm however, the original marine sediments are evidenced by higher pH and EC (Figure 3.7) and the chloride and sulfate concentrations (Figure 3.10). The comparatively less negative $\delta^{34}S_{(WS\ SO4)}$ values recorded at Site 4 can be explained by only occasional oxidation below 80 cm depth. The values are not as negative as would be expected of a pyrite dominant sulfate source and not positive enough for a seawater dominant sulfate source; rather they represent a mixing of these two main sources.

$\delta^{34}S_{(CRS)}$ and $\delta^{34}S_{(WS\ SO4)}$ at Site 5 are both lowest at the oxidation boundary at around 70 cm depth. Above this $\delta^{34}S_{(WS\ SO4)}$ values increase and the signatures appear similar to Site 2. At this site however, the $\delta^{34}S_{(WS\ SO4)}$ reflects the freshwater overlying the site. Sulfate concentrations were much lower at the surface which may have been limiting the reformation of sulfides (Habicht and Canfield 1997; Stam *et al* 2011; Mazumdar *et al* 2012).

The data clearly shows that changes in the stable sulfur isotopes in various soil fractions, when used in conjunction with other geochemical data, can be used to understand the geochemical processes that occur as sulfidic materials are oxidised and then affected by reinundation. It is a particularly useful technique to determine, at precise locations, the relative magnitude of the potential sources of the sulfate that are driving critical remediation processes such as sulfate reduction, as these provided

much of the alkalinity required for remediation (Johnston *et al* 2012) in these disturbed coastal landscapes.

The use of stable sulfur isotopes has also shed light on the stability of sulfate in the various fractions following inundation by tidal water. For example, the isotope signature of jarosite sulfate where present, is an indicator of conditions prior to remediation, whereas the sulfur isotope signatures of both water soluble and exchangeable sulfate reflect contemporary conditions.

The sulfur isotope signature of reformed pyrite in turn reflects the soluble sulfate source. In remediating environments where tidal water has been introduced the sulfate source is the result of both sulfate formed from pyrite oxidation and sulfate from the tidal water. The sulfur isotope signature of residual pyrite reflects conditions of formation solely under tidal conditions. Differences in the sources of sulfate are clearly reflected in the sulfur isotope signature of reformed pyrite.

Conclusion

The aim of this study was to examine the use of stable sulfur isotopes in understanding the geochemistry of acid sulfate soil materials undergoing remediation by lime assisted tidal exchange. The study was conducted on a severely degraded acid sulfate soil site at East Trinity near Cairns in northern Queensland. The remediation strategy has brought about many significant changes in the geochemistry of the East Trinity property.

Segregations of acid extractable sulfate such as jarosite provided information on the environmental conditions prior to the reintroduction of tidal water. Jarosite was also found to be less depleted in ^{34}S than the corresponding sulfide indicating some fractionation may be occurring during oxidation. Water soluble and exchangeable sulfate reflect the contemporary conditions and is likely derived from two potential sources. The oxidation of pyrite produces sulfate with an isotope signature similar to

the pyrite, which at these sites was isotopically negative, whereas sulfate provided in the tidal water carries a positive isotope signature similar to sea water sulfate.

At sites with tidal influence contemporary sulfide formations also reflected the varied soluble sulfate sources and could be isotopically distinguished from the relic pyrite found at depth. Reformed pyrite had an isotope signature that indicated sulfate reduction from two sulfate sources; sulfate derived from the oxidation of pyrite and sulfate in the tidal water. Relic pyrite indicated conditions of formation solely under tidal conditions.

This study has shown the examination of stable isotopes of sulfur in various soil fractions can be used to provide information on the environmental conditions prior to remediation of acid sulfate soils. It has also identified various soluble sulfate sources present pre and post remediation by lime assisted tidal exchange.

Acknowledgements

This study benefitted from financial assistance from CRC CARE as part of the East Trinity project 6-6-01-06/07, and the School of Environment, Science and Engineering. I would also like to thank Leigh Sullivan, Scott Johnston and Annabelle Keene for assistance with field sampling and Matheus Carvalho de Carvalho for the isotope analysis.

Chapter 4

Using stable sulfur isotopes to identify acidic discharges from acid sulfate soil materials

Introduction

Acid sulfate soils occur along extensive areas of the New South Wales and Queensland coastlines. The oxidation of acid sulfate soils through drainage and the lowering of water tables have attributed to severe environmental degradation, particularly in northern NSW (Johnston *et al* 2003a, b; Burton *et al* 2006). Amongst the most noticeable and publicised impacts are fish kills which result from the release of acid and heavy metals into the aquatic environment (White *et al.* 1993; Corfield 2000) or by the oxidation and mobilisation of monosulfidic black ooze (MBO) (Sullivan and Bush 2002). Other impacts associated with acid sulfate soils include habitat degradation, soil toxicity (Rassam *et al.* 2001), low nutrient availability (White and Sammut 1995) and damage to engineering structures (Bloomfield and Coulter 1973; Blunden and Indraratna 2000).

The principle iron sulfide mineral found in acid sulfate soil materials is pyrite. Pyrite is formed when sulfate, usually in seawater, is reduced to hydrogen sulfide (H_2S) and combines with reduced iron, to form iron disulfide (Equation 4.1) (Melville and White 2000). The majority of coastal acid sulfate soils occur in coastal embayments and estuaries where wave action is limited and sedimentation occurs. In addition to a supply of sulfate and iron, the formation of pyrite requires generally anaerobic conditions, chemically reducing microbes and a large supply of metabolisable organic matter (Melville *et al.* 1993). Such conditions existed during the last sea level rise approximately 6000–10 000 years ago which is when many acid sulfate soils were formed in eastern Australia.

$$4SO_4^{2-}{}_{(aq)} + Fe_2O_{3(aq)} + 8CH_2O_{(s)} + \tfrac{1}{2}\, O_{2(g)} \rightarrow 2FeS_{2(s)} + 8HCO_3^{-}{}_{(aq)} + 4H_2O_{(aq)}$$

Equation 4.1

The process of sulfate reduction is bacterially mediated (Mazumdar *et al* 2007). During this process, bacteria are able to preferentially uptake isotopically light sulfate which results in the H_2S and consequently the pyrite having a significantly different sulfur isotope signature from the original sulfate (Bottcher *et al* 1997; Farquhar *et al* 2008;

Stam *et al* 2011). Modern seawater sulfate has a sulfur isotope signature of +20.6 ‰ (Bottcher *et al* 2004), whereas the resulting pyrite may have a $\delta^{34}S$ signature of between -10 to -30 ‰ (Goldhaber and Kaplan 1974; Emery and Robinson 1993). This difference in signature is referred to as fractionation.

The oxidation of pyrite also releases sulfate which is discharged into drainage channels and subsequently into the surrounding rivers and estuaries (Equation 4.2) (Dent 1986; Cook *et al* 2000; Russell and Helmke 2002). Importantly, the oxidation of pyrite to produce sulfate results in only a slight change in the sulfur isotope signature (Taylor *et al* 1984). Therefore, it is possible to differentiate between the isotope signature of the original seawater sulfate and sulfate derived from the oxidation of acid sulfate soil materials (Mayer *et al* 2010; Kilminster and Cartwright 2011).

$$FeS_{2(s)} + 14Fe^{3+}_{(aq)} + 8H_2O_{(l)} \rightarrow 15Fe^{2+}_{(aq)} + 2SO_4^{2-}{}_{(aq)} + 16H^{+}_{(aq)} \quad \textbf{Equation 4.2}$$

One of the current techniques used for acid sulfate soil identification is the chloride to sulfate ratio (Mulvey 1993). In seawater the chloride to sulfate ratio is approximately 7.2. However in acid sulfate soil environments the oxidation of pyrite produces an excess of sulfate relative to chloride which reduces this ratio. Ratios below 1 were recorded at East Trinity in Chapter 3 of this thesis. Other studies have also recorded low chloride to sulfate ratios in acid sulfate soil landscapes (Rosicky *et al* 2002a, b; Johnston *et al* 2003b, c).

Dold and Spangenberg (2005) used isotopes of sulfur and oxygen to conclude water soluble sulfate resulted from the oxidation of pyrite in mine tailings. Their study differentiated the isotope signature of sulfate derived from pyrite oxidation from the isotope signature of primary sulfate dissolution. More recently, Kilminster and Cartwright (2011) used sulfur isotopes in dissolved sulfate as a screening tool for assessing the impact of acid sulfate soils in Western Australia. An indicator was developed based on $\delta^{34}S$ and chloride and sulfate concentrations that categorised samples into groups with similar isotopic influences (iso-groups). They identified disturbed acid sulfate soils in ~5% of sites examined and found corresponding poor water quality at those sites. Their study indicated that $\delta^{34}S$ values could be used to

provide an early warning signal for water affected by disturbed acid sulfate soils (Kilminster and Cartwright 2011).

Research conducted by Maher (2005) suggested that sulfur isotope ratios can be used as a potential technique for identifying the source of acidic discharge in acid sulfate soil landscapes by differentiating the $\delta^{34}S$ of the original sulfate source (taken as seawater sulfate) and the $\delta^{34}S$ of the sulfate derived from pyrite oxidation. When used in conjunction with background water characteristics such as pH, electrical conductivity, dissolved oxygen, metal and salt concentrations and chloride to sulfate ratio, stable sulfur isotopes may be able to further establish the link between acid sulfate soil oxidation and poor water quality.

Aim

The aim of this investigation was to examine the utility of sulfur isotope ratios in dissolved sulfate to identify the provenance of acidic waters draining from and within landscapes that contain acid sulfate soil materials. This investigation will link the use of sulfur isotopes to other water quality parameters such as pH, electrical conductivity, dissolved oxygen, metal and salt concentrations and the chloride to sulfate ratio which can be associated with contributions to waters from acid sulfate soil materials.

Methodology

Sampling site – Hendersons Drain, Tuckean Swamp

The Tuckean Swamp is located on the lower Richmond River floodplain in Northern NSW. It comprises an area of approximately 5000 ha with a catchment of approximately 22 000 ha (Sammut *et al* 1996a). The Tuckean Swamp is dissected by an extensive artificial drainage system, which has modified the natural drainage pattern (Sammut *et al* 1995). Hagley (1996) suggested this drainage system has resulted in

approximately 3000 ha of the Tuckean Swamp being strongly acidic with another 1000 ha having the potential to become acidic.

The primary regulatory structure for this extensive drainage system is the Bagotville Barrage, an eight-cell flood gate installed in 1971 to reduce periodic inundation by tidal influence (Hagley 1996). The barrage was constructed along a large drain commonly referred to as the Hendersons Drain (Figure 4.1). Acidic discharges from the Tuckean Swamp acid sulfate soils have been related to significant lowering of pH, release of heavy metals and other detrimental environmental impacts (Sammut *et al* 1996a).

Sampling commenced at the Bagotville Barrage and proceeded upstream along Hendersons Drain (Figure 4.1). Three drainage channels were identified as flowing into Hendersons Drain. The largest of these was the Tucki Canal (TC). Samples were collected 50–80 m upstream of the confluence with Hendersons Drain, at the mouth of the canal and 50–80 m downstream of the canal. Samples were also collected 50 m, 600 m and 2500 m upstream along the drain.

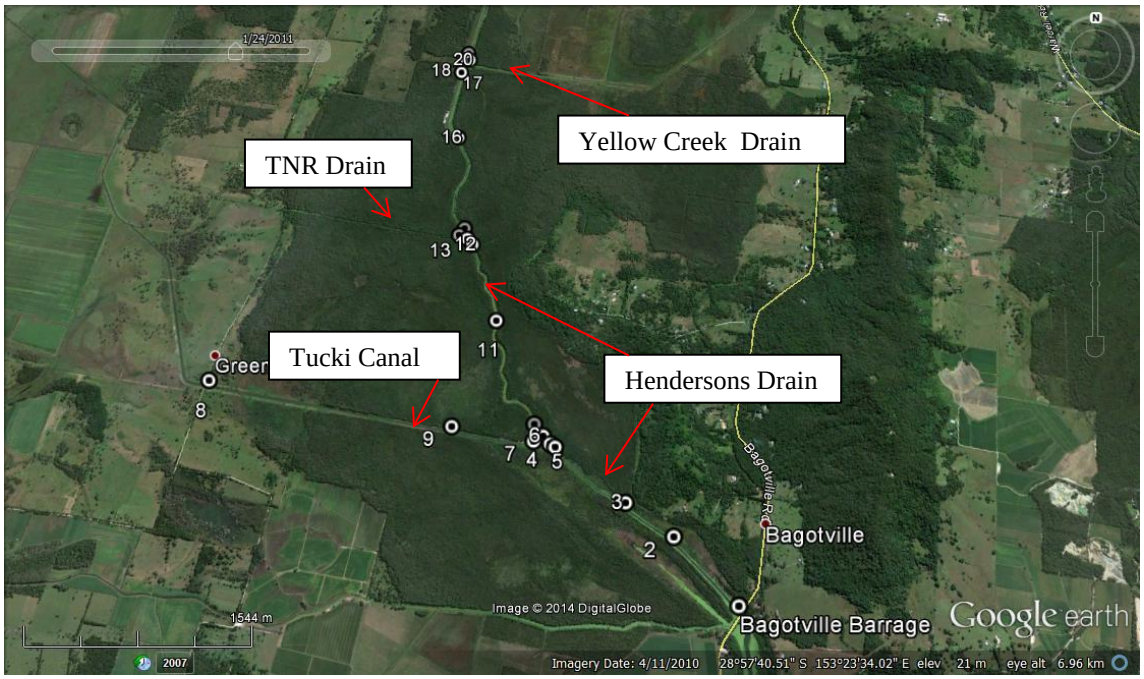

Figure 4.1. Google Earth image of the Tuckean Swamp with sample sites and drainage channels indicated.

The second drain investigated was the Tuckean Nature Reserve Drain (TNR). Samples were collected downstream, at the confluence and upstream from the confluence with Hendersons Drain. Another sample was collected from ~50 m into the drain. Field observations suggested there were considerable accumulations of monosulfidic black ooze at the mouth of the drain.

The final drain sampled was the Yellow Creek Drain (YCD). This drain contained abundant plant material and was inaccessible. Samples were collected from downstream, at and upstream of the confluence with Hendersons Drain. A final sample was again taken from the bank inside the drain. The water in the drain was extremely clear at the time of sampling.

A water sample was collected from the wharf at Wardell as a representative sample of the estuarine conditions in the Richmond River channel between the Bagotville Barrage and the sea. Similarly, another water sample was collected from the wharf at Coraki. This sample is typical of the environmental conditions up-stream from the Tuckean Swamp which are relatively unaffected by acid sulfate soils (Wong *et al* 2010).

Table 4.1 provides details of the sample collection sites including map grid coordinates, distance upstream from the Bagotville Barrage and a brief description. Hendersons Drain was examined upstream for a distance of 5.73 km. Samples 7–9, 15 and 20 were collected from within Tucki Canal, Tuckean Nature Reserve Drain and Yellow Creek Drain, respectively.

Water sample collection and preservation

Samples were collected from within the drainage channels. Plastic 1 L bottles were rinsed three times in the water before the sample was collected. The bottles were squeezed to expel air and then capped tightly. They were placed on ice in an esky for transport to the laboratory then stored at <4 °C until analysis.

Field data collection

Several water quality parameters were recorded at the time of sampling. These included pH, redox potential (Eh), electrical conductivity (EC), dissolved oxygen concentration (DO mg/L), dissolved oxygen saturation (DO % sat) and temperature using calibrated probes and a TPS meter. Readings were taken from approximately 30 cm below the surface. In addition, water samples were pipetted into the alkalinity trapping solutions to be analysed in the laboratory.

Table 4.1. Description of sampling sites

Site No.	Map Grid		Distance from Barrage (km)	Description
	56 J (E)	56 J (S)		
1	0539464	6794236	0	Adjacent to Bagotville Barrage
2	0539028	6794704	0.64	Near monitoring station
3	0538687	6794941	1.05	Upstream from Site 2
4	0538172	6795395	1.74	Downstream of Tucki Canal
5	0538136	6795367	1.75	Confluence of Hendersons Drain & Tucki Canal
6	0538081	6795428	1.83	Upstream of Tucki Canal
7	0538012	6795387	1.88	In Tucki Canal, ~50m upstream
8	0537403	6795489	2.49	In Tucki Canal, 600m upstream
9	0535548	6795819	4.38	In Tucki Canal, 2500m upstream
10	0538014	6795517	1.94	Between Tucki Canal & TNR Drain
11	0537692	6796347	2.94	Between Tucki Canal & TNR Drain
12	0537470	6797006	3.70	Downstream of TNR Drain
13	0537425	6797058	3.77	Confluence of Hendersons Drain & TNR Drain
14	0537398	6797153	3.87	Upstream of TNR Drain
15	0537357	6797091	3.86	In TNR Drain ~50m upstream
16	0537295	6798020	4.81	Between TNR Drain & Yellow Ck Drain
17	0537276	6798695	5.51	Downstream of Yellow Ck Drain
18	0537307	6798836	5.66	Confluence of Hendersons & Yellow Ck Drain
19	0537326	6798902	5.73	Upstream of Yellow Ck Drain
20	0537343	6798831	5.79	In Yellow Ck Drain, near monitoring station
21	0545386	6797115		Wardell wharf
22	0528133	6793374		Coraki wharf

Chemical analysis

The following chemical analyses were conducted on the water samples in the laboratories at Southern Cross University:

Alkalinity

Alkalinity was determined spectrophotometrically using the Bromophenol Blue method, and analysed by HACH spectrophotometer. Results were normalised by titrating with HCl of known concentration and the Gran Titration procedure (Sarazin *et al* 1999).

Metals

Water samples were filtered with a 0.45 µm cellulose acetate filter, preserved with HNO_3 and analysed for aluminium (Al, detection limit 0.05 mg/L), iron (Fe, detection limit 0.05 mg/L) and manganese (Mn (detection limit 0.001 mg/L). Samples were analysed by Inductively Coupled Plasma Optical Emission Spectrometry (ICP-OES) or Inductively Coupled Plasma Mass Spectrometry (ICP-MS) according to APHA method 3120 (APHA 2005). Duplicate analysis gave a precision of ± 3%.

Salts

Water samples were filtered with a 0.45 µm cellulose acetate filter, preserved with HNO_3 and analysed for salts. Chloride (Cl) analysis was conducted by Flow Injection Analyser (FIA) according to APHA method 4500 (APHA 2005). Sodium (Na), potassium (K), calcium (Ca), magnesium (Mg) and sulfate (SO_4) were determined by ICP-OES (APHA method 3120, APHA 2005). Chloride:sulfate ratios were calculated. Duplicate analysis gave a precision of ± 2% with a detection limit of 0.05 mg/L.

Sulfate Isotopes

The remaining water samples were used to precipitate sulfate for isotope analysis. Water samples were filtered directly into a prepared solution of 1 M $BaCl_2$ to precipitate $BaSO_4$. The precipitate was rinsed 3 times with 40 mL Milli-Q water and dried at 105 °C for 24 hours. Samples were analysed for $\delta^{34}S$ by Continuous Flow Isotope Ratio Mass Spectrometry (CF-IRMS) using a Thermo Flash EA 1112 coupled to a Thermo Delta V Plus IRMS. NIST reference material 8555 was used for calibration. $\delta^{34}S$ of the sulfate fraction is reported as ‰ deviations from the standard (Equation 12). Positive $\delta^{34}S$ values represent enrichment in ^{34}S while negative $\delta^{34}S$ indicate enrichment in ^{32}S. Duplicate analysis gave a precision of ± 0.3‰.

Results

Water quality in Hendersons Drain

The quality of the water discharging from the Tuckean Swamp was quite variable (Figure 4.2a–d). pH is highest (6.52) at the Bagotville Barrage and decreases to 3.62 between Tucki Canal and Tuckean Nature Reserve Drain (Figure 4.2a). Upstream of Yellow Creek Drain the pH again increases to 5.72.

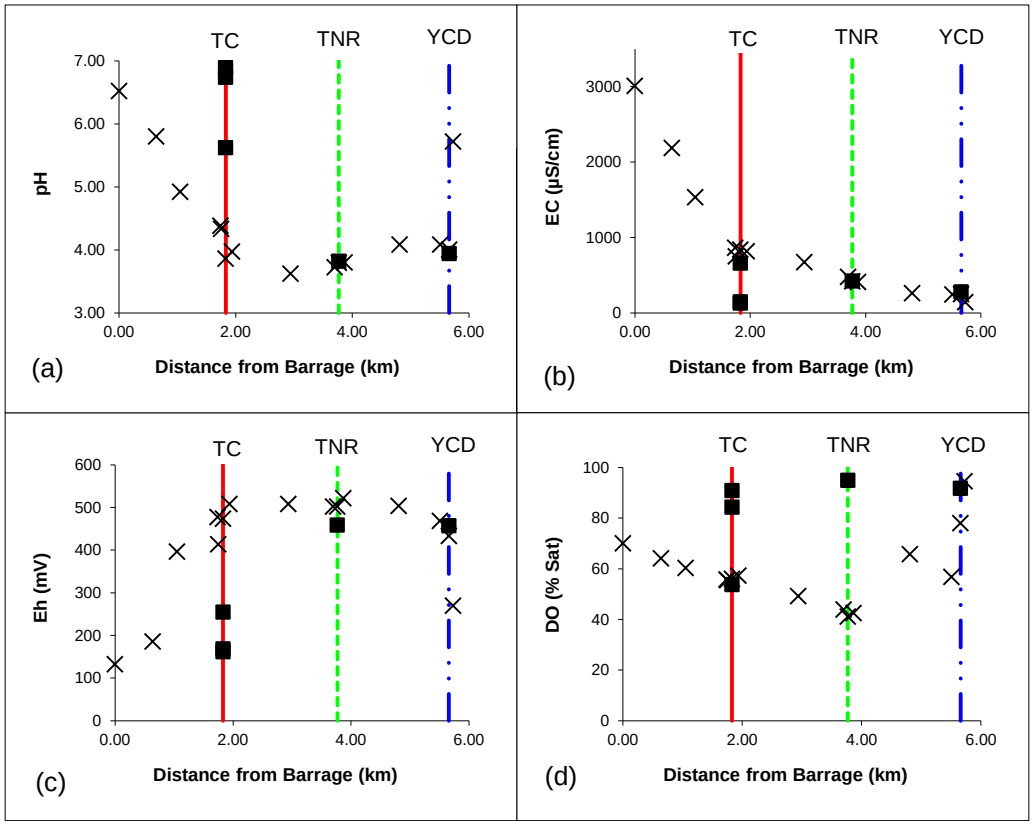

Figure 4.2. Background water quality for Hendersons Drain recorded upstream from the Bagotville Barrage for a) pH, b) EC, c) Eh, d) DO Sat. Vertical lines indicate where the drainage channels converge with Hendersons Drain (TC = Tucki Canal, TNR = Tuckean Nature Reserve Drain, YCD = Yellow Creek Drain). Solid squares represent samples collected from within the drains.

Eh followed an inverse pattern to pH with the lowest values recorded adjacent to the Bagotville Barrage and the highest values in the vicinity of the Tuckean Nature Reserve

Drain (Figure 4.2c). Values again decreased upstream of the Yellow Creek Drain. Eh is a measure of the redox potential of the water with high values indicating oxidising conditions (Evangelou 1998).

Dissolved oxygen levels were below ANZECC (2000) Guidelines for fresh waters along the majority of Hendersons Drain (Figure 4.2d). It was only upstream from the entrance of Yellow Creek Drain that dissolved oxygen increased above 90%. The lowest dissolved oxygen levels were recorded in the vicinity of the Tuckean Nature Reserve Drain.

Alkalinity, measured by HCO_3^-, provides a measure of the waters neutralising capacity (Wong *et al* 2010; Johnston *et al* 2012). In this study the highest alkalinity was recorded adjacent to the Bagotville Barrage (Figure 4.3a) however around the Tucki Canal and the Tuckean Nature Reserve Drain the alkalinity dropped considerably. Further upstream near the Yellow Creek Drain the alkalinity values again increased.

Metal concentrations for the three most elevated metals examined are displayed in Figure 4.3b–d. Manganese only varied marginally along the length of the Hendersons Drain (Figure 4.3d). However iron and particularly aluminium peaked at 1.0 and 1.8 mg/L, respectively, approximately 3 km upstream from the Bagotville Barrage between Tucki Canal and Tuckean Nature Reserve Drain (Figure 4.3b, c).

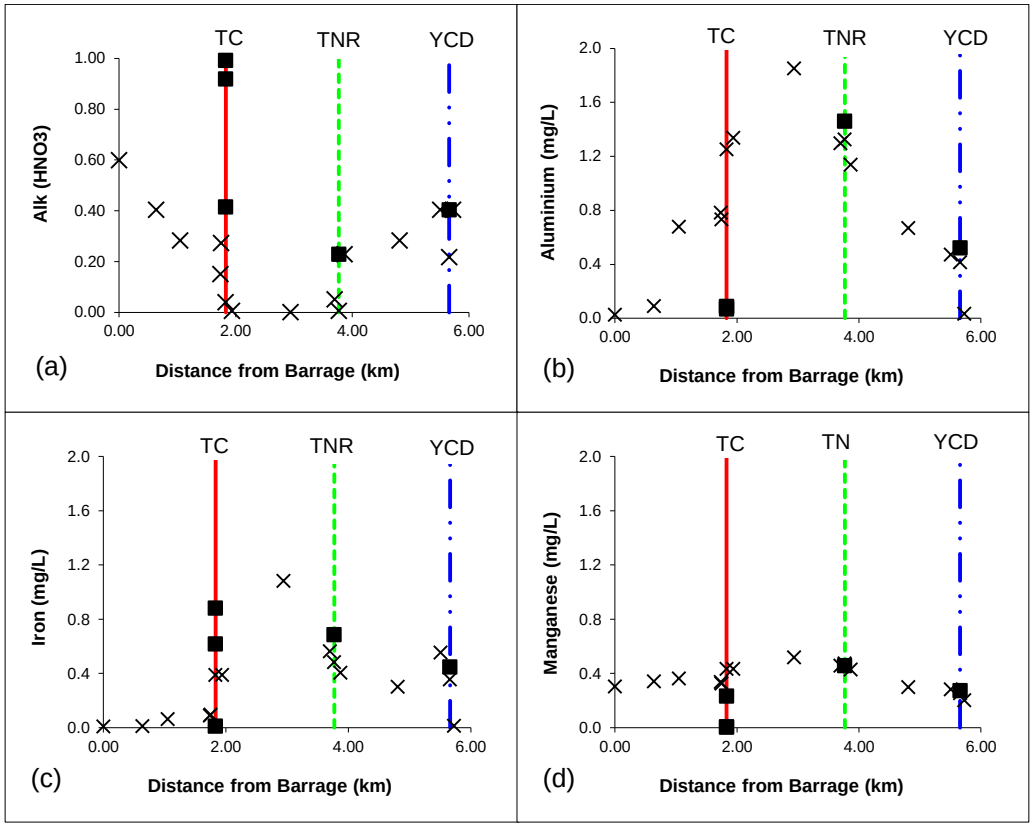

Figure 4.3 Background water quality for Hendersons Drain recorded upstream from the Bagotville Barrage for a) Alkalinity, b) Al, c) Fe, d) Mn. Vertical lines indicate where the drainage channels converge with Hendersons Drain (TC = Tucki Canal, TNR = Tuckean Nature Reserve Drain, YCD = Yellow Creek Drain). Solid squares represent samples collected from within the drains.

Soluble cation and anion concentrations for Hendersons Drain are displayed in Figure 4.4. For each of the salts examined, the concentration was highest at the Bagotville Barrage and reduced steadily further upstream. Salt concentrations just inside the Tucki Canal were similar to those recorded at the confluence and decreased further along Tucki Canal. The concentrations recorded in the Tuckean Nature Reserve Drain and Yellow Creek Drain was also similar to those recorded at their respective confluence with Hendersons Drain. Chloride:sulfate ratios decrease steady upstream from the Bagotville Barrage (Figure 4.5). In coastal environments a lowering of the chloride:sulfate ratio can indicate additional sulfate in the water which results from the oxidation of acid sulfate soil materials.

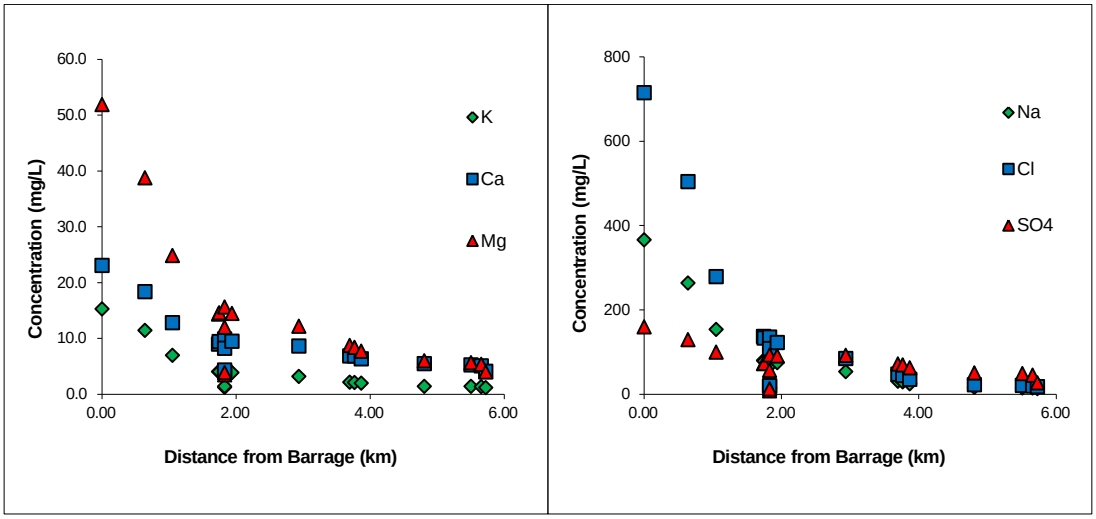

Figure 4.4. Soluble cation and anion concentrations recorded along Hendersons Drain, measured upstream from the Bagotville Barrage.

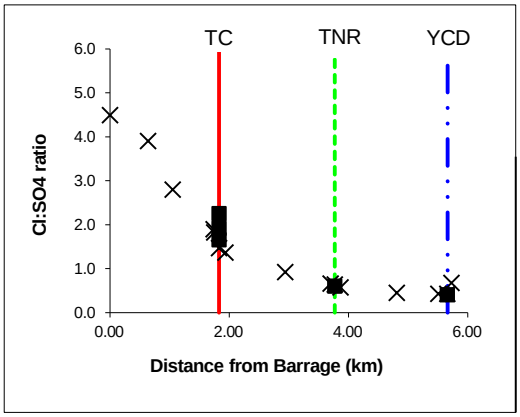

Figure 4.5. Chloride:sulfate ratios recorded along Hendersons Drain. Vertical lines indicate where the drainage channels converge with Hendersons Drain (TC = Tucki Canal, TNR = Tuckean Nature Reserve Drain, YCD = Yellow Creek Drain). Solid squares represent samples collected from within the drains.

Water quality above and below Tuckean Swamp

Tables 4.2 and 4.3 show the water quality sampled upstream and downstream of the Tuckean Swamp. Wardell Wharf is representative of samples downstream of the Tuckean Swamp and close to the sea. The sample from the Coraki Wharf is upstream from the Tuckean Swamp and should be unaffected by acid sulfate soils. Most of the

water quality parameters are similar between the two sites with the exception of EC which varied significantly. EC for the Wardell sample indicates a strong marine influence whereas the Coraki sample indicates a greater freshwater influence.

Table 4.2. Background water quality parameters for Wardell and Coraki Wharf samples

Parameter	Wardell Wharf Site 21	Coraki Wharf Site 22
pH	7.69	7.94
EC (mS/m)	23	0.36
Eh (mV)	188	159
DO sat (%)	98	94
Alkalinity (HNO_3^- mmol/L)	2.62	2.73
Aluminium (mg/L)	0.003	0.006
Iron (mg/L)	<0.001	0.007
Manganese (mg/L)	0.010	0.001

The distinction between marine and fresh water between the two sites is further evidenced by the salt concentrations (Table 4.3). For each of the salts measured the Wardell sample had higher levels than the Coraki sample.

Table 4.3. Major soluble cation and anion concentrations for Wardell and Coraki Wharf samples

Parameter	Wardell Wharf Site 21	Coraki Wharf Site 22
Sodium (mg/L)	3,501	30
Potassium (mg/L)	143	2.2
Calcium (mg/L)	164	17
Magnesium (mg/L)	451	11
Chloride (mg/L)	7,110	44
Sulfate (mg/L)	1117	12
Cl:SO_4	6.4	3.6

Stable isotope signatures

Stable isotope signatures from the dissolved sulfate fraction have been plotted in relation to the distance upstream along Hendersons Drain from the Bagotville Barrage (Figure 4.6). The isotope signature is highest at the Barrage and decreases steadily upstream. The maximum value recorded was 12 ‰ which shows some fractionation relative to a seawater sulfate signature. The lowest recorded value of 1.3 ‰ occurred just downstream of Yellow Creek Drain. Immediately upstream from Yellow Creek Drain the isotope signature begins to increase slightly (Figure 4.6).

Figure 4.6 also shows the stable isotope signature of samples collected from within the drainage channels. Immediately upstream from the Tucki Canal/Hendersons Drain confluence the $\delta^{34}S$ has increased slightly from the value recorded at the confluence (Table 4.4). The values continue to increase further upstream Tucki Canal which suggests the water flowing from Tucki Canal into Hendersons Drain is of slightly better quality and contains fewer acid sulfate soil derived sulfates.

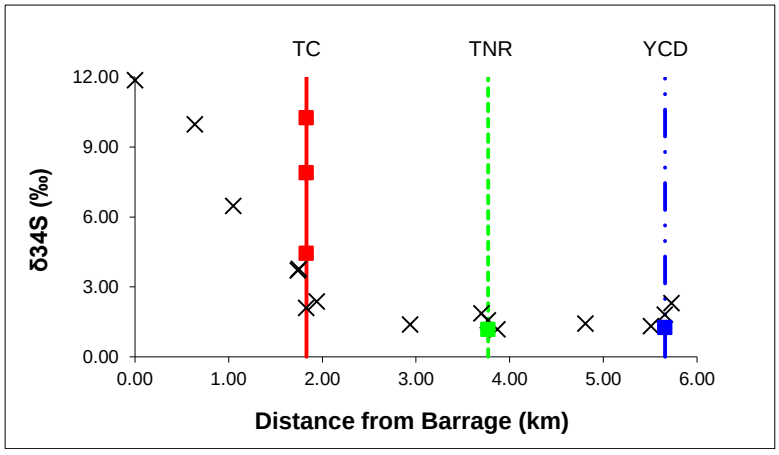

Figure 4.6. $\delta^{34}S$ (‰) in the dissolved sulfate fraction measured upstream from the Bagotville Barrage. Vertical lines indicate where the drainage channels converge with Hendersons Drain (TC = Tucki Canal, TNR = Tuckean Nature Reserve Drain, YCD = Yellow Creek Drain). Solid squares represent samples collected from within the drains.

Both Tuckean Nature Reserve Drain and Yellow Creek Drain showed slight decreases in $\delta^{34}S$ compared to their respective confluences with Hendersons Drain (Table 4.4).

Upstream from Tuckean Nature Reserve Drain $\delta^{34}S$ continues to decrease, whereas upstream from Yellow Creek Drain, $\delta^{34}S$ increases.

Table 4.4. $\delta^{34}S$ values recorded in drainage channels and at their respective confluence with Hendersons Drain

Site No	Canal/Drain Name	Distance upstream in drain (m)	$\delta^{34}S$ in drain (‰)	$\delta^{34}S$ at confluence (‰)
7	Tucki Canal	50	4.4	3.8
8	Tucki Canal	600	7.9	3.8
9	Tucki Canal	2500	10	3.8
15	TNR Drain	50	1.4	1.6
20	Yellow Creek Drain	50	1.3	1.8

The $\delta^{34}S$ recorded at Wardell Wharf was 19.81 ‰. This is very close to the seawater sulfate signature of 20.6 ‰ provided by Bottcher *et al* (2004). At the Coraki Wharf $\delta^{34}S$ is 14.91 ‰, which according to Holser and Kaplan (1966), is indicative of fresh water.

Figure 4.7 shows the relationship between the sulfur isotope signature and pH and the chloride:sulfate ratio for all samples. In this study the $\delta^{34}S$ of the sulfate fraction is strongly correlated with changes in pH and the chloride:sulfate ratio.

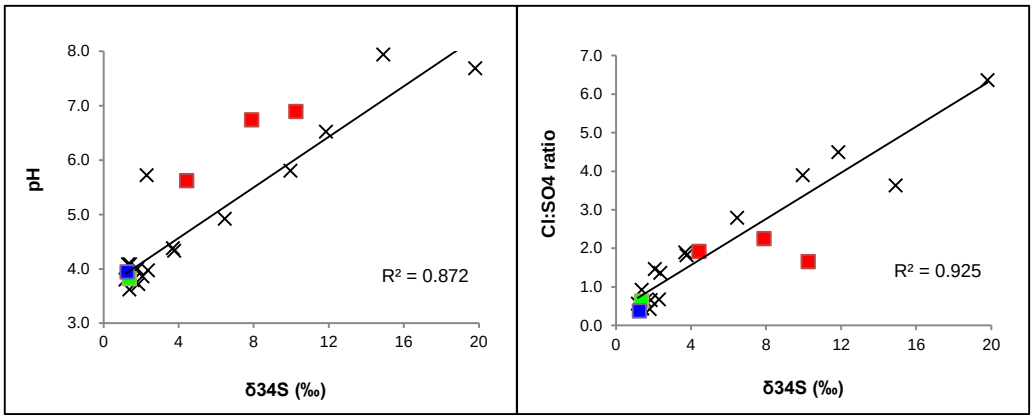

Figure 4.7. pH and chloride:sulfate ($Cl:SO_4$) ratio from all samples plotted against $\delta^{34}S$. X = samples from Hendersons Drain, red squares = Tucki Canal, green squares = Tuckean Nature Reserve Drain, blue squares = Yellow Creek Drain.

Discussion

The Tuckean Swamp has been the site of many acid sulfate soil investigations (Burton *et al* 2006; Wong *et al* 2010; Claff *et al* 2011). According to Hagley (1996) some of the issues facing the Tuckean Swamp include acid runoff, fish kills, poor water quality, land degradation, reduced agricultural productivity, loss of estuarine fisheries habitat and degraded native vegetation and wildlife values. Compared to some earlier studies the water quality currently found in Hendersons Drain is marginally better. Earlier studies have recorded pH values as low as 1.8 and concentrations of aluminium above 70 mg/L (Sammut *et al* 1996b). In 2002–2003, in an attempt to remediate the area, the floodgates at the Bagotville Barrage were opened and tidal water was allowed to flow into the swamp. This neutralised much of the acid generated from the oxidation of the acid sulfate soils (RRCC 2013).

At the Bagotville Barrage the high pH, EC (Figure 4.2) and alkalinity (Figure 4.3) are influenced by the inflowing tidal water. Upstream from the Barrage the EC drops significantly indicating a greater influence from fresh water derived from the upland areas. The low alkalinity values recorded in the vicinity of Tucki Canal and Tuckean Nature Reserve Drain may have resulted from the alkalinity being consumed by acidity released from the drainage channels (Wong *et al* 2010; Johnston *et al* 2012).

Several studies have reported low dissolved oxygen levels in the Tuckean Swamp particularly following significant rainfall events (Fyfe 2001; Sullivan and Bush 2001). This has been attributed in part to the oxidation of monosulfidic black ooze (MBO) accumulating in drainage channels associated with acid sulfate soil landscapes (Sullivan *et al* 2002; Bush *et al* 2004a, b). The elevated iron and aluminium concentrations found in this study (Figure 4.3) are consistent with previous studies and are associated with acidic discharges from acid sulfate soils landscapes and drain accumulations of monosulfidic black ooze (Ferguson and Eyre 1996; Burton *et al* 2006a, b; Wong *et al* 2010).

The results obtained in this study indicate that although there may have been some improvement since the opening of the floodgates, acid sulfate soils in the Tuckean

Swamp are still greatly influencing water quality. According to the water quality data, between Tucki Canal and Yellow Creek Drain, acidity was being mobilised, alkalinity was virtually exhausted and metals were being released. In addition, the chloride:sulfate ratio decreased to <1 (Figure 4.5) indicating pyrite oxidation has provided an additional source of sulfate to the water.

The water in Tucki Canal had a higher pH and lower EC than water at the confluence with Hendersons Drain. Alkalinity and dissolved oxygen were both higher in the Tucki Canal and the Eh lower than in Hendersons Drain. Overall the water quality improved with increasing distance upstream along Tucki Canal.

The water quality parameters measured within the Tuckean Nature Reserve Drain were similar to the values recorded in Hendersons Drain. However this is most likely due to the small size of the channel which limited the extent of sampling. The only parameter that was significantly different between the Tuckean Nature Reserve Drain and Hendersons Drain was dissolved oxygen (Figure 4.2). The elevated dissolved oxygen recorded in Tuckean Nature Reserve Drain may have resulted from the abundant plant material present at the time of sampling. In general Tuckean Nature Reserve Drain is contributing water of poor quality to Hendersons Drain.

At the time of sampling Yellow Creek Drain had an abundance of acid tolerate lillies and extremely clear water. These indicators are often associated with acidic discharges from acid sulfate soil landscapes. According to Figure 4.2, the water sampled within Yellow Creek Drain was very similar to the water sampled at the confluence with Hendersons Drain. Generally, the water quality improved between Tuckean Nature Reserve Drain and Yellow Creek Drain.

Along Hendersons Drain, $\delta^{34}S$ decreased from a maximum of 11 ‰ adjacent to the Bagotville Barrage to a minimum of 1.3 ‰ near Yellow Creek Drain (Figure 4.6). These values, particularly the lower values, show considerable fractionation from seawater. If seawater was the dominant sulfate source the isotope signature would be ~+20 ‰ as it was at Wardell. At the Bagotville Barrage, the isotope signature indicates some influence from the inflowing tidal water which was also suggested by the

background water quality parameters, however the $\delta^{34}S$ signature is diluted from sulfate derived from other sources.

The process of bacterial sulfate reduction is an example of kinetic fractionation and the major cause for the natural variation in the isotopic composition of sulfur (Nakai and Jensen 1964; Brownlow 1996). Fractionation occurs because the rate at which isotopically heavy sulfate is reduced is significantly slower than the rate that isotopically light sulfate is reduced (Emery and Robinson 1993). This means the resultant sulfide is isotopically lighter than the original sulfate. In the context of this study, bacterial sulfate reduction produces pyrite that has an isotope signature considerably lower than the precursor sulfate.

When this isotopically light pyrite is oxidised to produce dissolved sulfate there is little change in the isotope signature (Taylor *et al* 1984; Seal and Wandless 1997; Balci *et al* 2007). That means the pyrite and the product sulfate will have a similar isotope signature. It also means the produced sulfate can be readily distinguished from the original seawater sulfate. Upstream from the Bagotville Barrage the low $\delta^{34}S$ signatures recorded in this study indicate the water in Hendersons Drain contains sulfate derived from the oxidation of acid sulfate soil materials

The isotope signature in Tucki Canal increased from 3.8 ‰ at the confluence with Hendersons Drain to a maximum of 10.3 ‰, 2500 m along the drain (Table 4.4). These results suggest it is unlikely the source of sulfate was pyrite oxidation. This aligns with the water quality measurements and suggests the soils in this area are not contributing significantly to the poor water quality in Hendersons Drain.

The $\delta^{34}S$ value recorded within Tuckean Nature Reserve Drain was slightly lower than the value recorded at the confluence with Hendersons Drain. This suggests Tuckean Nature Reserve Drain is responsible for delivering sulfate derived from the oxidation of pyrite into Hendersons Drain. Consequently, the location of the oxidising acid sulfate soils are more likely to be found in the catchment of this drain rather than the Tucki Canal. A more detailed study along this drain would allow a more precise location to be identified.

In Chapter 2 of this thesis sulfur isotope ratios were determined on a range of sulfur fractions from a site within the Tuckean Swamp adjacent to the Tuckean Nature Reserve Drain. According to that study the isotope signature of the soluble sulfate fraction was -2.4 ‰ at the oxidation boundary. This sulfate has been derived from the oxidation of pyrite and has the potential be flushed into the nearby drainage network. The sulfate signature recorded in the drain was fairly similar to the value recorded in the soil profile however it is likely there has been some dilution of the sulfate with fresh water.

The $\delta^{34}S$ value recorded in Yellow Creek Drain was also slightly lower than at the confluence (Table 4.4). Similarly, the isotope signatures indicate Yellow Creek Drain is contributing sulfate derived from the oxidation of acid sulfate soils into Hendersons Drain. This conclusion is further supported by the water quality data and the observations of abundant water lillies and very clear water in the drain. The collection of additional water samples along Yellow Creek Drain may lead to a more precise discharge location being identified.

Upstream of Yellow Creek Drain, the water quality improved slightly and the $\delta^{34}S$ value increased. More samples need to be collected from further upstream to confirm if the improved trend continues. This one sampling point upstream suggests that the slight improvement in water quality observed between Tuckean Nature Reserve Drain and Yellow Creek Drain can be attributed to water coming from further upstream along Hendersons Drain and not from within Yellow Creek Drain.

In this study the $\delta^{34}S$ of the sulfate fraction was strongly correlated with changes in pH and the chloride:sulfate ratio (Figure 4.7). When the chloride:sulfate ratio drops there was a corresponding drop in $\delta^{34}S$. The chloride:sulfate ratio indicates there was an alternative source of sulfate in the drainage waters. The $\delta^{34}S$ values indicate this additional source was derived from the oxidation of acid sulfate soil materials. As expected, this was accompanied by a drop in pH. Although commonly used in the identification of acid sulfate soil landscapes, the chloride:sulfate ratio and the pH should be used with care. In combination with sulfur isotope signatures however, the accuracy with which acid sulfate soils can be identified is markedly improved.

The results of this study strongly indicate sulfur isotope signatures of the dissolved sulfate fraction can be used to identify the sources of acidic discharges in acid sulfate soil landscapes. Future studies could employ a coarser sampling regime along the primary drainage channel in addition to collecting samples at the confluence with inflowing drains. If the isotope signatures indicate previous pyrite oxidation within an area, a more detailed sampling regime along the drain may lead to a more precise source location being identified. This would allow for targeted management initiatives to be developed.

Furthermore, the establishment of characteristic isotope ratios for landscape elements (such as acid sulfate soil materials) would make possible the use of mass balance approaches, especially with the use of other water quality data such as chloride:sulfate ratios, to quantify the relative contributions of these landscape elements to water quality during flow events. This may include quantifying the contribution the oxidation of acid sulfate soil materials makes to water flows in landscapes during different stages of flow events. Such an approach could lead to improvements in our understanding of the hydrology of acid sulfate soils and how they affect the hydrology of catchments during and between flow events.

Conclusion

This study examined the utility of using stable sulfur isotopes of dissolved sulfate to identify acidic discharges to waterways from acid sulfate soil materials. The data shows a strong association between the sulfur isotope signature of the sulfate in drain water with other parameters commonly used identify the influence of acid sulfate soils on waterways, specifically the pH and chloride:sulfate ratio. This study indicates sulfur isotope ratios could be used to help identify and possibly quantify acidic discharges from acid sulfate soils, particularly when used in combination with other water quality parameters. This study further indicates that the isotopes of sulfur in sulfate in waterways can be used as a tool to improve our understanding of the hydrology of acid sulfate soil materials and how they affect the hydrology of catchments during and between flow events.

Acknowledgements

This study was made possible with financial assistance from CRC CARE as part of the East Trinity project (6-6-01-06/07) and the School of Environment, Science and Engineering. I would like to thank Diane Fyfe and Vanessa Wong for help with field and laboratory work and reviewing drafts. A special thanks to Trent McIntyre for assistance with getting Shane's boat back out of the drain.

Chapter 5

Understanding the formation of acid sulfate soil materials in eastern Australia through a study of mangrove environments

Introduction

In eastern Australia many coastal acid sulfate soil materials were formed in the Holocene Epoch as a consequence of sea level rise between 6000 and 10 000 years ago (Russell and Helmke 2002; Powell and Martens 2005). Sea level rise allowed mangrove forests to establish up to 30 km inland from the current coastline (Ferguson and Eyre 1996). The establishment of mangroves provided a source of organic matter that allowed bacteria to reduce the sulfate in sea water to hydrogen sulfide (H_2S) (Bouillon *et al* 2008; Fan *et al* 2012). When combined with reduced iron from the sediment, iron sulfides, particularly in the form of pyrite, were formed (Naylor *et al* 1998; Bottcher *et al* 1998; Wijsman *et al* 2001).

When the sea levels receded sedimentation began and the sulfides in these mangrove sediments were buried by eroding non-sulfidic sediments from higher up in the catchment. These buried sulfidic, largely mangrove sediments constitute the bulk of modern day acid sulfate soil materials on the eastern Australian floodplains (Powell and Martens 2005). At some locations, especially near the levees, the depth to acid sulfate soil materials may be several metres, however at other sites, especially in the back swamps, they may be at or very near the surface (Johnston *et al* 2003c). Acid sulfate soil materials that remain in a reduced state are relatively stable and cause no environmental harm. If they are allowed to oxidise, usually through a change in the water table height, acid sulfate soils can cause significant environmental degradation (Cook *et al* 2000; Johnston *et al* 2003a; Smith *et al* 2004; Unland *et al* 2012.

It is well established that redox conditions vary considerably in mangrove sediments. In order to understand this variation Clark *et al* (1998) proposed a four-zone geochemical model which includes an upper oxidised zone, upper reduction zone, lower oxidised zone and a lower reduction zone. The thickness and depth of each zone is dependent on the position of the water table and whether it lies within or above the sediment, the frequency of tidal inundation and the presence or absence of mangroves. In areas that are constantly inundated the upper reduction zone can extend to the sediment surface and replace the upper oxidised zone. In areas without mangroves

with well-developed lateral root systems the lower oxidation zone will be absent and the upper and lower reduction zones merge (Clark *et al* 1998).

Other studies have classified redox stratification into oxic, suboxic and anoxic zones (Otero *et al* 2006; Ferreira *et al* 2007a, b). Oxic and anoxic zones are similar to the upper oxidised and lower reduction zones provided by Clark *et al* (1998). The suboxic zone is a combination of the upper reduction zone and lower oxidised zone. The distinction Clark *et al* (1998) gave for these zones was based on the mechanism of oxygen incorporation into the soil profile. In the upper reduction zone suboxic conditions can be attributed to bioturbation and ventilation of sediments, whereas in the lower oxidation zone suboxic conditions result from the release of oxygen from mangrove roots.

At many of the sites examined in Chapters 2 and 3 of this thesis there was a similarity in the isotope signature between the sulfide and sulfate fractions. This was attributed to oxidation of sulfides as the primary source of sulfate in these sediments. At many sites this trend continued below the oxidation boundary. Two possible theories were put forth to explain this trend; (1) oxidation products including sulfates diffuse downward through the profile and (2) in-situ cycling between the sulfide and sulfate fraction occurred as the sediments were deposited. The purpose of this chapter is to examine the latter of these points by analysing the sulfur isotope signature of sulfate in mangrove sediments. In this study, mangrove sediments are used to represent acid sulfate soil materials that are currently forming.

Stable isotopes of various sulfur fractions have been used to understand geochemical cycling in estuarine and mangrove environments (Bruchert 1998; Bruchert and Pratt 1999; Bottcher *et al* 2010; Fan *et al* 2012). Bruchert (1998) found similarities between the $\delta^{34}S$ of elemental and acid volatile sulfide fractions and that these fractions were less depleted in ^{34}S than the pyrite fraction. That study suggested that elemental and acid volatile sulfides were recycled back into the porewaters and that isotopic exchange takes place in the upper 3 cm of sediment. More recently a study by Fan *et al* (2012) found similarities in the $\delta^{34}S$ of elemental and pyrite sulfur fractions which were depleted in ^{34}S and that the acid volatile sulfide fraction was enriched in ^{34}S.

Their study also found the $\delta^{34}S$ signature became increasingly enriched with depth due to sulfate limitation.

Aim

The aim of this chapter is to examine possible cycling between the sulfide and sulfate fractions in acid sulfate soil materials as they are being formed. In this study, mangrove sediments are being used to represent acid sulfate soil materials that are currently forming.

Methodology

Sample collection and preparation

Samples for this study were collected from an *Avicennia*-dominated mangrove environment along the borders of North Creek in Ballina, New South Wales (28°51'3.25"S, 153°34'15.21"E). North Creek is tidal and adjoins the Richmond River estuary, which discharges at Ballina (Figure 5.1).

This study was conducted in two parts: 1) a single low tide sampling and 2) an extended sampling. The single low tide sampling provides a snap shot of the geochemistry of mangrove sediments at low tide when the sediments are at their most drained condition. Samples were collected from two sites approximately 50 m apart using a sleeve corer to a depth of 40 cm. Cores were stored on ice to be transported to the laboratory then placed in the freezer for approximately 3 hours to 'firm up' slightly without freezing through. When sufficiently firm they were cut into 10 cm depth increments, homogenised and returned to the freezer.

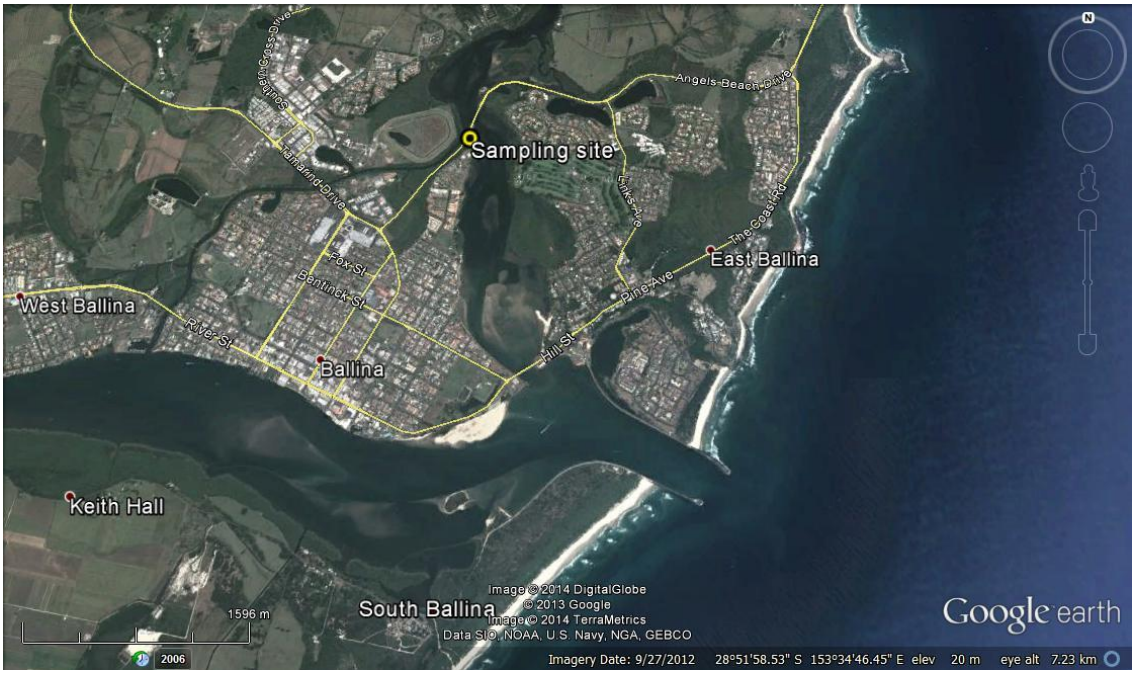

Figure 5.1. Google Earth image of Ballina showing sampling site

Chemical analysis

In the laboratories at Southern Cross University the following chemical analyses were performed on each depth increment. The moisture content of all samples was determined by drying a sub sample of the frozen soil at 105 °C for 7 days (Rayment and Lloyds 2011). The moisture content of the soils dried to 65 °C for total carbon was also determined. Where applicable, results are calculated on an oven dried mass.

pH, electrical conductivity

Frozen soil samples were placed in a centrifuge tube with Milli-Q water in a 1:5 soil:water ratio (Rayment and Lloyds 2011). The tubes were shaken in an end-over-end tumbler for 1 hour then allowed to settle for 15 minutes. pH was recorded using a calibrated Ionode IJ44 pH electrode and electrical conductivity recorded with a calibrated TPS Conductivity sensor.

Total carbon

Soil samples were dried at 65 °C then finely ground with a mortar and pestle for analysis of total carbon using a LECO-CNS 2000 induction furnace analyser with a detection limit of 0.01%.

Water soluble sulfate analysis

Sulfate was analysed by Inductively Coupled Plasma Optical Emission Spectrometry (ICP-OES) following extraction in a 1:5 soil:water suspension. Frozen soil samples (Maher *et al* 2004) were placed in centrifuge tubes with deoxygenated Milli-Q water and shaken for 1 hour. Samples were centrifuged and 10 mL of the supernatant extracted and filtered for analysis by ICP-OES according to APHA Method 3120 (APHA 2005). Duplicate analysis gave a precision of ± 8% with a detection limit of 0.05 mg/L. The remaining supernatant was retained for isotope analysis.

Acid volatile sulfur

The procedure used for the determination of acid volatile sulfur (AVS) is the same as that adopted by the Acid Sulfate Soil Laboratory Methods Guidelines (Ahern *et al* 2004). Approximately 10 g of frozen soil was weighed into a 200 mL conical flask. A vial containing 15 mL of 20% zinc acetate trapping solution was gently placed in the flask. To the flask, 2 mL of ascorbic acid was added and the stopper loosely fitted. The flask was purged with nitrogen gas for approximately 30 seconds. With the stopper firmly in place, a syringe was used to insert 15 mL of 6 M HCl into the flask. The flasks were then left for 24 hours to react.

After 24 hours, the zinc acetate trapping solution was titrated with iodine to a permanent blue end point. The amount of iodine was used to calculate the AVS content using the following formula:

$$\text{AVS (\%S)} = \frac{\text{(A–B) x C x 1600}}{\text{Mass of soil (mg)}} \qquad \textbf{Equation 5.1}$$

Where:

A = the volume of iodine (mL) used to titrate the soil sample

B = the volume of iodine (mL) used to titrate the blank

C = the molarity of the iodine solution as determined by titration of this solution with standardised 0.025 M sodium thiosulfate solution

$$C = \frac{0.025 \times \text{titration volume of standard thiosulfate solution (mL)}}{\text{Volume of iodine solution titrated (mL)}}$$

Duplicate analysis gave a precision of ± 8% with a detection limit of 0.001 %S.

Chromium reducible sulfur

In accordance with recommendations by Maher *et al* (2004), chromium reducible sulfur (CRS) analyses were performed on frozen soil using the method of Sullivan *et al* (2000). According to this method frozen soil was weighed into a reaction vessel and 2.059 g of chromium metal powder and 10 mL of ethanol (95% concentration) were added. The flask was connected to a condenser and 60 mL of 5.65 M HCl was added. The reaction evolved hydrogen sulfide gas which was trapped in a 100 mL Erlenmeyer flask containing 40 mL of zinc acetate trapping solution. The reaction vessel was brought to the boil and allowed to digest for 20 minutes.

At the completion of the digest the Erlenmeyer flask was removed and titrated with iodine to a permanent blue endpoint. The concentration of CRS was then calculated as follows:

$$\textbf{CRS (\%S)} = \frac{\textbf{(A–B) x C x 1600}}{\textbf{Mass of soil (mg)}} \qquad \textbf{Equation 5.2}$$

Where:

A = the volume of iodine (mL) used to titrate the soil sample

B = the volume of iodine (mL) used to titrate the blank

C = the molarity of the iodine solution as determined by titration of this solution with standardised 0.025 M sodium thiosulfate solution

$$C = \frac{0.025 \times \text{titration volume of standard thiosulfate solution (mL)}}{\text{Volume of iodine solution titrated (mL)}}$$

Duplicate analysis gave a precision of ± 9% with a detection limit of 0.001 %S.

Sulfur isotope analysis

Stable sulfur isotope analysis was conducted on selected layers from both sites. Both sulfide and sulfate fractions were examined. The sulfide fraction was extracted using the chromium reducible sulfur procedure detailed previously. When used as a stand-alone technique this process will extract all reduced inorganic sulfur species including acid volatile sulfur, elemental sulfur and pyrite sulfur (Sullivan *et al* 2000). To extract precipitate for isotope analysis additional chromium reducible sulfur runs were performed on selected samples. For these runs the trappings solutions were not titrated and the zinc sulfide precipitate was rinsed three times with Milli-Q water. The samples were centrifuged, the remaining water decanted and the precipitate dried in an oven overnight.

The isotope signature of the water soluble sulfate was examined on the supernatant remaining after sulfate analysis. The solution was extracted and syringe filtered into a new centrifuge tube. Approximately 10 mL of 1 M barium chloride ($BaCl_2$) solution was added to precipitate barium sulfate ($BaSO_4$). The precipitate was then rinsed, centrifuged and oven dried.

Zinc sulfide and barium sulfate precipitates were analysed for $\delta^{34}S$ by Continuous Flow Isotope Ratio Mass Spectrometry (CF-IRMS) using a Thermo Flash EA 1112 coupled to a Thermo Delta V Plus IRMS. NIST reference material 8555 was used for calibration. Results are presented as $\delta^{34}S_{(CRS)}$ for the sulfide fraction and $\delta^{34}S_{(SO4)}$ for the water soluble sulfate fraction. Duplicate analysis gave a precision of ± 0.3‰.

The extended sampling over a 12 hour period provided an examination of trends in sulfur cycling over an extended tidal draining period. The tidal cycle had no tidal recharge of the site during the 12 hour sampling period. Here, sediment samples were collected at the Site 1 location, in the same manner every 90 minutes for a period of 12 hours (a total of 9 sampling intervals). A piezometer was installed to a depth of 50 cm to monitor changes in the water level. The sampling period commenced at high tide. At each time interval, water in the piezometer was measured for pH, Eh, and EC by inserting a calibrated meter just below the water surface and recording the values. In addition, a sample was collected for sulfate analysis by ICP-OES.

Sediment soil samples were analysed for moisture content and chromium reducible sulfur. Isotope analysis was conducted on the water soluble sulfate fraction using a 1:5 soil:water extract. Methods for this part were the same as for the single low tide sampling.

Results and Discussion

Single low tide sampling

As Figure 5.2 suggests, there is considerable variation between the two sites despite being only 50 m apart. The apparent differences are most likely due to the different relative elevations of the profiles however, a change in the nature of the environment, whether depositional or eroding, may have also contributed. AVS was <0.0005 %S at both sites, consistent with a comparatively low iron concentration and a ready supply of sulfate encouraging transformation to pyrite (Gagnon *et al* 1995). However, other studies have recorded AVS concentrations up to two orders of magnitude greater than those recorded here (Fan *et al* 2012; Mazumdar *et al* 2012). Total carbon concentrations were relatively low particularly at depth at Site 2 and near the surface at Site 1. This indicates rapid organic matter decomposition in these sediments may be limiting the rate of sulfate reduction (Bottcher *et al* 1997).

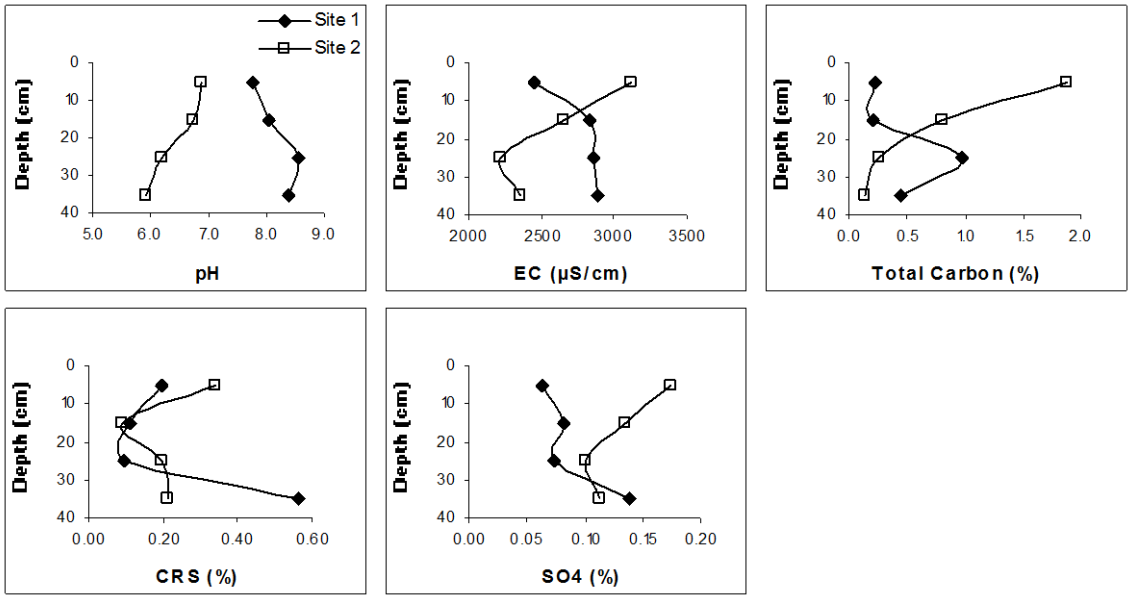

Figure 5.2. Selected soil characteristics for the mangrove profile examined in the single low tide sampling.

The $\delta^{34}S$ of the sulfate in the sediment pore waters were considerably less than recorded seawater sulfates (Bottcher *et al* 2004), despite proximity to the marine environment (Table 5.1). These values are different to the values reported in the literature for other marine environments where the $\delta^{34}S$ of the sulfate remained relatively constant at depths up to approximately 30 cm (Bates *et al* 1993; Bottcher *et al* 1997; Habicht and Canfield 1997). Bates *et al* (1993) found the $\delta^{34}S$ of sulfates decreased steadily from ~20 ‰ in the surface 20 cm layer to ~12 ‰ at 151 cm depth and suggested the difference was due to oxidation of sulfides during sample storage. In this study, considerable care was taken with all samples to prevent the oxidation of sulfides (Maher *et al* 2004), particularly during the procedure to extract sulfates for isotopic analysis. It is therefore unlikely, that oxidation after collection is responsible for the lower $\delta^{34}S$ values in the sulfate at this site.

Table 5.1. $\delta^{34}S$ of the CRS and SO_4 fractions for the Mangrove site studied in the single low tide sampling. Fractionation is calculated between $\delta^{34}S$ CRS and seawater SO_4 (SWS = 20.6‰).

Depth (cm)	$\delta^{34}S$ CRS (‰)	$\delta^{34}S$ water soluble SO_4 (‰)	Fractionation. from SWS (‰)
S1 0–10	-25.28	14.40	45.88
S1 30–40	-26.68	13.35	47.28
S2 0–10	-27.20	9.58	47.80
S2 30–40	-27.92	3.17	48.52

At these sites the lower than expected $\delta^{34}S$ values in the sulfate may have resulted from in-situ oxidation of sulfides brought about by bioturbational processes which either transport sulfides to the surface where they interact with oxygen, or by aerating the sediments below the surface. Although the rate of pyrite oxidation may be slow relative to tidal flushing events, the oxidation of dissolved and acid volatile sulfur species will proceed much faster and could therefore contribute to the low isotope values in the sulfate. The $\delta^{34}S$ of the Ballina sulfates may also be related to tidal variations. During low tide, which is when these samples were collected, sediments are more exposed and oxidation is more likely to occur. During high tide, the sediments are inundated with seawater and the products of oxidation may be washed from the profile, diluted or converted back to sulfides via sulfate reduction.

The $\delta^{34}S$ values of the CRS fraction showed little variation either in depth or between profiles. The fractionation from seawater is within the range for bacterial sulfate reduction and corresponds with other findings for sulfides formed in marine environments. These strongly negative sulfide values are consistent with a system that is open with respect to sulfate supply. At these sites, the burial of the sediments to a depth of 40 cm has not been sufficient to restrict the sulfate supply during sulfide formation and the system remains open.

Extended sampling over a draining phase

In order to examine the possibilities suggested in the single low tide sampling a closer examination of cycling between the sulfide and sulfate fractions over an extended period of 12 hours from a high tide peak was undertaken. In particular, the low isotope signature in the sulfate fraction required further examination. This was achieved by examining the changes in the sulfate isotope signature over a 12 hour period from a high tide (the following high tide did not inundate the trial site allowing an extended drainage cycle to be examined). This experiment was conducted at Site 1 from the single low tide sampling.

Sampling commenced at 05:30 am and ran for 12 hours giving a total of 9 sampling intervals. At the start of the experiment the site was overlain by tidal water. Figure 5.3 displays the water depth and chemistry results recorded in the piezometer at each time period. The water level at the site dropped from 3 cm above the sediment surface to 18 cm below the sediment surface over the 12 hours. Over this time the pH of the water in the piezometer also dropped from 6.93 to 6.30. Sulfate concentrations however increased nearly 30%. The pH and sulfate concentrations indicate there may have been some in-situ oxidation of pyrite occurring in the profile which was altering the chemistry of the water in the piezometer. The Eh however indicated a change from oxidising conditions at the start to reducing conditions after 12 hours.

Figure 5.4 shows the changes in CRS concentration and $\delta^{34}S_{(SO4)}$ at the upper and lower depths over the 12 hour study period. The surface concentration of CRS showed very little variation. At 30–40 cm depth however, CRS dropped from 1.08 %S at

05:30 to 0.25 %S at 14:30. In the last 90 minutes of the study the CRS increased to 1.2 %S. This supports the water chemistry results which indicate pyrite oxidation followed by a return to reducing conditions which favour pyrite formation (Marchand *et al* 2004). Hourly variations in pyrite content of this magnitude are very unlikely and it is assumed the observed variation in these samples is due to heterogeneity in the sediments giving rise to sample variability rather than geochemical processes. The $\delta^{34}S$ of the sulfate also varied considerably due to spatial heterogeneity over the study period particularly at depth. The sulfate signature fell to 14.8 ‰, which is still slightly higher than the maximum value recorded in the single low tide sampling.

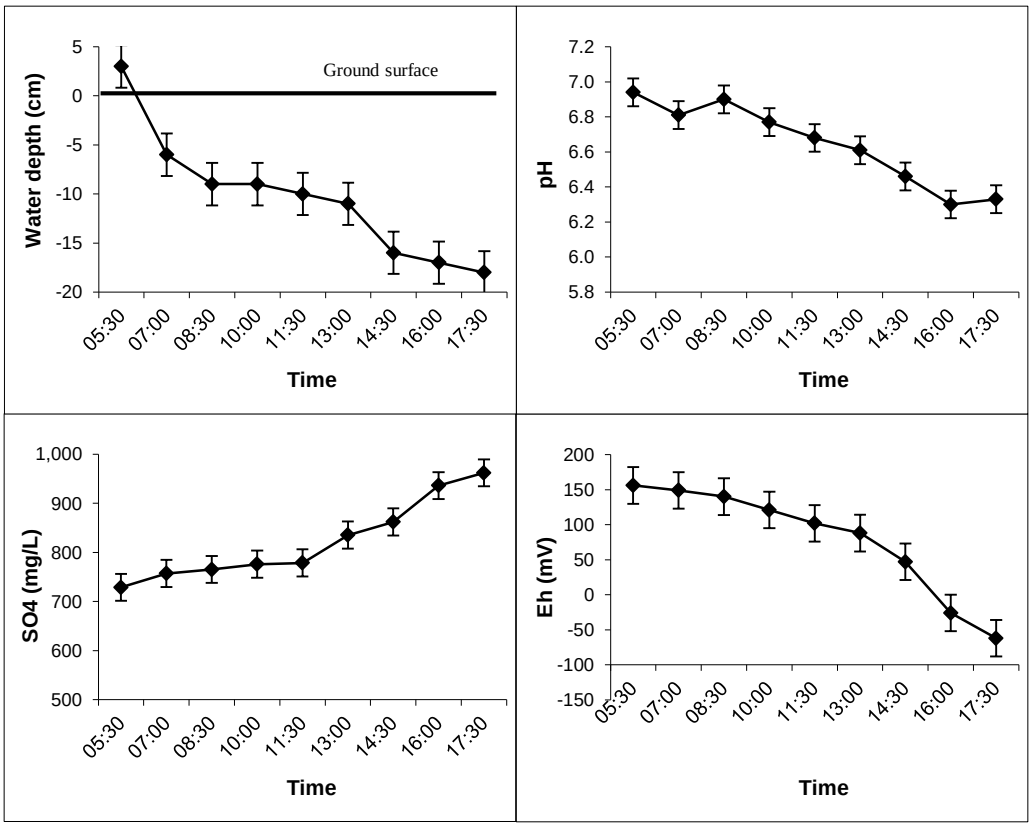

Figure 5.3. Water depth and chemistry recorded in the piezometer at each time interval in the extended sampling. Error bars are based on the standard error.

There is considerable variation in the CRS and $\delta^{34}S_{(SO4)}$ down the profiles and across the time periods which make it difficult to decipher any clear patterns or trends (Figure 5.5). It was expected that as the tide dropped there would be oxidation of pyrite in the soil which would provide a sulfate isotope signature less than seawater. There are indications that this has occurred in the 30–40 cm layers at 08:30 and again

at 13:00. However, at other times for example 10:00 and 14:30, there is a drop in CRS and an increase in $\delta^{34}S_{(SO4)}$.

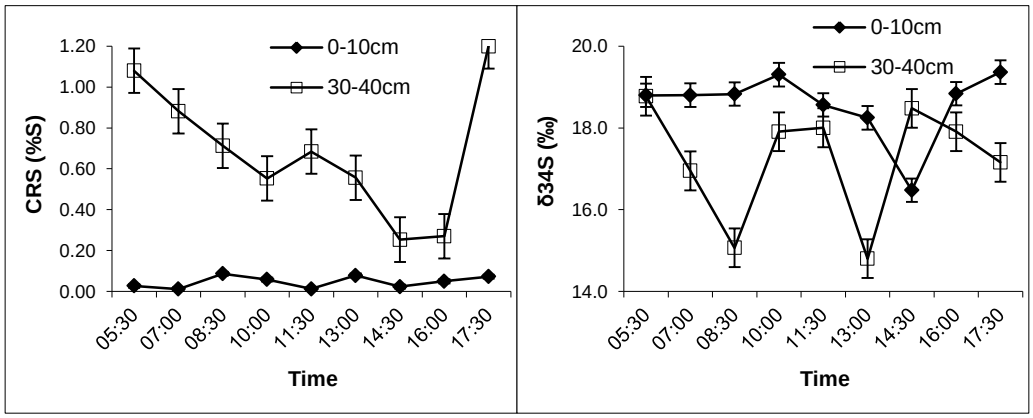

Figure 5.4. Changes in CRS concentration and $\delta^{34}S_{(SO4)}$ for 0–10 cm and 30–40 cm layers over 12 hours. Error bars are based on the standard error.

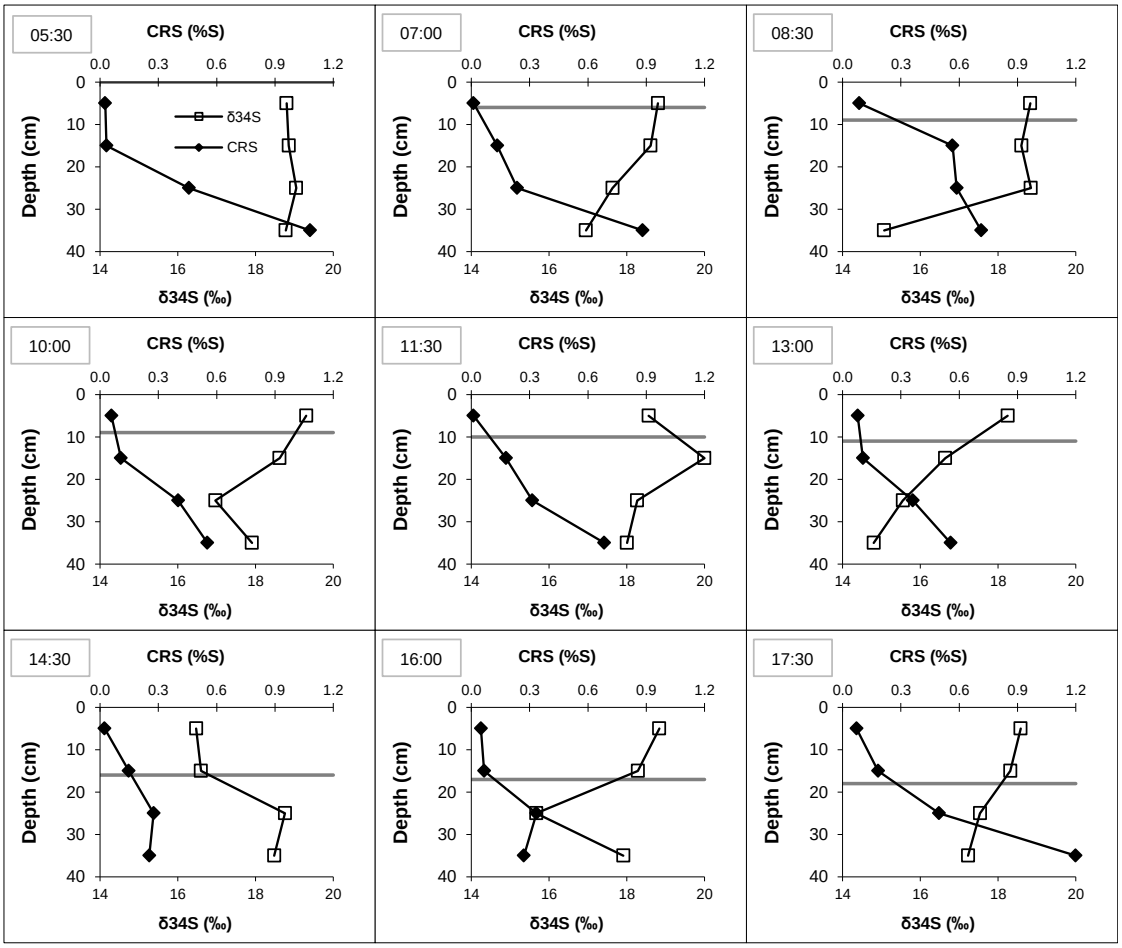

Figure 5.5. CRS concentrations and $\delta^{34}S_{(SO4)}$ recorded down the profile for each time interval. The grey horizontal line indicates the water level.

Figure 5.6 shows the CRS and $\delta^{34}S_{(SO4)}$ values averaged across all the time intervals for each depth. The figure indicates that CRS concentration increases with depth as would be expected with burial of the sediments. There is also a small decrease in the $\delta^{34}S_{(SO4)}$ values with depth.

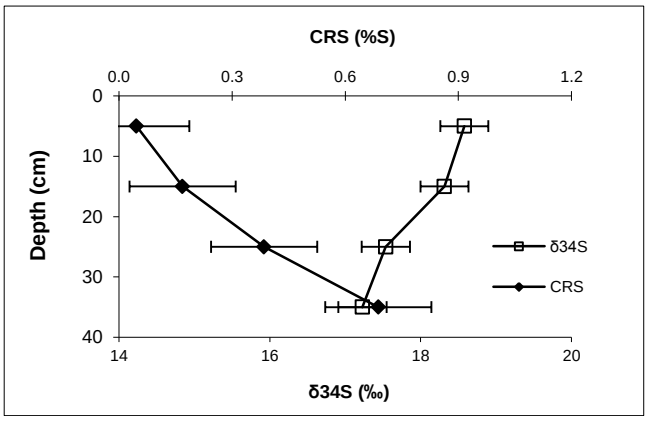

Figure 5.6. CRS and $\delta^{34}S_{(SO4)}$ values averaged across all the time intervals for each depth. Bars indicate the standard error.

Clark *et al* (1998) provided a four-zone geochemical model to explain the changes in redox potential in an environment similar to this study (Figure 5.7). According to that model the 'upper oxidised zone' is influenced by diffusion of atmospheric oxygen. The depth to which oxygen can diffuse is controlled by the sediment texture, the position of the water table and the nature and extent of sediment reworking by biota (Clark *et al* 1998). Sulfide oxidation in this zone would contribute sulfate that has a similar isotope signature to the sulfide thereby lowering the $\delta^{34}S$ in the sulfate fraction. In this study however, sulfide concentrations were quite low in the upper profile so they may not be affecting the sulfate signature.

In the 'upper reduction zone' microbial sulfate reduction is extensive which allows the formation of sulfide minerals (Clark *et al* 1998). This zone however, is also extremely dynamic and is often affected by burrowing and sediment turnover which can introduce oxygen into the profile (Gribsholt and Kristensen 2003; Ferreira *et al* 2007a; Volkenborn *et al* 2007). Throughout this study there is a trend of increasing CRS concentration with depth indicating extensive sulfate reduction. At sites which are constantly inundated the 'upper reduction zone' may extend to the sediment

surface (Clark *et al* 1998), however in this study the surficial sediments were exposed for nearly 12 hours.

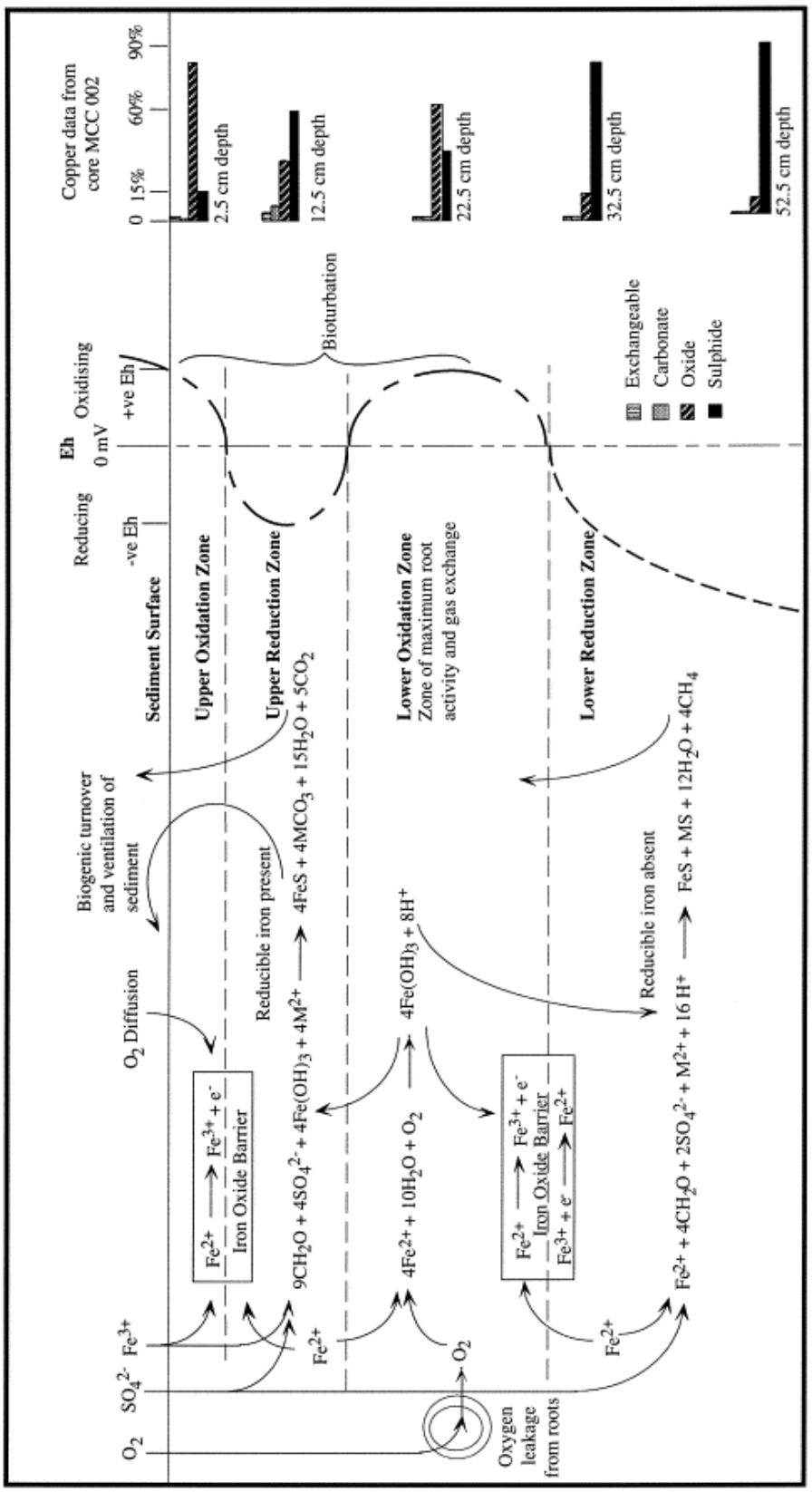

Figure 5.7. Four zone geochemical model proposed by Clark *et al* (1998).

The ‘lower oxidation zone’ occurs from the release of oxygen from mangrove roots (McKee *et al* 1988; Clark *et al* 1998). This oxidation is generally limited to the sediment near the mangrove roots and does not affect the surrounding sediment which remains reducing (Ferreira *et al* 2007a). In the current study the establishment of oxidising conditions around plant roots may have caused the considerable spatial and temporal variations seen in the CRS concentrations and sulfate isotope signatures.

The geochemical model provided by Clark *et al* (1998) also describes a ‘lower reduction zone’. In this zone redox potentials are likely to be at their lowest and sulfate reduction leads to the production of methane rather than carbon dioxide (Manahan 1990; Seralathan *et al* 2006). According to Clark *et al* (1998) sulfide formation in the ‘lower reduction zone’ may be limited by the availability of sulfate. Given the sediment in this study was covered with tidal water at the start and only dropped to 18 cm below ground surface after 12 hours it is unlikely that sulfate supply was limited at depth. The high CRS concentrations recorded at depth in this study and the $\delta^{34}S_{(CRS)}$ recorded in the single low tide sampling also indicate sulfate reduction was not limited by sulfate supply.

The varying redox conditions that typify mangrove sediments make it difficult to identify where pyrite is oxidising and sulfate is being reduced. In this study classifying the different redox zones is complicated by the influence of tidal water and the fact that the transition from one zone to another is often gradual with minor variations in Eh (Clark *et al* 1998). It was expected that oxidising conditions would bring about a lowering of the sulfate isotope signature due to sulfate being provided by the oxidation of pyrite. However, in the upper oxidised zone, there may not have been sufficient pyrite concentrations to significantly affect the sulfate signature. In the lower oxidation zone, if the extent of oxidising conditions is limited to the sediment near the mangrove roots, the sampling regime for this study may have been too coarse to pick up the in-situ oxidation that was seen in the single low tide sampling.

Although speculation, if reducing conditions prevail the sulfate isotope signature may be the same as seawater or slightly higher depending on the degree of tidal influence. If reducing conditions are established above the level of the tidal influence pyrite

would begin to form and there would be an increase in the sulfate isotope signature. This increase would occur due to removal of light sulfate to form sulfides leaving a greater abundance of heavy sulfate. If however, the reducing conditions were the result of tidal influence, it would be more difficult to detect a change in the sulfate isotope signature as the seawater signature would dominate. In this case, removal of the light sulfate would not affect the overall sulfate signature of the water.

Both parts of this study indicate that sulfide oxidation below the surface may contribute to low $\delta^{34}S$ values in the sulfate fraction. However, a change in CRS concentration and the consequent effect on the $\delta^{34}S_{(SO4)}$ values was extremely difficult to detect even during a prolonged drainage period due to the large degree of sample variability. The results indicate the $\delta^{34}S_{(SO4)}$ was lower at depth compared to the surface sediments which most likely results from natural long term sulfide oxidation processes in the sediment. Importantly, the lower $\delta^{34}S_{(SO4)}$ is clearly not an artefact of sulfide oxidation during sample handling and preparation as suggested by Bates *et al* (1993). If sampling handling were the cause of the low $\delta^{34}S_{(SO4)}$ the effect would have been seen in all samples.

In situ cycling of sulfides and sulfates in mangrove sediments is highly dynamic and controlled by redox conditions, which are in turn controlled by bioturbation, aeration from mangrove roots, sediment depth and texture, tidal range, etc. In order to more comprehensively understand the degree of cycling in these sediments and the effect it may have on the sulfide and sulfate composition, the redox conditions throughout the profile would need to be more closely examined and correlated with changes in the sulfate isotope signature. In addition, an experiment that employed a finer depth scale (e.g. 2–5 cm depth increments) could highlight smaller pockets of oxidation.

The problem of inherent heterogeneity on small and large spatial scales in mangrove areas may be addressed by the use of large scale sediment systems (mesocosms) where the experimental conditions can be controlled according to the study objectives (Alongi *et al* 2000; Gribsholt and Kristensen 2002; Kristensen and Alongi 2006). This would allow for more controlled monitoring of redox conditions, tidal influence and sulfide and sulfate concentrations and isotope signatures. A comparison study from

areas that contained mangroves of different species and development stages or where mangroves are excluded may help understand the occurrence and effect of the lower oxidation zone on sediment cycling (Clark *et al* 1998; Marchand *et al* 2004).

Conclusion

This study was conducted in two parts. The first part provided a snap shot of the geochemistry and isotope signature of mangrove sediments in a single low tide sampling. The second part attempted to assess changes in the sulfate isotope signature over a 12 hour extended drainage phase. Both parts were conducted in an *Avicennia* - dominated mangrove environment in Ballina, northern New South Wales.

The single low tide sampling indicated considerable variation in the geochemistry of mangrove sediments over small spatial distances. The $\delta^{34}S$ of the sulfide fraction was consistent between profiles and with depth however, the $\delta^{34}S$ of the sulfate fraction was considerably less than sea water sulfate despite the proximity to tidal water.

The extended sampling also showed considerable variation in CRS concentration and $\delta^{34}S_{(SO4)}$ down the profile and across the 12 hour study period. This variation was attributed to readily changing redox conditions which can be affected by bioturbation, aeration from mangrove roots, changes in tidal height and the inherent heterogeneity of mangrove sediments. These factors contribute to considerable sample variability and make it difficult to detect whether pyrite is oxidising or sulfate is reducing on very small spatial scales.

Both parts of this study indicate that sulfide oxidation below the surface could contribute to low $\delta^{34}S$ values in the sulfate fraction indicative of in-situ cycling between sulfide and sulfate fractions in mangrove sediments. However to determine if in-situ cycling during deposition was the cause of the similarity between the sulfide and sulfate isotope signature below the oxidation boundary in acid sulfate soils would require a more rigorous experimental strategy that accounted for the heterogeneity of these sediments.

Acknowledgements

This study benefitted from financial assistance from CRC CARE as part of the East Trinity project (6-6-01-06/07) and the School of Environment, Science and Engineering. I would like to also thank Shane Stenner for helping with field work, Diane Fyfe for transporting samples to the freezer and Debra Stokes for reviewing the draft.

Chapter 6

Conclusions

The natural variation and fractionation of stable sulfur isotopes makes them an ideal tool in many geochemical studies (Bottcher *et al* 1998; Bottcher and Lepland 2000; Wijsman *et al* 2001; Mazumdar *et al* 2007; Mayer *et al* 2010). The technique has been applied in many studies examining the formation environment of sulfide ores, differentiating sulfur sources and separating high and low temperature sulfur deposits. Despite their application in many related fields sulfur isotopes have only been used in a handful of studies relating to acid sulfate soils.

The overall aim of this thesis was to examine the geochemical processes in acid sulfate soil environments using stable sulfur isotopes. This was achieved by meeting the following specific objectives:

1) Establish a baseline for the use of stable sulfur isotopes in acid sulfate soils by examining the isotope signature of samples from different acid sulfate soil environments.

This chapter examined the sulfur isotope signature in the sulfide and sulfate fraction of acid sulfate soils formed under different conditions including coastal clay and peat dominated soils, coastal and inland monosulfidic black ooze samples. Clay dominated acid sulfate soils which were deposited during the last sea level rise gave strongly negative $\delta^{34}S$ signatures in both the sulfide and sulfate fractions. Peat dominated acid sulfate soils which form in more fresh or brackish water environments showed both positive and negative values in the sulfide fraction and only positive values in the sulfate fraction.

The isotope signatures recorded in these different environments can be linked to whether the environments were open or closed with respect to sulfate supply. The sulfate supply in sea water was abundant and therefore negative isotope signatures were recorded in the clay sediments. The sulfate supply in fresh water was more limited which resulted in positive isotope signatures recorded in the peat sediments. The monosulfidic black ooze samples were similar to the peat sediments and also closely aligned with their respective soil samples. The inland samples also gave both

positive and negative sulfide signatures, however the sulfate signature was strongly positive indicating a very different source from the other sites.

Understanding how the environment of formation can affect the isotope signature of the sulfide and sulfate fractions of acid sulfate soil materials may allow the identification of dissolved sulfate from sulfide oxidation. This may then allow the quantification of the sulfate that is supplied to nearby waterways from sulfide oxidation under different hydrological conditions.

2) Use sulfur isotope ratios to understand the geochemical processes operating in acid sulfate soils subject to remediation by lime assisted tidal exchange.

This study was conducted at the CRC CARE National Acid Sulfate Soil Demonstration Site near Cairns in far north Queensland. This site had been subjected to severe environmental degradation due to oxidising acid sulfate soils. In 2001 a lime assisted tidal exchange remediation strategy was implemented to address the problems. Remediation of the site brought about many geochemical changes which were examined using sulfur isotopes in the sulfide and sulfate fractions. The sulfide fraction was a combination of acid volatile sulfur, elemental sulfur and pyrite. The sulfate fractions included water soluble sulfate, exchangeable sulfate and acid soluble sulfate.

Deposits of acid extractable sulfate such as jarosite provided indications of the conditions prior to the reintroduction of tidal water. Jarosite was also found to be less depleted in ^{34}S than the corresponding sulfide indicating some fractionation may be occurring during oxidation. Water soluble and exchangeable sulfate reflect the contemporary conditions and are likely derived from two potential sources. The oxidation of pyrite produces sulfate with an isotope signature similar to the pyrite, which at these sites was isotopically negative, whereas sulfate provided in the tidal water carries a positive isotope signature similar to sea water sulfate.

At sites with tidal influence contemporary sulfide formations also reflected the varied soluble sulfate sources and could be isotopically distinguished from the relic pyrite

found at depth. Reformed pyrite had an isotope signature that indicated sulfate reduction from two sulfate sources; sulfate derived from the oxidation of pyrite and sulfate in the tidal water. Relic pyrite indicated conditions of formation solely under tidal conditions.

This study has shown the examination of stable isotopes of sulfur in various soil fractions can be used to provide information about the geochemical history of acid sulfate soils undergoing remediation by lime assisted tidal exchange.

3) Use stable sulfur isotopes in water to identify sites where acid sulfate soils may be oxidising and discharging acidity into waterways.

This study examined the use of stable sulfur isotopes of dissolved sulfate to identify acidic discharges to waterways from acid sulfate soil materials. The data showed a strong association between the sulfur isotope signature of sulfate in drain waters with other parameters commonly used to help identify the influence of acid sulfate soils on waterways, specifically pH and the chloride:sulfate ratio.

This study indicated sulfur isotope ratios could be used to help identify and possibly quantify acidic discharges from acid sulfate soils, particularly when used in combination with other water quality parameters. This study further indicated that sulfur isotopes of sulfate in waterways is a tool that could be used to improve our understanding of the hydrology of acid sulfate soil materials and how they affect the hydrology of catchments during and between flow events.

4) Use sulfur isotopes to examine the cycling between the sulfide and sulfate fractions of acid sulfate soil materials in eastern Australia as they are being formed.

The first part of this study provided a snap shot of the geochemistry and isotope signature of mangrove sediments in a single low tide sampling. The second part attempted to assess changes in the sulfate isotope signature over a 12 hour extended drainage phase. Both parts were conducted in an *Avicennia* - dominated mangrove environment in Ballina, northern New South Wales.

The single low tide sampling indicated considerable variation in the geochemistry of mangrove sediments over small spatial distances. The $\delta^{34}S$ of the sulfide fraction was consistent between profiles and with depth however, the $\delta^{34}S$ of the sulfate fraction was considerably less than sea water sulfate despite the proximity to tidal water.

The extended sampling showed considerable variation in CRS concentration and $\delta^{34}S_{(SO4)}$ down the profile and across the 12 hour study period. This variation was attributed to readily changing redox conditions which can be affected by bioturbation, aeration from mangrove roots and changes in tidal height and the inherent heterogeneity of mangrove sediments. These factors contribute to considerable sample variability and make it difficult to detect whether pyrite is oxidising or sulfate is reducing on very small spatial scales.

Both parts of this study indicate sulfide oxidation below the surface could contribute to low $\delta^{34}S$ values in the sulfate fraction which indicates that in-situ cycling between the sulfide and sulfate fraction may occur in mangrove sediments. However, to determine if in-situ cycling during deposition may be the cause of the similarity between the sulfide and sulfate isotope signature below the oxidation boundary in acid sulfate soils would require a more rigorous experimental strategy that accounted for the heterogeneity of these sediments.

Chapter 7

References

Ahern CR, Blunden B, Stone Y, Sullivan LA, Tulau MJ (2000) Acid sulfate soils laboratory methods guidelines. In 'Acid sulfate soils manual, draft 2000 (Eds Y Stone, CR Ahern, B Blunden & MJ Tulau). (Acid Sulfate Soil Management Advisory Committee: Wollongbar, New South Wales, Australia).

Ahern CR, McElnea AE, Sullivan LA (2004) Acid sulfate soils laboratory methods guidelines. (Queensland Department of Natural Resources, Mines and Energy: Indooroopilly, Queensland, Australia).

Allery S (2002) Distribution of pyrite and marcasite in a peat profile: Boggy Creek Drainage System, northern NSW. Integrated Project. (Southern Cross University: Lismore, New South Wales, Australia).

Allery S (2003) Sulfide mineralogy, oxidation behaviour and acidification of peat acid sulfate soil materials. Honours Thesis. (Southern Cross University: Lismore, New South Wales, Australia).

Alongi DM, Tirendi F, Clough BF (2000) Below ground decomposition of organic matter in forests of the mangroves *Rhizophoa stylosa* and *Avicennia marina* along the arid coast of Western Australia. *Aquatic Botany*, **68,** 97-122.

Andersen R, Chapman SJ, Artz RRE (2013) Microbial communities in natural and disturbed peatlands: A review. *Soil Biology and Biochemistry,* **57,** 979-994.

Andrews JE, Brimblecombe TD, Liss PS (2000) 'An introduction to environmental chemistry'. (Blackwell Science: Oxford, London, England).

APHA (2005). 'Standard methods for the examination of water and wastewater, 21st Edition' (American Public Health Association – American Water Works Association: Baltimore, United States of America).

Astrom M, Spiro B (2000) Impact of isostatic uplift and ditching of sulfidic sediments on the hydrochemistry of major and trace elements and sulfur isotope ratios in streams, western Finland. *Environmental Science and Technology,* **34,** 1182-1188.

Backlund K, Boman A, Frojdo S, Astrom M (2005) An analytical procedure for determination of sulfur species and isotopes in boreal acid sulfate soils and sediments. *Agricultural and Food Science,* **14,** 70-82.

Balci N, Shanks WC, Mayer B, Mandernack KW (2007) Oxygen and sulfur isotope systematics of sulfate produced by bacterial and abiotic oxidation of pyrite. *Geochimica et Cosmochimica Acta,* **71**, 3796-3811.

Bates AL, Spiker EC, Orem WH, Burnett WC (1993) Speciation and isotopic composition of sulfur in sediments from Jellyfish Lake, Palau. *Chemical Geology,* **106,** 63-76.

Berglund M, Wieser ME (2011) Isotopic compositions of the elements 2009 (IUPAC Report). *Journal of the Chemical Society*, **83,** 397-410.

Berndmeyer C, Birgel D, Brunner B, Wehrmann LM, Jons N, Bach W, Arning ET, Follmi KB, Peckmann J (2012) The influence of bacterial activity of phosphorate formation in the Miocene Monterey Formation, California. *Palaeogeography, Palaeoclimatology, Palaeoecology,* **317-318,** 171-181.

Berner RA (1964) An idealized model of dissolves sulfate distribution in recent sediments. *Geochimica et Cosmochimica Acta,* **28,** 1497-1503.

Berner RA (1970) Sedimentary pyrite formation: an update. *American Journal of Science,* **268,** 1-23.

Berner RA (1984) Sedimentary pyrite formation: an update. *Geochimica et Cosmochimica Acta,* **48,** 605-615.

Bloch J, Krouse HR (1992) Sulfide diagenesis and sedimentation in the Albian Harmon Member, Western Canade. *Journal of Sedimentary Petrology*, **62,** (2), 235-249.

Bloomfield C, Coulter JK (1973) Genesis and management of acid sulfate soils. *Advances in Agronomy,* **25**, 265-326.

Blunden BG, Indraratna B (2000) Evaluation of surface and groundwater management strategies for drained sulfidic soil using numerical simulation models. *Australian Journal of Soil Science,* **38**, 569-590.

Bolton KGE (2001) Byron Bay effluent reuse project. Consultant's report prepared for Byron Bay Shire Council: Australia.

Bolton KGE, Sullivan LA, Rosicky MA, Ward NJ, Balson A, Bruce JJ (2002a) Changes in water and soil chemistry in response to effluent irrigation in a peat acid sulfate soil. Oral Paper, 5th International acid sulfate soil conference, 25-30 August, 2002 (Tweed Heads, New South Wales, Australia).

Bolton KGE, Warner P (2002b) Effluent reuse for acid sulfate soil management, wetland regeneration and carbon credits. Poster Paper 5th International acid sulfate soil conference, 25-30 August 2002 (Tweed Heads, New South Wales, Australia).

Boman A, Astrom M, Frojdo S (2008) Sulfur dynamics in boreal acid sulfate soils rich in metastable iron sulfide – the role of artificial drainage. *Chemical Geology,* **255,** 68-77.

Boman A, Frojdo S, Bucklund K, Astrom ME (2010) Impact of isostatic land uplift and artificial drainage on oxidation of brackish-water sediments rich in metastable iron sulfide. *Geochimica et Cosmochimica Acta,* **74,** 1268-1281.

Bottcher ME, Khim B, Suzuki A, Gehre M, Wortmann UG, Brumsack H (2004) Microbial sulfate reduction in deep sediments of the Southwest Pacific (ODP Leg

181, sites 1119-1125): evidence from stable sulfur isotope fractionation and pore water modelling. *Marine Geology* **205**, 249-260.

Bottcher ME, Lepland A (2000) Biogeochemistry of sulfur in a sediment core from the west-central Baltic Sea: Evidence from stable isotopes and pyrite textures. *Journal of Marine Systems,* **25,** 299-312.

Bottcher ME, Rusch A, Hopner T, Brumsack HJ (1997) Stable sulfur isotope effects related to local intense sulfate reduction in a tidal sandflat (southern North Sea): results from loading experiments. *Isotopes in Environmental Health Studies,* **33,** 109-129.

Bottcher ME, Smock AM, Cypionka H (1998) Sulfur isotope fractionation during experimental precipitation of iron (II) and manganese (II) sulfide at room temperature. *Chemical Geology,* **146,** 127-134.

Bottcher ME, Voss M, Schulz-Bull D, Schneider R, Leipe T, Knoller K (2010) Environmental changes in the Pearl River Estuary (China) as reflected by light stable isotopes and organic contaminants. *Journal of Marine Systems,* **82,** 543-553.

Bottrell SH, Louie PKK, Timpe RC, Hawthorne SB (1994) The use of stable sulfur isotopes to assess selectivity of chemical analyses and extractions of forms of sulfur in coal. *Fuel,* **73,** (10), 1578-1582.

Bouillon S, Connolly RM, Lee SY (2008) Organic matter exchange and cycling in mangrove ecosystems: Recent insights from stable isotope studies. *Journal of Sea Research,* **59,** 44-58.

Bradley AS, Leavitt WD, Johnston DT (2011) Revisiting the dissimilatory sulfate reduction pathway. *Geobiology,* **9,** 446-457.

Branch A (2001) The influence of benthic microalgae on sulfur cycling in an estuarine sediment. Honours Thesis. (Southern Cross University: Lismore, New South Wales, Australia).

Bridgeman HA (1989) Acid rain studies in Australia and New Zealand. *Archives of Environmental Contamination and Toxicology,* **18,** 137-146.

Brown TL, LeMay Jr. HE, Bursten BE (2000) 'Chemistry the central science. 8th Edition'. (Prentice Hall International Inc.: New Jersey, United States of America).
Brownlow AH (1996) 'Geochemistry, 2nd Edition'. (Prentice Hall Inc,: New Jersey, United States of America).

Bruchert V (1998) Early diagenesis of sulfur in estuarine sediments: The role of sedimentary humic and fulvic acids. *Geochimica et Cosmochimica Acta,* **62,** 1567-1586.

Bruchert V, Pratt LM (1999) Stable sulfur isotopic evidence for historical changes of sulfur cycling in estuarine sediments from northern Florida. *Aquatic Geochemistry,* **5,** 249-268.

Bureau of Meteorology (BOM) (2012). http://www.bom.gov.au [accessed 12 December 2012].

Burton ED, Bush RT, Johnston SG, Sullivan LA, Keene AF (2011a). Sulfur biogeochemical cycling and novel Fe-S mineralisation pathways in a tidally re-flooded wetland. *Geochimica et Cosmochimica Acta,* **75,** 3434-3451.

Burton ED, Bush RT, Sullivan LA (2006a) Sedimentary iron geochemistry in acidic waterways associated with coastal lowland acid sulfate soils. *Geochimica et Cosmochimica Acta,* **70,** 5455-5468.

Burton ED, Bush RT, Sullivan LA (2006b) Acid volatile sulfide oxidation in coastal flood plain drains: Iron-sulfur cycling and effects on water quality. *Environmental Science and Technology,* **40,** 1217-1222.

Burton ED, Bush RT, Sullivan LA (2006c) Fractionation and extractability of sulfur, iron and trace elements in sulfidic sediments. *Chemosphere,* **64,** 1421-1428.

Burton ED, Bush RT, Sullivan LA (2006d) Reduced inorganic sulfur speciation in drain sediments from acid sulfate soil landscapes. *Environmental Science and Technology,* **40,** 888-893.

Burton ED, Bush RT, Sullivan LA (2009) Iron-monosulfide oxidation in natural sediments: Resolving microbially mediated S transformations using XANES, electron microscopy and selective extractions. *Environmental Science and Technology,* **43,** 3128-3134.

Burton ED, Bush RT, Sullivan LA, Johnston SG, Hocking RK (2008) Mobility of arsenic and selected metals during reflooding of iron and organic rich acid sulfate soil. *Chemical Geology,* **253,** 64-73.

Burton ED, Bush RT, Sullivan LA, Mitchell DRG (2007) Reductive transformation of iron and sulfur in schwertmannite-rich accumulations associated with acidified coastal lowlands. *Geochimica et Cosmochimica Acta,* **71,** 4456-4473.

Burton ED, Johnston SG, Bush RT (2011b) Microbial sulfidogenesis in ferrihydrite-rich environments: Effects on iron mineralogy and arsenic mobility. *Geochimica et Cosmochimica Acta,* **75,** 3072-3087.

Burton ED, Johnston SG, Watling K, Bush RT, Keene AF, Sullivan LA (2010) Arsenic effects and behavior in association with the Fe(II) catalysed transformation of schwertmannite. *Environmental Science and Technology,* **44,** 2016-2021.

Bush RT (2000) Micromorphology and mineralogy of iron sulfides in acid sulfate soils: their formation and behaviour. PhD Thesis. (University of New South Wales: Australia).

Bush RT, Fyfe D, Sullivan LA (2002) Distribution and occurrence of monosulfidic black ooze (MBO) in coastal acid sulfate soil landscapes. Poster Paper 5th International Acid Sulfate Soil Conference, 25-30 August 2002 (Tweed Heads, New South Wales, Australia).

Bush RT, Fyfe D, Sullivan LA (2004a) Occurrence and abundance of monosulfidic black ooze in coastal acid sulfate soil landscapes. *Australian Journal of Soil Research,* **42**, 609-616.

Bush RT, Sullivan LA (2002) Iron monosulfides at the oxidation front of a coastal acid sulfate soil. In 'Acid sulfate soils in Australia and China'. (Eds C Lin, M Melville, L Sullivan). (Science Press: Beijing, China).

Bush RT, Sullivan LA, Fyfe DM, Johnston SG (2004b) Redistribution of monosulfidic black ooze by flood waters in a coastal acid sulfate soil floodplain. *Australian Journal of Soil Research*, **42**, 603-607.

Butler IB, Bottcher ME, Rickard D, Oldroyd A (2004) Sulfur isotope partitioning during experimental formation of pyrite via the polysulfide and hydrogen sulfide pathways: implications for the interpretation of sedimentary and hydrothermal pyrite isotope records. *Earth and Planetary Science Letters,* **228,** 495-509.

Callinan RB, Sammut J, Fraser GC (1996) Epizootic ulcerative syndrome (red spot disease) in estuarine fish – confirmation that exposure to acid sulfate soil runoff and an invasive aquatic fungus *Aphanomyces* sp., are causative factors. In 'Proceedings of the 2nd national conference of acid sulfate soils' (Robert J Smith and Associates and ASSMAC: Australia)

Canfield DE (2004) The evolution of the Earth surface sulfur reservoir. *American Journal of Science,* **304,** 839-861.

Canfield DE, Raiswell R, Bottrell S (1992) The reactivity of sedimentary iron minerals toward sulfide. *American Journal of Science*, **292**, 659-683.

Canfield DE, Thamdrup B.B (1994) The production of ^{34}S-depleted sulfide during bacterial disproportionation of elemental sulfur. *Science,* **266**, 1973-1975.

Cibilic, A (2003a) McLeods Creek – Main Trust Canal acid sulfate soil hot spot remediation concept plan. (Department of Infrastructure, Planning and Natural Resources, Unpubl.).

Cibilic, A (2003b) Sandy Creek-Bungawalbyn Creek acid sulfate soil hot spot remediation concept plan. (Department of Infrastructure, Planning and Natural Resources, Unpubl.).

Claff SR, Burton ED, Sullivan LA, Bush RT (2011) Metal partitioning dynamics during the oxidation and acidification of sulfidic soil. *Chemical Geology*, **286,** 146-157.

Clark MW, McConchie D, Lewis DW, Saenger P (1998) Redox stratification and heavy metal partitioning in *Avicennia*-dominated mangrove sediments: A geochemical model. *Chemical Geology,* **149,** 147-171.

Claypool GE, Holser WT, Kaplan IR, Sakai H, Zak I (1980) The age curves of sulfur and oxygen isotopes in marine sulfate and their mutual interpretation. *Chemical Geology*, **28,** 199-260.

Cook FJ, Hicks W, Gardner EA, Carlin GD, Froggatt DW (2000) Export of acidity in drainage water from acid sulfate soils. *Marine Pollution Bulletin,* **41,** 319-326.

Corfield J (2000) The effects of acid sulfate run-off on a subtidal estuarine macrobenthic community in the Richmond River, NSW, Australia. *ICES Journal of Marine Science,* **57,** 1517-1523.

Dellwig O, Bottcher ME, Lipinski M, Brumsack HJ (2002) Trace metals in Holocene coastal peats and their relation to pyrite formation (NW Germany). *Chemical Geology*, **182,** 423-442.

Dent DL (1986) Acid sulfate soils: a baseline for research and development. ILRI Publication No. 39. (International Institute for Land Reclamation and Improvement: Wageningen, The Netherlands).

Dent DL (2000) An International Perspective. In 'Acid sulfate soils: environmental issues, assessment and management, Technical Papers'. (Eds CR Ahern, KM Hey, KM Watling, VJ Eldershaw) pp. 12-1 to 12-4. (Queensland Department of Natural Resources: Brisbane, Queensland, Australia).

Dent DL, Pons L (1993) Acid and muddy thoughts. In 'Proceedings 1st national conference on acid sulfate soils'. (Ed RT Bush) (CSIRO, NSW Agriculture, Tweed Shire Council: Australia).

Dent DL, Pons L (1995) A world perspective on acid sulfate soils. *Geoderma*, **67,** 263-276.

Dold B, Spangenberg JE (2005) Sulfur speciation and stable isotope trends of water soluble sulfates in mine tailings profiles. *Environmental Science and Technology*, **39,** (15), 5650-5656.

Dowuona GN, Mermut AR, Krouse HR (1992) Stable isotopes of salts in some acid sulfate soils of North America. *Soil Science Society of America*, **56,** 1646-1653.

Drake H, Astrom ME, Tullborg E, Whitehouse M, Fallick AE (2013) Variability of sulfur isotope ratios in pyrite and dissolved sulfate in granitoid fractures down to 1km

depth – Evidence for widespread activity of sulfur reducing bacteria. *Geochimica et Cosmochimica Acta,* **102,** 143-161.

Easton C (1989) The trouble with the Tweed. *Fishing World,* March, 58-59.

Eckert T, Brunner B, Edwards EA, Wortmann UG (2011) Microbially mediated re-oxidation of sulfide during dissimilatory sulfate reduction of *Desulfobacto latus*. *Geochimica et Cosmochimica Acta,* **75,** 3469-3485.

Ehleringer JR, Cerling TE (2002) Stable isotopes. In 'Volume 2, The earth system; biological and ecological dimensions of global environmental change' (Eds HA Mooney and JG Canadell), pp 544-550, In 'Encyclopaedia of global environmental change'. (Editor in Chief T Munn). (John Wiley and Sons, Ltd.: Chichester, England).

Emery D, Robinson A (1993) 'Inorganic geochemistry: applications to petroleum geology'. (Blackwell Scientific Publications: Oxford, England).

Enginuity Design (2003) Collombatti-Clybucca acid sulfate soil 'hot spot' area management plan. Final report prepared for Kempsey Shire Council. (Civil and Environmental Engineering Consultants: Bellingen, New South Wales, Australia).

Environmental Protection Authority (EPA) (2000) 'New South Wales state of the environment report, land backgrounder 4'.
http://www.epa.nsw.gov.au/soe/soe2000/bl/bl_4.htm [accessed 3rd October 2002].

Evangelou VP (1998) 'Environmental soil and water chemistry: principals and applications'. (John Wiley and Sons Inc.: New York, United States of America).

Fan LF, Lin S, He KM, Chen CP, Hsieh HL (2012) Effect of sulfate availability on the isotopic signature of reduced sulphurous compounds in the sediments of a subtropical estuary. *Wetlands,* **32,** 907-917.

Fanning D (1993) 'Salinity problems in acid sulfate soils'. (Eds H Lieth, A Al Mosson) *Towards the National Use of High Salinity Tolerant Plants,* **1,** 491-500.

Farquhar J, Canfield DE, Masterson A, Bao H, Johnston D (2008) Sulfur and oxygen isotope study of sulfate reduction in experiments with natural populations from Faellestrand, Denmark. *Geochimica et Cosmochimica Acta,* **72,** 2805-2821.

Farquhar J, Johnston D, Wing BA (2007) Implications of conservation of mass effects on mass-dependent isotope fractionation: influence of network structure on sulfur isotope phase space of dissimilatory sulfate reduction. *Geochimica et Cosmochimica Acta,* **71,** 5862-5875.

Farquhar J, Wu N, Canfield DE, Oduro H (2010) Connections between sulfur cycle evolution, sulfur isotopes, sediments and base metal sulfide deposits. *Economic Geology,* **105,** 509-533.

Ferguson A, Eyre B (1996) Floodplain hydrology and the transport of acid sulfate soil products. In 'Proceedings 2nd national conference on acid sulfate soils'. (Robert J. Smith and Associates and ASSMAC: Australia).

Ferreira TO, Otero XL, Vidal-Torrado P, Macias F (2007a) Effects of bioturbation by root and crab activity on iron and sulfur biogeochemistry in mangrove substrate. *Geoderma,* **142,** 36-46.

Ferreira TO, Vidal-Torrado P, Otero XL, Macias F (2007b) Are mangrove forest substrates sediments or soils? A case study in southeastern Brazil. *Catena,* **70,** 79-91.

Fitzpatrick RW, Fox D, Hicks WS (1999) *Acid sulfate soils in East Trinity Inlet.* Workshop in Cairns, May 19, 1999.

Fitzpatrick RW, Fritsch E, Self PG (1993) Australia's unique saline acid sulfate soils associated with dryland salinity. In 'Proceedings 1st national conference on acid

sulfate soils'. (Ed. RT Bush). (CSIRO, NSW Agriculture, Tweed Shire Council: Australia).

Fitzpatrick RW, Powell B, McKenzie NJ, Macshmedt DJ, Schoknecht N, Jacquier DW (2003) Demands on soil classification in Australia. In 'Soil classification, a global desk reference'. (Eds H Eswaran, T Rice, R Ahrens, BA Stewart). CRC Press.

Fitzpatrick RW, Shand P, Merry RH (2009) Acid sulfate soils. In 'Natural history of the Riverlands and Murraylands'. (Ed. JT Jennings). (Royal Society of South Australia Inc.: Adelaide, South Australia, Australia).

Fyfe D (2001) Abundance and mobility of iron monosulfide-rich drain sludge. Honours Thesis. (Southern Cross University: Lismore, New South Wales, Australia).

Gagnon C, Mucci A, Pelletier E (1995) Anomalous accumulation of acid volatile sulfides (AVS) in a coastal marine sediment Saguenay Fjord, Canada. *Geochimica et Cosmochimica Acta,* **59,** (13), 2663-2675.

Gautier DL (1985) Interpretation of early diagenesis in ancient marine sediments. In 'Relationships of organic matter and mineral diagenesis' SEPM short course no. 17. (Society of Economic Palaeontologists and Mineralogists: Tulsa, United States of America).

Goldhaber MB (2004) Sulfur-rich sediments. In 'Treatise on Geochemistry, Vol 5'. (Ed. FT Mackenzie). Pp 569-655. (Elsevier, Oxford, UK).

Goldhaber MB, Kaplan IR (1974) The sulfur cycle. In 'The sea, Vol. 5. Marine Chemistry'. (Ed. ED Goldberg) pp 569-655. (Wiley-Interscience: New York, United States of America).

Green R, Waite TD, Melville MD, Macdonald BCT (2006) Characteristics of the acidity in acid sulfate soil drainage waters, McLeods Creek, north-eastern NSW, Australia. *Environmental Chemistry,* **3,** 225-232.

Gribsholt B, Kristensen E (2003) Benthic metabolism and sulfur cycling along an inundation gradient in a tidal *Spartina anglica* salt marsh. *Limnology and Oceanography,* **48,** (6), 2151-2162.

Gribsholt B, Kristensen E (2002) Effects of bioturbation and plant roots on salt marsh biogeochemistry: A mesocosm study. *Marine Ecological Progress Series*, **241,** 71-87.

Grogan KL, Gilkes RJ, Lottermoser BG (2003) Maghemite formation in burnt plant litter at East Trinity, north Queensland. *Clays and Clay Minerals,* **51,** (4), 390-396.

Habicht KS, Canfield DE (1997) Sulfur isotope fractionation during bacterial sulfate reduction in organic-rich sediments. *Geochimica et Cosmochimica Acta,* **61,** (24), 5351-5361.

Hagley R (1996) The Tuckean project. In 'Proceedings 2nd national conference on acid sulfate soils'. (Robert J. Smith and Associates and ASSMAC: Australia).

Hatzinger PB, Bohlke JK, Sturchio NC (2012) Applications of stable isotope ratio analysis for biodegradation monitoring in groundwater. *Current Opinions in Biotechnology,* **24,** 1-8.

Hendry JM, Krouse HR, Shakur MA (1989) Interpretation of oxygen and sulfur isotopes from dissolved sulfates in tills of Southern Alberta, Canada. *Water Resources Research,* **25,** (3), 567-572.

Hicks WS, Bowman GM, Fitzpatrick RW (1999) East Trinity acid sulfate soils Part 1: Environmental hazards. (CSIRO Land and Water Technical Report 14/99, pp. 79).

Hoefs J (2009) Stable Isotope Geochemistry. Springer-Verlag, Heidelberg.

Holser WT and Kaplan IR (1966) Isotope geochemistry of sedimentary sulfates. *Chemical Geology,* **1,** 93-135.

Howarth RW, Teal JM (1979) Sulfate reduction in a New England salt marsh. *Limnology and Oceanography*, **24,** 999-1013.

Hsieh YP, Chung SW, Tsau YJ, Sue CT (2002) Analysis of sulfides in the presence of ferric minerals by diffusion methods. *Chemical Geology*, **182,** 195-201.

Hunger S, Benning LG (2007) Greigite: a true intermediate on the polysulfide pathway to pyrite. *Geochemical Transactions*, **8,** 1-20.

Isaacson LS, Burton ED, Bush RT, Mitchell DRG, Johnston SG, Macdonald BCT, Sullivan LA, White I (2009) Iron (III) accumulations in inland saline waterways, Hunter Valley, Australia: Mineralogy, micromorphology and pore-water geochemistry. *Applied Geochemistry*, **24,** 1825-1834.

Isbell RF (1996) 'The Australian soil classification scheme' (CSIRO Publishing: Collingwood, Victoria, Australia).

Johnston D (2011) Multiple sulfur isotopes and the evolution of Earth's surface sulfur cycle. *Earth-Science Reviews*, **106,** 161-183.

Johnston SG, Burton ED, Bush RT, Keene AF, Sullivan LA, Smith D, McElnea AE, Ahern CR, Powell B (2010). Abundance and fractionation of Al, Fe and trace metals following tidal inundation of a tropical acid sulfate soil. *Applied Geochemistry*, **25,** 323-335.

Johnston SG, Bush RT, Sullivan LA, Burton ED, Smith D, Martens MA, McElnea AE, Ahern CR, Powell B, Stephens LP, Wilbraham ST, van Heel S (2009a). Changes in water quality following tidal inundation of coastal lowland acid sulfate soil landscapes. *Estuarine, Coastal and Shelf Science*, **81,** 257-266.

Johnston SG, Keene AF, Burton ED, Bush RT, Sullivan LA (2012) Quantifying alkalinity generating processes in a tidally remediating acidic wetland. *Chemical Geology*, **304-305,** 106-116.

Johnston SG, Keene AF, Bush RT, Burton ED, Sullivan LA, Isaacson L, McElnea AE, Ahern CR, Smith CD, Powell B (2011b) Iron geochemical zonation in a tidally inundated acid sulfate soil wetland. *Chemical Geology*, **280,** 257-270.

Johnston SG, Keene AF, Bush RT, Burton ED, Sullivan LA, Smith D, McElnea AE, Martens ME, Wilbraham S (2009b). Contemporary pedogenesis of severely degraded tropical acid sulfate soils after introduction of regular tidal inundation. *Geoderma*, **149,** 335-346.

Johnston SG, Keene AF, Bush RT, Sullivan LA, Wong VNL (2011a). Tidally driven water column hydro-chemistry in a remediating acidic wetland. *Journal of Hydrology*, **409,** 128-139.

Johnston SG, Kroon F, Slavich P, Cibilic A, Bruce A (2003c) Restoring the balance: Guidelines for managing floodgates and drainage systems on coastal floodplains. (NSW Agriculture: Wollongbar, New South Wales, Australia).

Johnston SG, Slavich PG, Hirst P (2003b) Alteration of groundwater and sediment geochemistry in a sulfidic backswamp due to *Melaleuca quinquenervia* encroachment. *Australian Journal of Soil Research*, **41,** 1343-1367.

Johnston SG, Slavich PG, Sullivan LA, Hirst P (2003a) Artificial drainage of flood waters from sulfidic backswamps: Effects of deoxygenation in an Australian estuary. *Marine and Freshwater Research*, **54,** 781-795.

Jones DS, Fike DA (2013) Dynamic sulfur and carbon cycling through the end-Ordovician extinction revealed by paired sulfate-pyrite $\delta^{34}S$. *Earth and Planetary Science Letters*, **363,** 144-155.

Jorgensen, BB (1990) A thiosulfate shunt in the sulfur cycles of marine sediments. *Science*, **249,** (4965), 152-155.

Kamyshny Jr. A, Zerkle AL, Mansaray ZF, Ciglenecki I, Bura-Nakic E, Farquhar J, Ferdelman TC (2011) Biogeochemical sulfur cycling in the water column of a shallow stratified sea-water lake: Speciation and quadruple sulfur isotope composition. *Marine Chemistry,* **127,** 144-154.

Kaplan IR, Rittenberg SC (1964) Microbiological fractionation of sulfur isotopes. *Journal of General Microbiology,* **34**, 195-212.

Keene AF, Johnston SG, Bush RT, Burton ED, Sullivan LA (2010) Reactive trace element enrichment in a highly modified, tidally inundated acid sulfate soil wetland: East Trinity, Australia. *Marine Pollution Bulletin,* **60,** 620-626.

Keene AF, Johnston SG, Bush RT, Sullivan LA, Burton ED, McElnea AE, Ahern CR, Powell B (2011) Effects of hyper-enriched reactive Fe on sulfidisation in a tidally inundated acid sulfate soil wetland. *Biogeochemistry,* **103,** 263-280.

Kelly ID (1996) Shallow groundwater management and acid sulfate soil environments. In 'Proceedings 2nd national conference on acid sulfate soils'. (Robert J. Smith and Associates and ASSMAC: Australia).

Kilminster K, Cartwright I (2011) A sulfur-stable-isotope-based screening tool for assessing impact of acid sulfate soils on waterways. *Marine and Freshwater Research,* **62,** 152-161.

Knoller K, Schubert M (2010) Interaction of dissolved and sedimentary sulfur compounds in contaminated aquifers. *Chemical Geology,* **276,** 284-293.

Knoller K, Trettin R, Strauch G (2005) Sulfur cycling in the drinking water catchment area of Torgau-Mockritz (Germany): Insights from hydrochemical and stable isotope investigations. *Hydrological Processes,* **19,** 3445-3465.

Kostka, JE & Luther III, GW (1994) Partioning and speciation of solid phase Fe in saltmarsh sediments. *Geochimica et Cosmochimica Acta,* **58,** 1701-1710.

Kristensen E, Alongi DM (2006) Control of fiddler crabs (*Uca vocans*) and plant roots (*Avicennia marina*) on carbon, iron and sulfur biogeochemistry in mangrove sediment. *Limnology and Oceanography,* **51,** (4), 1557-1571.

Leadbitter D, (1993) The acid test: basic concerns in the fishing industry about coastal floodplain management in NSW. In 'Proceedings 1st national conference on acid sulfate soils'. (Ed RT Bush) (CSIRO, NSW Agriculture, Tweed Shire Council: Australia).

Lines-Kelly R (2000) 'Soil sense: soil management for north coast farmers'. (NSW Agriculture: Wollongbar, New South Wales, Australia).

Luther III GW (1991) Pyrtie synthesis via polysulfide compounds. *Geochimica et Cosmochimica Acta,* **55,** 2839-2849.

Macdonald BCT, Smith J, Melville MD, White I (2002) Acid sulfate soil research in Australia. In, 'Acid sulfate soils in Australia and China'. (Eds C Lin, MD Melville, LA Sullivan). (Science Press: Beijing, China).

Maher CA (2005) Sulfur isotope ratios applied to acid sulfate soil materials. Honours Thesis. (Southern Cross University, Lismore, New South Wales, Australia)

Maher CA, Sullivan LA, Ward NJ (2004) Sample pre-treatment and the determination of some chemical properties of acid sulfate soil materials. *Australian Journal of Soil Research,* **42,** 667-670.

Makhnach A, Mikhajlov N, Kolosov I, Gulis L, Shimanovich V, Demeneva O (2000) Comparative analysis of sulfur isotope behaviour in basins with evaporates of chloride and sulfate types. *Sedimentary Geology,* **134,** 343-360.

Manahan SE (1990) 'Environmental Chemistry'. (Lewis Publishers: Boston, United States of America).

Mandernack KW, Lynch L. Krouse HR, Morgan MD (2000) Sulfur cycling in wetland peat of the New Jersey Pinelands and its effect on stream water quality. *Geochimica et Cosmochimica Acta,* **64,** (23), 3949-3964.

Marchand C, Baltzer F, Lallier-Verges E, Alberic P (2004) Pore water chemistry in mangrove sediments: relationship with species composition and development stages (French Guiana). *Marine Geology,* **208,** 361-381.

Mayer B, Shanley JB, Bailer SW, Mitchell MJ (2010) Identifying sources of stream water sulfate after a summer drought in the Sleepers River watershed (Vermont, USA) using hydrological, chemical and isotopic techniques. *Applied Geochemistry,* **25,** 747-754.

Mazumdar A, Paropkari AL, Barole DV, Rao BR, Khadge NH, Karisiddaiah SM, Kocherla M, Joao HM (2007) Pore water sulfate concentration profiles of sediment cores from Krishna-Godavari and Goa basins, India. *Geochemical Journal,* **41,** 259-269.

Mazumdar A, Peketi A, Joao H, Dewangan P, Borole DV, Kocherla M (2012) Sulfidisation in a shallow coastal depositional setting: Diagenetic and palaeoclimatic implications. *Chemical Geology,* **322-323,** 68-78.

McConville P, Boyce AJ, Fallick AE, Harte B, Scott EM (2000) Sulphur isotope variations in diagenetic pyrite from core plug to sub-millimetre scales. *Clay Minerals,* **35**, 303-311.

McElnea AE, Ahern CR (2004) KCl extractable pH (pH_{KCl}) and titratable actual acidity (TAA) – Method codes 23A and 23F. In 'Acid sulfate soils laboratory methods guidelines'. (Eds CR Ahern, AE McElnea, LA Sullivan). (Department of Natural Resources, Mines and Energy, Indooroopilly, Queensland, Australia.

McKee KL, Mendelssohn IA, Hester MW (1988) Re-examination of pore water sulfide concentrations and redox potentials near the aerial roots of *Rhizophora mangle* and *Avicennia germinans. American Journal of Botany,* **75,** 1352-1359.

McKibben MA, Eldridge CS (1989) Sulfur isotope variations among minerals and aqueous species in the Salton Sea geothermal system: A SHRIMP ion microprobe and conventional study of active ore genesis in a sediment-hosted environment. *American Journal of Science,* **289,** 661-707.

Melville MD, White I (2000) Acid sulfate soils. In 'Soils: their properties and management'. (Eds PEV Charman, BW Murphy). (Oxford University Press)

Melville MD, White I, Lin C (1993) The origins of acid sulfate soils. In 'Proceedings 1st national conference on acid sulfate soils'. (Ed RT Bush) (CSIRO, NSW Agriculture, Tweed Shire Council: Australia).

Moncaster SJ, Bottrell HS, Tellam JH, Lloyd JW, Konhauser KO (2000) Migration and attenuation of agrochemical pollutants: Insights from isotopic analysis of groundwater sulfate. *Journal of Contaminant Hydrology*, **43,** 147-163.

Morand DT (1993) Interim definitions for locating and defining coastal potential and actual acid sulfate soils. In 'Proceedings 1st national conference on acid sulfate soils'. (Ed RT Bush) (CSIRO, NSW Agriculture, Tweed Shire Council: Australia).

Morgan B, Rate AW, Burton ED (2012a) Trace element reactivity in FeS-rich estuarine sediments: Influence of formation environment and acid sulfate soil drainage. *Science of the Total Environment,* **438,** 463-476.

Morgan B, Rate AW, Burton ED, Smirk MN (2012b) Enrichment and fractionation of rare earth elements in FeS and organic rich estuarine sediments receiving acid sulfate soil drainage. *Chemical Geology,* **308-309,** 60-73.

Morgan B, Burton ED, Rate AW (2012c) Iron monosulfide enrichment and the presence of organosulfur in eutrophic estuarine sediments. *Chemical Geology*, **296-297,** 119-130.

Morse JW (1991) Oxidation kinetics of sedimentary pyrite in seawater. *Geochimica et Cosmochimica Acta*, **55**, 3665-3667.

Morse JW, Cornwell JC (1987) Analysis and distribution of iron sulfide minerals in recent anoxic marine sediments. *Marine Chemistry*, **22**, 55-69.

Morse JW, Rickard D (2004) Chemical dynamics of sedimentary acid volatile sulfide. *Environmental Science and Technology,* **38,** 131-136.

Mulvey P (1993) Pollution, prevention and management of sulfidic clays and sands. In 'Proceedings 1st national conference on acid sulfate soils'. (Ed. RT Bush). (CSIRO, NSW Agriculture, Tweed Shire Council: Australia).

Mulvey PJ, Willett IR (1996) Analyses of sulfidic sediments and acid sulfate soils. In 'Proceedings 2nd national conference on acid sulfate soils'. (Robert J. Smith and Associates and ASSMAC: Australia).

Nakai N, Jensen ML (1964) The kinetic isotope effect in the bacterial reduction and oxidation of sulfur. *Geochimica et Cosmochimica Acta*, **28**, 1893-1912.

National Working Party on Acid Sulfate Soils (2000) 'National strategy for the management of coastal acid sulfate soils'. (NSW Agriculture: Wollongbar, New South Wales, Australia).

Naylor SD, Chapman GA, Atkinson G, Murphy CL, Tulau MJ, Flewin TC, Milford HB, Morand DT (1998) 'Guidelines for the use of acid sulfate soil risk maps'. (NSW Soil Conservation Service, Department of Land and Water Conservation: Sydney, New South Wales, Australia).

Otero XL, Ferreira TO, Vidal-Torrado P, Macias F (2006) Spatial variation in pore water geochemistry in a mangrove system (Pai Matos Island, Cananeia-Brazil). *Applied Geochemistry,* **21,** 2171-2186.

Peck AJ (1993) Salinity. In 'Land degradation processes in Australia'. (Ed. GH McTainsh & WC Broughton). (Longman: Melbourne, Australia).

Poulton SW, Bottrell SH, Underwood CJ (1998) Porewater sulfur geochemistry and fossil preservation during phosphate diagenesis in a Lower Cretaceous shelf mudstone. *Sedimentology,* **45,** 875-887.

Powell B, Martens M (2005) A review of acid sulfate soil impacts, actions and policies that impact on water quality in Great Barrier Reef catchments, including a case study on remediation at East Trinity. *Marine Pollution Bulletin,* **51,** 149-164.

Raiswell R (1982) Pyrite texture, isotopic composition and the availability of iron. *American Journal of Science,* **282,** 1244-1263.

Rassam DW, Cook FJ, Gardner E (2001) A field investigation of acid sulfate soils. In 'Environmental Geotechnics - Proceedings of the 2nd Australia and New Zealand conference on environmental geotechnics'. (Eds D Smith, S Fityus, M Allman). (Australian Geomechanics Society Incorporated: Newcastle, New South Wales, Australia).

Rayment GE, Higginson FR (1992) 'Australian laboratory handbook of soil and water chemical methods'. (Inkata Press: Melbourne, Victoria, Australia).

Rayment GE, Lloyds DJ (2011) 'Soil chemical methods – Australasia' (CSIRO Publishing: Collingwood, Victoria, Australia).

Rees CE (1973) A steady state model for sulphur isotope fractionation in bacterial reduction processes. *Geochimica et Cosmochimica Acta,* **37,** 1141-1162.

Rickard DT (1975) The kinetics and mechanisms of pyrite formation at low temperatures. *American Journal of Science,* **275,** 636-652.

Rickard DT (2012) 'Sulfidic sediments and sedimentary rocks'. Developments in Sedimentology Volume 65. (Elsevier: Oxford, England).

Rickard DT, Luther III GW (2007) Chemistry of iron sulfides. *Chemical Reviews,* **107,** 514-562.

Rickard DT, Luther III GW (1997) Kinetics of pyrite formation by the H_2S oxidation of iron (II) monosulfide in aqueous solutions between 25 and 125°C: the mechanism. *Geochimica et Cosmochimica Acta,* **61,** (1), 135-147.

Rickard DT, Morse JW (2005) Acid volatile sulfide (AVS). *Marine Chemistry,* **97,** 141-197.

Rickard DT, Schoonen MAA, Luther III GW (1995) Chemistry of iron sulfides in sedimentary environments. In 'Geochemical transformations of sedimentary sulfur'. (Eds. MA Vairavamurthy & MAA Schoonen). ACS Symposium Series 612. (American Chemical Society: Washington, United States of America).

Ritsema CJ, Groenenberg JE (1993) Pyrite oxidation, carbonate weathering and gypsum formation in a drained potential acid sulfate soil. *Soil Science Society American Journal,* **57,** 968 – 976.

Ritsema CJ, Groenenberg JE, Bisdom EBA (1992) The transformation of potential into actual acid sulfate soils studied in column experiments. *Geoderma,* **55,** 259-271.

Ritsema CJ, Van Mensvoort MEF, Dent DC, Tan Y, Van den Bosch H, Van Wijk ALM (2000) Acid sulfate soils. In 'Handbook of soil science'. (Ed. M Sumner) (CRC Press: Boca Raton, United States of America).

Rosicky M, Slavich P, Sullivan L, Hughes M, Wood M (2000) Acid sulfate scalds on the NSW coast: characterisation and potential vegetation techniques. In 'Proceedings of workshop on remediation and assessment of broadacre acid sulfate soils'. (Ed. P Slavich) pp. 111-121 (ASSMAC, Southern Cross University: Lismore, New South Wales, Australia).

Rosicky M, Sullivan LA, Slavich P (2002a) Pyrite concentration and surface reformation in and around acid sulfate soil scalds on the NSW coast. Oral Paper, 5th International acid sulfate soil conference, 25-30 August, 2002 (Tweed Heads, New South Wales, Australia).

Rosicky M, Sullivan LA, Slavich P (2002b) Characterisation and management of acid sulfate soil scalds on the New South Wales Coast of southeast Australia. In 'Acid sulfate soils in Australia and China'. (Eds C Lin, M Melville, L Sullivan). (Science Press: Beijing, China).

Rosicky M, Sullivan LA, Slavich P, Hughes M (2004) Factors contributing to the acid sulfate soil scalding process in the coastal floodplains of New South Wales, Australia. *Australian Journal of Soil Research*, **42,** 587-594.

Russell DJ, Helmke SA (2002) Impacts of acid leachate on water quality and fisheries resources of a coastal creek in northern Australia. *Marine and Freshwater Research*, **53,** 19-33.

Sahlstedt E, Karhu JA, Pitkanen P, Whitehouse M (2013) Implications of sulfur isotope fractionation in fracture filling sulfides in crystalline bedrock, Olkiluoto, Finland. *Applied Geochemistry*, **32,** 52-69.

Sammut J, Callinan R, Fraser G (1993) The impact of acidified water on estuarine fish populations in acid sulfate soil environments. In 'Proceedings 1st national conference on acid sulfate soils'. (Ed. RT Bush). (CSIRO, NSW Agriculture, Tweed Shire Council: Australia).

Sammut J, Callinan RB, Fraser GC (1996a) The impact of acidified water on freshwater and estuarine fish populations in acid sulfate soil environments. In 'Proceedings 2nd national conference on acid sulfate soils'. (Robert J. Smith and Associates and ASSMAC: Australia).

Sammut J, Lines-Kelly R (2000) 'An Introduction to Acid Sulfate Soils, 2nd Edition'. (Environment Australia, Natural Heritage Trust, Coastal Acid Sulfate Soils Program and Agriculture, Fisheries and Forestry)

Sammut J, Melville MD, Callinan RB, Fraser GC (1995) Estuarine acidification: impacts on aquatic biota of draining acid sulfate soils. *Australian Geographical Studies*, **33**, 89-100.

Sammut J, White I, Melville MD (1996b) Acidification of an estuarine tributary in eastern Australian due to drainage of acid sulfate soils. *Marine and Freshwater Research*, **47,** 669-684.

Sarazin G, Michard G, Prevot F (1999) A rapid and accurate spectroscopic method for alkalinity measurements in sea water samples. *Water Research*, **33,** 290-294.

Scheiderich K, Zerkle AL, Helz GR, Farquhar J, Walker RJ (2010) Molybdenum isotope, multiple sulfur isotope and redox sensitive element behaviour in early Pleistocene Mediterranean sapropels. *Chemical Geology*, **279,** 134-144.

Schippers A, Jorgensen BB (2002) Biogeochemistry of pyrite and iron sulfide oxidation in marine sediments. *Geochimica et Cosmochimica Acta*, **66,** (1), 85-92.

Schoonen MAA, Barnes HL (1991) Reactions forming pyrite and marcasite from solution: II, via FeS precursors below 100 °C. *Geochimica et Cosmochimica Acta*, **55,** 1505-1514.

Seal RR, Wandless GA (1997) Stable isotope characteristics of waters draining massive sulfide deposits in the eastern United States. In 'Fourth international

symposium on environmental geochemistry proceedings'. (Eds. RB Wanty, SP Marsh, LP Gough).

Seralathan P, Rajkumar MS, Sunilkumar V, Anandaraj N (2006) Interstitial water chemistry of mangrove sediments, Kerala. *Journal of the Geological Society of India,* **68,** 251-258.

Singer PC, Stumm W (1970) Acid mine drainage: the rate determining step. *Science,* **167**, 1121-1123.

Smith J (2004) Chemical changes during oxidation of iron monosulfide-rich sediments. *Australian Journal of Soil Research,* **42,** 659-666.

Smith CD, Martens MD, McElnea AE, Powell B (2004) *East Trinity acid sulfate soil remediation action plan report*. (Department of Natural Resources and Mines, Queensland Government).

Smith J, Melville MD (2004) Iron monosulfide formation and oxidation in drain-bottom sediments of an acid sulfate soil environment. *Applied Geochemistry*, **19,** 1837-1853.

Smith J, van Oploo P, Marston H, Melville MD, Macdonald BCT (2003) Spatial distribution and management of total actual acidity in an acid sulfate soil environment, McLeods Creek, north-eastern NSW, Australia. *Catena,* **51,** 61-79.

Stam MC, Mason PRD, Laverman AM, Pallud C, Van Cappellen P (2011) $^{34}S/^{32}S$ fractionation by sulfate reducing microbial communities in estuarine sediments. *Geochimica et Cosmochimica Acta,* **75,** 3903-3914.

Sullivan LA, Bush RT (2001) Deoxygenation and acidification of water by monosulfidic black ooze. Report to the 'Floods and fish kills workshop'. 15 May 2001. (Alstonville Tropical Fruit Research Station: Alstonville, New South Wales, Australia).

Sullivan LA, Bush RT (2002) The chemistry of drain sludge material: implications for acidification of waterways and drain maintenance. In 'Acid sulfate soils in Australia and China'. (Eds C Lin, M Melville, L Sullivan). (Science Press: Beijing, China).

Sullivan LA, Bush RT, Burton ED, Ritsema CJ, van Mensvoort MEF (2012) Acid sulfate soils. In 'Handbook of soil science, volume II: Resource management and environmental impacts, 2nd Edition'. (Eds. PM Huang, YC Li, ME Sumner). (Taylor and Francis: Boca Raton, Florida, United States of America).

Sullivan LA, Bush RT, McConchie D (2000) A modified chromium reducible sulfur method for reduced inorganic sulfur: optimum reaction time for acid sulfate soils, *Australian Journal of Soil Research*, **38**, (3), 729.

Sullivan LA, Bush RT, Ward NJ (2002) Sulfidic sediments and salinisation in the Murray Darling Basin. Poster Paper 5th International acid sulfate soil conference, 25-30 August 2002 (Tweed Heads, New South Wales, Australia).

Sullivan LA, Ward NJ, Bush RT (2001) Chemical analysis for acid sulfate soil management. In 'Environmental Geotechnics - Proceedings of the 2nd Australia and New Zealand conference on environmental geotechnics'. (Eds D Smith, S Fityus, M Allman). (Australian Geomechanics Society Incorporated: Newcastle, New South Wales, Australia).

Taylor BE, Wheeler MC, Nordstrom DK (1984) Stable isotope geochemistry of acid mine drainage: Experimental oxidation of pyrite. *Geochimica et Cosmochimica Acta*, **48,** 2669-2678.

Taylor P, Rummery TE, Owen DG (1979) Reactions of iron monosulfide solids with aqueous hydrogen sulfide up to 160°C. *Journal of Inorganic Nuclear Chemistry*, **41,** 1683-1687.

Tulau MJ (2000) Acid sulfate soil remediation guidelines. In 'Acid sulfate soil remediation guidelines'. (Ed MJ Tulau). (DLWC unpublished).

Unland NP, Taylor HL, Bolton BR, Cartwright I (2012) Assessing the hydrogeochemical impact and distribution of acid sulfate soils, Heart Morass, West Gippsland, Victoria. *Applied Geochemistry,* **27,** 2001-2009.

Vandemarsen T, Kristensen E, Holmer M (2009) Metabolic threshold and sulfide buffering in diffusion controlled marine sediments impacted by continuous organic enrichment. *Biogeochemistry,* **95,** 335-353.

van Oploo P (2000) Soil and pore water relations of a coastal acid sulfate soil in northern NSW, Australia. PhD Thesis (University of New South Wales: Sydney, New South Wales, Australia).

Volkenborn N, Polerecky L, Hedtkamp SIC, Seusekom JEE, de Beer D (2007) Bioturbation and bioirrigation extend the open exchange regions in permeable sediments. *Limnology and Oceanography,* **52,** (5), 1898-1909.

Wallmann K, Hennies K, Konig I, Petersen W, Knauth HD (1993). New procedure for determining reactive Fe(III) and Fe(II) minerals in sediments. *Limnology and Oceanography*, **38,** 1803-1812.

Werner RA, Brand WA (2001) Referencing strategies and techniques in stable isotope ratio analysis. *Rapid Communications in Mass Spectrometry,* **15,** 501-519.

White I, Melville MD, Wilson BP, Price CB, Willett IR (1993) Understanding acid sulfate soils in canelands. In 'Proceedings 1st national conference on acid sulfate soils'. (Ed. RT Bush). (CSIRO, NSW Agriculture, Tweed Shire Council: Australia).

White I, Sammut J (1995) Acid sulfate coastal soils. *Trees and Natural Resources,* **37,** (2), 15-18.

White I, Wilson BP, Melville MD, Sammut J, Lin C (1996) Hydrology and drainage of acid sulfate soils. In 'Proceedings 2nd national conference on acid sulfate soils'. (Robert J. Smith and Associates and ASSMAC: Australia).

Widdel F, Hansen TA (1992) The dissimilatory sulfate and sulfur reducing bacteria. In 'The Prokaryotes'. (Ed. A Barlows) pp. 583-624. (Springer Verlag).

Wijsman JWM, Middelburg JJ, Merman PMJ, Bottcher ME, Heip CHR (2001) Sulfur and iron speciation in surface sediments along the northwestern margin of the Black sea. *Marine Chemistry*, **74,** 261-278.

Williams BJ, Watford FA, Hannan J, Copeland C (1996) Audit of tidal control structures in NSW. In 'Proceedings 2nd national conference on acid sulfate soils'. (Robert J. Smith and Associates and ASSMAC: Australia).

Wong VNL, Johnston SG, Burton ED, Bush RT, Sullivan LA, Slavich PG (2010) Seawater causes rapid trace metal mobilisation in coastal lowland acid sulfate soils: Implications of sea level rise for water quality. *Geoderma,* **160,** 252-263.

Wong VNL, Johnston SG, Burton ED, Bush RT, Sullivan LA, Slavich PG (2013) Seawater induced mobilisation of trace metals from mackinawite-rich estuarine sediments. *Water Research,* **47,** 821-832.

Wu S, Jeschke C, Dong R, Paschke H, Kuschk P, Knoller K (2011) Sulfur transformations in pilot-scale constructed wetland treating high sulfate-contaminated groundwater: A stable isotope assessment. *Water Research,* **45,** 6688-6698.

Yang X (1997) Applications of remote sensing and GIS to acid drainage management in an estuary floodplain agricultural environment. PhD Thesis. (University of New South Wales: Sydney, New South Wales, Australia).

Zaback DA, Pratt LM (1992) Isotopic composition and speciation of sulfur in the Miocene Monterey Formation: re-evaluation of sulfur reactions during early diagenesis in marine environments. *Geochimica et Cosmochimica Acta,* **56,** 763-774.

Zhu MX, Shi XN, Yang GP, Hao XC (2013) Formation and burial of pyrite and organic sulfur in mud sediments of the East China Sea inner shelf: Constraints from

solid phase sulfur speciation and stable sulfur isotope. *Continental Shelf Research,* **54,** 24-36.

Appendices

Appendix 1 – Data tables for Chapter 2

	Depth (cm)	pH Water	EC (µS/cm)	Total Carbon (%)	AVS (%)	CRS (%)	Soluble SO4 (%)
Kempsey	0-5	5.90	237	21.4	0.161	0.615	0.001
	5-10	4.49	446	16.5	0.003	0.072	0.030
	10-20	4.32	750	9.38	<0.001	0.022	0.110
	20-40	4.51	1166	2.82	<0.001	0.019	0.092
	40-60	4.25	2880	1.27	<0.001	0.011	1.40
	60-80	6.99	3090	0.95	<0.001	0.142	2.01
	80-100	5.74	1996	0.87	<0.001	0.487	0.168
	100-120	7.31	1715	0.84	<0.001	0.696	0.097
	120-140	7.90	1119	0.91	<0.001	0.601	0.039
	140-160	7.93	1224	0.92	<0.001	0.681	0.025
	160-180	8.06	1264	2.11	<0.001	0.413	0.038

	Depth (cm)	pH Water	EC (µS/cm)	Total Carbon (%)	AVS (%)	CRS (%)	Soluble SO4 (%)
McLeods Creek	0-10	4.90	85	3.70	0.002	0.007	0.011
	10-20	4.61	91	3.65	<0.001	0.010	0.022
	20-30	4.56	146	3.56	0.002	0.015	0.045
	30-40	4.02	551	3.20	0.002	0.007	0.106
	40-50	3.94	665	2.66	0.001	0.007	0.222
	50-60	3.92	680	1.29	0.002	0.004	0.253
	60-70	4.26	720	1.33	0.003	0.025	0.294
	70-80	5.77	740	1.50	0.001	1.12	0.267
	80-90	5.66	786	1.54	0.002	1.25	0.297
	90-100	5.30	783	1.46	<0.001	0.558	0.264
	100-110	4.62	711	1.36	0.002	0.007	0.290
	110-120	6.10	383	1.53	0.001	1.30	0.233
	120-130	6.80	840	1.62	0.001	1.94	0.239
	130-140	6.73	851	1.64	0.005	1.77	0.217
	140-150	6.74	884	1.57	0.005	2.12	0.203
	150-160	6.94	849	1.48	0.004	1.97	0.166
	160-170	6.98	851	1.53	<0.001	2.45	0.190

	Depth (cm)	pH Water	EC (µS/cm)	Total Carbon (%)	AVS (%)	CRS (%)	Soluble SO4 (%)
Shark Creek	0-10	4.33	115	15.8	0.013	0.055	0.033
	10-20	4.34	277	7.44	0.007	0.022	0.018
	20-30	4.18	474	4.75	0.005	0.018	0.093
	30-40	4.29	435	3.32	0.007	0.011	0.093
	40-50	4.27	362	3.04	0.005	0.008	0.116
	50-60	4.18	280	3.99	0.006	0.009	0.121
	60-70	4.05	291	1.85	0.007	0.012	0.156
	70-80	3.83	481	1.88	0.006	0.053	0.145
	80-90	4.10	337	1.90	0.006	0.107	0.137
	90-100	4.23	542	2.01	0.005	0.065	0.162
	100-110	4.21	539	1.87	0.003	0.093	0.169
	110-120	4.30	526	1.78	0.004	0.506	0.179
	120-130	3.83	1142	1.83	0.007	1.13	0.165
	130-140	4.01	1316	2.27	0.006	2.04	0.190
	140-150	3.97	1234	1.55	0.007	0.828	0.207
	150-160	5.03	1031	1.46	0.004	1.17	0.202
	160-170	5.57	1003	1.51	0.008	0.980	0.223
	170-180	6.21	834	1.57	0.009	1.16	0.235

	Depth (cm)	pH Water	EC (µS/cm)	Total Carbon (%)	AVS (%)	CRS (%)	Soluble SO4 (%)
Tuckean Nature Reserve	0-10	3.80	1036	3.64	0.001	0.036	0.406
	10-20	4.03	876	2.33	0.001	0.012	0.639
	20-30	3.91	750	2.63	0.002	0.021	0.184
	30-40	3.92	606	1.30	0.002	0.009	0.141
	40-50	3.87	557	1.06	0.001	0.009	0.168
	50-60	3.75	489	0.82	0.001	0.004	0.184
	60-70	3.68	448	0.42	0.002	0.007	0.172
	70-80	3.42	991	0.58	0.001	0.003	0.326
	80-90	3.68	1086	0.84	0.002	0.012	0.421
	90-100	3.76	1108	0.70	0.002	1.40	0.400
	100-110	3.99	1513	0.89	0.002	2.53	0.698
	110-120	4.17	1622	1.17	0.003	2.88	0.497
	120-130	3.37	1929	1.06	0.002	2.68	1.47
	130-140	3.43	1350	0.92	0.002	2.38	1.60
	140-150	3.63	1581	0.75	0.002	1.98	1.71
	150-160	3.69	1372	1.02	0.003	2.44	2.47
	160-170	4.62	1425	1.34	0.002	3.22	3.08
	170-180	4.93	1757	1.22	0.003	4.57	0.668

	Depth (cm)	pH Water	EC (µS/cm)	Total Carbon (%)	AVS (%)	CRS (%)	Soluble SO4 (%)
Byron Bay	0 - 5	5.52	157	41.7	0.002	0.163	0.022
	5 - 10	4.76	196	44.1	0.001	0.080	0.013
	10 - 15	4.38	236	48.8	0.001	0.097	0.012
	15 - 20	4.30	266	46.7	0.002	0.078	0.015
	20 - 30	4.14	300	50.6	0.001	0.090	0.013
	30 - 40	4.08	291	50.3	0.004	0.083	0.076
	40 - 50	4.10	327	50.6	0.004	0.092	0.125
	50 - 60	4.20	313	49.0	0.004	0.055	0.106
	60 - 70	4.25	294	51.2	0.004	0.094	0.093
	70 - 80	4.32	295	51.8	0.002	0.134	0.066
	80 - 90	4.40	264	52.6	0.003	0.089	0.047
	90 - 100	4.43	278	55.3	0.003	0.106	0.084
	100 - 110	4.52	242	52.0	0.003	0.262	0.066
	110 - 120	4.61	234	52.9	0.003	0.197	0.042
	120 - 130	4.61	251	52.0	0.004	0.264	0.046
	130 - 140	4.69	206	52.4	0.003	0.449	0.060
	140 - 150	4.69	206	52.9	0.005	0.620	0.064
	150 - 160	4.79	165	51.0	0.002	0.378	0.017
	160 - 170	4.99	98	21.1	0.001	0.095	0.004
	170 - 180	4.96	109	17.3	0.001	0.076	0.001
	180 - 190	4.86	138	14.4	0.001	0.090	0.000
	190 - 200	4.90	129	15.4	0.001	0.060	0.002

	Depth (cm)	pH Water	EC (µS/cm)	Total Carbon (%)	AVS (%)	CRS (%)	Soluble SO4 (%)
Boggy Creek	0 - 10	3.90	683	8.16	0.001	0.017	0.330
	10 - 30	3.97	625	11.0	0.001	0.013	0.297
	30 - 50	3.82	375	32.2	0.001	0.039	0.217
	50 - 70	3.74	516	38.0	0.002	0.087	0.468
	70 - 90	4.53	387	34.6	0.002	0.765	0.345
	90 - 110	5.09	254	20.3	0.002	2.92	0.199
	110 - 130	5.61	172	28.2	0.002	1.45	0.118
	130 - 150	5.91	103	11.1	0.001	1.90	0.035
	150 - 170	5.98	81	5.04	0.001	0.877	0.004
	170 - 190	6.05	76	2.59	0.002	0.911	0.006

	Depth (cm)	pH Water	EC (µS/cm)	Total Carbon (%)	AVS (%)	CRS (%)	Soluble SO4 (%)
Bora Codrington	0-10	4.47	119	13.16	0.002	0.031	0.124
	10-20	4.6	331	8.74	<0.001	0.022	0.188
	20-30	4.29	338	5.59	0.002	0.014	0.140
	30-40	3.94	353	4.19	0.003	0.009	0.140
	40-50	3.84	366	7.54	<0.001	0.007	0.149
	50-60	3.63	526	7.43	0.002	0.009	0.216
	60-70	3.58	544	8.74	0.001	0.013	0.181
	70-80	3.48	639	21.5	0.006	0.105	0.510
	80-90	3.4	608	38.0	0.006	0.242	0.597
	90-100	3.49	602	26.9	0.002	0.140	0.668
	100-110	3.46	626	13.4	0.005	0.211	0.567
	110-120	3.63	588	4.85	<0.001	0.480	0.297
	120-130	3.69	523	3.01	<0.001	0.969	0.292
	130-140	2.66	2777	1.67	0.003	1.62	1.488
	140-150	2.98	1918	1.92	0.002	0.641	1.281
	150-160	3.46	1151	1.48	0.003	0.966	0.700
	160-170	4.46	720	1.45	0.002	0.754	0.518
	170-180	5.02	498	1.43	0.002	0.870	0.212

	Depth (cm)	pH Water	EC (µS/cm)	Total Carbon (%)	AVS (%)	CRS (%)	Soluble SO4 (%)
Boggy Creek MBO	0 - 5	4.39	459	12.5	0.005	3.39	0.365
	5 - 10	4.40	387	16.3	0.001	1.56	0.250
	10 - 15	4.44	353	19.8	0.007	3.91	0.373
	15 - 20	4.50	428	21.9	0.001	4.26	0.396
	20 - 25	4.52	433	22.9	0.006	5.99	0.560
	25 - 30	4.35	535	24.0	0.004	4.25	0.682
	30 - 35	4.50	448	16.7	0.001	1.22	0.275
	35 - 40	5.06	217	10.0	0.001	0.459	0.093
	40 - 45	4.66	328	6.10	0.004	1.51	0.163
	45 - 50	4.87	256	6.52	0.002	1.13	0.138
	50 - 55	4.74	323	4.66	0.005	2.02	0.219
	55 - 60	4.53	332	3.03	0.000	1.06	0.127

	Depth (cm)	pH Water	EC (µS/cm)	Total Carbon (%)	AVS (%)	CRS (%)	Soluble SO4 (%)
Tuckean Swamp MBO	0 - 5	6.75	1476	10.0	0.115	4.19	0.207
	5 - 10	6.81	1253	8.76	0.431	2.67	0.134
	10 - 15	6.69	1307	8.44	0.101	3.59	0.142
	15 - 20	6.71	1401	7.92	0.135	3.22	0.099
	20 - 25	6.97	1213	4.37	0.043	1.15	0.049
	25 - 30	7.51	955	1.83	0.015	1.17	0.024
	30 - 35	7.50	783	1.84	0.016	0.602	0.021
	35 - 40	7.36	1212	0.92	0.004	0.627	0.030
	40 - 45	7.54	1152	1.15	0.118	0.930	0.015
	45 - 50	7.69	739	0.96	0.003	0.704	0.017
	50 - 55	8.05	598	0.76	0.001	0.386	0.006

	Depth (cm)	pH Water	EC (µS/cm)	Total Carbon (%)	AVS (%)	CRS (%)	Soluble SO4 (%)
Inland Samples	Calabria	8.73	364	4.88	0.337	0.855	0.032
	Leonards	7.95	320	3.24	0.075	0.095	0.011
	Boomley	7.93	1659	2.18	0.052	0.129	0.096
	Widden	8.63	9600	4.17	0.136	0.371	0.794
	Piccaninny	8.29	6080	1.98	0.379	0.714	0.319
	Barr	8.42	4700	1.45	0.347	0.642	0.242

	Depth (cm)	$\delta^{34}S$ AVS (‰)	$\delta^{34}S$ CRS (‰)	$\delta^{34}S$ SO_4^{2-} (‰)	Fract. from SWS (‰)	Fract. from SS (‰)
Kempsey	Surfacewater			-18.0		
	0-5	-19.0	-20.1	-2.7	40.7	17.4
	60-80		-28.6	-17.3	49.2	11.3
	160-180		-18.3	-16.4	38.9	1.9
McLeods Creek	20-30		-9.0	-5.4	29.6	3.5
	60-70			-7.1		
	70-80		-13.6	-6.7	34.2	6.9
	80-90		-10.5	-8.6	31.1	1.9
	90-100		-10.9	-7.4	31.5	3.5
	110-120		-22.6		43.2	
	160-170		-16.5	-6.3	37.1	10.2
Shark Creek	0-10		-12.4	-2.8	33.0	9.6
	10-20		-22.2	-5.1	42.8	17.1
	90-100		-17.3	-8.7	37.9	8.5
	100-110		-12.9	-8.4	33.5	4.5
	110-120		-14.6	-8.6	35.2	6.0
	170-180		-13.1	-6.0	33.7	7.2
Tuckean Swamp	0-10		-20.5	-4.4	41.1	16.0
	80-90		-2.1	-2.2	22.7	-0.1
	90-100		-2.5	-2.5	23.1	0.1
	100-110		-4.8	-2.4	25.4	2.4
	110-120		-4.1	-2.5	24.7	1.7
	170-180		12.4	-2.8	8.2	-15.2
Byron Bay	0-5					
	100-110		-1.5		22.1	
	140-150		-7.2		27.8	
Boggy Creek	0-10		-	13.0		
	90-110		9.8	12.9	10.8	3.1
	170-190		10.5	-	10.1	

	Depth (cm)	$\delta^{34}S$ AVS (‰)	$\delta^{34}S$ CRS (‰)	$\delta^{34}S$ SO_4^{2-} (‰)	Fract. from SWS (‰)	Fract. from SS (‰)
Bora Codrington	0-10		5.6	11.3	15.0	5.7
	80-90		-7.3	12.5	27.9	19.9
	90-100		-6.4	12.7	27.0	19.1
	110-120		9.9	11.4	10.7	1.6
	120-130		10.8	10.6	9.8	-0.2
	170-180		-17.4	7.3	38.0	24.7
Boggy Creek MBO	0-5		8.8	14.4	11.8	5.7
	20-25		2.8	4.8	17.8	1.9
	50-55		12.3	10.0	8.3	-2.3
T. Swamp MBO	5-10	-2.0	-5.0		25.6	
	15-20	4.0	2.3		18.3	
	40-45	16.8	-6.3	24.6	26.9	30.8
Inland sites	Calabria	-8.6	-9.2	26.7	29.8	35.8
	Leonards	5.1	2.3		18.3	
	Boomley	8.8	8.4	11.1	12.2	2.7
	Widden	-12.4	-13.5	24.0	34.1	37.5
	Piccaninny	-9.5	-7.5	29.1	28.1	36.6
	Barr Ck	4.4	3.0	26.0	17.7	23.0

Appendix 2 – Data tables for Chapter 3

	Depth (cm)	pH Water	EC (µS/cm)	FeR 2+ (mg/g)	FeR 3+ (mg/g)	FeR Total (mg/g)	Fe CDE (mg/g)
East Trinity Site 1	0-10	4.29	1231	0.094	0.236	0.330	0.088
	10-20	4.37	913	0.074	0.195	0.269	0.113
	20-30	4.70	604	0.077	0.488	0.565	0.233
	30-40	5.24	724	0.067	0.373	0.440	0.196
	40-50	5.67	793	0.067	0.203	0.270	0.215
	50-60	5.65	675	0.068	0.198	0.266	0.227
	60-70	5.68	1931	0.065	0.172	0.238	0.213
	70-80	7.24	2890	0.076	0.210	0.286	0.249
	80-90	7.47	3170	0.081	0.210	0.291	0.240
	90-100	7.61	3460	0.073	0.167	0.240	0.210
	100-110	7.74	3680	0.073	0.164	0.237	0.199
	110-120	8.04	3110	0.072	0.191	0.263	0.097
	120-130	7.85	2640	0.068	0.174	0.242	0.066
	130-140	8.32	1755	0.074	0.189	0.263	0.074
	140-150	8.46	1983	0.071	0.176	0.247	0.069

	Depth (cm)	Total Sulfur (%)	Total Carbon (%)	Total Nitrogen (%)	AVS (%S)	E.S (%S)	CRS (%S)
East Trinity Site 1	0-10	0.34	14.4	0.651	<0.001	0.002	0.018
	10-20	0.47	5.35	0.233	0.001	0.004	0.004
	20-30	0.62	3.34	0.113	<0.001	<0.001	0.005
	30-40	0.56	3.70	0.118	<0.001	<0.001	0.006
	40-50	0.71	2.25	0.082	0.001	<0.001	0.007
	50-60	0.46	1.54	0.059	<0.001	<0.001	0.006
	60-70	0.77	1.29	0.049	0.002	<0.001	0.006
	70-80	1.79	1.38	0.035	<0.001	<0.001	0.261
	80-90	1.85	1.63	0.037	<0.001	<0.001	0.355
	90-100	1.18	2.47	0.035	<0.001	0.001	0.454
	100-110	1.11	1.89	0.043	<0.001	0.052	0.319
	110-120	1.33	1.86	0.036	<0.001	0.259	1.287
	120-130	1.49	2.38	0.047	<0.001	<0.001	1.654
	130-140	1.54	2.19	0.042	<0.001	<0.001	1.690
	140-150	1.61	2.28	0.040	<0.001	0.001	1.644

	Depth (cm)	WS Cl (%)	WS SO4 (%)	Cl:SO4 Ratio	KCl SO4 (%)	HCl SO4 (%)
East Trinity Site 1	0-10	0.196	0.386	0.51	0.226	0.381
	10-20	0.100	0.211	0.47	0.208	0.678
	20-30	0.075	0.125	0.60	0.082	1.89
	30-40	0.081	0.162	0.50	0.031	2.17
	40-50	0.089	0.197	0.45	0.057	2.53
	50-60	0.064	0.158	0.41	0.106	0.628
	60-70	0.065	0.886	0.07	0.509	0.451
	70-80	0.120	1.32	0.09	1.17	0.189
	80-90	0.182	1.15	0.16	1.21	0.080
	90-100	0.348	1.00	0.35	0.536	0.130
	100-110	0.519	0.872	0.60	0.550	0.060
	110-120	0.548	0.577	0.95	0.403	0.046
	120-130	0.747	0.375	1.99	0.265	0.023
	130-140	0.768	0.376	2.04	0.285	0.037
	140-150	0.772	0.379	2.04	0.237	0.045

	Depth (cm)	$\delta^{34}S$ CRS (‰)	$\delta^{34}S$ WS SO4 (‰)	$\delta^{34}S$ KCl SO4 (‰)	$\delta^{34}S$ HCl SO4 (‰)
East Trinity Site 1	0-10		-20.3	-19.5	-19.4
	10-20		-21.0	-19.2	-21.0
	20-30		-21.9	-20.1	-19.0
	30-40		-21.9		
	40-50		-21.7		
	50-60		-22.1	-10.7	-24.5
	60-70		-23.9		
	70-80	-33.6	-22.9	-22.8	-23.6
	80-90	-32.3	-22.8	-21.8	-22.1
	90-100	-32.0	-21.0	-19.8	-16.1
	100-110		-19.7	-3.6	
	110-120		-16.7		
	120-130		-13.7	-2.6	
	130-140	-28.4	-12.9	-12.5	
	140-150	-29.1	-11.9	-10.7	

	Depth (cm)	pH Water	EC (µS/cm)	FeR 2+ (mg/g)	FeR 3+ (mg/g)	FeR Total (mg/g)	Fe CDE (mg/g)
East Trinity Site 2	0-10	5.80	3180	0.263	0.425	0.688	0.073
	10-20	6.29	2780	0.237	0.051	0.288	0.076
	20-30	5.76	2960	0.207	0.067	0.274	0.192
	30-40	6.20	1440	0.109	0.149	0.258	0.200
	40-50	6.17	1368	0.071	0.162	0.233	0.195
	50-60	6.06	1379	0.072	0.021	0.093	0.103
	60-70	6.17	1299	0.079	0.000	0.070	0.124
	70-80	6.33	1775	0.069	0.016	0.085	0.109
	80-90	6.43	2220	0.066	0.016	0.082	0.111
	90-100	6.48	3100	0.074	0.020	0.094	0.231
	100-110	6.71	4390	0.069	0.149	0.218	0.219
	110-120	7.47	4180	0.084	0.023	0.107	0.118
	120-130	7.85	3750	0.077	0.017	0.093	0.074
	130-140	8.05	3070	0.067	0.013	0.080	0.065
	140-150	8.12	2990	0.074	0.014	0.088	0.076

	Depth (cm)	Total Sulfur (%)	Total Carbon (%)	Total Nitrogen (%)	AVS (%S)	E.S (%S)	CRS (%S)
East Trinity Site 2	0-10	0.86	19.8	0.686	0.009	0.027	0.030
	10-20	0.69	11.1	0.429	0.006	0.023	0.024
	20-30	0.58	4.27	0.242	0.006	0.012	0.010
	30-40	0.53	3.28	0.148	0.024	0.018	0.019
	40-50	0.52	3.01	0.130	<0.001	0.006	0.033
	50-60	0.39	2.45	0.110	<0.001	0.001	0.136
	60-70	0.25	2.12	0.099	<0.001	<0.001	0.055
	70-80	0.23	1.67	0.081	<0.001	<0.001	0.110
	80-90	0.28	1.33	0.066	<0.001	<0.001	0.102
	90-100	0.35	1.16	0.053	<0.001	0.001	0.062
	100-110	1.38	1.16	0.048	<0.001	0.001	0.133
	110-120	1.52	1.64	0.052	<0.001	0.001	0.467
	120-130	1.28	1.85	0.053	<0.001	<0.001	0.832
	130-140	1.06	1.96	0.039	<0.001	<0.001	1.02
	140-150	1.23	1.65	0.040	<0.001	<0.001	1.26

	Depth (cm)	WS Cl (%)	WS SO4 (%)	Cl:SO4 Ratio	KCl SO4 (%)	HCl SO4 (%)
East Trinity Site 2	0-10	0.822	0.323	2.54	0.409	0.462
	10-20	0.759	0.240	3.16	0.180	0.462
	20-30	0.642	0.264	2.43	0.071	2.59
	30-40	0.628	0.257	2.45	0.184	2.56
	40-50	0.490	0.203	2.42	0.070	1.21
	50-60	0.518	0.216	2.40	0.050	0.573
	60-70	0.504	0.215	2.35	0.196	0.243
	70-80	0.434	0.187	2.32	0.097	0.380
	80-90	0.391	0.229	1.71	0.853	0.161
	90-100	0.440	0.634	0.69	0.690	0.076
	100-110	0.507	1.205	0.42	2.399	0.105
	110-120	0.751	1.109	0.68	0.825	0.073
	120-130	0.787	0.505	1.56	0.609	0.031
	130-140	0.682	0.257	2.65	0.612	0.036
	140-150	0.711	0.233	3.04	0.240	0.023

	Depth (cm)	$\delta^{34}S$ CRS (‰)	$\delta^{34}S$ WS SO4 (‰)	$\delta^{34}S$ KCl SO4 (‰)	$\delta^{34}S$ HCl SO4 (‰)
East Trinity Site 2	0-10	-32.2	-7.1	-5.1	-9.5
	10-20	-30.0	3.9	5.2	-16.3
	20-30		-1.3		
	30-40	-29.2	-3.5		
	40-50		-6.2		
	50-60	-29.8	-11.0	-6.6	-17.5
	60-70		-9.9		
	70-80	-31.2	-10.4	-6.4	
	80-90		-16.7		
	90-100		-18.9		
	100-110	-31.9	-18.6	-22.2	-20.5
	110-120				
	120-130		-11.5		
	130-140	-29.3	-6.3	-3.3	
	140-150	-27.6	-7.6	-4.5	

	Depth (cm)	pH Water	EC (µS/cm)	FeR 2+ (mg/g)	FeR 3+ (mg/g)	FeR Total (mg/g)	Fe CDE (mg/g)
East Trinity Site 3	0-10	6.90	1955	0.344	1.11	1.46	0.281
	10-20	7.23	2330	0.223	0.043	0.267	0.115
	20-30	6.93	1880	0.203	0.051	0.254	0.212
	30-40	6.66	3380	0.211	0.068	0.279	0.216
	40-50	6.91	3410	0.162	0.037	0.198	0.082
	50-60	6.80	1903	0.093	0.015	0.108	0.060
	60-70	7.00	1990	0.044	0.007	0.051	0.066
	70-80	6.91	2240	0.046	0.008	0.054	0.039
	80-90	6.73	1873	0.053	0.009	0.062	0.032
	90-100	6.64	2110	0.040	0.006	0.047	0.039
	100-110	6.44	1180	0.042	0.007	0.048	0.040
	110-120	6.09	4400	0.055	0.009	0.064	0.052
	120-130	6.06	3890	0.037	0.006	0.043	0.033
	130-140	6.14	4800	0.042	0.007	0.049	0.040
	140-150	6.53	2470	0.054	0.009	0.063	0.051

	Depth (cm)	Total Sulfur (%)	Total Carbon (%)	Total Nitrogen (%)	AVS (%S)	E.S (%S)	CRS (%S)
East Trinity Site 3	0-10	0.40	6.73	0.306	0.021	0.019	0.018
	10-20	0.21	2.76	0.134	0.054	0.089	0.028
	20-30	0.34	2.37	0.117	0.031	0.048	0.021
	30-40	0.58	2.68	0.127	0.028	0.041	0.024
	40-50	0.68	2.39	0.129	0.040	0.034	0.057
	50-60	0.37	2.35	0.111	<0.001	0.002	0.199
	60-70	0.32	2.52	0.110	<0.001	0.001	0.136
	70-80	0.54	3.11	0.124	<0.001	0.001	0.273
	80-90	1.76	4.22	0.107	<0.001	0.001	0.584
	90-100	2.32	6.22	0.133	<0.001	0.001	1.53
	100-110	1.75	4.20	0.112	<0.001	0.001	1.72
	110-120	1.86	4.23	0.118	<0.001	0.002	1.67
	120-130	1.84	4.34	0.103	<0.001	0.001	1.42
	130-140	1.41	4.00	0.099	<0.001	0.001	1.37
	140-150	1.59	4.27	0.105	<0.001	0.001	1.61

	Depth (cm)	WS Cl (%)	WS SO4 (%)	Cl:SO4 Ratio	KCl SO4 (%)	HCl SO4 (%)
East Trinity Site 3	0-10	0.794	0.128	6.18	0.132	0.320
	10-20	0.372	0.052	7.11	0.035	0.151
	20-30	0.751	0.121	6.23	0.063	0.745
	30-40	0.896	0.155	5.79	0.029	0.990
	40-50	1.16	0.211	5.50	0.081	1.068
	50-60	0.800	0.154	5.20	0.151	0.331
	60-70	1.21	0.197	6.13	0.130	0.110
	70-80	1.19	0.223	5.31	0.120	0.123
	80-90	1.31	0.276	4.75	0.103	0.124
	90-100	1.36	0.321	4.22	0.217	0.163
	100-110	1.01	0.410	2.47	0.101	0.110
	110-120	1.30	0.395	3.30	0.125	0.136
	120-130	1.37	0.491	2.80	0.115	0.166
	130-140	1.11	0.537	2.07	0.143	0.117
	140-150	1.32	0.541	2.43	0.148	0.129

	Depth (cm)	$\delta^{34}S$ CRS (‰)	$\delta^{34}S$ WS SO4 (‰)	$\delta^{34}S$ KCl SO4 (‰)	$\delta^{34}S$ HCl SO4 (‰)
East Trinity Site 3	0-10	-17.4	24.6	22.4	
	10-20	-22.7	29.3	25.6	
	20-30	-24.1	25.5		
	30-40	-22.5	20.0		
	40-50	-25.8	21.1	18.2	-13.9
	50-60	-23.2	19.1	16.3	
	60-70	-22.1	22.2	18.8	
	70-80	-26.1	16.0	11.9	
	80-90	-27.7	5.6		
	90-100	-28.0	3.1		
	100-110	-28.2	-6.8	-11.1	
	110-120	-28.4	-2.3		
	120-130	-28.1	-6.5	-14.8	
	130-140	-27.8	-10.8		
	140-150	-26.9	-9.1		

	Depth (cm)	pH Water	EC (µS/cm)	FeR 2+ (mg/g)	FeR 3+ (mg/g)	FeR Total (mg/g)	Fe CDE (mg/g)
East Trinity Site 4	0-10	5.23	709	0.331	0.995	1.33	0.284
	10-20	4.56	559	0.053	0.091	0.144	0.112
	20-30	4.44	492	0.042	0.013	0.055	0.068
	30-40	3.96	741	0.041	0.118	0.160	0.204
	40-50	3.75	748	0.039	0.452	0.492	0.429
	50-60	3.79	750	0.042	0.246	0.289	0.485
	60-70	3.88	785	0.040	0.218	0.259	0.444
	70-80	4.36	718	0.042	0.159	0.201	0.345
	80-90	4.26	944	0.050	0.193	0.243	0.919
	90-100	4.28	856	0.052	0.055	0.107	0.084
	100-110	4.39	685	0.068	0.072	0.139	0.112
	110-120	7.29	1620	0.073	0.072	0.145	0.115
	120-130	7.90	1430	0.061	0.060	0.122	0.101
	130-140	7.93	1330	0.058	0.054	0.111	0.090
	140-150	8.28	949	0.053	0.025	0.078	0.094

	Depth (cm)	Total Sulfur (%)	Total Carbon (%)	Total Nitrogen (%)	AVS (%S)	E.S (%S)	CRS (%S)
East Trinity Site 4	0-10	0.21	6.25	0.390	0.025	0.059	0.033
	10-20	0.12	3.70	0.224	<0.001	0.002	0.008
	20-30	0.08	2.53	0.128	<0.001	0.002	0.003
	30-40	0.37	2.84	0.119	<0.001	<0.001	0.003
	40-50	0.74	1.87	0.098	<0.001	<0.001	0.004
	50-60	0.89	1.73	0.095	<0.001	<0.001	0.003
	60-70	0.83	1.71	0.094	<0.001	<0.001	0.004
	70-80	0.40	1.77	0.102	<0.001	<0.001	<0.001
	80-90	0.73	1.86	0.095	<0.001	<0.001	0.030
	90-100	1.57	1.88	0.094	<0.001	0.001	1.83
	100-110	1.68	2.10	0.094	<0.001	0.001	1.40
	110-120	1.59	1.81	0.086	<0.001	<0.001	2.19
	120-130	1.77	2.33	0.090	<0.001	<0.001	1.61
	130-140	1.59	2.16	0.081	<0.001	<0.001	1.64
	140-150	1.33	2.22	0.064	<0.001	<0.001	0.862

	Depth (cm)	WS Cl (%)	WS SO4 (%)	Cl:SO4 Ratio	KCl SO4 (%)	HCl SO4 (%)
East Trinity Site 4	0-10	0.090	0.081	1.11	0.083	0.189
	10-20	0.065	0.057	1.14	0.073	0.103
	20-30	0.050	0.060	0.84	0.000	0.066
	30-40	0.113	0.131	0.86	0.112	1.57
	40-50	0.108	0.123	0.87	0.075	2.89
	50-60	0.108	0.113	0.95	0.156	3.12
	60-70	0.117	0.127	0.91	0.086	3.79
	70-80	0.116	0.122	0.95	0.131	3.36
	80-90	0.147	0.174	0.84	0.164	1.85
	90-100	0.148	0.441	0.34	0.241	2.25
	100-110	0.227	0.694	0.33	0.146	0.274
	110-120	0.243	0.377	0.65	0.372	0.216
	120-130	0.286	0.330	0.87	0.276	0.159
	130-140	0.283	0.288	0.98	0.138	0.147
	140-150	0.287	0.228	1.26	0.205	0.148

	Depth (cm)	$\delta^{34}S$ CRS (‰)	$\delta^{34}S$ WS SO4 (‰)	$\delta^{34}S$ KCl SO4 (‰)	$\delta^{34}S$ HCl SO4 (‰)
East Trinity Site 4	0-10		-0.95	-4.4	
	10-20		-9.9	-19.7	
	20-30		-12.1		
	30-40		-20.3	-16.8	-21.8
	40-50		-20.3		
	50-60		-20.4		
	60-70		-19.8		
	70-80		-20.2		
	80-90		-22.7		
	90-100	-21.8	-25.1	-21.5	-20.0
	100-110		-24.7		
	110-120	-16.3	-21.1	-17.5	
	120-130		-17.8		
	130-140		-17.5		
	140-150		-16.4		

	Depth (cm)	pH Water	EC (µS/cm)	FeR 2+ (mg/g)	FeR 3+ (mg/g)	FeR Total (mg/g)	Fe CDE (mg/g)
East Trinity Site 5	0-10	5.62	364	0.131	0.176	0.307	0.219
	10-20	4.40	548	0.103	0.871	0.974	0.394
	20-30	4.64	1690	0.068	0.465	0.532	0.382
	30-40	5.32	1680	0.075	0.172	0.247	0.204
	40-50	5.35	1383	0.072	0.071	0.143	0.217
	50-60	5.25	1257	0.065	0.022	0.087	0.196
	60-70	5.70	2040	0.072	0.022	0.095	0.209
	70-80	7.68	3050	0.097	0.069	0.165	0.121
	80-90	7.90	3460	0.072	0.043	0.115	0.090
	90-100	8.06	3800	0.083	0.057	0.139	0.115
	100-110	8.36	3850	0.086	0.016	0.102	0.119
	110-120	8.64	3070	0.076	0.016	0.092	0.097
	120-130	8.52	3660	0.074	0.016	0.089	0.097
	130-140	8.38	3380	0.075	0.015	0.089	0.102
	140-150	8.46	3100	0.065	0.013	0.078	0.060

	Depth (cm)	Total Sulfur (%)	Total Carbon (%)	Total Nitrogen (%)	AVS (%S)	E.S (%S)	CRS (%S)
East Trinity Site 5	0-10	0.60	10.9	0.534	0.007	0.010	0.015
	10-20	0.17	3.16	0.164	<0.001	0.003	0.005
	20-30	0.24	2.45	0.115	<0.001	0.001	0.002
	30-40	0.20	2.16	0.109	0.001	0.002	0.015
	40-50	0.27	1.64	0.086	<0.001	0.001	0.013
	50-60	0.76	1.73	0.086	<0.001	0.002	0.638
	60-70	1.13	1.76	0.090	<0.001	0.001	1.19
	70-80	1.11	1.79	0.085	0.002	<0.001	1.27
	80-90	1.46	2.09	0.078	<0.001	0.001	1.92
	90-100	1.49	2.03	0.080	<0.001	<0.001	1.66
	100-110	1.74	2.10	0.077	<0.001	<0.001	1.86
	110-120	1.58	2.01	0.069	0.001	<0.001	1.31
	120-130	1.74	2.14	0.072	<0.001	<0.001	1.73
	130-140	1.71	2.18	0.076	<0.001	<0.001	1.51
	140-150	1.72	2.17	0.114	<0.001	0.001	1.48

	Depth (cm)	WS Cl (%)	WS SO4 (%)	Cl:SO4 Ratio	KCl SO4 (%)	HCl SO4 (%)
East Trinity Site 5	0-10	0.065	0.047	1.38	0.041	1.05
	10-20	0.091	0.077	1.19	0.062	0.162
	20-30	0.343	0.160	2.14	0.061	0.213
	30-40	0.377	0.131	2.88	0.090	0.332
	40-50	0.320	0.130	2.47	0.067	1.249
	50-60	0.350	0.217	1.62	0.138	0.107
	60-70	0.433	0.350	1.24	0.130	0.080
	70-80	0.667	0.617	1.08	0.264	0.054
	80-90	0.733	0.410	1.79	0.380	0.048
	90-100	0.795	0.412	1.93	0.315	0.034
	100-110	0.971	0.488	1.99	0.232	0.049
	110-120	0.981	0.494	1.99	0.450	0.054
	120-130	1.17	0.603	1.93	0.512	0.057
	130-140	1.34	0.667	2.01	0.527	0.061
	140-150	1.24	0.628	1.98	0.463	0.054

	Depth (cm)	$\delta^{34}S$ CRS (‰)	$\delta^{34}S$ WS SO4 (‰)	$\delta^{34}S$ KCl SO4 (‰)	$\delta^{34}S$ HCl SO4 (‰)
East Trinity Site 5	0-10		10.7	7.8	-1.4
	10-20		2.5	3.7	
	20-30		-6.9		
	30-40		-2.0		
	40-50		-4.9	-3.4	-17.7
	50-60	-29.6	-13.7		-21.5
	60-70		-17.6		
	70-80		-10.1		
	80-90		-4.6		
	90-100		-5.4		
	100-110	-22.5	-4.1		
	110-120		-4.5		
	120-130	-13.4	-3.3		
	130-140		-2.3		
	140-150		-1.5		

Appendix 3 – Data tables for Chapter 4

Site No.	pH Water	EC (µS/cm)	Eh (mV)	DO (mg/L)	DO Sat (%)	Temp (°C)	Alk (mmol/L)
1	6.52	3010	132	5.65	70.0	26.9	0.599
2	5.80	2186	185	5.14	64.1	27.4	0.403
3	4.92	1530	396	4.84	60.3	27.3	0.283
4	4.38	860	477	4.46	55.7	27.3	0.150
5	4.33	746	413	4.45	55.5	27.4	0.272
6	3.86	835	473	4.46	55.9	27.5	0.039
7	5.62	659	254	4.30	53.7	27.4	0.414
8	6.74	128	168	7.16	90.8	28.2	0.992
9	6.89	144	161	6.67	84.3	28.1	0.918
10	3.97	814	508	4.55	57.2	27.7	0.005
11	3.62	670	508	3.92	49.2	27.6	0.000
12	3.72	476	502	3.50	43.8	27.5	0.050
13	3.79	414	502	3.29	41.1	27.3	0.005
14	3.80	409	521	3.38	42.5	27.6	0.228
15	3.82	419	458	7.28	94.9	29.8	0.172
16	4.08	259	503	5.21	65.7	27.8	0.283
17	4.08	241	468	4.44	56.7	28.6	0.403
18	4.00	244	433	6.18	77.9	27.8	0.217
19	5.72	142	269	7.51	94.5	27.8	0.403
20	3.94	274	457	7.16	91.7	28.7	0.072
21	7.69	23350	188	7.83	98.4	27.6	2.62
22	7.94	357	159	7.36	94.1	28.6	2.73

Site No.	Na (mg/L)	K (mg/L)	Ca (mg/L)	Mg (mg/L)	Cl (mg/L)	SO4 (mg/L)	Cl:SO4 Ratio
1	366	15.3	23.0	51.9	715	159	4.49
2	263	11.4	18.4	38.8	504	129	3.90
3	154	6.96	12.8	24.8	279	100	2.79
4	79.8	4.01	8.96	14.4	137	72.3	1.89
5	78.0	4.05	9.40	14.6	133	73.3	1.81
6	79.6	4.15	9.89	15.6	135	92.4	1.46
7	66.7	3.45	8.23	12.0	108	56.5	1.91
8	13.6	1.24	4.03	3.47	18.2	8.1	2.25
9	15.0	1.38	4.34	3.86	19.8	12.0	1.65
10	74.5	3.88	9.45	14.4	122	90.1	1.36
11	53.5	3.19	8.62	12.1	84.7	92.2	0.92
12	30.9	2.15	6.82	8.72	47.0	71.6	0.66
13	29.3	2.07	6.81	8.41	44.0	69.2	0.64
14	24.2	1.94	6.34	7.69	35.4	62.6	0.57
15	27.6	1.93	6.57	8.17	41.2	65.7	0.63
16	16.5	1.37	5.49	5.95	22.2	50.4	0.44
17	14.9	1.38	5.24	5.61	20.5	48.7	0.42
18	14.6	1.33	5.05	5.35	19.1	45.1	0.42
19	13.0	1.14	4.10	3.97	17.9	26.7	0.67
20	14.7	1.39	5.29	5.81	19.3	51.6	0.37
21	3501	143	164	451	7110	1117	6.36
22	29.8	2.25	17.15	10.9	43.9	12.1	3.63

Site No.	Ag (mg/L)	Al (mg/L)	As (mg/L)	Cd (mg/L)	Cr (mg/L)	Cu (mg/L)	Fe (mg/L)
1	<0.001	0.025	0.004	<0.001	0.001	0.001	0.008
2	<0.001	0.090	0.003	<0.001	0.001	<0.001	0.012
3	<0.001	0.679	0.001	<0.001	0.001	0.001	0.063
4	<0.001	0.781	0.001	<0.001	0.001	0.000	0.088
5	<0.001	0.732	0.001	<0.001	0.001	0.001	0.095
6	<0.001	1.25	0.001	<0.001	<0.001	0.001	0.387
7	<0.001	0.087	0.001	<0.001	0.001	<0.001	0.011
8	<0.001	0.084	<0.001	<0.001	0.001	0.001	0.617
9	<0.001	0.068	<0.001	<0.001	0.001	0.001	0.882
10	<0.001	1.34	0.001	<0.001	<0.001	0.001	0.389
11	<0.001	1.85	0.001	<0.001	0.000	0.001	1.08
12	<0.001	1.30	<0.001	<0.001	0.001	0.001	0.562
13	<0.001	1.32	<0.001	<0.001	<0.001	0.001	0.482
14	<0.001	1.14	<0.001	<0.001	<0.001	0.001	0.404
15	<0.001	1.46	<0.001	<0.001	<0.001	0.001	0.685
16	<0.001	0.667	<0.001	<0.001	<0.001	0.001	0.300
17	<0.001	0.472	<0.001	<0.001	<0.001	0.001	0.554
18	<0.001	0.414	<0.001	<0.001	<0.001	<0.001	0.354
19	<0.001	0.032	<0.001	<0.001	<0.001	<0.001	0.013
20	<0.001	0.521	<0.001	<0.001	<0.001	0.000	0.446
21	<0.001	0.003	0.038	<0.001	0.004	0.005	0.000
22	<0.001	0.006	0.001	<0.001	0.002	0.001	0.007

Site No.	Mn (mg/L)	Ni (mg/L)	Pb (mg/L)	Se (mg/L)	Zn (mg/L)	Hg (mg/L)	$\delta^{34}S$ SO4 (‰)
1	0.304	0.005	<0.001	0.010	0.011	<0.001	11.9
2	0.340	0.005	<0.001	0.008	0.015	<0.001	9.97
3	0.363	0.006	<0.001	0.004	0.022	<0.001	6.47
4	0.337	0.005	<0.001	0.002	0.020	<0.001	3.69
5	0.324	0.005	<0.001	0.002	0.019	<0.001	3.77
6	0.433	0.006	<0.001	0.002	0.028	<0.001	2.09
7	0.233	0.003	<0.001	0.002	0.012	<0.001	4.43
8	0.006	0.001	<0.001	0.001	<0.001	<0.001	7.90
9	0.003	0.001	<0.001	<0.001	<0.001	<0.001	10.3
10	0.434	0.006	<0.001	0.002	0.029	<0.001	2.36
11	0.518	0.007	<0.001	0.002	0.035	<0.001	1.37
12	0.458	0.009	<0.001	0.001	0.027	<0.001	1.85
13	0.472	0.009	<0.001	0.001	0.027	<0.001	1.56
14	0.428	0.006	<0.001	0.001	0.023	<0.001	1.17
15	0.456	0.006	<0.001	0.001	0.028	<0.001	1.38
16	0.299	0.003	<0.001	0.001	0.012	<0.001	1.42
17	0.282	0.003	<0.001	0.001	0.010	<0.001	1.31
18	0.253	0.002	<0.001	0.001	0.008	<0.001	1.80
19	0.201	0.002	<0.001	<0.001	0.003	<0.001	2.29
20	0.273	0.002	<0.001	<0.001	0.010	<0.001	1.26
21	0.010	0.008	<0.001	0.115	0.003	<0.001	19.8
22	0.001	0.002	<0.001	0.001	<0.001	<0.001	14.9

Appendix 4 – Data tables for Chapter 5

	Depth (cm)	pH Water	EC (µS/cm)	Total Carbon (%)	AVS (%)	CRS (%)	Soluble SO4 (%)
Mangroves single low tide sampling	S1 0-10	7.77	2449	0.23	<0.001	0.195	0.063
	10-20	8.04	2830	0.21	<0.001	0.111	0.083
	20-30	8.55	2860	0.98	<0.001	0.096	0.074
	30-40	8.40	2880	0.44	<0.001	0.564	0.139
	S2 0-10	6.88	3120	1.87	0.001	0.340	0.174
	10-20	6.74	2660	0.79	<0.001	0.091	0.136
	20-30	6.19	2215	0.26	<0.001	0.198	0.102
	30-40	5.94	2350	0.13	<0.001	0.214	0.112

	Depth (cm)	$\delta^{34}S$ CRS (‰)	$\delta^{34}S$ SO_4^{2-} (‰)	Fract. from SWS (‰)	Fract. from SS (‰)
Mangroves single low tide sampling	S1 0-10	-25.3	14.4	39.7	45.9
	20-30	-26.7	13.4	40.0	47.3
	S2 0-10	-27.2	9.6	36.8	47.8
	20-30	-27.9	3.2	31.1	48.5

	Time	Depth (cm)	CRS (%S)	$\delta^{34}S\ SO_4^{2-}$ (‰)	Water depth (cm)	Piezometer readings			
						pH	EC (mS/cm)	Eh (mV)	SO_4 (mg/L)
Mangroves extended sampling	05:30	0-10	0.027	18.8	3	6.94	48.4	156	729
		10-20	0.033	18.9					
		20-30	0.457	19.0					
		30-40	1.08	18.8					
	07:00	0-10	0.011	18.8	-6	6.81	49.6	149	757
		10-20	0.133	18.6					
		20-30	0.236	17.6					
		30-40	0.882	16.9					
	08:30	0-10	0.086	18.8	-9	6.90	51.4	140	765
		10-20	0.566	18.6					
		20-30	0.587	18.8					
		30-40	0.713	15.1					
	10:00	0-10	0.058	19.3	-9	6.77	51.6	121	776
		10-20	0.107	18.6					
		20-30	0.402	17.0					
		30-40	0.552	17.9					
	11:30	0-10	0.012	18.6	-10	6.68	53.5	102	779
		10-20	0.178	20.0					
		20-30	0.314	18.3					
		30-40	0.684	18.0					
	13:00	0-10	0.078	18.2	-11	6.61	55.7	88	835
		10-20	0.105	16.6					
		20-30	0.361	15.6					
		30-40	0.556	14.8					
	14:30	0-10	0.023	16.5	-16	6.46	59.3	47	862
		10-20	0.147	16.6					
		20-30	0.275	18.8					
		30-40	0.253	18.5					
	16:30	0-10	0.049	18.8	-17	6.30	61.3	-26	936
		10-20	0.066	18.3					
		20-30	0.335	15.7					
		30-40	0.270	17.9					
	17:00	0-10	0.072	19.4	-18	6.33	62.4	-62	962
		10-20	0.182	18.6					
		20-30	0.497	17.1					
		30-40	1.41	17.2					